PHASE 2 INITIAL BOREHOLE DRILLING AND TESTING, IGNACE AREA

WP04C Data Report: Porewater Extraction and Analysis for IG_BH06

APM-REP-01332-0349 **December 2024**

WSP Canada LTD. (and Hydroisotop GmbH)

nwmo
NUCLEAR WASTE MANAGEMENT ORGANIZATION
SOCIÉTÉ DE GESTION DES DÉCHETS NUCLÉAIRES

This report has been prepared under contract to NWMO. The report has been reviewed by NWMO, but the views and conclusions are those of the authors and do not necessarily represent those of the NWMO.

All copyright and intellectual property rights belong to NWMO.

Nuclear Waste Management Organization
22 St. Clair Avenue East, 4th Floor
Toronto, Ontario
M4T 2S3
Canada

Tel: 416-934-9814
Web: www.nwmo.ca

REPORT

PHASE 2 INITIAL BOREHOLE DRILLING AND TESTING AT IG_BH04/05/06

WP04C Data Report - Porewater Extraction and Analysis for IG_BH06

Submitted to:

Nuclear Waste Management Organization

4th Floor
22 St. Clair Avenue East
Toronto, Ontario, M4T 2S3

Submitted by:

WSP Canada Inc.
6925 Century Avenue, Suite #600, Mississauga, Ontario, L5N 7K2, Canada

+1 905 567 4444

NWMO Document: APM-REP-01332-0349

2001102 / 20253946

December 2024

Distribution List

e-copy - NWMO

e-copy - WSP

e-copy - Hydroisotop

WP4C DATA REPORT
POREWATER EXTRACTION AND ANALYSIS FOR IG_BH06

CLIENT INFORMATION

Project Name: Phase 2 Initial Borehole Drilling and Testing at IG_BH04/05/06, Ignace Area
Project Number: 20253946
Client PO Number: 2000141
Document Name: 20253946 IG_BH06 WP04C Rpt_Dec2024_R6a

Client:	Nuclear Waste Management Organization (NWMO)	
Address:	22 St. Clair Avenue East, 4th Floor	
City:	Toronto	
Province:	Ontario	
Postal Code:	M4T 2S3	
Client Contact:	Laura Kennell-Morrison	Warwick Watt
Telephone:	647-259-3737	437-972-3669
Email:	lkennell@nwmo.ca	wwatt@nwmo.ca

ISSUE/REVISION INDEX

Issue Code	Revision No.	By	Revd.	App.	Date	Revision Details
RR	0	JI/FE	GWS	-	11-Mar-2023	Draft released for review and comment
RR	1	JI/FE	GWS	-	21-Dec-2023	Revised draft for review and comment
RR	2	JI/FE	GWS	-	08-Mar-2024	Final report for NWMO acceptance
RI	3	FE	GWS	KDV	01-Aug-2024	Revised final report for NWMO acceptance
RI	4	FE	GWS	KDV	05-Aug-2024	Revised final report for NWMO acceptance
RI	5	FE	GWS	KDV	18-Nov-2024	Revised final report for NWMO acceptance
RI	6	FE	GWS	KDV	09-Dec-2024	Final report released for information

Issue Codes: RR = Released for Review and Comments, RI = Released for Information

SIGNATURES

Prepared by: _____

Dr. Florian Eichinger
Hydroisotop GmbH

Reviewed by: _____

George Schneider, M.Sc., P.Geo.
Senior Geoscientist

Approved by: _____

Ken DeVos, M.Sc., P.Geo.
Senior Hydrogeochemist

Table of Contents

1.0 INTRODUCTION 1

1.1 Geological Setting 2

1.2 Technical Objectives 4

2.0 SAMPLING AND SAMPLE PREPARATION 6

2.1 Porewater Samples 6

2.2 Porewater Gas Samples 10

2.3 Core Logging Depth Correction 11

3.0 EXPERIMENTAL SET-UPS AND ANALYTICAL METHODS 11

3.1 Water Content and Water-Loss Porosity 11

3.2 Porewater Extraction Methods 13

3.2.1 Aqueous Extraction Experiments 13

3.2.2 Out-Diffusion Experiments 13

3.2.3 Isotope Diffusive Exchange Technique 15

3.3 Out-gassing Experiments to Extract Gases Dissolved in Porewater 16

3.3.1 Extraction and Quantification of Non-Inert gases (DG) Dissolved in Porewater 16

3.3.1.1 Quantification of Extracted Non-Inert Gases 16

3.3.1.2 Stable Isotope Analyses on Non-Inert Gases 18

3.3.2 Determination of Noble Gases (NG) Dissolved in Porewater 18

4.0 RESULTS OF WATER CONTENT AND WATER-LOSS POROSITY INVESTIGATIONS 19

4.1 Water Contents 19

4.1.1 Gravimetric Water Contents Determined on Aqueous Extraction Core Samples 20

4.1.2 Gravimetric Water Contents Determined on Porewater Cores 22

4.1.2.1 Gravimetric Water Contents Determined on End Pieces 22

4.1.3 Gravimetric Water Contents Determined on Out-Diffusion Cores 23

4.1.4 Gravimetric Water Contents Determined by Isotope Diffusive Exchange 26

4.1.6 Summary and Depth Profiles of Water Content Results 30

4.2 Bulk Dry/Wet Density and Water-Loss Porosity 32

5.0 RESULTS OF CHEMICAL COMPOSITION OF EXPERIMENT SOLUTIONS OF AQUEOUS EXTRACTION AND OUT-DIFFUSION EXPERIMENTS 34

5.1 Chemical Composition of Aqueous Extraction Solutions 35

5.2 Chemical Composition of Out-Diffusion Experiment Solutions 39

6.0 RESULTS FROM ELEMENTAL TIME SERIES AND PORE DIFFUSION COEFFICIENT OF CHLORIDE 46

6.1 Elemental Elution Curves 46

6.2 Modelling of Pore Diffusion Coefficients 78

7.0 CHLORIDE, BROMIDE AND CHLORIDE ISOTOPES IN POREWATER OF CORE SAMPLES FROM BOREHOLE IG_BH06 87

7.1 Porewater Chloride Concentrations Estimated by Aqueous Extraction Experiments 87

7.2 Porewater Chloride Concentrations and Bromide Concentrations and $\delta^{37}Cl$ Isotope Ratios Determined by Out-Diffusion Experiments 88

8.0 $\delta^{18}O$ AND $\delta^{2}H$ OF POREWATER OF CORE SAMPLES FROM IG_BH06 92

9.0 RESULTS FROM DISSOLVED GASES IN MATRIX POREWATER OF CORE SAMPLES FROM IG_BH06 95

9.1 Non-Inert Gases 97

9.1.1 Concentrations of Reactive, Non-Inert Gases Dissolved in Porewater 97

9.1.1.1 Porewater Nitrogen-, Hydrogen- and Carbon Dioxide Concentrations 98

9.1.1.2 Porewater Hydrocarbon Gas Concentrations 99

9.1.2 Stable Isotope Signatures of Non-Inert Gases Dissolved in Porewater 101

9.2 Noble Gases 107

10.0 REFERENCES 113

TABLES

Table 2-1: Overview of the core samples taken from IG_BH06 for porewater investigations (PW = porewater samples, AQ = cores dedicated for aqueous extraction experiments, AR = retained samples, decided to be investigated after borehole completion). 7

Table 2-2: Overview of the analytical porewater program conducted on core samples from IG_BH06 (PW: porewater extraction, AQ: aqueous extraction, AR = retained samples, decided to be investigated after borehole completion) 8

Table 4-1: Gravimetric water contents (WC) of aliquots of AQ core samples from IG_BH06 used for aqueous extraction experiments using wet (WC_{wet}) and dry masses (WC_{dry}) of the individual core

pieces. The weighted values are calculated by using the individual masses; (G / T: granodiorite / tonalite, D: diabase) 21

Table 4-2: Gravimetric water contents (WC) of aliquots of PW core samples from IG_BH06 used for out-diffusion experiments using wet (WC_{wet}) and dry masses (WC_{dry}) of the individual core pieces. The weighted values are calculated by using the individual masses; (G / T: granodiorite / tonalite, D: diabase) 22

Table 4-3: Gravimetric water contents of out-diffusion core samples from IG_BH06 calculated by the mass of cores determined before (b.e.) and after (a.e.) experiments using wet (WC_{wet}) and dry masses (WC_{dry}) of the individual core pieces; the error of the water content is determined by Gaussian error propagation (Appendix C); (G / T: granodiorite / tonalite, D: diabase) 24

Table 4-4: Gravimetric water contents determined on core samples from IG_BH06 used for isotope diffusive exchange experiments ($WC_{IsoEx,\ grav}$); Water contents are corrected for weight changes during experiments (b.e. = before experiment, a.e. = after experiment); the gravimetric water contents determined on the rock pieces used in the experiments with LAB – and ICE water are weighted taking their weights into account; the error of the water content is determined by Gaussian error propagation (Appendix C) 27

Table 4-5: Water contents of core samples from IG_BH06 calculated by isotope diffusive exchange method (eq. 7); the error of the water content is determined by Gaussian error propagation (Appendix C) 28

Table 4-7: Weighted gravimetric water contents of aqueous extraction and porewater core samples taken from borehole IG_BH06 and their corresponding total masses; the uncertainties of the water content values are the weighted standard deviations of the individual aliquots showing the density of water contents in one entire sample; (G / T: granodiorite / tonalite, D: diabase) 30

Table 4-8: Bulk wet and dry density and water-loss (=WL-) porosity determined by water contents calculated for dry ($\Phi_{WL,dry}$) and wet ($\Phi_{WL,wet}$) core samples from borehole IG_BH06; the errors are calculated by Gaussian error propagation (Appendix C); (G / T: granodiorite / tonalite, D: diabase) 32

Table 5-1: Analytical results of the aqueous extraction solutions of crushed core samples from borehole IG_BH06; Test solution types are classified after Jäckli (1970) 36

Table 5-2: Analytical results of test solutions of out-diffusion experiments using core samples from borehole IG_BH06 41

Table 6-1: Minimum (min), maximum (max) and average (avg) pore and effective diffusion coefficients determined by 1-dimensional modelling of Cl elution curves of out-diffusion experiments on core samples from IG_BH06 at 45 °C and calculated by the Stoke-Einstein-equation for 10 °C and 25 °C; (G / T: granodiorite / tonalite, D: diabase) 86

Table 7-1: Porewater Cl and Br concentrations and Br*1000/Cl mass ratios estimated using aqueous extraction experiments; the errors of porewater Cl and Br concentrations and Br*1000/Cl mass ratios are calculated by Gaussian error propagation (Appendix C). 87

Table 7-2: Porewater Cl and Br concentrations, Br*1000/Cl mass ratios and $\delta^{37}Cl$ isotope signatures. Cl concentrations are determined by out-diffusion experiments; the errors of porewater Cl and Br concentrations and Br*1000/Cl mass ratios are calculated by Gaussian error propagation (Appendix C); the errors of $\delta^{37}Cl$ values are the standard deviation of triplicate analyses; (G / T: granodiorite / tonalite, D: diabase). 89

Table 8-1: $\delta^{18}O$ and $\delta^{2}H$ values of porewater of core samples from borehole IG_BH06; the errors are calculated by Gaussian error propagation; (G / T: granodiorite / tonalite, D: diabase) 94

Table 9-1: Concentrations of gases dissolved in porewater of core samples from borehole IG_BH06; the volumes in NmL/L_{PW} are given normalised to standard conditions (273 K = 0°C, 1 bar); the errors are estimated to be ±20 %. 101

Table 9-2: Stable isotope signatures of gases dissolved in porewater of core samples from borehole IG_BH06....107

Table 9-3: Noble gas concentrations and ratios dissolved in porewater of cores taken from borehole IG_BH06....109

FIGURES

Figure 1-1: Location of IG_BH06 in relation to the Revell Site....1

Figure 1-2: Geological Setting and Location of Boreholes IG_BH04, IG_BH05, and IG_BH06 in the Northern Portion of the Revell Batholith....3

Figure 4-1: Mass of core samples from IG_BH06 before and after the out-diffusion experiments; the uncertainty of the core mass is ± 0.05 g 25

Figure 4-2: Water content calculated from the wet mass (dry surface) before and after the out-diffusion experiments of core sections from IG_BH06; the error of the water content is determined by Gaussian error propagation (Appendix C). 25

Figure 4-3: Comparison of water contents determined by isotope diffusive exchange (WC_{IsoEx}) and gravimetrically ($WC_{IsoEx, grav, corr.}$ by wet weight, corrected for weight change during experiments) on the same core pieces; the error of the water content is determined by Gaussian error propagation (Appendix C) 29

Figure 4-4: Water content and water-loss porosity of core samples from IG_BH06. 34

Figure 5-1: Schoeller diagram of experiment solutions from aqueous extraction experiments conducted with core samples from borehole IG_BH06. 38

Figure 5-2: Schoeller diagram of experiment solutions from out-diffusion experiments. 44

Figure 6-1: Elution curves of anions and cations set-up by the periodic sampling of the test solutions from out-diffusion experiments using core samples from borehole IG_BH06; the errors are the analytical uncertainty of ± 5 %. 48

Figure 6-2: Maximum (Dp(max)) and minimum (Dp(min)) pore diffusion coefficients (45 °C) determined ba a best fit of Cl elution curves in linear and logarithmic time and concentration scale; the solid lines mark the average diffusion coefficients (45 °C, Dp (ave)) 79

Figure 7-1: Borehole IG_BH06: Estimated porewater Cl and Br concentrations and Br*1000/Cl mass ratios versus depth by aqueous extraction experiments....88

Figure 7-2: Porewater chloride, bromide, Br*1000/Cl mass ratios and $\delta^{37}Cl$ isotope signatures from cores from borehole IG_BH06 as function of depth....90

Figure 7-3: Porewater Cl versus Br concentrations determined by out-diffusion experiments on core samples from IG_BH06. 91

Figure 7-4: Porewater $\delta^{37}Cl$ isotope signatures versus porewater Cl concentrations. 91

Figure 8-1: $\delta^{18}O$ and $\delta^{2}H$ porewater signatures as function of depth along borehole IG_BH06; errors are calculated by Gaussian error propagation (depth in mbgs (downhole)). 93

Figure 8-2: $\delta^{18}O$ versus $\delta^{2}H$ values of porewater; the black line marks the global meteoric water line; the errors of the stable isotope ratios are calculated by Gaussian error propagation. 94

Figure 8-3: Errors of the determination of the $\delta^{18}O$ (left) and $\delta^{2}H$ (right) porewater isotope signatures versus the mass ratio of test water and porewater (R(tw/pw)). 95

Figure 9-1: Diffusive equilibration of gases dissolved in porewater. The model calculations show that the equilibration time in days is sufficient to achieve equilibrium with respect to the analysed gases. The diffusive exchange in the experiments of the non-inert gases and noble gases with the lowest (Butane, Xenon) and the highest diffusion coefficient in free water (Methane, Helium) were modelled ($D_{(He)}$ = 7.2*10^{-9} m^2/s, $D_{(Xe)}$ = 1.5*10^{-9} m^2/s, $D_{(CH4)}$ = 1.9*10^{-9} m^2/s, $D_{(C4H10)}$ = 9.6*10^{-10} m^2/s at 20°C, Jähne et al. 1987). The conversion of these diffusion coefficients in free water to pore diffusion coefficients of the single gases in the rock samples was done according to Equation 14 using an average geometry factor of 0.04 as estimated for chloride (cf. Section 6.2)....96

Figure 9-2: Porewater nitrogen (N_2, left), hydrogen (H_2, center) and carbon dioxide (CO_2, right) concentrations as function of depth along borehole IG_BH06; errors are ± 20% (depth in mbgs (downhole)). 98

Figure 9-3: Porewater methane (CH_4, top, left), saturated (C_2-C_5, bottom left) and unsaturated (C_2-C_4, bottom right) higher hydrocarbon concentrations and hydrocarbon ratios (top, right) as function of depth along borehole IG_BH06; errors are ± 20%....100

Figure 9-4: Stable isotope signatures of nitrogen ($\delta^{15}N$-N_2, left) and methane ($\delta^{13}C$-CH_4, center, $\delta^{2}H$-CH_4, right) dissolved in porewater as function of depth along borehole IG_BH06; errors are ± 0.1 ‰ for $\delta^{15}N$-N_2, ± 2.0 ‰ for $\delta^{13}C$-CH_4 and ± 10.0 ‰ for $\delta^{2}H$-CH_4. 102

Figure 9-5: Stable carbon isotope signatures of higher hydrocarbons dissolved in porewater as function of depth along borehole IG_BH06; errors are ± 2.0 ‰ 103

Figure 9-6: Isotopic classification of methane dissolved in porewater from core samples from borehole IG_BH06. The porewater results are compared to end-member signatures according to Whiticar (2020). 104

Figure 9-8: Carbon isotope signatures of methane versus the hydrocarbon ratio of methane over ethane plus propane (C_1/C_2+C_3) dissolved in porewater of cores from borehole IG_BH06 compared to end-member fields according to Faber (1987), Whiticar (1999) and Kietäväinen et al. (2017) and references therein. 106

Figure 9-9: Helium (left) and argon concentrations of porewater as function of depth along borehole IG_BH06; errors are ± 20.0%....110

Figure 9-10: $^{40}Ar/^{36}Ar$ and $^{3}He/^{4}He$ isotope ratios dissolved in porewater as function of depth along borehole IG_BH06 compared to end-members of air and crustal and mantle He.....111

Figure 9-11: $^{3}He/^{4}He$ isotope ratios versus helium concentrations dissolved in porewater of cores taken from borehole IG_BH06 compared to end-member concentration of air saturated water (ASW), crust and mantle signature and potential mantle mixing paths (Osenbrück 1996).....112

APPENDICES

APPENDIX A
Core Logging Depth Correction and Photo Documentation

APPENDIX B
Analytical Raw Data

APPENDIX C
Error Calculations

1.0 INTRODUCTION

The Initial Borehole Drilling and Testing project in the Wabigoon Lake Ojibway Nation (WLON) – Ignace Area, Ontario, is part of Phase 2 Geoscientific Preliminary Field Investigations of the Nuclear Waste Management Organization's (NWMO) Adaptive Phased Management Site Selection Phase. This project includes the drilling and testing of six deep boreholes at the Revell site, as well as additional on-going studies located within the northern portion of the Revell batholith.

This project involves testing of deep borehole IG_BH04 and the drilling and testing of deep boreholes IG_BH05 and IG_BH06 in the Revell site within the identified Potential Repository Area (PRA), as shown on Figure 1-1. The work comprises a total of eleven work packages and was carried out by a team led by WSP Canada Inc. (WSP) on behalf of the NWMO. The IG_BH06 program is described in a Borehole Characterization Plan (BCP) for IG_BH06.

This data report describes the methodology, activities, and results for Work Package 4C (WP04C): Porewater Extraction and Analysis for IG_BH06.

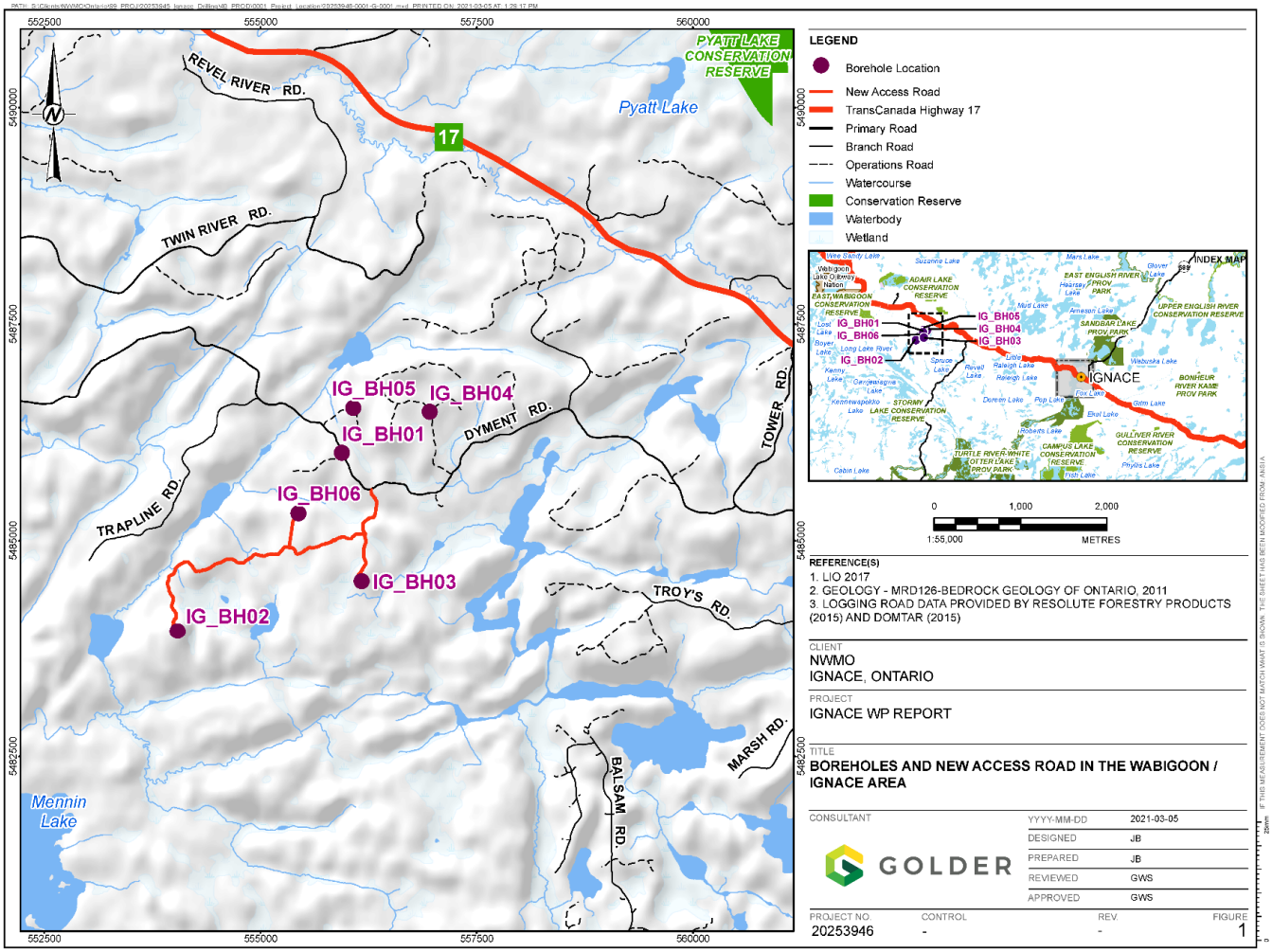


Figure 1-1: Location of IG_BH06 in relation to the Revell Site

Given that the permeability of the crystalline rock units being characterized is expected to be very low, it is unlikely that groundwater can be sampled beyond a few opportunistic groundwater samples from conductive fractures. As such, core samples were collected and preserved on site and sent for porewater extraction and analysis. Core samples were taken with the overall objective of characterizing porewater geochemistry and gas composition at depth. The geochemical results provide information about the paleohydrogeological evolution of the bedrock system in the crystalline rock units at depth. Sampling depths and intervals were selected based on the geological and structural conditions of the bedrock and on the observations and investigation results gained from previous boreholes.

Thin section petrographic analyses will be carried out in the same core sample intervals on adjacent core sections to characterize mineralogy and support the evaluation of the porewater chemistry, which is obtained by indirect extraction methods, requiring the determination of both the in situ water content and the connected porosity. The evaluation of the petrophysical parameters requires a correlation with the petrographic and mineralogical characteristics of the investigated lithologies. Thin section petrographic analysis was completed under WP04D (WSP 2023).

1.1 Geological Setting

The approximately 2.7 billion years old Revell batholith is located in the western part of the Wabigoon Subprovince of the Archean Superior Province. The batholith is roughly elliptical in shape trending northwest, is approximately 40 km in length, 15 km in width, and covers an area of approximately 455 km^2. Based on geophysical modelling, the batholith is approximately 2 km to 3 km thick through the center of the northern portion (SGL 2015). The batholith is surrounded by supracrustal rocks of the Raleigh Lake (to the north and east) and Bending Lake (to the southwest) greenstone belts (Figure 1-2).

IG_BH06 is located within an investigation area of approximately 19 km^2 in size, situated in the northern portion of the Revell batholith. Bedrock exposure in the area is generally very good due to minimal overburden, few water bodies, and relatively recent logging activities. Ground elevations generally range from 400 to 450 m above sea level. The ground surface broadly slopes towards the northwest as indicated by the flow direction of the main rivers in the area. Local water courses tend to flow to the southwest towards Mennin Lake (Figure 1-1).

Four main rock units are identified in the supracrustal rock group: mafic metavolcanic rocks, intermediate to felsic metavolcanic rocks, metasedimentary rocks, and mafic intrusive rocks (Figure 1-2). Sedimentation within the supracrustal rock assemblage was largely synvolcanic, although sediment deposition in the Bending Lake area may have continued past the volcanic period (Stone 2009; Stone 2010a; Stone 2010b). All supracrustal rocks are affected, to varying degrees, by penetrative brittle-ductile to ductile deformation under greenschist- to amphibolite-facies metamorphic conditions (Blackburn and Hinz 1996; Stone et al. 1998). In some locations, primary features, such as pillow basalt or bedding in sedimentary rocks are preserved, in other locations, primary relationships are completely masked by penetrative deformation. Uranium-lead (U-Pb) geochronological analysis of the supracrustal rocks produced ages that range between 2734.6 +/-1.1 Ma and 2725 +/-5 Ma (Stone et al. 2010).

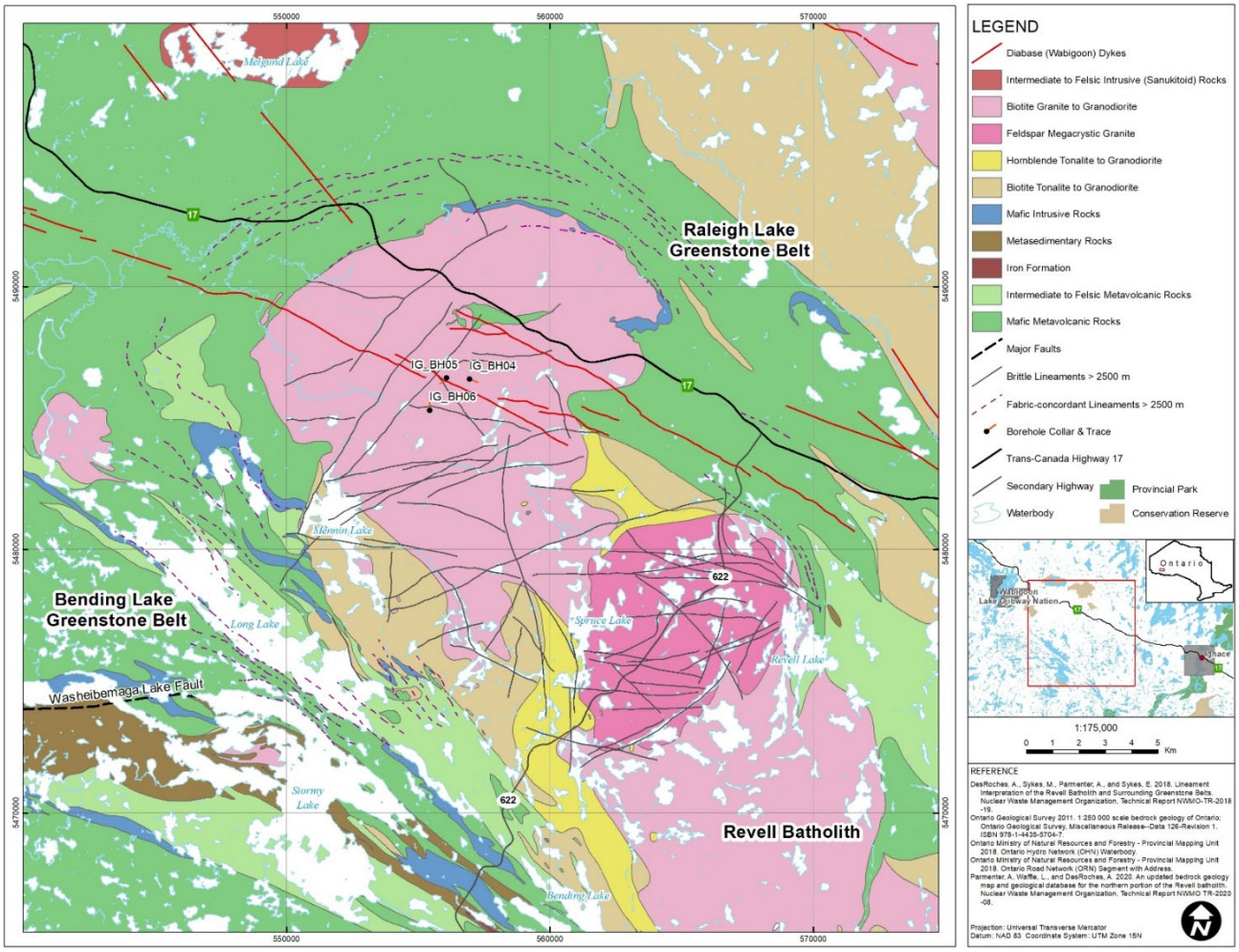


Figure 1-2: Geological Setting and Location of Boreholes IG_BH04, IG_BH05, and IG_BH06 in the Northern Portion of the Revell Batholith

Three main suites of plutonic rock are recognized in the Revell batholith, including, from oldest to youngest: a Biotite Tonalite to Granodiorite suite, a Hornblende Tonalite to Granodiorite suite, and a Biotite Granite to Granodiorite suite (Figure 1-2). Plutonic rocks of the Biotite Tonalite to Granodiorite suite occur along the southwestern and northeastern margins of the Revell batholith. The principal type of rock within this suite is a white to grey, medium-grained, variably massive to foliated or weakly gneissic, biotite tonalite to granodiorite. One sample of foliated and medium-grained biotite tonalite produced a U-Pb age of 2734.2+/-0.8 Ma (Stone et al. 2010). The Hornblende Tonalite to Granodiorite suite occurs in two irregularly-shaped zones surrounding the central core of the Revell batholith. Rocks of the Hornblende Tonalite to Granodiorite suite range compositionally from tonalite through granodiorite to granite, and include significant proportions of quartz diorite and quartz monzodiorite. One sample of coarse-grained grey mesocratic hornblende tonalite produced a U-Pb age of 2732.3+/-0.8 Ma (Stone et al. 2010). Rocks of the Biotite Granite to Granodiorite suite underlie most of the northern, central and southern portions of the Revell batholith. Rocks of this suite are typically coarse-grained, massive to weakly foliated, and white to pink in colour. The Biotite Granite to Granodiorite suite ranges compositionally from granite through granodiorite to tonalite. A distinct potassium (K)-Feldspar Megacrystic

Granite phase of the Biotite Granite to Granodiorite suite occurs as an oval-shaped body in the central portion of the Revell batholith (Figure 1-2). One sample of coarse-grained, pink, massive K-feldspar megacrystic biotite granite produced a U-Pb age of 2694.0+/-0.9 Ma (Stone et al. 2010).

The bedrock surrounding IG_BH06 is composed mainly of massive to weakly foliated felsic intrusive rocks that vary in composition between granodiorite and tonalite, and together form a relatively homogeneous intrusive complex. Bedrock identified as tonalite transitions gradationally into granodiorite and no distinct contact relationships between these two rock types are typically observed (SRK and Golder 2015; Golder and PGW 2017). Massive to weakly foliated granite is identified at the ground surface to the northwest of the feldspar-megacrystic granite. The granite is observed to intrude into the granodiorite-tonalite bedrock, indicating it is distinct from, and younger than, the intrusive complex (Golder and PGW 2017).

West-northwest trending mafic dykes interpreted from aeromagnetic data extend across the northern portion of the Revell batholith and into the surrounding greenstone belts. One mafic dyke occurrence, located to the northwest of IG_BH01, is approximately 15-20 m wide (Figure 1-2). All of these mafic dykes have a similar character and are interpreted to be part of the Wabigoon dyke swarm. One sample from the same Wabigoon swarm produced a U-Pb age of 1887+/-13 Ma (Stone et al. 2010), indicating that these mafic dykes are Proterozoic in age. It is assumed based on surface measurements that these mafic dykes are sub-vertical (Golder and PGW 2017).

Long, narrow valleys are located along the western and southern limits of the investigation area (Figure 1-1). These local valleys host creeks and small lakes that drain to the southwest and may represent the surface expression of structural features that extend into the bedrock. A broad valley is located along the eastern limits of the investigation area and hosts a more continuous, un-named water body that flows to the south. The linear and segmented nature of this waterbody's shorelines may also represent the surface expression of structural features that extend into the bedrock.

Regional observations from mapping have indicated that structural features are widely spaced (typical 30 to 500 cm spacing range) and dominantly comprised of sub-vertical joints with two dominant orientations, northeast and northwest trending (Golder and PGW 2017). Interpreted bedrock lineaments generally follow these same dominant orientations in the northern portion of the Revell batholith (Figure 1-2; DesRoches et al. 2018). Minor sub-horizontal joints have been observed with minimal alteration, suggesting they are younger and perhaps related to glacial unloading. One mapped regional-scale fault, the Washeibemaga Lake fault, trends east and is located to the west of the Revell batholith (Figure 1-2). Ductile lineaments, also shown on Figure 2, follow the trend of foliation mapped in the surrounding greenstone belts. Additional details of the lithological units and structures found at surface within the investigation area are reported in Golder and PGW (2017).

1.2 Technical Objectives

The technical objectives of the porewater testing program are to assess the key chemical and transport properties of the crystalline host rock with depth and within the repository horizon (presently assumed to be at depths of > 600 m). The geochemical results will provide information about the palaeohydrogeological evolution of the bedrock system. The porewater chemistry will be evaluated using indirect extraction methods which require the determination of the in situ water content and connected porosity.

The associated work tasks include:

- Aqueous extraction experiments to determine initial estimates of pore fluid composition and Total Dissolved Solids (TDS);
- Isotope diffusive exchange experiments, for the determination of stable water isotopes ($\delta^{18}O$ and $\delta^{2}H$);
- Out-diffusion experiments, for determination of porewater stable ion concentrations (Cl and Br), as well as the determination of pore and effective diffusion coefficients, D_p, D_e, for Cl;
- Determination of elemental elution curves during out-diffusion experiments;
- $\delta^{37}Cl$ analyses; and
- Determination of density, water content and porosity for the various subsamples used in the above-listed analytical suites.

Further objectives within this study are to extract and characterise gases dissolved in porewater. This includes:

- The extraction of non-inert gases (N_2, CO_2, H_2, O_2, CH_4, C_xH_x) from porewater by out-gassing experiments;
- Quantification of the gas concentrations dissolved in porewater using the water content of the naturally saturates core samples;
- The isotopic characterisation of non-inert gases ($\delta^{13}C$-CO_2, -CH_4, -C_xH_x, $\delta^{2}H$-CH_4, $\delta^{15}N$-N_2) dissolved in porewater;
- The extraction of noble gases (He, Ar, Ne, Kr, Xe) from porewater by out-gassing experiments;
- Quantification of the noble-gas concentrations dissolved in porewater using the water content of the naturally saturated core samples; and
- The isotopic characterisation of noble gases ($^{3}He/^{4}He$, $^{40}Ar/^{36}Ar$, ^{132}Xe, ^{84}Kr) dissolved in porewater

The characterization of porewater composition, including gases and the solute transport processes in the rock matrix, contribute important information for the long-term safety assessment of deep geological repositories for radioactive waste. Thus, knowledge of the porewater composition will allow better constraints on the processes affecting the near-field of a repository. In designs where repository construction is restricted to bedrock of low permeability, the first water to interact with the repository barrier materials (e.g., bentonite, Cu-canister) will be the porewater. This interaction could result in changes of the physical and chemical properties of the various barrier materials. Knowledge of the porewater composition and its evolution over recent geological time – particularly during the last thousand to hundreds of thousands of years, in accordance with the expected lifespan of a geologic repository – is considered to be of high importance.

In combination with the knowledge gained about solute transport in the rock matrix, characterization of porewater also contributes to a better understanding of processes related to the far-field environment around the repository. Thus, it provides valuable information about matrix diffusion as a potential retardation factor for radionuclides, and allows better constraints to be placed on the palaeohydrogeological history of a repository site. Due to the exchange by diffusion between fracture groundwater and matrix porewater, released radionuclides may be temporally immobilized by matrix diffusion, and possible subsequent sorption onto mineral surfaces. For radionuclides susceptible to sorption, the accessible surface areas are greatly enhanced by matrix diffusion when compared to the accessible surface area on fracture surfaces alone. Matrix diffusion therefore has the potential to

increase solute transport times. The chemical and isotopic characterisation and quantification of gases dissolved in porewater is important to estimate the potential gas flow in the bedrock. It gives first information about the gas behaviour in the bedrock, which can act as sink or source for gases occurring during the deposition of radioactive waste. The combination of the characterisation of non-inert and noble gases allows for the source characterisation of detected gases. Additionally, the noble gas investigations allow an estimate of the residence times of porewater to be made.

In contrast to fracture groundwater, porewater cannot be sampled by conventional groundwater sampling techniques; it has to be derived by indirect extraction techniques. In most of these indirect extraction techniques – especially in case of rocks of a porosity below about 2 vol.% – the original porewater concentrations are diluted and need to be back-calculated to in situ concentrations. This requires a well-defined value for the connected porosity – accessible to different solutes under in situ conditions. The derivation of connected porosity values, as well as solute concentrations, is prone to various perturbations during drilling, core sampling, storage, and experiments in the laboratory. The obtained data have to be carefully evaluated for potential perturbations induced by drilling activities, rock stress release and sample treatment in the laboratory in order to derive values that are representative of in situ conditions. This requires detailed characterization of the rock composition, the rock texture, and the local stress field.

Matrix porewater of 31 core samples taken from 212 m to 971 mbgs (downhole) in the borehole IG_BH06, were investigated for their chemical and isotopic composition. Additionally, the same set of core samples were characterised for their petrophysical properties, including water content, water-loss porosity, bulk density and chloride pore diffusion coefficients. Additionally, 10 core samples taken from 510 m to 940 mbgs (downhole) were investigated for their non-inert and noble gas composition. These cores were also characterised for their water contents and water-loss porosities.

2.0 SAMPLING AND SAMPLE PREPARATION

2.1 Porewater Samples

A total of 31 samples were taken from borehole IG_BH06 between September 24, 2021 and November 3, 2021 for the porewater characterization program (Table 2-1). Sampling was conducted by WSP according to the instructions provided by Hydroisotop GmbH (Hydroisotop) via personnel training. After recovery from the borehole, the individual core sections were photographed and immediately packed in a plastic (PE) bag, evacuated and sealed airtight. This procedure was repeated for a second PE bag and a final Al-coated plastic layer. The samples were stored in a refrigerator on site and then sent to Hydroisotop, Germany, in a cooler.

The samples arrived in the lab between October 8 and November 9, 2021. Eleven additional archived core samples arrived on October 29, 2021 (IG_BH06_DG003) and January 21, 2022 (IG_BH06_AR010, AR013, AR019, AR020, AR027, AR038, AR039, AR045, AR049, AR064). All samples were well packed and arrived in the lab with preserved vacuum. At Hydroisotop, the samples were stored in the refrigerator at 4°C and prepared between November 8 and December 4, 2021. The 11 additional archived core samples were prepared on March 14, 2022.

The assigned samples were unpacked and immediately wrapped into Parafilm™ and cut by dry-sawing into full-diameter sections. After sawing, the surfaces of the obtained pieces were cleaned with paper towels and again wrapped into Parafilm™. The entire sample preparation was conducted as rapidly as possible (within 10 minutes) after opening the sealed bags, in order to minimize evaporation. During sample preparation it was observed that three of the porewater core samples (IG_BH06_AR010, IG_BH06_AR038 and IG_BH06_AR039) were of a

different lithology (tonalite, amphibolite and tonalite, respectively) compared to the other core samples (biotite granodiorite / tonalite). The analytical program conducted on each sample is summarized in Table 2-2.

Table 2-1: Overview of the core samples taken from IG_BH06 for porewater investigations (PW = porewater samples, AQ = cores dedicated for aqueous extraction experiments, AR = retained samples, decided to be investigated after borehole completion).

			Depth								
Interval	Sample ID	Hydro Lab Nr.	from	to	mid-point	Length	Test Type	Date sampled	Time recovered	Date sent	Date arrived
			mbgs	mbgs	mbgs	m			hh:mm		
1	IG_BH06_PW001	373158	212.09	212.44	212.27	0.26	PW	24-Sep-2021	23:14	01.10.2021	08.10.2021
	IG_BH06_AQ001	373159	212.79	212.94	212.87	0.15	AQ	24-Sep-2021	23:06	01.10.2021	08.10.2021
2	IG_BH06_PW002	373160	291.28	291.69	291.49	0.41	PW	27-Sep-2021	11:45	01.10.2021	08.10.2021
	IG_BH06_AQ002	373161	292.44	292.68	292.56	0.17	AQ	27-Sep-2022	11:38	01.10.2021	08.10.2021
3	IG_BH06_PW003	373162	369.33	369.73	369.53	0.18	PW	30-Sep-2021	14:55	01.10.2021	08.10.2021
	IG_BH06_AQ003	373163	370.13	370.53	370.33	0.40	AQ	30-Sep-2021	14:45	01.10.2021	08.10.2021
4	IG_BH06_PW004	373164	453.00	453.40	453.20	0.40	PW	6-Oct-2021	10:18	12.10.2021	18.10.2021
	IG_BH06_AQ004	373165	453.40	453.62	453.51	0.22	AQ	6-Oct-2021	10:22	12.02.2021	18.10.2021
5	IG_BH06_PW005	373166	503.91	504.30	504.11	0.39	PW	8-Oct-2021	12:40	12.10.2021	18.10.2021
	IG_BH06_AQ005	373167	504.3	504.47	504.39	0.17	AQ	8-Oct-2021	12:37	12.02.2021	18.10.2021
6	IG_BH06_PW006	373168	562.25	562.62	562.44	0.37	PW	10-Oct-2021	14:04	12.10.2021	18.10.2021
	IG_BH06_AQ006	373169	562.62	562.81	562.72	0.19	AQ	10-Oct-2021	14:02	12.02.2021	18.10.2021
7	IG_BH06_PW007	373170	574.00	574.35	574.18	0.35	PW	11-Oct-2021	00:32	12.10.2021	18.10.2021
	IG_BH06_AQ007	373171	574.35	574.50	574.43	0.15	AQ	11-Oct-2021	00:38	12.02.2021	18.10.2021
8	IG_BH06_PW008	373835	612.01	612.38	612.20	0.37	PW	12-Oct-2021	18:21	18.10.2021	25.10.2021
	IG_BH06_AQ008	373836	612.38	612.57	612.48	0.19	AQ	12-Oct-2021	18:18	18.10.2021	25.10.2021
9	IG_BH06_PW009	373837	647.69	648.06	647.88	0.37	PW	20-Oct-2021	04:35	25.10.2021	29.10.2021
	IG_BH06_AQ009	373838	648.06	648.24	648.15	0.18	AQ	20-Oct-2021	04:23	25.10.2021	29.10.2021
10	IG_BH06_PW010	373839	665.70	666.08	665.89	0.38	PW	20-Oct-2021	15:50	25.10.2021	29.10.2021
	IG_BH06_AQ010	373840	666.08	666.28	666.18	0.20	AQ	20-Oct-2021	15:58	25.10.2021	29.10.2021
11	IG_BH06_PW011	373841	690.75	691.23	690.99	0.48	PW	21-Oct-2021	16:48	25.10.2021	29.10.2021
12	IG_BH06_PW012	373843	693.49	693.87	693.68	0.38	PW	21-Oct-2021	23:20	25.10.2021	29.10.2021
	IG_BH06_AQ011	373842	693.87	694.03	693.95	0.16	AQ	21-Oct-2021	23:23	25.10.2021	29.10.2021
13	IG_BH06_PW013	373844	720.34	720.73	720.54	0.39	PW	23-Oct-2021	00:57	25.10.2021	29.10.2021
	IG_BH06_AQ012	373845	720.73	720.90	720.82	0.17	AQ	23-Oct-2021	01:01	25.10.2021	29.10.2021
14	IG_BH06_PW014	373846	747.35	747.71	747.53	0.36	PW	24-Oct-2021	12:19	25.10.2021	29.10.2021
	IG_BH06_AQ013	373847	747.71	747.85	747.78	0.14	AQ	24-Oct-2021	14:32	25.10.2021	29.10.2021
15	IG_BH06_AQ014	374203	771.16	771.33	771.25	0.17	AQ	25-Oct-2021	12:07	29.10.2021	05.11.2021
	IG_BH06_PW015	374200	774.69	775.04	774.87	0.35	PW	25-Oct-2021	13:46	29.10.2021	05.11.2021
16	IG_BH06_PW016	374201	804.47	804.84	804.66	0.37	PW	27-Oct-2021	00:39	29.10.2021	05.11.2021
	IG_BH06_AQ015	374204	804.84	805.02	804.93	0.18	AQ	27-Oct-2021	00:33	29.10.2021	05.11.2021
17	IG_BH06_PW017	368213	839.99	840.37	840.18	0.38	PW	29-Oct-2021	06:13	29.10.2021	05.11.2021
	IG_BH06_AQ016	374205	840.98	841.38	841.18	0.40	AQ	29-Oct-2021	06:19	29.10.2021	05.11.2021
18	IG_BH06_PW018	374206	852.83	853.18	853.01	0.35	PW	29-Oct-2021	22:16	03.11.2021	09.11.2021
	IG_BH06_AQ017	374207	853.18	853.42	853.30	0.24	AQ	29-Oct-2021	22:20	03.11.2021	09.11.2021
19	IG_BH06_PW019	374208	885.14	885.50	885.32	0.36	PW	31-Oct-2021	10:43	03.11.2021	09.11.2021
	IG_BH06_AQ018	374209	885.50	885.66	885.58	0.16	AQ	31-Oct-2021	10:40	03.11.2021	09.11.2021
20	IG_BH06_PW020	374210	927.41	927.81	927.61	0.40	PW	2-Nov-2021	01:12	03.11.2021	09.11.2021
	IG_BH06_AQ019	374211	927.81	928.09	927.95	0.28	AQ	2-Nov-2021	01:05	03.11.2021	09.11.2021
AR	IG_BH06_AR010	378926	398.49	398.91	398.70	0.42	PW (AR)	2-Oct-2021	15:56	17.01.2022	21.01.2022
	IG_BH06_AR013	378927	421.39	421.79	421.59	0.40	PW (AR)	3-Oct-2021	16:54	17.01.2022	21.01.2022
	IG_BH06_AR019	378928	533.79	534.16	533.98	0.37	PW (AR)	9-Oct-2021	15:43	17.01.2022	21.01.2022
	IG_BH06_AR020	378929	542.66	543.04	542.85	0.38	PW (AR)	9-Oct-2021	23:37	17.01.2022	21.01.2022
	IG_BH06_AR027	378930	594.78	595.14	594.96	0.36	PW (AR)	12-Oct-2021	01:49	17.01.2022	21.01.2022
	IG_BH06_AR038	378931	722.38	722.83	722.61	0.45	PW (AR)	23-Oct-2021	04:25	17.01.2022	21.01.2022
	IG_BH06_AR039	378932	728.58	728.94	728.76	0.36	PW (AR)	23-Oct-2021	12:17	17.01.2022	21.01.2022
	IG_BH06_AR045	378933	796.49	796.85	796.67	0.36	PW (AR)	26-Oct-2021	10:23	17.01.2022	21.01.2022
	IG_BH06_AR049	378934	820.06	820.42	820.24	0.36	PW (AR)	27-Oct-2021	15:22	17.01.2022	21.01.2022
	IG_BH06_AR064	378935	971.18	971.54	971.36	0.36	PW (AR)	3-Nov-2021	14:45	17.01.2022	21.01.2022
	IG_BH06_DG003	373848	743.92	744.13	744.03	0.21	PW (DG)	24-Oct-2021	10:32	25.10.2021	29.10.2021

*mbgs (downhole)

Table 2-2: Overview of the analytical porewater program conducted on core samples from IG_BH06 (PW: porewater extraction, AQ: aqueous extraction, AR = retained samples, decided to be investigated after borehole completion)

					Experimental and analytical programme													
					Aqueous Extraction			Diffusive isotope exchange experiments			Out-diffusion experiments							Grav. WC
Sample ID	Hydro Lab Nr.	Depth	Date prepared	Experiment	Exp. Set-Up	Chemical analyses	Grav. WC	Exp. Set-Up	Isotope Analyses	Grav. WC	Exp. Set-Up	Time Series	Analyses ions	Analyses $\delta^{37}Cl$	Grav. WC	Density	Modelling D_P	Extra Pieces
		mbgs																
IG_BH06_PW001	373158	212.3	08.11.2021	PW	X	X	X											
IG_BH06_AQ001	373159	212.9	21.10.2021	AQ				X	X	X	X	X	X	X	X	X	X	X
IG_BH06_PW002	373160	291.5	08.11.2021	PW				X	X	X	X	X	X	X	X	X	X	X
IG_BH06_AQ002	373161	292.6	21.10.2021	AQ	X	X	X											
IG_BH06_PW003	373162	369.5	08.11.2021	PW	X	X	X											
IG_BH06_AQ003	373163	370.3	21.10.2021	AQ				X	X	X	X	X	X	X	X	X	X	X
IG_BH06_PW004	373164	453.2	08.11.2021	PW	X	X	x											
IG_BH06_AQ004	373165	453.5	21.10.2021	AQ				X	X	X	X	X	X	X	X	X	X	X
IG_BH06_PW005	373166	504.1	08.11.2021	PW				X	X	X	X	X	X	X	X	X	X	X
IG_BH06_AQ005	373167	504.4	21.10.2021	AQ	X	X	X											
IG_BH06_PW006	373168	562.4	08.11.2021	PW				X	X	X	X	X	X	X	X	X	X	X
IG_BH06_AQ006	373169	562.7	21.10.2021	AQ	X	X	X											
IG_BH06_PW007	373170	574.2	08.11.2021	PW				X	X	X	X	X	X	X	X	X	X	X
IG_BH06_AQ007	373171	574.4	21.10.2021	AQ	X	X	X											
IG_BH06_PW008	373835	612.2	08.11.2021	PW				X	X	X	X	X	X	X	X	X	X	X
IG_BH06_AQ008	373836	612.5	21.10.2021	AQ	X	X	X											
IG_BH06_PW009	373837	647.9	04.12.2021	PW	X	X	X											
IG_BH06_AQ009	373838	648.2	21.10.2021	AQ				X	X	X	X	X	X	X	X	X	X	X
IG_BH06_PW010	373839	665.9	04.12.2021	PW				X	X	X	X	X	X	X	X	X	X	X
IG_BH06_AQ010	373840	666.2	21.10.2021	AQ	X	X	X											
IG_BH06_PW011	373841	691.0	04.12.2021	PW				X	X	X	X	X	X	X	X	X	X	X
IG_BH06_AQ011	373842	694.0	21.10.2021	AQ	X	X	X											
IG_BH06_PW012	373843	693.7	04.12.2021	PW					X	X	X	X	X	X	X	X	X	X
IG_BH06_AQ012	373845	720.8	21.10.2021	AQ	X	X	X											
IG_BH06_PW013	373844	720.5	04.12.2021	PW					X	X	X	X	X	X	X	X	X	X
IG_BH06_AQ013	373847	747.8	21.10.2021	AQ	X	X	X											

*mbgs (downhole)

Table 2-2: Continued

					Experimental and analytical programme													
					Aqueous Extraction			Diffusive isotope exchange experiments			Out-diffusion experiments							Grav. WC
Sample ID	Hydro Lab Nr.	Depth	Date prepared	Experiment	Exp. Set-Up	Chemical analyses	Grav. WC	Exp. Set-Up	Isotope Analyses	Grav. WC	Exp. Set-Up	Time Series	Analyses ions	Analyses $\delta^{37}Cl$	Grav. WC	Density	Modelling D_P	Extra Pieces
		mbgs																
IG_BH06_PW014	373846	747.5	04.12.2021	PW					X	X	X	X	X	X	X	X	X	X
IG_BH06_AQ014	374203	771.2	21.10.2021	AQ	X	X	X											
IG_BH06_PW015	374200	774.9	04.12.2021	PW				X	X	X	X	X	X	X	X	X	X	X
IG_BH06_AQ015	374204	804.9	21.10.2021	AQ	X	X	X											
IG_BH06_PW016	374201	804.7	04.12.2021	PW				X	X	X	X	X	X	X	X	X	X	X
IG_BH06_AQ016	374205	841.2	21.10.2021	AQ	X	X	X											
IG_BH06_PW017	368213	840.2	04.12.2021	PW				X	X	X	X	X	X	X	X	X	X	X
IG_BH06_AQ017	374207	853.3	21.10.2021	AQ	X	X	x											
IG_BH06_PW018	374206	853.0	04.12.2021	PW				X	X	X	X	X	X	X	X	X	X	X
IG_BH06_AQ018	374209	885.6	21.10.2021	AQ	X	X	x											
IG_BH06_PW019	374208	885.3	04.12.2021	PW				X	X	X	X	X	X	X	X	X	X	X
IG_BH06_AQ019	374211	928.0	21.10.2021	AQ	X	X	x											
IG_BH06_PW020	374210	927.6	04.12.2021	PW				X	X	X	X	X	X	X	X	X	X	X
IG_BH06_AR010	378926	398.7	14.03.2022	PW				X	X	X								
IG_BH06_AR013	378927	421.6	14.03.2022	PW				X	X	X	X	X	X	X	X	X	X	X
IG_BH06_AR019	378928	534.0	14.03.2022	PW				X	X	X	X	X	X	X	X	X	X	X
IG_BH06_AR020	378929	542.9	14.03.2022	PW				X	X	X								
IG_BH06_AR027	378930	595.0	14.03.2022	PW				X	X	X	X	X	X	X	X	X	X	X
IG_BH06_AR038	378931	722.6	14.03.2022	PW				X	X	X								
IG_BH06_AR039	378932	728.8	14.03.2022	PW				X	X	X	X	X	X	X	X	X	X	X
IG_BH06_AR045	378933	796.7	14.03.2022	PW				X	X	X								
IG_BH06_AR049	378934	820.2	14.03.2022	PW				X	X	X	X	X	X	X	X	X	X	X
IG_BH06_AR064	378935	971.4	14.03.2022	PW				X	X	X	X	X	X	X	X	X	X	X
IG_BH06_DG003	373848	744.0	14.03.2022	PW							X	X	X	X	X	X	X	X

*mbgs (downhole)

2.2 Porewater Gas Samples

A total of 15 samples from 5 depth intervals were taken from borehole IG_BH06 between October 08, 2021 and November 02, 2021 for the porewater gas characterization program (Table 2-3). Sampling was conducted by WSP according to the instructions provided by Hydroisotop GmbH (Hydroisotop) via video and video tutorial training. After recovery from the borehole, the individual core sections were photographed, weighed, and immediately placed in stainless-steel cylinders.

The cylinders were vacuum tight closed and repeatedly flushed with nitrogen (for the noble gas (NG) samples) or helium (for the non-inert dissolved gas (DG) samples) and evacuated.

Afterwards the samples were stored at room temperature and sent in one batch to Hydroisotop and University of Oxford. At Hydroisotop, the cylinders were also stored at room temperature. The samples were allowed to equilibrate for 349 to 374 days for DG samples and 637 to 668 days for NG samples, respectively.

The analytical program conducted on each sample is summarized in Table 2-4.

Table 2-3: Overview of the core samples taken from IG_BH06 for porewater gas investigations (NG = noble gas; DG = non-inert dissolved gas; Hydro = HI = Hydroisotop; UoO = University of Oxford).

Sample ID	Lab	Depth					Sampling Date	Recovery Time	m (cyl)	m (core)
		from	to	Mid-point	Core Length	Test Type				
		mbgs	mbgs	mbgs	m				g	g
IG_BH06_DG001	Hydro	510.09	510.29	510.2	0.20	DG	08.10.2021	22:37	5018.16	1627.46
IG_BH06_NG001	Hydro	512.40	512.62	512.5	0.22	NG (HI)	09.10.2021	01:00	5120.00	1726.20
IG_BH06_NG002	UoO	512.62	512.83	512.7	0.21	NG (UoO)	09.10.2021	01:04	5005.07	1613.18
IG_BH06_DG002	Hydro	620.74	620.96	620.9	0.22	DG	19.10.2021	04:35	5145.25	1750.23
IG_BH06_NG003	Hydro	623.54	623.75	623.6	0.21	NG (HI)	19.10.2021	10:05	4990.53	1602.71
IG_BH06_NG004	UoO	623.75	623.96	623.9	0.21	NG (UoO)	29.10.2021	09:57	4536.61	1619.99
IG_BH06_NG005	Hydro	735.51	735.74	735.6	0.23	NG (HI)	23.10.2021	16:36	5176.00	1784.00
IG_BH06_NG006	UoO	736.04	736.28	736.2	0.24	NG (UoO)	23.10.2021	16:48	5254.00	1864.00
IG_BH06_DG004	Hydro	802.31	802.51	802.4	0.20	DG	26.10.2021	22:30	4919.04	1519.57
IG_BH06_DG005	Hydro	842.56	842.76	842.7	0.20	DG	29.10.2021	11:40	4894.00	1428.00
IG_BH06_NG007	Hydro	846.84	847.04	846.9	0.20	NG (HI)	29.10.2021	13:49	4950.00	1632.00
IG_BH06_NG008	UoO	847.04	847.24	847.1	0.20	NG (UoO)	29.10.2021	13:57	4888.00	1492.00
IG_BH06_DG006	Hydro	936.30	936.50	936.4	0.20	DG	02.11.2021	11:54	4972.48	1576.83
IG_BH06_NG009	Hydro	939.48	939.69	939.6	0.21	NG (HI)	02.11.2021	14:20	5015.88	1629.26
IG_BH06_NG010	UoO	939.69	939.89	939.8	0.20	NG (UoO)	02.11.2021	14:23	4929.28	1546.97

*mbgs (downhole)

Table 2-4: Overview of the analytical porewater gas program conducted on core samples from IG_BH06 (NG = noble gas; DG = non-inert dissolved gas).

					Experimental and analytical programme					
Sample ID	Hydro Lab Nr.	Depth mbgs	Test Type	Date analysed	Exp. Set-Up	DG analyses	DG isotope analyses	NG analyses	NG isotope analyses	Water content
IG_BH06_DG001	378520	510.2	DG	15.09.2022	x	x	x			x
IG_BH06_DG002	378521	620.9	DG	15.09.2022	x	x	x			x
IG_BH06_DG004	378522	802.4	DG	15.09.2022	x	x	x			x
IG_BH06_DG005	378523	842.7	DG	15.09.2022	x	x	x			x
IG_BH06_DG006	378524	936.4	DG	15.09.2022	x	x	x			x
IG_BH06_NG001	378525	512.5	NG	27.07.2023	x	x	x	x	x	x
IG_BH06_NG003	378526	623.6	NG	03.08.2023	x		x	x	x	x
IG_BH06_NG005	378527	735.6	NG	07.08.2023	x		x	x	x	x
IG_BH06_NG007	378528	846.9	NG	31.07.2023	x		x	x	x	x
IG_BH06_NG009	378529	939.6	NG	31.07.2023	x		x	x	x	x

*mbgs (downhole)

2.3 Core Logging Depth Correction

During the core logging of borehole IG_BH06, the logged depths were not reconciled with the depths obtained by the drilling supervisor calculated from measurement of the drill string and drill rod stick-up. This resulted in the WP03 core logging depths and core sample depths to be recorded as being slightly deeper than the actual sample depths. Refer to the WP03 Report for IG_BH06 for details of the correction applied to the core logging data.

All sample depths referred to in this report and appendices are the original, uncorrected sample depths in metres below ground surface (mbgs) downhole.

An Addendum to the Laboratory Report summarizing the original and corrected core depths for each sample is provided in Appendix A.

3.0 EXPERIMENTAL SET-UPS AND ANALYTICAL METHODS

Porewater investigations included: 1) the determination of the water content and water-loss porosity on the respective samples, 2) aqueous extraction and out-diffusion experiments to characterise porewater using chemical tracers, 3) isotope diffusive exchange experiments used to determine the porewater $\delta^{18}O$ and $\delta^{2}H$ composition, 4) out-gassing experiments to determine the composition and volume as well as isotopic signatures and ratios of non-inert gases and noble gases dissolved in porewater.

Unless otherwise specified, the analytical work has been conducted at Hydroisotop GmbH, Germany.

3.1 Water Content and Water-Loss Porosity

The water content was determined on core material used for aqueous extraction and out-diffusion experiments, as well as on the core pieces used for the isotope diffusive exchange experiments and out-gassing experiments.

Water contents also were determined on extra pieces of core available from those used for the out-diffusion experiments.

The quality of sample preservation upon arrival in the laboratory was assessed by the condition of the sample bags and of the core surface (wet vs. dry). Core pieces used for out-gassing experiments were weighed directly in the field before placing them in the cylinders and after the experiments.

For water content measurements, drill-core pieces were placed in a crystallization dish, weighed and subsequently dried at 105 °C until stable weight conditions. According to the experience and knowledge gained from the investigations of cores from boreholes IG_BH01 to IG_BH03, the first drying step at 45 °C was considered unnecessary. Before taking the initial wet weight of the full diameter core sections, the surface was allowed to dry on the balance until stable weight was achieved for ≈10 sec. During the following drying process, weighing was carried out every 14 days until the sample weight remained constant (±0.002 g) for at least 14 days.

Water contents were determined on core samples used for aqueous extraction experiments (Table 2-2). Therefore, one half of the full disc core (282 – 549 g) was broken by a mortar to an edge length of approximately 1 cm, placed in a crystallization dish, weighed and put in the oven at 105 °C for drying. Additionally, the two cut uneven head pieces with weights between 141 and 471 g were also weighed and put in the oven to determine the water content. Drying times varied between 35 and 105 days for crushed pieces, and 32 to 117 days for full core discs.

Water contents also were determined on core pieces used for out-diffusion experiments, with weights between 1217 – 1628 g and drying times between 36 and 174 days. Two extra pieces of the core sample used for out-diffusion and isotope exchange experiments were also taken for the determination of the water content. These sections had weights between 123 and 999 g and drying times between 21 and 143 days.

Gravimetric water contents were further determined on crushed core sections used for the single isotope diffusive exchange experiments after equilibration. The crushed core material was placed in a crystallizing dish and put in the oven at 105 °C. These samples had weights between 316 g and 503 g and drying times between 21 and 101 days.

Water contents were determined on the full-size cores used for out-gassing experiments (NG and DG) with weights between 1,504 g and 1,784 g also in the oven at 105°C. Drying to constant weight needed between 65 and 155 days.

The calculation of the water-loss porosity (i.e., the connected porosity) from the gravimetric water content requires a measure of the grain density. In rocks of low porosity, the bulk wet density can be used as a proxy for the grain density. A measure for the bulk wet density of the rocks used for out-diffusion and aqueous extraction experiments was obtained from the volume and saturated mass of the core samples. The volume was calculated from measurements of height and diameter of the core samples using a Vernier Caliper, with an error of ± 0.01 mm.

Core lengths varied between 3.6 and 8.1 cm for aqueous extraction cores, and between 15.7 and 20.6 cm for out-diffusion cores.

From known sample volume and wet mass, the bulk, wet and dry density is obtained by

$$\rho_{bulk,wet} = \frac{m_{rock,wet}}{V_{rock}}, \qquad \rho_{bulk,dry} = \frac{m_{rock,dry}}{V_{rock}} \qquad \text{eq. 1}$$

and the water-loss (connected) porosity, ϕWL, can be calculated according to

$$\emptyset_{WL} = WC_{wet} \times \frac{\rho_{bulk,wet}}{\rho_{water}} \quad \emptyset_{WL} = \frac{m_{pw} \times 100}{r^2 \times h \times \pi \times \rho_{water}} \qquad \text{eq. 2}$$

where WC_{wet} is the water content based on the wet weight of the rock sample and $\rho_{bulk,wet}$ the bulk wet density of the rock. In a first approximation, the density of water, ρ_{water}, is assumed to be 1 g/cm^3. Due to the low water content of the investigated crystalline rocks, the water content and water-loss porosity determined by the wet weight and bulk, wet density of the sample is essentially equal to those values calculated using the dry weight and bulk, dry density.

As shown by Gaussian error propagation (Appendix C), the error of the water content and the water-loss porosity depends predominately on the accuracy of the determination of the mass of porewater measured after unpacking (i.e., on the measured initial wet weight) and the final dry weight of the cores.

3.2 Porewater Extraction Methods

3.2.1 Aqueous Extraction Experiments

Aqueous extraction experiments were conducted prior to out-diffusion and isotope exchange experiments to estimate the salinity of the investigated porewaters.

Saturated full disc core sections were crushed by a mortar and sieved by an analytical sieve to a grain size of < 2 mm and 85 to 155 g of rock material were put in a PE bottle, where 49 to 157 ml of deionized water were added. Subsequently the bottle was gently shaken for 24 h. Afterward, the elution was decanted, filtered (0.45 µm) and immediately analysed for their alkalinity, pH and specific electrical conductivity (EC) using a Metrohm Titrino 785 and WTW LF 325 system.

The main anion and cation concentrations were analysed by ion chromatography (IC) using a Dionex ICS 1500 system. The analytical error of the ion concentration analyses is ± 5 %. Aluminium concentrations were analysed using a ContrAA800 G graphite tube atomic absorption spectrometer (AAS) from ThermoFischer with an analytical error of ±10 % and silica concentrations were determined photometrically with an analytical error of ±5 %. DOC concentrations were analysed using a Shimazu TOC-VCSH analyser (analytical error of 3-5 % depending on the concentration range).

The porewater Cl concentration was further calculated according to

$$C_{i,pw} = \frac{C_{i,sol} \times V_{sol} \times 0.001}{m_{pw}} \qquad \text{eq. 3}$$

where $C_{i,pw}$ = porewater elemental concentration, $C_{i,sol}$ = analyzed elemental concentration in the aqueous extraction solution, V_{sol} = Volume of aqueous extraction solution, and m_{pw} = mass of porewater.

3.2.2 Out-Diffusion Experiments

Out-diffusion experiments were performed on intact full disc cores by immersion into ultrapure water. The volume of test water varied between 128 and 154 ml, resulting in test water to core mass ratios between 0.09 and 0.11. During the experiments the two water reservoirs, i.e., porewater and test water, were allowed to exchange until equilibrium. Equilibrium with respect to chloride is reached when the Cl concentration has been constant within the analytical error range (= ±5 %) over a minimum of 14 days.

After placing the core sample in the PE-vessel, the vessel was sealed and put in a vibrating water bath (40 rpm) at a constant temperature of 45 °C to accelerate diffusion. The PE-vessels were covered by a vapour-tight lid, which is equipped with two Swagelok™ valves and PEEK™ sampling lines. The core, the experiment container and the test water were weighed before and after the experiment to ensure that no loss of test water occurred during the entire experiment. At specific time intervals of initially a few days, and later a few weeks, 0.5 ml of solution were sampled using a PVC-syringe to determine the chloride concentration as a function of time. The experimental time depended on the equilibration grade in the individual experiments. All out-diffusion experiments were ended between 253 and 324 days.

After equilibrium with respect to chloride was achieved, the vessels were removed from the water bath and cooled to room temperature. Subsequently, the cylinder, the core and the remaining test water were weighed and the supernatant solution was filtered (0.45 µm) and analysed immediately for pH, sp. el. conductivity (EC) and alkalinity (total alkalinity (pH 4.3) and base capacity 8.2), and later for major cations and anions and certain trace elements and isotopes.

The major cations (Na^+, K^+, Ca^{2+}, Mg^{2+}, Sr^{2+}) and anions (F^-, Cl^-, NO_3^-, Br^-, SO_4^{2-}) of the 0.5 ml time series and final test solutions of the out-diffusion experiments were analysed by IC using a Dionex ICS 1500 system or a Thermo Scientific Dionex Aquion and Integrion IC system. The relative analytical error of these analyses is ± 5 % based on multiple measurements of external check standard solutions (1σ). The final test solutions with a volume of app. 100 ml were analysed undiluted and in different dilutions (1:10 and, if necessary, 1:20). The time series samples were analysed timely after sampling. Due to the low volume, the samples could only be measured once in a 1:10 dilution. As such, the detection limit is different for each element in the two different solutions.

The alkalinity titration, pH-value and specific electrical conductivity measurements were performed using Metrohm titration systems and a WTW LF325 probe. TOC and TIC concentrations were analysed on the final solutions using a Shimadzu VCSH analyser with a relative analytical error of ± 5 % based on multiple measurements of external check standard solutions (1σ). Aluminium and lithium concentrations were analysed using a ContrAA800G graphite tube atomic absorption spectrometer (AAS) from ThermoFischer and silica concentrations were determined photometrically. Boron of out-diffusion test solutions was analysed at Analytik Institut Rietzler GmbH, Germany, using an ICP-MS system with a detection limit of 0.0001 mg/l and an analytical uncertainty of ±5 %.

The $^{37}Cl/^{35}Cl$ isotope ratio, expressed as $\delta^{37}Cl$ relative to SMOC, was measured by a GC-MS-IRMS system (Thermo Fischer Delta S), according to the method described in Ertl et al. (2024). Analytical errors were determined by the standard deviation of triplicate analyses of every sample. Strontium isotope signatures were analysed at Iso Analysis UG, Germany, by a Thermo Fischer MC-ICP-MS system with an analytical uncertainty of 0.0005.

Chloride and bromide concentrations of the experiment solution can be converted to porewater concentrations by applying mass balance calculations if equilibrium between test water and porewater is achieved. With knowledge of the mass of porewater in the rock sample, the chloride and bromide concentration of the porewater can be calculated according to:

$$C_{pw} = \frac{(m_{pw}+m_{TWi}-\sum^n m_s)\times C_{TW\infty}-(m_{TWi}\times C_{TWi})+\sum^n m_s\times C_s}{m_{pw}} \quad \text{eq. 4}$$

where C_{pw} = porewater concentration, m_{pw} = mass of porewater, m_{TWi} = initial mass of test water, C_{TWi} = initial Cl concentration of test water, m_s = mass of sub sample used for time series, and C_s = Cl concentration of sub sample used for time series.

The term $\sum m_s * C_s$ (equation 4) describes the amount of Cl removed from the initial experiment solution for Cl time-series samples. A correction for chloride and bromide in the initial experiment solution ($m_{TWi} * C_{TWi}$) is necessary if this solution is not entirely free of chloride and bromide.

The unit for the porewater concentration is given in mg/kg H_2O (and not mg/l) because it is derived on a mass basis rather than a volumetric basis. This is due to the fact that the density of the porewater is not known beforehand, because it depends on the in situ salinity of the water (which is unknown).

3.2.3 Isotope Diffusive Exchange Technique

The isotope diffusive exchange technique to determine the water isotope composition, $\delta^{18}O$ and $\delta^{2}H$, of the porewater and the mass of porewater was originally developed by Rogge (1997) and Rübel et al. (2002) for sedimentary rocks and later adapted for crystalline rocks by Waber and Smellie (2005, 2006) and Eichinger et al. (2006). In this method, initially saturated rock material is placed into two vapour-tight containers together with different test waters of known isotope composition. The porewater and test water are then allowed to isotopically equilibrate via the vapour phase without any direct contact between the core material and the test water. The porewater isotope composition and the water content of the rock sample can then be derived by isotope mass balance relationships. It has been shown that the uncertainty of the derived isotope composition largely depends on the ratio of porewater to test water used in the experiments (e.g., Rübel et al. 2002). For crystalline rocks, this ratio was optimised by using larger volumes of rock and smaller volumes of test water in the experiments (e.g., Waber and Smellie 2005, 2006; Eichinger et al. 2006).

For the present samples, 1.8 ml of test water were placed in a Petri dish in the centre of a glass vessel and surrounded by hand crushed core pieces 4-6 cm^3 in size and with a total mass of 316 to 504 g. After an equilibration time of 60 days, the two test waters were removed and analysed by Cavity Ring Down Spectroscopy using a Picarro L 2130-I Analyser. The results for the test waters are reported relative to the VSMOW (Vienna Standard Mean Ocean Water) standard with a precision of ± 0.15 ‰ for $\delta^{18}O$ and ± 1.5 ‰ for $\delta^{2}H$.

Test water and core material were weighed before and after the experiment to assess if test water was lost on the container walls and/or rock material due to evaporation and/or condensation. To minimise condensation, about 0.3 mol of NaCl were dissolved in the test water to lower its water vapour pressure. For every sample, two experiments were performed, one using test water with an isotope composition close to that expected in the porewater ("LAB-sample") and one using test water with an isotope composition far from that expected for the porewater ("ICE-sample").

The test water used for the LAB-sample was normal laboratory tap water ($\delta^{18}O$ = -10.30 to -10.16 ‰ V-SMOW; $\delta^{2}H$ = -73.0 to -72.8 ‰ V-SMOW), while that for the ICE-sample was water from an ice core drilled in the Antarctic ($\delta^{18}O$ = -31.74 to -31.59 ‰ V-SMOW; $\delta^{2}H$ = -247.3 to -246.8 ‰ V-SMOW). The equilibration time in the three reservoirs – rock porewater, test water, and the air inside the container as a diaphragm – depends on the volume of the container, the size of the rock pieces and the distance of the rock pieces to the test water (see Rogge 1997). Based on the estimations of the minimum time period required for complete isotopic equilibration (Eichinger et al. 2006) an experimental time of 60 days was chosen.

The isotope diffusive exchange technique can be used to determine porewater $\delta^{18}O$ and $\delta^{2}H$ values and the mass of the porewater present in the connected pore space of the rock sample. These parameters are calculated from the analytical results obtained for the two test water solutions, using mass balance relationships, according to

$$m_{pw} * c_{pw}\Big|_{t=0} + m_{tw} * c_{tw}\Big|_{t=0} = (m_{pw} + m_{tw}) * c_{tw}\Big|_{t=\infty} \qquad \text{eq. 5}$$

where *m* = mass, *c* = isotope ratios expressed in the δ notation, *pw* = porewater, *tw* = test water, *t = 0* represents the isotope concentrations at the beginning of the experiment, and *t* = ∞ represents the isotope concentrations at the end of the experiment.

The water content of the applied samples is calculated by transformation of equation 5 to

$$WC_{IsoEx} = \left[\frac{m_{TW(Std2)} \times m_{Rock(Std1)} \times (C_{TW^0(Std2)} - C_{TW\infty(Std2)}) + m_{TW(Std1)} \times m_{Rock(Std2)} \times (C_{TW\infty(Std1)} - C_{TW^0(Std1)})}{m_{Rock(Std1)} \times m_{Rock(Std2)} \times (C_{TW\infty(Std2)} - C_{TW\infty(Std1)})} \right] \times 100 \qquad \text{eq. 6}$$

where m_{Rock} = mass of rock, *Std 1* = test solution 1 and *Std 2* = test solution 2.

Equation 6 can be set up for oxygen and hydrogen isotope ratios of the test water, resulting in two independent values for the mass of porewater.

The $\delta^{18}O$- and $\delta^{2}H$- values of the porewater are calculated by transformation of equation 5 to

$$C_{PW} = \frac{C_{TW\infty(Std1)} \times m_{TW(Std2)} \times m_{Rock(Std1)} \times (C_{TW\infty(Std2)} - C_{TW^0(Std2)}) - C_{TW\infty(Std2)} \times m_{TW(Std1)} \times m_{Rock(Std2)} \times (C_{TW\infty(Std1)} - C_{TW^0(Std1)})}{m_{TW(Std2)} \times m_{Rock(Std1)} \times (C_{TW\infty(Std2)} - C_{TW^0(Std2)}) - m_{TW(Std1)} \times m_{Rock(Std2)} \times (C_{TW\infty(Std1)} - C_{TW^0(Std1)})} \qquad \text{eq. 7}$$

The errors of the calculated $\delta^{18}O$, $\delta^{2}H$ and the mass of porewater are computed for each sample using Gauss' law of error propagation (Appendix C).

3.3 Out-gassing Experiments to Extract Gases Dissolved in Porewater

3.3.1 Extraction and Quantification of Non-Inert gases (DG) Dissolved in Porewater

Gases in porewater were allowed to outgas into the void volume of the gas tight cylinder during sampling over a time period of 349 to 374 days at room temperature. Non-inert gases include oxygen, hydrogen, nitrogen and carbon dioxide as well as saturated and unsaturated hydrocarbons. These were analysed at Hydroisotop GmbH, Germany. The experimental set-up and the analytical gas programme performed on the core samples is given in Table 2-3 and Table 2-4.

Non-inert gases were analysed on one sample dedicated for noble gas analyses, after the analyses of noble gases was completed, because one cylinder dedicated for non-inert gas analyses was not tight and showed an almost atmospheric pressure.

3.3.1.1 Quantification of Extracted Non-Inert Gases

Prior to gas analysis, the cylinders were brought to a constant temperature of 22°C to guarantee controlled water vapour conditions. Afterward, the cylinder was plugged directly onto the gas chromatograph, the attached valve was opened, and the total gas pressure in the cylinder was measured by a connected pressure gauge (Druck Limited) with a determination range of 0.1 to 1100 mbar. The total pressures in the cylinders varied between 33 and 917 mbar. The gas composition was then analysed by a Shimadzu GC 17A gas chromatograph equipped with a GC-WLD detector for the detection of gaseous O_2, N_2, H_2 and CO_2, and a GC-FID detector for the detection

of saturated and unsaturated hydrocarbon gases. The gas chromatograph was calibrated with control standards before each group of measurements was conducted. The detection limits of these methods vary for the different gas species and are listed in Appendix B. The errors of the gas analyses are calculated by Gaussian error propagation and depend on the gas pressure and composition. The control of the quality of the total gas analyses is given by the sum of the gases, which should sum to ~100 %.

For the calculation of the exact volume of the liberated gas mixture and the individual gas species, the void volume in the gas cylinder had to be determined. This void volume corresponds to the sum of the cylinder volume and the copper tube volume minus the volume of the rock sample. All cylinders, including the valve, have a constant volume of 860 ml. The volume of the cores was determined by taking the weight of the individual cores and density determined on adjacent pieces.

Possible air-contamination due to leakage of the cylinder or valve during equilibration and/or during measurement was corrected based on the analysed O_2 concentrations in the extracted gas, based on the assumption that the in situ porewater is O_2-free. Where necessary, a correction was applied to the measured concentrations of N_2, CO_2 and CH_4 in the extracted gas. The concentrations of higher hydrocarbons in air are very low and even a large air contamination will not alter the measured concentrations. The gas composition of atmospheric air, as used for any required corrections, is shown in Appendix B.

The original volume of a gas in the cylinder is corrected for air contamination according to:

$$V_{X,Sample,corrected} = V_{X,Sample,measured} - \frac{C_{O_2,Sample,measured} * C_{X,air}}{C_{O_2,air}} \quad (8),$$

where V_X is the volume of a gas species X in vpm (volume per million = 10^{-5} Vol.%) and V_{O2} is the volume of oxygen in vpm.

The volumetric proportion of the single gas species of the total extracted gas volume is calculated according to:

$$V_X = \frac{V_{x,tot}}{V_{gas,tot}} \text{ with } V_{gas,tot} = P_{gas} * V_{Void} \quad (9),$$

where V_x is the volume of a certain gas species X in ml, $V_{x,tot}$ the concentration of the gas species X in ml/L of the total amount of gas, $V_{gas,tot}$ the total volume of the extracted gas in mL, P_{gas} the final gas pressure in the cylinder in mbar and V_{void} the void volume in the cylinder in ml.

The gas pressure measured in the cylinder after equilibration is a mixture of the gases liberated from the porewater and the water vapour pressure at a certain temperature, here 21°C. Therefore, the gas pressure measured in each cylinder after equilibration was corrected according to:

$$P_{WV} = 5.268721 + 0.663623 * T - 0.002364 * T^2 + 0.000716 * T^3 \quad (10)$$

where P_{WV} is the water vapour pressure at a temperature T in mbar (Lide, 1994).

All given gas concentrations are related to standard temperature and pressure conditions (STP = 0°C, 1.013 bar; referred to by 'N' in the units NmL/L for the reported gas concentrations) according to:

$$V_{gas,tot,STP} = \frac{V_{gas,corr} * 273K}{(273K + T_{anal.})} \quad (11)$$

Where $V_{gas,tot,STP}$ is the standardized total gas volume, $V_{gas,corr}$ is the measured and corrected (air contamination and water vapour) gas volume and $T_{anal.}$ Is the temperature during analyses (=21°C).

Finally, the gas contents of the single gas species dissolved in matrix porewater is calculated according to:

$$V_{X,PW} = \frac{V_X}{V_{PW}} * 1000 \quad (12)$$

where $V_{X,PW}$ is the gas content of a gas species X dissolved in porewater in ml_{gas}/kg_{PW}, V_X the volume of a certain gas species X in ml_{gas} and V_{PW} the volume of porewater in the used drillcore segment in kg_{H2O}.

The volume of porewater was determined gravimetrically by drying as described in Section 3.1.

3.3.1.2 Stable Isotope Analyses on Non-Inert Gases

Carbon stable isotope ratios ($\delta^{13}C$) of CH_4, higher hydrocarbons and CO_2, hydrogen stable isotope ratios ($\delta^{2}H$) of CH_4 and nitrogen stable isotope ratios ($\delta^{15}N$) of N_2 could be determined on four of the five DG samples and on all five NG samples.

For the gas isotope analyses, the gas cylinders with the remaining sample gas were filled with He as a carrier gas to a pressure of 1.5 to 2 bar. Before an aliquot of the gas was transferred to gas tight GC-IRMS glass vials, the gas mixture was allowed to equilibrate for about an hour at a temperature of about 60 °C. Afterwards, the carbon and hydrogen isotope ratios of hydrocarbons and CO_2 as well as nitrogen isotope signatures of N_2were determined by a Thermo V GC-IRMS, which is equipped with a purge and trap system and a direct dual inlet system. The results are reported relative to the V-PDB and V-SMOW standards. The analytical error of $\delta^{13}C$ in hydrocarbons and CO_2 is $\pm$ 2 ‰, that of $\delta^{2}H$ ± 10 ‰, and that of $\delta^{15}N$-N_2 $\pm$ 0.1 ‰

3.3.2 Determination of Noble Gases (NG) Dissolved in Porewater

The porewater noble gas method is based on the quantitative release of the noble gases from the rock sample by out-gassing from the porewater into the void volume of the stainless-steel container (Eichinger et al. 2011, 2013, 2018; Rufer et al., 2019; Osenbrück et al. 1998). This assumption is based on the chemical inertness and the low solubility of noble gases in water (Weiss 1971).

After sealing the sample in an evacuated steel container, the noble gases are quantitatively released from the porewater by molecular diffusion into the container void volume. The time required to reach equilibrium conditions depends on the transport properties of the rock material as well as the sample size and geometry. The equilibration time was estimated according to diffusive scoping calculations (cf. Section 9.0).

In order to allow equilibration with respect to all noble gases (cf. Section 9.0 and Eichinger et al. 2013), the noble gases dissolved in porewater of the IG_BH06 drill core samples were allowed to outgas into the void volume of the He-tight sample cylinders for 487 to 50 days at room temperature (approximately 20 °C).

All noble gas analyses were conducted at the Institute of Environmental Physics, University of Heidelberg, Germany according to the procedure described in detail in Friedrich (2007). The concentrations of the noble gas isotopes, ^{3}He, ^{4}He, ^{20}Ne, ^{22}Ne, ^{36}Ar and ^{40}Ar in the gas mixture were measured by a GV 5400He Noble Gas Mass Spectrometer. The analytical errors of the single noble gases were determined by multiple measurements of atmospheric air. The volume of an individual noble gas species in mL/L_{PW} was calculated according to Equations 9, 10 and 12, ensuring the correction for water vapour and the normalisation to standard temperature and pressure conditions (reported as NmL/L_{PW}).

The degree of air contamination of the extracted gas was monitored by the measured neon content (= $^{20}Ne+^{22}Ne$). As outlined in Section 9.2 there is negligible in situ production of ^{20}Ne and ^{22}Ne even over a geological time span of more than 1 Ga. Consequently, the Ne isotope concentrations in matrix porewater cannot exceed that of the air saturated water (i.e. the concentrations brought into the system by surface-derived water). The time of such infiltration is unknown and could have taken place under different climatic conditions. To account for the temperature dependent solubility of Ne, the Ne content in air saturated water was taken as a range ($[Ne]_{asw}$ = (1.9 ± 0.2)*10^{-7} cc STP Ne/g_{H2O}, Weiss 1971) corresponding to an infiltration temperature between 5 and 25 °C. An air contamination is present in the gas samples once the measured total Ne ($^{20}Ne+^{22}Ne$) content in the gas sample exceeds that range. The excess of the single noble gas species ($C(X)_{ex}$), introduced to the gas samples by air contamination is calculated using the measured Ne isotope contents, the Ne/C(X) ratio in air, and the range of Ne ($[Ne]_{asw}$) during infiltration according to:

$$C(X)_{ex} = \frac{(C_{Ne_{tot}} - 1.9*10^{-7})}{\frac{C_{Ne_{air}}}{C(X)_{air}}} \quad (13)$$

where $C(X)_{ex}$ is the excess of the single noble gas species, C_{Neair} the concentration of Ne in air in cc/cc_{air}, and $C(X)_{air}$ the concentration of the single noble gas species in air in cc/cc_{gas}.

4.0 RESULTS OF WATER CONTENT AND WATER-LOSS POROSITY INVESTIGATIONS

Water content, bulk density and water-loss porosity were determined on originally saturated segments of the core samples from IG_BH06. The water content was determined by two independent methods: gravimetrically by drying rock sections at 105 °C to stable weight conditions, and by using the isotope diffusive exchange technique (see Section 3). The gravimetric water content (WC_{grav}) was determined on different segments of the core samples used for the individual experiments. The initial saturated weight of all these samples was recorded directly after unpacking and preparation of the samples in the laboratory. This ensures that the calculation of the porewater mass is not affected by any possible changes induced during the experiments. Such possible changes were monitored by recording the sample weight right after termination of the experiment and before the drying process began. The water loss was calculated using the initial wet weight measured in the lab and the final weight after drying.

The exact determination of the in situ mass of porewater is of particular importance when using indirect extraction methods because porewater tracer concentrations are calculated by mass balance equations using the mass of porewater (Section 3). Knowledge of the water-loss porosity (calculated from the water content and density) is further required for the derivation of diffusion coefficients (Section 6.2).

4.1 Water Contents

Gravimetric water contents were determined on different segments used for individual experiments (see Section 3).

4.1.1 Gravimetric Water Contents Determined on Aqueous Extraction Core Samples

The gravimetric water contents were determined on different aliquots of the 19 aqueous extraction core samples (AQ) taken between 213 and 982 mbgs (downhole). These values were used for the estimation of porewater Cl- and Br-concentrations derived from the aqueous extraction experiments (cf. chapter 6.1).

The gravimetric water contents determined on individual aliquots of the AQ samples vary between 0.06 wt.% and 0.22 wt.%, with weighted values ranging between 0.08 ± 0.02 and 0.20 ± 0.02 wt.% (Table 4-1).

The water contents determined by taking the wet (WC_{wet}) and dry weight (WC_{dry}) are similar within the first two decimal places due to the low water masses in the investigated cores.

The water contents determined on the individual aliquots of the different AQ samples can vary significantly, which is interpreted to be due to mineralogical heterogeneities.

Table 4-1: Gravimetric water contents (WC) of aliquots of AQ core samples from IG_BH06 used for aqueous extraction experiments using wet (WC_{wet}) and dry masses (WC_{dry}) of the individual core pieces. The weighted values are calculated by using the individual masses; (G / T: granodiorite / tonalite, D: diabase)

Sample	Depth	Lithology	Aq.ex. subsample A			Aq.ex. subsample B			Aq.ex. subsample C			WC weighted		
	mbgs*		Mass	WC_{wet}	WC_{dry}	mass	WC_{wet}	WC_{dry}	mass	WC_{wet}	WC_{dry}	WC_{wet}	WC_{dry}	Stdev
			g	wt.%	wt.%	g	wt.%	wt.%	g	wt.%	wt.%	wt.%	wt.%	wt.%
IG_BH06_AQ001	212.9	G / T	382.906	0.19	0.19	189.248	0.21	0.21	140.611	0.21	0.21	**0.20**	**0.20**	**0.02**
IG_BH06_AQ002	221.1	G / T	548.698	0.20	0.20	189.597	0.18	0.18	217.817	0.19	0.19	**0.19**	**0.19**	**0.01**
IG_BH06_AQ003	370.3	G / T	468.663	0.17	0.17	305.547	0.18	0.18	250.922	0.19	0.19	**0.18**	**0.18**	**0.01**
IG_BH06_AQ004	453.5	G / T	430.873	0.14	0.14	258.145	0.16	0.16	213.685	0.16	0.16	**0.15**	**0.15**	**0.01**
IG_BH06_AQ005	504.4	G / T	436.519	0.16	0.16	209.231	0.19	0.20	227.437	0.19	0.19	**0.18**	**0.18**	**0.02**
IG_BH06_AQ006	562.7	G / T	467.748	0.17	0.17	248.065	0.22	0.19	237.024	0.21	0.21	**0.19**	**0.18**	**0.02**
IG_BH06_AQ007	574.4	G / T	363.942	0.15	0.15	253.582	0.19	0.21	183.527	0.19	0.19	**0.17**	**0.18**	**0.02**
IG_BH06_AQ008	612.5	G / T	428.712	0.15	0.15	240.901	0.18	0.18	191.262	0.20	0.20	**0.17**	**0.17**	**0.03**
IG_BH06_AQ009	648.2	G / T	406.212	0.13	0.13	223.275	0.14	0.14	245.082	0.14	0.14	**0.14**	**0.14**	**0.01**
IG_BH06_AQ010	666.2	G / T	364.965	0.14	0.14	235.961	0.15	0.15	180.562	0.14	0.14	**0.14**	**0.14**	**0.01**
IG_BH06_AQ011	694.0	G / T	369.857	0.12	0.12	199.990	0.13	0.13	200.987	0.16	0.16	**0.13**	**0.13**	**0.02**
IG_BH06_AQ012	720.8	G / T	399.975	0.15	0.15	211.840	0.16	0.16	179.699	0.15	0.15	**0.15**	**0.15**	**0.01**
IG_BH06_AQ013	747.8	G / T	330.828	0.11	0.11	144.421	0.13	0.13	182.180	0.12	0.12	**0.12**	**0.12**	**0.01**
IG_BH06_AQ014	771.2	G / T	376.261	0.08	0.08	220.136	0.09	0.10	251.894	0.09	0.09	**0.09**	**0.09**	**0.01**
IG_BH06_AQ015	804.9	G / T	439.133	0.10	0.10	235.377	0.09	0.09	243.307	0.06	0.06	**0.08**	**0.08**	**0.02**
IG_BH06_AQ016	841.2	G / T	304.983	0.14	0.14	222.457	0.15	0.15	278.934	0.15	0.15	**0.15**	**0.15**	**0.01**
IG_BH06_AQ017	853.3	G / T	422.460	0.11	0.11	470.544	0.11	0.11	206.448	0.15	0.15	**0.12**	**0.12**	**0.02**
IG_BH06_AQ018	885.6	G / T	469.096	0.14	0.14	181.852	0.14	0.14	240.019	0.14	0.14	**0.14**	**0.14**	**0.01**
IG_BH06_AQ019	928.0	G / T	281.611	0.12	0.12	248.772	0.13	0.13	333.295	0.12	0.12	**0.12**	**0.12**	**0.01**

* mbgs (downhole)

4.1.2 Gravimetric Water Contents Determined on Porewater Cores

Gravimetric water contents were determined on different aliquots of the 31 PW samples taken between 212 and 971 mbgs (downhole).

4.1.2.1 Gravimetric Water Contents Determined on End Pieces

During sample preparation, the head pieces with weights between 123 and 999 g were cut, weighed and dried at 105 °C to obtain a first estimate about the water contents of the investigated core samples.

The gravimetric water contents determined on the head pieces of the PW core samples vary between 0.05 wt.% and 0.24 wt.%, with weighted WC_{grav} values between 0.04 ± 0.02 wt.% and 0.22 ± 0.03 wt.% (Table 4-2).

The water contents determined by taking the wet (WC_{wet}) and dry weight (WC_{dry}) are similar within the first two decimal places due to the low water masses in the investigated cores. The water contents determined on the two head pieces of the different PW samples vary, which is attributed to mineralogical heterogeneities.

Table 4-2: Gravimetric water contents (WC) of aliquots of PW core samples from IG_BH06 used for out-diffusion experiments using wet (WC_{wet}) and dry masses (WC_{dry}) of the individual core pieces. The weighted values are calculated by using the individual masses. G / T = granodiorite / tonalite; A = amphibolite ; T = feldspar phyric tonalite.

Sample	Depth	Lithology	Subsample A			Subsample B			WC weighted		
			mass	WC_{wet}	WC_{dry}	mass	WC_{wet}	WC_{dry}	WC_{wet}	WC_{dry}	Stdev
	mbgs*		g	wt.%	wt.%	g	wt.%	wt.%	wt.%	wt.%	wt.%
IG_BH06_PW001	212.3	G / T	204.163	0.20	0.20	123.970	0.19	0.19	**0.20**	**0.20**	**0.01**
IG_BH06_PW002	291.5	G / T	402.012	0.18	0.18	132.467	0.16	0.16	**0.17**	**0.18**	**0.01**
IG_BH06_PW003	253.2	G / T	294.034	0.21	0.21	216.351	0.19	0.19	**0.20**	**0.20**	**0.01**
IG_BH06_AR010	398.7	T	222.230	0.07	0.07	240.404	0.06	0.06	**0.06**	**0.06**	**0.01**
IG_BH06_AR013	421.6	G / T	166.039	0.15	0.15	197.478	0.15	0.15	**0.15**	**0.15**	**0.01**
IG_BH06_PW004	453.2	G / T	265.522	0.17	0.17	171.877	0.17	0.17	**0.17**	**0.17**	**0.00**
IG_BH06_PW005	504.1	G / T	311.563	0.18	0.18	228.281	0.21	0.21	**0.19**	**0.19**	**0.02**
IG_BH06_AR019	534.0	G / T	151.167	0.15	0.15	122.555	0.15	0.15	**0.15**	**0.15**	**0.01**
IG_BH06_AR020	542.9	G / T	156.354	0.18	0.18	195.457	0.17	0.17	**0.17**	**0.17**	**0.01**
IG_BH06_PW006	562.4	G / T	229.293	0.21	0.21	221.933	0.20	0.20	**0.21**	**0.21**	**0.01**
IG_BH06_PW007	574.2	G / T	189.634	0.20	0.20	173.533	0.24	0.24	**0.22**	**0.22**	**0.03**
IG_BH06_AR027	595.0	G / T	177.513	0.16	0.16	135.901	0.18	0.18	**0.17**	**0.17**	**0.01**
IG_BH06_PW008	612.2	G / T	202.920	0.20	0.20	237.895	0.19	0.19	**0.20**	**0.20**	**0.01**
IG_BH06_PW009	647.9	G / T	257.477	0.14	0.14	214.687	0.14	0.14	**0.14**	**0.14**	**0.01**
IG_BH06_PW010	665.9	G / T	267.202	0.14	0.14	207.762	0.16	0.16	**0.15**	**0.15**	**0.01**
IG_BH06_PW011	691.0	G / T	334.129	0.11	0.11	998.637	0.15	0.15	**0.14**	**0.14**	**0.03**
IG_BH06_PW012	693.7	G / T	297.375	0.15	0.15	201.589	0.13	0.13	**0.14**	**0.14**	**0.01**
IG_BH06_PW013	720.5	G / T	200.758	0.12	0.12	336.481	0.13	0.13	**0.13**	**0.13**	**0.01**
IG_BH06_AR038	722.6	A	432.989	0.05	0.05	518.587	0.03	0.03	**0.04**	**0.04**	**0.02**
IG_BH06_AR039	728.8	T	225.143	0.07	0.07	266.965	0.07	0.07	**0.07**	**0.07**	**0.01**
IG_BH06_DG003	744.0	G / T	159.390	0.06	0.06	177.494	0.04	0.04	**0.05**	**0.05**	**0.01**
IG_BH06_PW014	747.5	G / T	154.315	0.10	0.10	246.196	0.11	0.11	**0.11**	**0.11**	**0.01**

Sample	Depth	Lithology	Subsample A			Subsample B			WC weighted		
			mass	WC_{wet}	WC_{dry}	mass	WC_{wet}	WC_{dry}	WC_{wet}	WC_{dry}	Stdev
	mbgs*		g	wt.%	wt.%	g	wt.%	wt.%	wt.%	wt.%	wt.%
IG_BH06_PW015	774.9	G / T	177.961	0.12	0.12	162.565	0.13	0.13	**0.12**	**0.12**	**0.01**
IG_BH06_AR045	796.7	G / T	240.111	0.08	0.08	160.960	0.08	0.08	**0.08**	**0.08**	**0.01**
IG_BH06_PW016	804.7	G / T	276.769	0.10	0.10	214.060	0.11	0.11	**0.11**	**0.11**	**0.00**
IG_BH06_AR049	820.2	G / T	178.466	0.11	0.11	198.742	0.12	0.12	**0.11**	**0.11**	**0.01**
IG_BH06_PW017	840.2	G / T	259.401	0.17	0.17	199.229	0.15	0.15	**0.16**	**0.16**	**0.01**
IG_BH06_PW018	853.0	G / T	134.135	0.14	0.14	185.486	0.11	0.11	**0.12**	**0.12**	**0.02**
IG_BH06_PW019	885.3	G / T	144.969	0.16	0.16	169.721	0.16	0.16	**0.16**	**0.16**	**0.01**
IG_BH06_PW020	927.6	G / T	430.933	0.14	0.14	243.933	0.13	0.13	**0.13**	**0.13**	**0.01**
IG_BH06_AR064	971.4	G / T	170.920	0.13	0.13	188.784	0.11	0.12	**0.12**	**0.12**	**0.01**

* mbgs (downhole)

4.1.3 Gravimetric Water Contents Determined on Out-Diffusion Cores

Gravimetric water contents determined on the large sized 1,217 – 1,628 g heavy core pieces were determined by the weights taken before and after their long-term immersion in deionised water during the out-diffusion experiments. For 24 samples, the weights of cores were higher, beyond the assumed error of 0.05 g (uncertainty in the determination of the weight with dry surface) after the experiment than before the experiment (Table 4-3, Figure 4-1). The weight gain and hence intake of water during the experiments, which is between 0.152 and 0.968 g can be caused by:

- The filling of pore space by drilling fluid created post drilling by stress release;
- The filling of pore space that was desaturated during the time period between core recovery (during drilling) and packaging; or
- Uncertainty of the determination of the initial wet weight during drying of the surface water.

Five samples showed lower (>0.05 g) weights after the experiments than before (0.012 – 0.101 g, negative Δ-values in Table 4-3). The differences are presumed to be due to the fact that determination of the initial weight is done after drying the surfaces of the cores.

The gravimetric water contents determined on the out-diffusion cores vary between 0.04 ± 0.02 wt.% and 0.25 ± 0.02 wt.%, as calculated using the wet weight (dry surface) of the core before the experiment (b.e.), and between 0.056± 0.02 wt.% and 0.22 ± 0.02 wt.%, as calculated using the wet weight (dry surface) of the core after the experiment (a.e.) (Table 4-3). The weight differences of the core samples determined before (b.e.) and after the experiments (a.e.) result in water content variations of 0.01-0.08 wt.% (Table 4-3, Figure 4-2). These differences are within the error ranges determined by Gaussian error propagation (Table 4-3, Figure 4-2). The weight differences before and after the experiments, and the corresponding differences in porewater masses expressed as water content, are considered for the calculation of the porewater Cl and Br concentrations.

The water contents determined by taking the wet (WC_{wet}) and dry weight (WC_{dry}) are similar within the first two decimal places due to the low water masses in the investigated cores (Table 4-3).

Table 4-3: Gravimetric water contents of out-diffusion core samples from IG_BH06 calculated by the mass of cores determined before (b.e.) and after (a.e.) experiments using wet (WC_{wet}) and dry masses (WC_{dry}) of the individual core pieces; the error of the water content is determined by Gaussian error propagation (Appendix C). G / T = granodiorite / tonalite; A = amphibolite; T = feldspar phyric tonalite.

Sample	Depth	Lithology	mass core			mass porewater		$WC_{grav,wet}$		$WC_{grav,dry}$		error WC_{grav}
			wet b.e.	wet a.e.	Δm_{core}	m_{core} b.e.	m_{core} a.e.	m_{core} b.e.	m_{core} a.e.	m_{core} b.e.	m_{core} a.e.	
	mbgs*		g	g	g	g	g	wt. %	wt. %	wt. %	wt. %	wt.%
IG_BH06_PW001	212.3	G / T	1428.860	1429.364	0.205	2.956	3.161	0.21	0.22	0.21	0.22	0.02
IG_BH06_PW002	291.5	G / T	1438.036	1438.861	0.585	2.543	3.128	0.18	0.22	0.18	0.22	0.04
IG_BH06_PW003	253.2	G / T	1453.468	1453.653	0.006	2.836	2.842	0.20	0.20	0.20	0.20	0.00
IG_BH06_AR010	398.7	T	1627.420	1627.98	0.475	1.183	1.658	0.07	0.10	0.07	0.10	0.03
IG_BH06_AR013	421.6	G / T	1477.362	1477.882	0.325	2.359	2.684	0.16	0.18	0.16	0.18	0.03
IG_BH06_PW004	453.2	G / T	1451.726	1452.180	0.253	2.456	2.709	0.17	0.19	0.17	0.19	0.02
IG_BH06_PW005	504.1	G / T	1463.569	1463.622	-0.075	2.834	2.759	0.19	0.19	0.19	0.19	0.01
IG_BH06_AR019	534.0	G / T	1451.617	1452.094	0.313	2.296	2.609	0.16	0.18	0.16	0.18	0.02
IG_BH06_AR020	542.9	G / T	1425.077	1425.146	-0.037	2.607	2.570	0.18	0.18	0.18	0.18	0.01
IG_BH06_PW006	562.4	G / T	1452.990	1453.103	-0.012	2.807	2.795	0.19	0.19	0.19	0.19	0.00
IG_BH06_PW007	574.2	G / T	1441.778	1441.857	-0.110	2.683	2.573	0.19	0.18	0.19	0.18	0.01
IG_BH06_AR027	595.0	G / T	1454.975	1455.430	0.211	2.667	2.878	0.18	0.20	0.18	0.20	0.02
IG_BH06_PW008	612.2	G / T	1452.143	1452.194	-0.101	2.519	2.418	0.17	0.17	0.17	0.17	0.01
IG_BH06_PW009	647.9	G / T	1464.375	1464.723	0.168	2.120	2.288	0.14	0.16	0.14	0.16	0.01
IG_BH06_PW010	665.9	G / T	1472.497	1472.868	0.187	2.109	2.296	0.14	0.16	0.14	0.16	0.02
IG_BH06_PW011	691.0	G / T	1406.002	1406.100	0.014	1.847	1.861	0.13	0.13	0.13	0.13	0.00
IG_BH06_PW012	693.7	G / T	1467.348	1468.106	0.587	2.105	2.692	0.14	0.18	0.14	0.18	0.04
IG_BH06_PW013	720.5	G / T	1440.077	1440.446	0.234	1.951	2.185	0.14	0.15	0.14	0.15	0.02
IG_BH06_AR038	722.6	A	1602.754	1603.089	0.219	0.721	0.940	0.04	0.06	0.05	0.06	0.02
IG_BH06_AR039	728.8	T	1431.104	1431.916	0.581	1.044	1.625	0.07	0.11	0.07	0.11	0.04
IG_BH06_DG003	744.0	G / T	1216.271	1217.415	0.968	0.690	1.658	0.06	0.14	0.06	0.14	0.08
IG_BH06_PW014	747.5	G / T	1407.998	1408.330	0.174	1.850	2.024	0.13	0.14	0.13	0.14	0.02
IG_BH06_PW015	774.9	G / T	1474.894	1475.494	0.422	1.877	2.299	0.13	0.16	0.13	0.16	0.03
IG_BH06_AR045	796.7	G / T	1417.982	1418.839	0.600	1.349	1.949	0.10	0.14	0.10	0.14	0.05
IG_BH06_PW016	804.7	G / T	1479.106	1480.152	0.881	1.898	2.779	0.13	0.19	0.13	0.19	0.06
IG_BH06_AR049	820.2	G / T	1368.428	1369.431	0.721	1.772	2.493	0.13	0.18	0.13	0.18	0.06
IG_BH06_PW017	840.2	G / T	1396.776	1397.086	0.152	2.308	2.460	0.17	0.18	0.17	0.18	0.01
IG_BH06_PW018	853.0	G / T	1451.021	1451.581	0.375	1.778	2.153	0.12	0.15	0.12	0.15	0.03
IG_BH06_PW019	885.3	G / T	1440.235	1441.001	0.615	2.257	2.872	0.16	0.20	0.16	0.20	0.05
IG_BH06_PW020	927.6	G / T	1465.050	1465.826	0.591	1.978	2.569	0.14	0.18	0.14	0.18	0.04
IG_BH06_AR064	971.4	G / T	1439.354	1440.154	0.607	1.964	2.571	0.14	0.18	0.14	0.18	0.05

* mbgs (downhole)

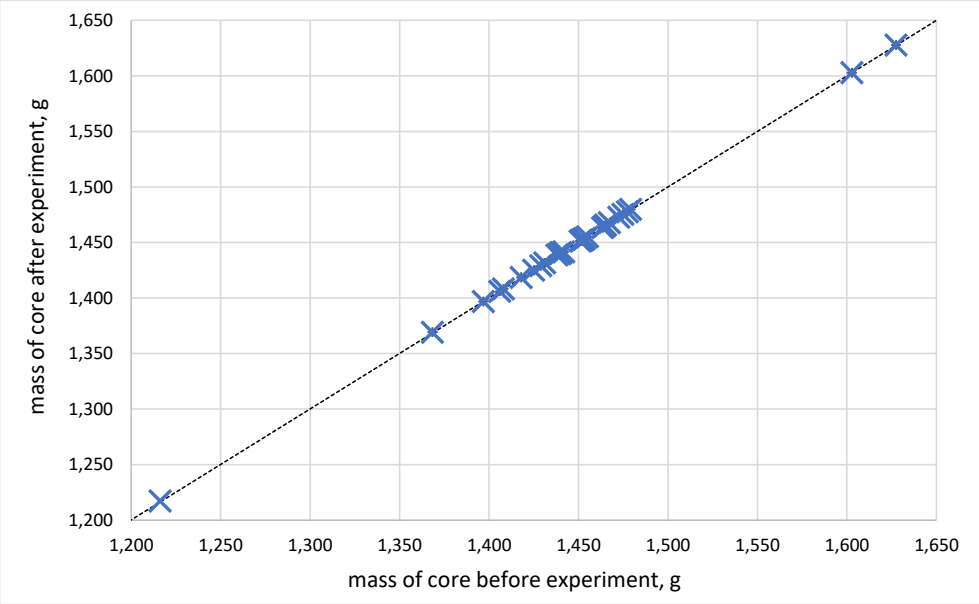


Figure 4-1: Mass of core samples from IG_BH06 before and after the out-diffusion experiments; the uncertainty of the core mass is ± 0.05 g

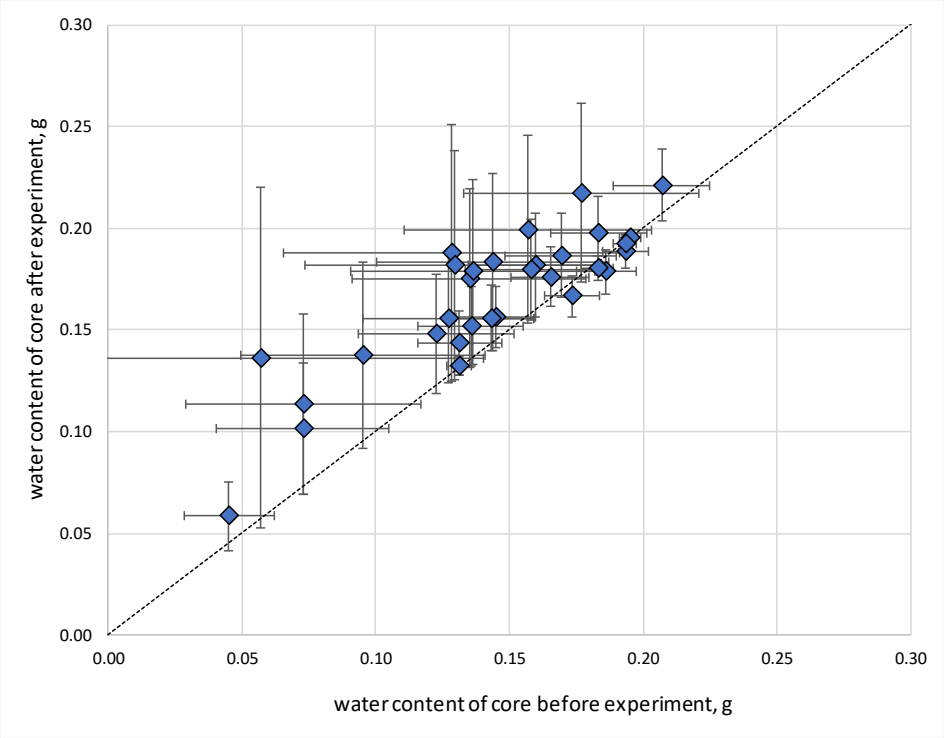


Figure 4-2: Water content calculated from the wet mass (dry surface) before and after the out-diffusion experiments of core sections from IG_BH06; the error of the water content is determined by Gaussian error propagation (Appendix C).

4.1.4 Gravimetric Water Contents Determined by Isotope Diffusive Exchange

Gravimetric water contents were determined on crushed core pieces used for the isotope diffusive exchange experiments. The masses of the used rock material were measured before and after the experiments. During the experiments the rocks remain saturated. A weight change of the rocks above the analytical uncertainty of ± 0.05 g at constant total weight was observed in almost all experiments (Table 4-4). Therefore, the water contents were corrected for the weight loss or gain.

The gravimetric water contents determined on rock pieces used for isotope diffusive exchange experiments ($WC_{IsoEx,grav,corr.}$) vary between 0.03 wt.% and 0.18 wt.% with weighted $WC_{IsoEx,grav}$ values ranging from 0.03 ± 0.01 wt.% to 0.18 ± 0.01 wt.% (Table 4-4). For the three diabase rock type samples (IG_BH06_AR010, IG_BH06_AR038 and IG_BH06_AR039) the gravimetric water contents were not corrected for potential uptake of water because water contents of these samples are very low and a correction leads to extremely low water content values (0.01 to 0.02 wt.%) or water content values below detection limit (< 0.01 wt.%) (Table 4-4).

The water contents determined by the isotope diffusive exchange technique ($WC_{IsoEx,average}$) for core samples from borehole IG_BH06 vary between 0.06 ± 0.01 wt.% and 0.16 ± 0.1 wt.% (Table 4-5).

During the isotope diffusive exchange experiment water uptake of 0.004 to 0.367 g was observed for almost all individual experiments. For six of the individual experiments the rock mass was 0.001 g to 0.053 g lower after the experiment.

Hence, the gravimetric water content of crushed rock samples used for isotope diffusive exchange experiments were corrected by calculating the mass difference ($\Delta m_{(rock,wet)} = m_{(rock,wet)}$ after experiment – $m_{(rock,wet)}$ before experiment) of the crushed rock sample in the container. The porewater mass was then corrected by this mass difference and the gravimetric water contents were calculated using the corrected porewater mass values.

For the most samples (n=20) the water contents determined by the isotope diffusive exchange technique agree well within 0.02 wt.% compared gravimetric values determined on the same core pieces (Table 4-4) and Table 4-5, Figure 4-3). For ten samples the water contents determined by isotope diffusive exchange are between 0.03 et.% and 0.06 wt% higher than those determined gravimetrically (Table 4-4). Based on the experimental quality check, it was decided to classify these values as reliable.

It is known from many sites, that generally the water contents determined by the isotope diffusive exchange (WC_{IsoEx}) technique are slightly higher than those determined gravimetrically ($WC_{IsoEx,\ grav}$) (e.g. Eichinger et al., 2010, 2018, Eichinger, 2021). This can be observed in argillaceous and crystalline rocks and is explained by the isotopic exchange of the test water with interlayer and bound water. This effect is generally more pronounced in argillaceous rocks and altered crystalline rocks (e.g. Pearson et al., 2003; Gimmi et al., 2022).

Table 4-4: Gravimetric water contents determined on core samples from IG_BH06 used for isotope diffusive exchange experiments ($WC_{IsoEx,\ grav}$); Water contents are corrected for weight changes during experiments (b.e. = before experiment, a.e. = after experiment); the gravimetric water contents determined on the rock pieces used in the experiments with LAB – and ICE water are weighted taking their weights into account; the error of the water content is determined by Gaussian error propagation (Appendix C)

Sample	LAB				ICE				
	mass	Δm (a.e.-b.e.)	$WC_{IsoEx,\ grav}$	$WC_{IsoEx,\ grav,corr.}$	mass	Δm (a.e.-b.e.)	$WC_{IsoEx,\ grav}$	$WC_{IsoEx,\ grav,corr.}$	$WC_{IsoEx,grav}$ weighted
	g	g	wt.%	wt.%	g	g	wt.%	wt.%	wt. %
IG_BH06_PW001	367.2	-0.053	0.17	0.18	370.8	-0.032	0.17	0.18	**0.18**
IG_BH06_PW002	468.8	-0.001	0.16	0.16	472.9	0.004	0.16	0.16	**0.16**
IG_BH06_PW003	451.3	0.049	0.17	0.16	445.9	0.051	0.16	0.15	**0.15**
IG_BH06_PW004	432.8	0.050	0.12	0.11	426.7	0.089	0.14	0.11	**0.11**
IG_BH06_PW005	378.9	-0.004	0.15	0.15	379.6	0.011	0.16	0.16	**0.16**
IG_BH06_PW006	408.6	0.017	0.17	0.16	406.1	0.042	0.17	0.16	**0.16**
IG_BH06_PW007	341.9	-0.002	0.15	0.15	343.0	0.083	0.15	0.13	**0.14**
IG_BH06_PW008	403.5	-0.027	0.14	0.14	402.3	0.108	0.14	0.11	**0.13**
IG_BH06_PW009	399.4	0.032	0.13	0.12	397.4	0.052	0.13	0.11	**0.12**
IG_BH06_PW010	399.1	0.044	0.13	0.11	396.7	0.056	0.13	0.11	**0.11**
IG_BH06_PW011	408.0	0.099	0.12	0.09	412.5	0.104	0.12	0.09	**0.09**
IG_BH06_PW012	408.6	0.061	0.13	0.12	407.0	0.085	0.14	0.12	**0.12**
IG_BH06_PW013	403.1	0.088	0.13	0.10	402.5	0.103	0.13	0.10	**0.10**
IG_BH06_PW014	381.9	0.196	0.12	0.07	402.0	0.156	0.13	0.09	**0.08**
IG_BH06_PW015	461.2	0.100	0.09	0.07	456.0	0.124	0.11	0.08	**0.08**
IG_BH06_PW016	374.7	0.183	0.11	0.07	375.8	0.184	0.11	0.07	**0.07**
IG_BH06_PW017	449.0	0.225	0.18	0.13	450.6	0.314	0.18	0.11	**0.12**
IG_BH06_PW018	390.2	0.283	0.15	0.08	393.9	0.254	0.14	0.08	**0.08**
IG_BH06_PW019	373.7	0.174	0.15	0.10	387.7	0.163	0.14	0.09	**0.10**
IG_BH06_PW020	323.5	0.296	0.17	0.08	316.2	0.252	0.16	0.08	**0.08**
IG_BH06_AR010	466.9	0.275	0.09	0.03	464.3	0.323	0.09	0.02	***0.09**
IG_BH06_AR013	501.2	0.079	0.14	0.13	502.4	0.095	0.14	0.12	**0.13**
IG_BH06_AR019	430.9	0.114	0.14	0.12	430.7	0.117	0.15	0.12	**0.12**
IG_BH06_AR020	497.7	0.128	0.16	0.13	498.8	0.152	0.16	0.13	**0.13**
IG_BH06_AR027	419.1	0.154	0.14	0.10	418.3	0.168	0.14	0.10	**0.10**
IG_BH06_AR038	503.3	0.337	0.08	0.01	503.5	0.335	0.07	0.01	***0.08**
IG_BH06_AR039	352.8	0.360	0.10	< 0.01	351.6	0.367	0.11	0.01	***0.11**
IG_BH06_AR045	383.3	0.314	0.12	0.04	382.9	0.367	0.13	0.03	**0.03**
IG_BH06_AR049	362.9	0.277	0.14	0.07	363.1	0.311	0.15	0.06	**0.07**
IG_BH06_AR064	373.5	0.304	0.15	0.07	372.7	0.346	0.15	0.06	**0.06**

* no correction for potential water uptake

Table 4-5: Water contents of core samples from IG_BH06 calculated by isotope diffusive exchange method (eq. 7); the error of the water content is determined by Gaussian error propagation (Appendix C)

Sample	WC_{IsoEx} ($\delta^{18}O$)	WC_{IsoEx} ($\delta^{2}H$)	WC_{IsoEx} average
	wt.%	wt.%	wt.%
IG_BH06_PW001	0.17±0.01	0.16±0.01	0.16±0.02
IG_BH06_PW002	0.15±0.01	0.14±0.01	0.14±0.01
IG_BH06_PW003	0.17±0.01	0.16±0.01	0.16±0.01
IG_BH06_PW004	0.13±0.02	0.12±0.02	0.13±0.02
IG_BH06_PW005	0.16±0.01	0.15±0.01	0.16±0.01
IG_BH06_PW006	0.16±0.01	0.14±0.01	0.15±0.01
IG_BH06_PW007	0.17±0.01	0.14±0.01	0.16±0.01
IG_BH06_PW008	0.16±0.01	0.13±0.01	0.14±0.01
IG_BH06_PW009	0.12±0.01	0.17±0.01	0.15±0.01
IG_BH06_PW010	0.13±0.01	0.11±0.01	0.12±0.01
IG_BH06_PW011	0.12±0.01	0.11±0.01	0.11±0.01
IG_BH06_PW012	0.14±0.01	0.13±0.01	0.13±0.01
IG_BH06_PW013	0.12±0.01	0.11±0.01	0.11±0.01
IG_BH06_PW014	0.08±0.01	0.08±0.01	0.08±0.01
IG_BH06_PW015	0.13±0.01	0.12±0.01	0.12±0.01
IG_BH06_PW016	0.12±0.01	0.11±0.01	0.12±0.01
IG_BH06_PW017	0.15±0.01	0.13±0.01	0.14±0.01
IG_BH06_PW018	0.11±0.01	0.10±0.01	0.10±0.01
IG_BH06_PW019	0.18±0.01	0.14±0.01	0.16±0.01
IG_BH06_PW020	0.13±0.01	0.11±0.01	0.12±0.01
IG_BH06_AR010	0.07±0.01	0.07±0.01	0.07±0.01
IG_BH06_AR013	0.12±0.01	0.12±0.01	0.12±0.01
IG_BH06_AR019	0.12±0.01	0.12±0.01	0.12±0.01
IG_BH06_AR020	0.16±0.01	0.15±0.01	0.16±0.01
IG_BH06_AR027	0.13±0.01	0.12±0.01	0.13±0.01
IG_BH06_AR038	0.07±0.01	0.06±0.01	0.06±0.01
IG_BH06_AR039	0.09±0.01	0.08±0.01	0.09±0.01
IG_BH06_AR045	0.08±0.01	0.07±0.01	0.08±0.01
IG_BH06_AR049	0.11±0.01	0.10±0.01	0.11±0.01
IG_BH06_AR064	0.11±0.01	0.10±0.01	0.11±0.01

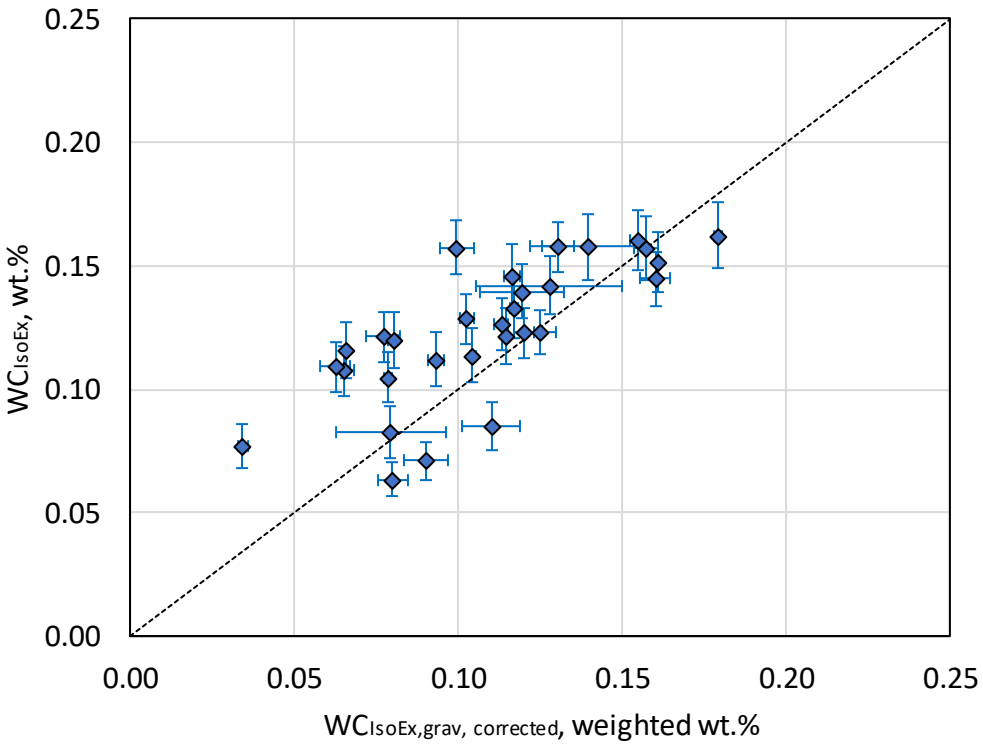


Figure 4-3: Comparison of water contents determined by isotope diffusive exchange (WC_{IsoEx}) and gravimetrically ($WC_{IsoEx,\ grav,\ corr.}$ by wet weight, corrected for weight change during experiments) on the same core pieces; the error of the water content is determined by Gaussian error propagation (Appendix C)

4.1.5 Gravimetric Water Contents Determined on Out-Gassing Cores

Gravimetric water contents were determined on the full-sized cores used for out-gassing experiments (NG and DF) with weights between 1,504 and 1,784 g by taking the weights determined after recovery on site. For all samples, except IG_BH06_DG001 and IG_BH06_NG005, the weights of cores were lower after the experiment than before the experiment (Table 4-6)

The weight loss during the experiments, which is between 0.29 and 0.96 g, is most likely caused by evacuating and flushing the cylinders with helium (DG samples) or nitrogen (NG samples) and by the outtake of various gas aliquots for the analyses.

The gravimetric water contents determined on the out-gassing cores vary between 0.13 ± 0.02 wt.% and 0.22 ± 0.03 wt.%, as calculated using the weight of the core before the experiment (b.e.) (Table 4-6).

Table 4-6: Gravimetric water contents of out-gassing core samples from IG_BH06 calculated by the mass of cores determined before experiments of the individual cores; the error of the water content is determined by Gaussian error propagation (Appendix C); G / T = granodiorite / tonalite.

Sample	Depth	Lithology	m_{core} b.e.	m_{core} a.e.	Δm_{core}	m_{PW} (m_{core} b.e.)	WC (m_{core} b.e.)	error WC_{grav}
	mbgs*		g	g	g	g	wt.%	wt.%
IG_BH06_DG001	510.2	G / T	1627.46	1627.544	-0.08	3.01	0.18	0.01
IG_BH06_DG002	620.9	G / T	1750.23	1749.563	0.67	3.62	0.21	0.03
IG_BH06_DG004	802.4	G / T	1519.57	1518.612	0.96	2.66	0.18	0.04
IG_BH06_DG005	842.7	G / T	1504.00	1503.458	0.54	3.39	0.23	0.03
IG_BH06_DG006	936.4	G / T	1576.83	1576.418	0.41	2.82	0.18	0.02
IG_BH06_NG001	512.5	G / T	1726.20	1725.423	0.76	3.76	0.22	0,03
IG_BH06_NG003	623.6	G / T	1601.71	1600.778	0.93	3.19	0.20	0,04
IG_BH06_NG005	735.6	G / T	1784.00	1784.635	-0.63	1.58	0.09	0,03
IG_BH06_NG007	846.9	G / T	1632.00	1631.297	0.70	3.32	0.20	0,03
IG_BH06_NG009	939.6	G / T	1629.26	1628.972	0.29	2.69	0.17	0,01

* mbgs (downhole)

4.1.6 Summary and Depth Profiles of Water Content Results

The gravimetric water contents determined on different portions of the core pieces for the AQ and the PW investigations are weighted using the masses of the individual rock pieces (Table 4-7). The weighted water contents represent the entire cores, with masses between 657 g and 1,099 g for AQ cores and between 1,554 g and 3,561 g for PW cores. As shown in the previous paragraphs, the water contents of the individual aliquots can vary significantly, which is inferred to be caused by mineralogical heterogeneities. This indicates that water content values cannot be extrapolated.

The weighted gravimetric water contents of the AQ- and PW-core samples taken between 212.3 and 971.4 mbgs (downhole) vary between 0.03±0.02 wt.% and 0.20 ±0.02 wt.% (Table 4-7, Figure 4-4).

The water contents of the individual sub-samples, and of the AQ and PW samples, which are generally collected close, or adjacent, to one another (e.g. AQ001 and PW001), can differ significantly. This is demonstrated by the large error bars associated with the weighted water content values (Table 4-7, Figure 4-4). A clear trend in the water content values with depth cannot be observed.

Table 4-7: Weighted gravimetric water contents of aqueous extraction and porewater core samples taken from borehole IG_BH06 and their corresponding total masses; the uncertainties of the water content values are the weighted standard deviations of the individual aliquots showing the density of water contents in one entire sample; G / T = granodiorite / tonalite; A = amphibolite; T = feldspar phyric tonalite.

Sample	Depth	Lithology	$m_{rock,tot}$	$WC_{grav,weighted}$	Bulk,wet density	$Vol._{core}$	$WC_{grav,\ weighted}$
	mbgs		g	wt. %	g/cm³	cm³	Vol.%
IG_BH06_AQ001	212.9	G / T	712.8	0.20±0.02	2.64	172.7	0.52±0.07
IG_BH06_AQ002	221.1	G / T	956.1	0.19±0.01	2.65	158.9	0.51±0.10
IG_BH06_AQ003	370.3	G / T	1025.1	0.18±0.01	2.65	149.9	0.47±0.11

Sample	Depth	Lithology	$m_{rock,tot}$	$WC_{grav,weighted}$	Bulk,wet density	$Vol._{core}$	$WC_{grav,\ weighted}$
	mbgs		g	wt. %	g/cm³	cm³	Vol.%
IG_BH06_AQ004	453.5	G / T	902.7	0.15±0.01	2.63	194.3	0.39±0.05
IG_BH06_AQ005	504.4	G / T	873.2	0.18±0.02	2.65	149.6	0.47±0.09
IG_BH06_AQ006	562.7	G / T	952.8	0.19±0.02	2.64	141.2	0.50±0.12
IG_BH06_AQ007	574.4	G / T	801.1	0.17±0.02	2.63	117.9	0.46±0.13
IG_BH06_AQ008	612.5	G / T	860.9	0.17±0.03	2.66	172.1	0.44±0.07
IG_BH06_AQ009	648.2	G / T	874.6	0.14±0.01	2.68	154.6	0.37±0.07
IG_BH06_AQ010	666.2	G / T	781.5	0.14±0.01	2.66	121.3	0.37±0.10
IG_BH06_AQ011	694.0	G / T	770.8	0.13±0.02	2.68	128.1	0.36±0.09
IG_BH06_AQ012	720.8	G / T	791.5	0.15±0.01	2.67	140.6	0.40±0.08
IG_BH06_AQ013	747.8	G / T	657.4	0.12±0.01	2.67	105.1	0.32±0.10
IG_BH06_AQ014	771.2	G / T	848.3	0.09±0.01	2.66	120.8	0.24±0.08
IG_BH06_AQ015	804.9	G / T	917.8	0.08±0.02	2.67	145.0	0.22±0.06
IG_BH06_AQ016	841.2	G / T	806.4	0.15±0.01	2.65	152.0	0.39±0.07
IG_BH06_AQ017	853.3	G / T	1099.5	0.12±0.02	2.65	238.4	0.31±0.04
IG_BH06_AQ018	885.6	G / T	891.0	0.14±0.01	2.57	109.1	0.36±0.14
IG_BH06_AQ019	928.0	G / T	863.7	0.12±0.01	2.68	177.4	0.33±0.05
IG_BH06_PW001	212.3	G / T	2495.3	0.20±0.01	2.66	536.6	0.55±0.05
IG_BH06_PW002	291.5	G / T	2914.8	0.17±0.01	2.66	541.8	0.47±0.12
IG_BH06_PW003	253.2	G / T	2861.0	0.18±0.02	2.67	545.0	0.52±0.02
IG_BH06_PW004	453.2	G / T	2748.9	0.15±0.03	2.67	543.2	0.45±0.06
IG_BH06_PW005	504.1	G / T	2761.8	0.18±0.02	2.68	546.2	0.52±0.03
IG_BH06_PW006	562.4	G / T	2718.8	0.19±0.02	2.68	542.7	0.52±0.02
IG_BH06_PW007	574.2	G / T	2489.8	0.18±0.04	2.70	534.5	0.50±0.04
IG_BH06_PW008	612.2	G / T	2698.7	0.16±0.03	2.68	541.8	0.46±0.03
IG_BH06_PW009	647.9	G / T	2733.5	0.14±0.02	2.69	544.1	0.39±0.04
IG_BH06_PW010	665.9	G / T	2743.4	0.14±0.02	2.69	548.2	0.38±0.05
IG_BH06_PW011	691.0	G / T	3559.3	0.13±0.03	2.73	515.9	0.36±0.02
IG_BH06_PW012	693.7	G / T	2782.5	0.14±0.01	2.68	546.8	0.39±0.12
IG_BH06_PW013	720.5	G / T	2783.1	0.12±0.02	2.69	536.2	0.36±0.05
IG_BH06_PW014	747.5	G / T	2592.6	0.11±0.03	2.68	525.8	0.35±0.04
IG_BH06_PW015	774.9	G / T	2733.0	0.11±0.03	2.70	545.8	0.34±0.09
IG_BH06_PW016	804.7	G / T	2721.3	0.11±0.03	2.70	547.9	0.35±0.17
IG_BH06_PW017	840.2	G / T	2755.2	0.15±0.03	2.66	524.6	0.44±0.04
IG_BH06_PW018	853.0	G / T	2555.1	0.11±0.03	2.66	544.7	0.33±0.08
IG_BH06_PW019	885.3	G / T	2516.9	0.14±0.03	2.65	543.9	0.42±0.12
IG_BH06_PW020	927.6	G / T	2780.2	0.12±0.03	2.69	545.3	0.36±0.12
IG_BH06_AR010	398.7	T	3021.7	0.08±0.01	2.70	603.4	0.21±0.08
IG_BH06_AR013	421.6	G / T	2844.9	0.15±0.02	2.66	554.7	0.43±0.07
IG_BH06_AR019	534.0	G / T	2587.3	0.14±0.02	2.66	545.3	0.42±0.07
IG_BH06_AR020	542.9	G / T	2773.3	0.16±0.03	2.67	533.1	0.49±0.03

Sample	Depth	Lithology	$m_{rock,tot}$	$WC_{grav,weighted}$	Bulk,wet density	Vol.core	$WC_{grav,\ weighted}$
	mbgs		g	wt. %	g/cm³	cm³	Vol.%
IG_BH06_AR027	595.0	G / T	2606.0	0.16±0.04	2.67	545.6	0.49±0.05
IG_BH06_AR038	722.6	A	3561.3	0.05±0.02	3.00	533.6	0.16±0.05
IG_BH06_AR039	728.8	T	2628.2	0.08±0.02	2.69	532.2	0.22±0.08
IG_BH06_AR045	796.7	G / T	2585.8	0.07±0.03	2.70	525.2	0.26±0.12
IG_BH06_AR049	820.2	G / T	2472.4	0.11±0.03	2.62	522.2	0.34±0.15
IG_BH06_AR064	971.4	G / T	2545.8	0.11±0.04	2.68	536.9	0.37±0.12
IG_BH06_DG003	744.03	G / T	1554.1	0.06±0.01	2.69	453.4	0.15±0.22

* mbgs (downhole)

4.2 Bulk Dry/Wet Density and Water-Loss Porosity

The bulk dry and wet density is calculated according to equation 1 (Section 3.2) using the dry and wet mass of the full diameter cylindrical cores and the volume of the core samples determined by measuring the height and core diameter by a Vernier Calliper. Bulk wet densities were determined for the cores used for out-diffusion and aqueous extraction experiments before crushing, and bulk dry density was determined only for out-diffusion cores.

Bulk dry and wet density values of the core samples from borehole IG_BH06 are similar, differing by a maximum of 0.01 g/cm³, due to the low water content of the samples, and vary between 2.62 and 3.00 g/cm³ (Table 4-8).

The water-loss (connected) porosity was calculated according to equation 2 (Section 3.2) using the water content calculated by the dry and wet weight and the bulk dry/wet density of the samples. Water-loss porosities are calculated for core sections used for the out-diffusion and aqueous extraction experiments, for which the water content and the bulk dry/wet density were determined. Water-loss porosities calculated using the wet mass and density differ by a maximum of 0.01 Vol.% from those determined by the dry mass and density (Table 4-8).

Water-loss porosity values of core samples taken between 212 and 971 mbgs (downhole) from borehole IG_BH06 vary between 0.14 ± 0.05 Vol.% and 0.55 ± 0.05 Vol.% (Table 4-8, Figure 4-4). Trends in the porosity values for the samples follow the same trends as described by the water contents (Figure 4-4).

Table 4-8: Bulk wet and dry density and water-loss (=WL-) porosity determined by water contents calculated for dry ($\Phi_{WL,dry}$) and wet ($\Phi_{WL,wet}$) core samples from borehole IG_BH06; the errors are calculated by Gaussian error propagation (Appendix C); (G / T: granodiorite / tonalite, D: diabase)

Sample	Depth	Lithology	bulk, wet density	bulk, dry density	water-loss porosity $\Phi_{WL,wet}$	water-loss porosity $\Phi_{WL,dry}$
	mbgs*		g/ccm	g/ccm	Vol.%	Vol.%
IG_BH06_AQ001	212.9	G / T	2.64		0.52±0.07	
IG_BH06_AQ002	221.1	G / T	2.65		0.51±0.10	
IG_BH06_AQ003	370.3	G / T	2.65		0.47±0.11	
IG_BH06_AQ004	453.5	G / T	2.63		0.39±0.05	
IG_BH06_AQ005	504.4	G / T	2.65		0.47±0.09	
IG_BH06_AQ006	562.7	G / T	2.64		0.50±0.12	
IG_BH06_AQ007	574.4	G / T	2.63		0.46±0.13	
IG_BH06_AQ008	612.5	G / T	2.66		0.44±0.07	
IG_BH06_AQ009	648.2	G / T	2.68		0.37±0.07	
IG_BH06_AQ010	666.2	G / T	2.66		0.37±0.10	

Sample	Depth mbgs*	Lithology	bulk, wet density g/ccm	bulk, dry density g/ccm	water-loss porosity $\Phi_{WL,wet}$ Vol.%	water-loss porosity $\Phi_{WL,dry}$ Vol.%
IG_BH06_AQ011	694.0	G / T	2.68		0.36±0.09	
IG_BH06_AQ012	720.8	G / T	2.67		0.40±0.08	
IG_BH06_AQ013	747.8	G / T	2.67		0.32±0.10	
IG_BH06_AQ014	771.2	G / T	2.66		0.24±0.08	
IG_BH06_AQ015	804.9	G / T	2.67		0.22±0.06	
IG_BH06_AQ016	841.2	G / T	2.65		0.39±0.07	
IG_BH06_AQ017	853.3	G / T	2.65		0.31±0.04	
IG_BH06_AQ018	885.6	G / T	2.57		0.36±0.14	
IG_BH06_AQ019	928.0	G / T	2.68		0.33±0.05	
IG_BH06_PW001	212.3	G / T	2.66	2.66	0.55±0.05	0.55±0.05
IG_BH06_PW002	291.5	G / T	2.66	2.66	0.47±0.12	0.47±0.12
IG_BH06_PW003	253.2	G / T	2.67	2.67	0.52±0.02	0.52±0.02
IG_BH06_PW004	453.2	G / T	2.67	2.67	0.45±0.06	0.45±0.06
IG_BH06_PW005	504.1	G / T	2.68	2.68	0.52±0.03	0.52±0.03
IG_BH06_PW006	562.4	G / T	2.68	2.68	0.52±0.02	0.52±0.02
IG_BH06_PW007	574.2	G / T	2.70	2.70	0.50±0.04	0.50±0.04
IG_BH06_PW008	612.2	G / T	2.68	2.68	0.46±0.03	0.47±0.03
IG_BH06_PW009	647.9	G / T	2.69	2.69	0.39±0.04	0.39±0.04
IG_BH06_PW010	665.9	G / T	2.69	2.69	0.38±0.05	0.39±0.05
IG_BH06_PW011	691.0	G / T	2.73	2.73	0.36±0.02	0.36±0.02
IG_BH06_PW012	693.7	G / T	2.68	2.68	0.39±0.12	0.39±0.12
IG_BH06_PW013	720.5	G / T	2.69	2.69	0.36±0.05	0.36±0.05
IG_BH06_PW014	747.5	G / T	2.68	2.68	0.35±0.04	0.35±0.04
IG_BH06_PW015	774.9	G / T	2.70	2.70	0.34±0.09	0.34±0.09
IG_BH06_PW016	804.7	G / T	2.70	2.70	0.35±0.17	0.35±0.17
IG_BH06_PW017	840.2	G / T	2.66	2.66	0.44±0.04	0.44±0.04
IG_BH06_PW018	853.0	G / T	2.66	2.66	0.33±0.08	0.33±0.08
IG_BH06_PW019	885.3	G / T	2.65	2.65	0.42±0.12	0.42±0.12
IG_BH06_PW020	927.6	G / T	2.69	2.69	0.36±0.12	0.36±0.12
IG_BH06_AR010	398.7	T	2.70	2.70	0.21±0.08	0.21±0.08
IG_BH06_AR013	421.6	G / T	2.66	2.66	0.43±0.07	0.43±0.07
IG_BH06_AR019	534.0	G / T	2.66	2.66	0.42±0.07	0.42±0.07
IG_BH06_AR020	542.9	G / T	2.67	2.67	0.49±0.03	0.49±0.03
IG_BH06_AR027	595.0	G / T	2.67	2.67	0.49±0.05	0.49±0.05
IG_BH06_AR038	722.6	A	3.00	3.00	0.16±0.05	0.16±0.05
IG_BH06_AR039	728.8	T	2.69	2.69	0.22±0.08	0.22±0.08
IG_BH06_AR045	796.7	G / T	2.70	2.70	0.26±0.12	0.26±0.12
IG_BH06_AR049	820.2	G / T	2.62	2.62	0.34±0.15	0.34±0.15
IG_BH06_AR064	971.4	G / T	2.68	2.68	0.37±0.12	0.37±0.12
IG_BH06_DG003	744.0	G / T	2.69	2.68	0.15±0.22	0.15±0.22

* mbgs (downhole)

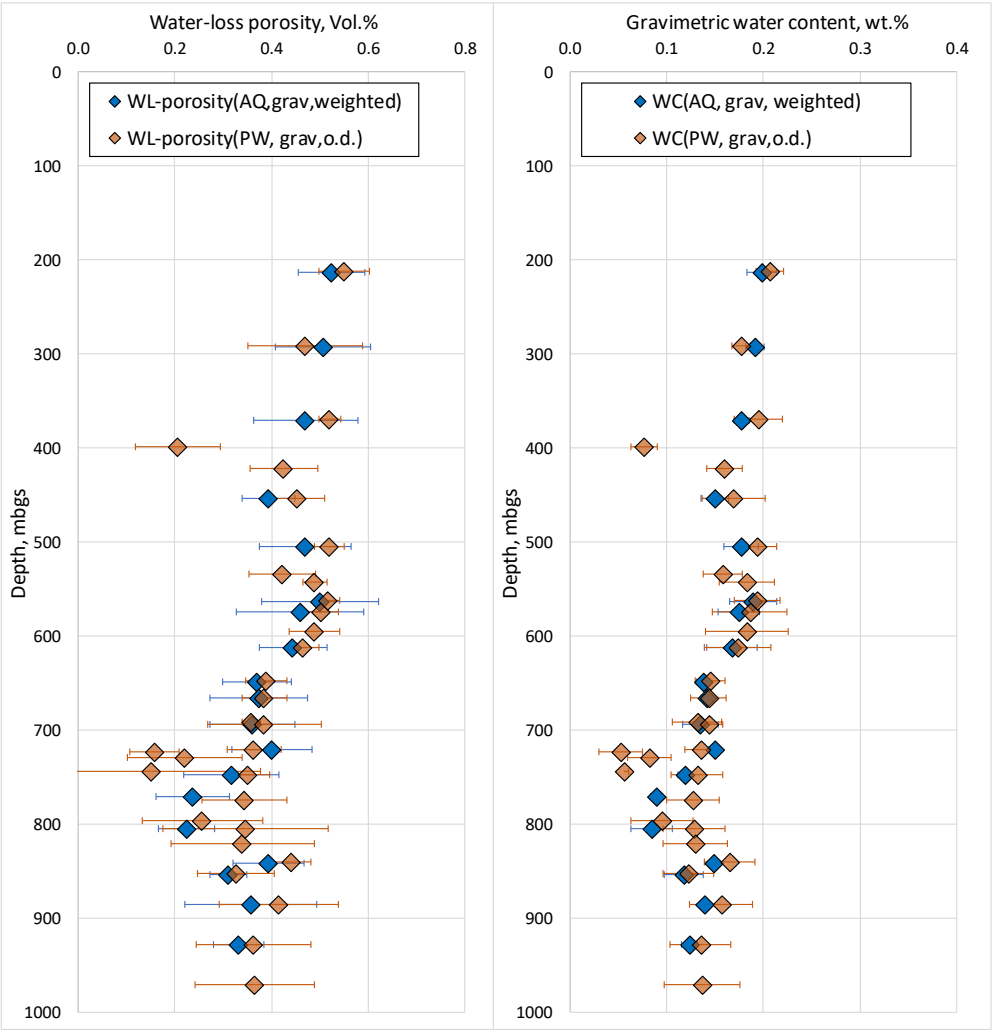


Figure 4-4: Water content and water-loss porosity of core samples from IG_BH06.

5.0 RESULTS OF CHEMICAL COMPOSITION OF EXPERIMENT SOLUTIONS OF AQUEOUS EXTRACTION AND OUT-DIFFUSION EXPERIMENTS

Out-diffusion and aqueous extraction experiments were performed on 31 PW and 19 AQ core samples taken from borehole IG_BH06, respectively. In both experiments the investigated rock samples were immersed in test water. The concentrations of dissolved constituents in the test solutions originate from:

a) porewater, which exchanges and mixes with test water;

b) water-rock interactions, releasing reactive elements in the test water; and

c) fluid inclusions (only aqueous extractions), which are liberated during crushing of the rocks.

5.1 Chemical Composition of Aqueous Extraction Solutions

The purpose of aqueous extraction experiments is to obtain an initial estimate of the porewater salinity, which is necessary for the adjustment of the ion concentration in the test waters for the indirect porewater extraction methods.

Crushing and grinding of the rock material additionally liberates fluid trapped in mineral fluid inclusions. During leaching, all salts will become dissolved in addition to the limited dissolution of the original mineral assemblage. The mineralization of a leach solution is therefore the sum of: (i) the constituents originally dissolved in the porewater, (ii) the constituents present in fluid inclusions, and (iii) water-rock interactions during the leaching process. Aqueous leach solutions represent a complex composition in rocks with abundant fluid inclusions and/or rapidly reacting mineral phases.

The aqueous extraction solutions produced by the immersion of crushed cores from IG_BH06 in deionized water (procedure cf. Section 3.2.1) have pH values between 9.3 and 9.8, and a mineralization between 94 and 179 mg/L (specific electrical conductivity = 127 – 304 µS/cm, Table 5-1). The dissolved constituents consist predominately of Na^+, K^+, Ca^{2+}, HCO_3^-, Cl^-, SO_4^{2-} and Si in different concentrations and proportions (Table 5-1, Figure 5-1). Minor concentrations of Mg^{2+}, F^- and Br^- could be detected. Concentrations of Sr were below detection limit or very low (0.02 to 0.14 mg/L (Table 5-1). Silicon and aluminium could be detected in concentrations between 4.00 and 12.2 mg/L (Si) and between 0.252 and 14.5 mg/L (Al).

The estimated porewater Cl-concentrations of core samples from IG_BH06, extracted by aqueous extraction experiments using the weighted water contents of the AQ samples (cf. Table 4-7), vary between 3,534 mg/kg_{PW} and 25,777 mg/kg_{PW} (Table 7-2).

Table 5-1: Analytical results of the aqueous extraction solutions of crushed core samples from borehole IG_BH06; Test solution types are classified after Jäckli (1970)

Sample		IG_BH06_AQ001	IG_BH06_AQ002	IG_BH06_AQ003	IG_BH06_AQ004	IG_BH06_AQ005	IG_BH06_AQ006	IG_BH06_AQ007	IG_BH06_AQ008	IG_BH06_AQ009	IG_BH06_AQ010
Interval	m BHL	212.9	221.1	370.3	453.5	504.4	562.7	574.4	612.5	648.2	666.2
Hydroisotop No.		374064	374065	374066	374067	374109	374110	374111	374513	374514	374515
MASTER VARIABLES											
pH (lab)	-log(H+)	9.6	9.6	9.5	9.4	9.5	9.5	9.4	9.6	9.6	9.6
Electr. Conductivity	µS/cm	254	127	176	208	176	200	225	160	152	170
Sample Temperature	°C	22.8	22.4	22.6	22.8	22.1	22.2	22.1	23.2	23.3	23.2
Alkalinity (pH 4,3) Lab.	mmol/l	1.45	0.81	0.86	0.91	0.75	0.9	1.0	0.7	0.73	0.67
Alkalinity (pH 8,2) Lab.	mmol/l	0.35	0.21	0.19	0.19	0.18	0.18	0.21	0.18	0.19	0.19
DISSOLVED CONSTITUENTS											
CATIONS	mg/l										
Sodium (Na^+)	mg/l	43.3	18.5	25.3	30.3	26.4	30.1	37.5	19.6	20.9	21.2
Potassium (K^+)	mg/l	10.9	7.1	10.1	12	8.6	9.9	8.8	10.3	9.7	10.9
Magnesium (Mg^{2+})	mg/l	0.36	0.23	0.26	0.3	0.24	0.37	0.37	0.32	0.28	0.26
Calcium (Ca^{2+})	mg/l	3.3	4.1	4.6	4.4	4	4.5	3.1	5.6	4.1	5.4
Strontium (Sr^{2+})	mg/l	0.02	< 0,02	< 0,02	< 0,02	< 0,02	< 0,02	< 0,02	0.03	< 0,02	< 0,02
Silicon (Si^{4+})	mg/l	7.63	8.38	9.17	10.71	9.77	10.11	12.17	7.4	8.5	9
Aluminium (Al^{3+})	mg/l	7.18	4.35	3.61	5.67	1.20	8.26	12.0	2.19	2.57	-
ANIONS											
Fluoride (F^-)	mg/l	0.79	0.28	0.29	0.37	0.22	0.23	0.27	0.12	0.13	0.17
Chloride (Cl^-)	mg/l	22	11.6	22.7	31.5	24.4	30.1	32	24.9	20	26.2
Bromide (Br^-)	mg/l	0.35	0.26	1.9	1.1	3.3	0.78	0.89	0.55	0.47	0.75
Sulfate (SO_4^{2-})	mg/l	9	2.1	2.7	2.9	2.9	3	4.3	1.9	2.5	1.9
Nitrate (NO_3^-)	mg/l	< 0,2	< 0,2	0.23	< 0,2	0.43	< 0,2	< 0,2	< 0,2	< 0,2	< 0,2
Total Alkalinity as HCO_3^-	mg/l	88.7	49.5	52.4	55.4	45.6	52.2	59.3	39.7	44.5	40.6
PARAMETERS CALCULATED FROM ANALYTICAL DATA											
Sum of analysed constituents	mg/l	179	94	120	138	116	131	146	103	103	107
Charge balance	%	1.14%	0.45%	0.33%	-0.61%	0.93%	0.67%	1.34%	0.61%	0.94%	0.84%
Water type		Na-(K)-HCO3-Cl	Na-(Ca)-(K)-HCO3-Cl	Na-(K)-(Ca)-HCO3-Cl	Na-(K)-(Ca)-HCO3-Cl	Na-(K)-(Ca)-HCO3-Cl	Na-(K)-(Ca)-HCO3-Cl	Na-(K)-HCO3-Cl	Na-(K)-(Ca)-Cl-HCO3	Na-(K)-(Ca)-HCO3-Cl	Na-(K)-(Ca)-Cl-HCO3

Note: m BHL is equivalent to mbgs (downhole).

Table 5-1: Continued

Sample		IG_BH06_AQ_011	IG_BH06_AQ_012	IG_BH06_AQ_013	IG_BH06_AQ_014	IG_BH06_AQ_015	IG_BH06_AQ_016	IG_BH06_AQ_017	IG_BH06_AQ_018	IG_BH06_AQ_019
Interval	m BHL	694.0	720.8	747.8	771.2	804.9	841.2	853.3	885.6	928.0
Hydroisotop No.		374754	374755	374756	376067	376068	376069	376070	376071	376072
MASTER VARIABLES										
pH (lab)	-log(H+)	9.7	9.7	9.4	9.6	9.8	9.5	9.3	9.4	9.7
Electr. Conductivity	µS/cm	167	168	189	237	139	223	304	193	156
Sample Temperature	°C	23.2	23.6	23.4	22.6	22.9	22.3	22.1	23.2	23.5
Alkalinity (pH 4,3) Lab.	mmol/l	0.87	0.8	0.58	0.57	0.83	0.5	0.4	0.4	0.75
Alkalinity (pH 8,2) Lab.	mmol/l	0.33	0.22	0.22	0.22	0.43	0.22	0.15	0.22	0.35
DISSOLVED CONSTITUENTS										
CATIONS	mg/l									
Sodium (Na^+)	mg/l	24.6	23	19.8	18.5	18.2	17.5	22.6	15.6	16.7
Potassium (K^+)	mg/l	9.7	8.7	12.1	32.4	12.8	15.4	20.5	12.9	15
Magnesium (Mg^{2+})	mg/l	0.27	0.24	0.34	0.57	0.49	0.61	0.68	0.56	0.48
Calcium (Ca^{2+})	mg/l	3.7	5.2	8.2	6.26	3.6	13.4	19.0	11.2	6.03
Strontium (Sr^{2+})	mg/l	< 0,02	< 0,02	< 0,02	0.08	0.02	0.11	0.14	0.07	0.03
Silicon (Si^{4+})	mg/l	7.1	6.9	6.4	4.48	5.9	4.33	3.99	4.55	5.9
Aluminium (Al^{3+})	mg/l	4.18	7.06	2.41	8.22	9.85	0.9	0.3	1.8	14.5
ANIONS										
Fluoride (F^-)	mg/l	0.18	0.16	0.12	0.24	0.13	0.18	0.22	0.12	0.12
Chloride (Cl^-)	mg/l	21.7	23.3	33.1	44.4	13.9	28.1	35.4	28.4	23.4
Bromide (Br^-)	mg/l	1.4	0.56	1.1	1.17	0.52	2.08	0.87	0.58	0.49
Sulfate (SO_4^{2-})	mg/l	2.1	2.4	5.4	8.62	3.78	28.4	55	20.5	2.36
Nitrate (NO_3^-)	mg/l	< 0,2	0.24	< 0,2	< 0,2	< 0,2	< 0,2	< 0,2	< 0,2	< 0,2
Total Alkalinity as HCO_3^-	mg/l	52.8	49.0	35.6	34.9	50.8	29.3	23.5	24.7	45.9
PARAMETERS CALCULATED FROM										
Sum of analysed constituents	mg/l	116	113	116	147	104	135	178	115	110
Charge balance	%	-0.90%	-0.80%	-1.18%	-0.86%	0.95%	-0.61%	-0.82%	-0.81%	-0.70%
Water type		Na-(K)-(Ca)-HCO3-Cl	Na-(Ca)-(K)-HCO3-Cl	Na-Ca-(K)-Cl-HCO3	K-Na-(Ca)-Cl-HCO3	Na-K-(Ca)-HCO3-Cl	Na-Ca-K-Cl-SO4-HCO3	Na-Ca-K-SO4-Cl-(HCO3)	Na-Ca-K-Cl-SO4-HCO3	Na-K-Ca-HCO3-Cl

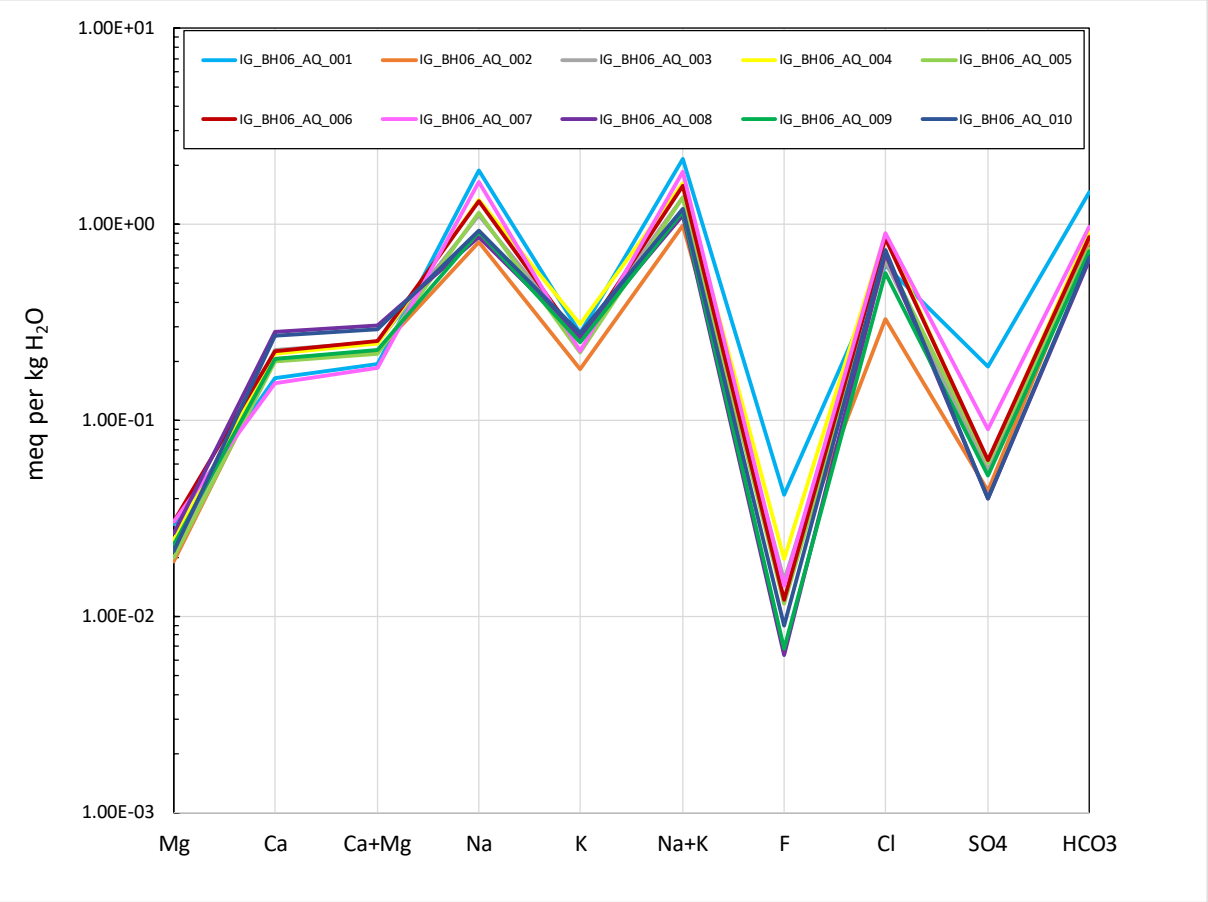


Figure 5-1: Schoeller diagram of experiment solutions from aqueous extraction experiments conducted with core samples from borehole IG_BH06.

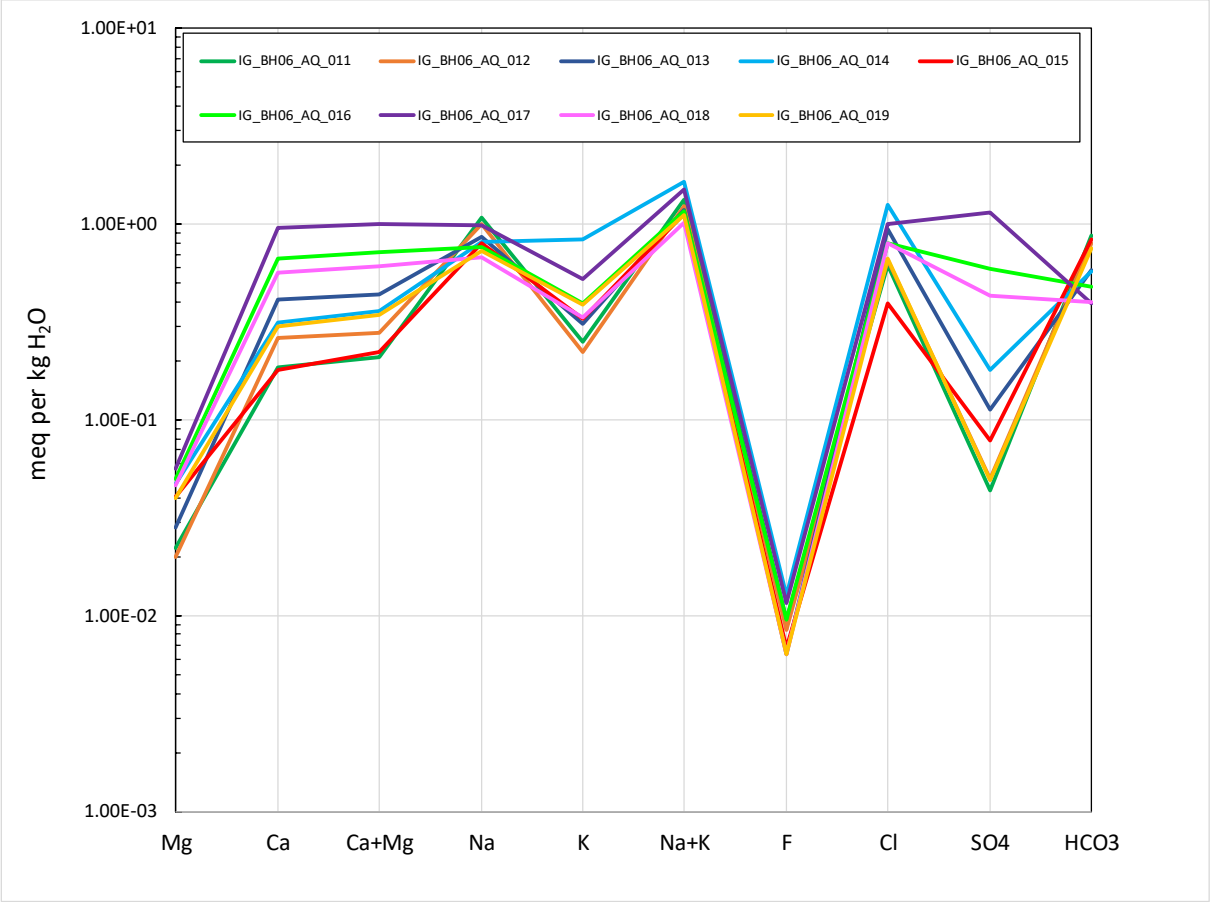


Figure 5-1 continued

5.2 Chemical Composition of Out-Diffusion Experiment Solutions

Out-diffusion experiments were performed on 31 core samples from IG_BH06 to derive the porewater chloride and bromide concentrations, porewater $\delta^{37}Cl$ isotopic ratios, and chemical composition of the test solutions - which are the basis for the hydrogeochemical modelling of porewater chemical compositions. The core sections varied in diameter between 60.6 mm and 61.1 mm, with lengths between 157 mm and 206 mm. The corresponding volume of the sections varied between 453 cm^3 and 603 cm^3 and the saturated mass was between 1,217 g and 1,639 g. In the out-diffusion experiments, the mass ratio of experiment solution to rock samples was between 0.086 and 0.112 (Table 5-2).

During the out-diffusion experiments, a continuous exchange between porewater and test water takes place until equilibrium conditions with respect to conservative, non-reactive compounds are achieved. The experiments use intact large-sized core pieces and there is no release and/or influence of fluids from within fluid inclusions. The exchange appears to occur mainly by diffusion (Section 6). For chemically conservative elements, such as chloride and bromide, for which the porewater is the only source, the porewater concentration can be calculated using the gravimetrically determined porewater mass of the rock sample. For reactive elements and compounds, such as Ca^{2+}, Mg^{2+}, Na^{+}, K^{+}, Sr^{2+}, Si, Al, SO_4^{2-} and HCO_3^{-}, the contribution of mineral dissolution reactions during the experiment has to be taken into account. Those reactions are evaluated by the determination of the concentrations of the non-conservative elements taken in time-series (Section 6.1).

The pH of the experiment solutions varies between 7.3 and 8.0, with a total mineralization between 126 mg/L and 787 mg/L (EC = 177 - 1277 µS/cm, Table 5-2). It should be noted that the total mineralization obtained for the experiment solutions depends on the water content of the sample and the water/rock ratio used in the experiment (Table 4-3) and does not directly reflect differences in porewater salinity.

The experimental solutions contain Na^+ (14.8 – 37.1 mg/L), Ca^{2+} (15.2 – 202 mg/L), K^+ (2.5 – 11.0 mg/L), HCO_3^- (48.6 – 139 mg/L), Cl^- (7.8 – 210 mg/L), Br (0.12 to 14.2 mg/L) and SO_4^{2-} (4.8 – 335 mg/L) in varying proportions and concentrations (Table 5-2, Figure 5-2).

Based on the out-diffusion test solutions, samples are characterized by Na^+ and HCO_3^- dominated water between 212 and 291.5 mbgs (downhole), and transition to Na^+, Ca^{2+}, HCO_3^- and Cl^- dominated water types between 253 and 562 mbgs (downhole). Between 574 and 721 mbgs (downhole) samples are characterized by Ca^{2+}- and Cl^--dominated water followed by two samples from 723 and 729 mbgs (downhole) showing again Na^+ and HCO_3^--dominated water. Samples from depths between 744 and 971 mbgs (downhole) are mainly characterized by Ca^{2+}- and Cl^-- dominated water, and some of the samples show high proportions of sulphate.

Silicon (expressed as Si) is present in concentrations between 6.20 and 12.2 mg/L. Magnesium, strontium, aluminium, boron, fluoride and nitrate are below detection limit or present in low or trace concentrations (Table 5-2).

The concentrations of dissolved organic carbon (DOC) vary between 4.42 and 27.8 mg/L (Table 5-2).

The DIC/TIC concentrations (DIC = TIC, because analyses are performed on filtered samples) determined by TIC analyser vary between 11.5 and 31.6 mg/L. The comparison of the TIC concentrations determined by direct analyses with those determined by acid titration (AC4.3) shows that the total alkalinity is mainly determined by HCO_3.

The strontium $^{87}Sr/^{86}Sr$ isotope ratios of the out-diffusion test solutions vary between 0.719688 and 0.743598 with Sr^{2+} concentrations between 0.136 and 1.61 mg/L (Table 5-2).

Table 5-2: Analytical results of test solutions of out-diffusion experiments using core samples from borehole IG_BH06

Sample		IG_BH06_PW001	IG_BH06_PW002	IG_BH06_PW003	IG_BH06_AR010	IG_BH06_AR013	IG_BH06_PW004	IG_BH06_PW005	IG_BH06_AR019	IG_BH06_AR020	IG_BH06_PW006
Hydroisotop Nr.		389375	389376	389377	392239	392240	389378	389379	392241	392242	389380
Interval	m BHL	212.3	291.5	253.2	398.7	421.6	453.2	504.1	534.0	542.9	562.4
Ratio Exp.Water : Rock	g/g	0.101	0.100	0.104	0.086	0.091	0.100	0.098	0.094	0.097	0.097
Ratio TW:PW	g/g	48.9	56.6	53.3	118.3	57	59	50.8	60	53.0	50
MASTER VARIABLES											
pH (lab)	-log(H+)	8.0	7.6	7.6	7.6	7.6	7.5	7.6	7.7	7.6	7.5
Spec. Electr. Conductivity	µS/cm	177	243	233	271	269	293	184	225	196	229
Acid Capacity (4.3)	mmol	1.23	1.39	1.04	1.42	1.13	1.25	0.87	1.21	1.02	0.96
Base Capacity (8.2)	mmol	-	-	-	-	-	-	-	-	-	-
Sample Temperature	°C	23.9	24	24.1	23.1	22.9	24.2	24.3	23	22.4	24.5
DOC	mg/l	10.7	23.9	16.7	8.13	7.14	11.7	9.9	10.2	7.89	8.46
TIC	mg/l	14.2	14.1	14.0	21.1	15.4	16.4	11.5	18.4	16.6	14.0
DISSOLVED CONSTITUENTS											
CATIONS	mg/l										
Sodium (Na^+)	mg/l	19.4	19	17.4	18.8	16.1	15.6	17.7	15.9	14.9	16.4
Potassium (K^+)	mg/l	2.6	2.5	4.2	3.68	2.77	4	4.1	5.54	3.31	6.8
Calcium (Ca^{2+})	mg/l	15.2	30.2	27.1	32.9	33.5	40.8	19.0	24.9	21.9	26.9
Magnesium (Mg^{2+})	mg/l	< 0,2	< 0,2	< 0,2	0.3	< 0,2	< 0,2	< 0,2	0.28	0.37	< 0,2
Strontium (Sr^{2+})	mg/l	< 0,1	< 0,1	< 0,1	0.184	0.136	< 0,1	< 0,1	0.159	0.14	< 0,1
Aluminium (Al^{3+})	mg/l	0.124	0.041	0.061	0.094	0.137	0.037	0.092	0.08	0.08	0.091
Silicon (Si^{4+})	mg/l	8.87	10.14	10.44	8.12	8.12	9.35	12.17	8.83	8.79	9.35
Boron (B)	mg/l	0.473	0.102	0.086	0.141	0.070	0.068	0.094	0.089	0.094	0.093
ANIONS											
Fluoride (F^-)	mg/l	3.10	2.60	1.00	0.28	0.92	1.70	0.67	0.37	0.30	0.40
Chloride (Cl^-)	mg/l	7.8	21.6	29.1	22.1	39.6	45.5	24	23.7	21.2	33.4
Bromide (Br^-)	mg/l	0.12	0.3	0.74	0.66	0.96	0.91	0.91	0.83	0.8	0.58
Nitrate (NO_3^-)	mg/l	< 0,2	< 0,2	< 0,2	1.92	0.35	< 0,2	< 0,2	0.43	0.44	< 0,2
Sulphate (SO_4^{2-})	mg/l	5.2	8.9	9.2	21.0	6.96	7.1	7	7.1	7.41	6.5
Total Alkalinity	meq/l	1.23	1.39	1.04	1.42	1.13	1.25	0.87	1.21	1.02	0.96
Total Alkalinity as HCO_3^-	mg/l	75.2	84.9	63.5	86.9	68.8	76.2	53.0	73.7	62.5	58.6
PARAMETERS CALCULATED FROM ANALYTICAL DATA											
Sum of Analysed Constituents	mg/l	129	170	152	189	170	192	126	153	133	150
Charge Balance:	%	-1.66%	1.48%	2.36%	0.85%	-0.21%	0.65%	2.40%	1.01%	1.36%	3.81%
WATER TYPE		Na-Ca-HCO3-(Cl)	Na-Ca-HCO3-Cl	Na-Ca-HCO3-Cl	Ca-Na-HCO3-Cl-(SO4)	Ca-Na-HCO3-Cl	Ca-Na-Cl-HCO3	Na-Ca-HCO3-Cl	Na-Ca-HCO3-Cl	Na-Ca-HCO3-Cl	Na-Ca-HCO3-Cl
ION-ION RATIOS											
Br*1000/Cl weight		15.4	13.9	25.4	29.9	24.2	20.0	37.9	35.0	37.7	17.4
Br*1000/Cl molal	mol/mol	6.8	6.2	11.3	13.3	10.8	8.9	16.8	15.5	16.7	7.7
Na/Cl molal	mol/mol	3.8	1.4	0.9	1.3	0.6	0.5	1.1	1.0	1.1	0.8
K/Na molal	mol/mol	0.079	0.077	0.142	0.115	0.101	0.151	0.136	0.205	0.131	0.244
SO4/Cl molal	mol/mol	0.246	0.152	0.117	0.351	0.065	0.058	0.108	0.110	0.129	0.072
Na/(Cl+SO4)	mol/mol	3.1	1.2	0.8	1.0	0.6	0.5	1.0	0.9	1.0	0.7
ISOTOPE RATIOS											
$\delta^{37}Cl$	pm SMOC	-0.12	0.17	0.42	1.02	0.99	0.89	0.11	0.62	0.62	0.31
error $\delta^{37}Cl$	pm SMOC	0.10	0.10	0.10	0.10	0.10	0.14	0.10	0.10	0.11	0.10
$^{87}Sr/^{86}Sr$		0.733616	0.737978	0.743598	0.731986	0.732974	0.731654	0.737411	0.738412	0.728584	0.734827
error $^{87}Sr/^{86}Sr$		0.00005	0.00005	0.00005	0.00003	0.00003	0.00005	0.00005	0.00003	0.00003	0.00005

Table 5-2: Continued

Sample		IG_BH06_PW007	IG_BH06_AR027	IG_BH06_PW008	IG_BH06_PW009	IG_BH06_PW010	IG_BH06_PW011	IG_BH06_PW012	IG_BH06_PW013	IG_BH06_AR038	IG_BH06_AR039
Hydroisotop Nr.		389381	392243	389382	389383	389384	389385	390167	390168	392244	392245
Interval	m BHL	574.2	595.0	612.2	647.9	665.9	691.0	693.7	720.5	722.6	728.8
Ratio Exp.Water : Rock	g/g	0.098	0.099	0.099	0.096	0.101	0.106	0.098	0.107	0.087	0.098
Ratio TW:PW	g/g	52.9	53.8	57.2	66.4	70.6	80.9	68.0	79.1	192.4	134.4
MASTER VARIABLES											
pH (lab)	-log(H+)	7.6	7.5	7.8	7.9	7.8	7.9	7.8	7.9	7.7	7.7
Spec. Electr. Conductivity	µS/cm	266	305	276	269	288	292	390	282	329	309
Acid Capacity (4.3)	mmol	1.64	1.30	1.11	1.05	1.09	1.14	1.10	1.03	2.28	1.31
Base Capacity (8.2)	mmol	-	-	-	-	-	-	-	-	-	-
Sample Temperature	°C	25	22.1	24.6	24.6	24.6	24.6	24.6	24.6	23.1	22.7
DOC	mg/l	11.7	8.79	9.81	5.65	6	4.42	8.85	6.42	13.7	11.8
TIC	mg/l	20.7	18.6	14.4	14.3	14.4	16.9	14.7	14.3	31.6	20.6
DISSOLVED CONSTITUENTS											
CATIONS	mg/l										
Sodium (Na^+)	mg/l	15.6	15.8	17.1	17.5	15.6	14.8	21.5	17.9	25	22.6
Potassium (K^+)	mg/l	6.6	6.58	5.7	4.8	5.6	5.7	6.4	6.2	9.06	6.78
Calcium (Ca^{2+})	mg/l	38.1	37.2	37.8	37.4	39.1	40.3	49.2	33.2	31.1	32.1
Magnesium (Mg^{2+})	mg/l	0.3	< 0,2	< 0,2	< 0,2	< 0,2	0.48	0.63	< 0,2	0.49	0.36
Strontium (Sr^{2+})	mg/l	< 0,1	0.2	< 0,1	< 0,1	< 0,1	< 0,1	< 0,1	< 0,1	0.385	0.293
Aluminium (Al^{3+})	mg/l	0.03	0.12	0.06	0.04	0.03	0.04	0.06	0.07	0.03	0.09
Silicon (Si^{4+})	mg/l	10.14	6.73	9.2	7.18	7.74	7.82	6.99	6.62	9.13	8.79
Boron (B)	mg/l	0.111	0.074	0.062	0.084	0.091	0.101	0.146	0.100	0.222	0.335
ANIONS											
Fluoride (F^-)	mg/l	0.11	0.44	0.27	< 0,1	0.32	0.20	0.65	< 0,1	< 0,1	< 0,1
Chloride (Cl^-)	mg/l	29.2	45.6	51.9	55.3	56.5	53.7	74.4	52	16.3	35.2
Bromide (Br^-)	mg/l	0.37	1.07	0.65	0.9	1.1	1.3	6.4	1.1	0.37	0.81
Nitrate (NO_3^-)	mg/l	< 0,2	0.59	< 0,2	< 0,2	< 0,2	< 0,2	< 0,2	< 0,2	< 0,2	0.34
Sulphate (SO_4^{2-})	mg/l	8.6	6.19	6.3	5.7	5	4.8	10.5	5.1	12.9	23.4
Total Alkalinity	meq/l	1.64	1.30	1.11	1.05	1.09	1.14	1.10	1.03	2.28	1.31
Total Alkalinity as HCO_3^-	mg/l	100.3	79.6	67.6	63.9	66.4	69.8	67.4	63.0	138.9	79.8
PARAMETERS CALCULATED FROM ANALYTICAL DATA											
Sum of Analysed Constituents	mg/l	199	193	187	186	190	191	237	178	235	202
Charge Balance:	%	2.13%	-0.89%	0.91%	0.22%	-0.78%	0.97%	0.98%	-0.48%	-1.52%	-0.17%
WATER TYPE		Ca-Na-HCO3-Cl	Ca-Na-HCO3-Cl	Ca-Na-Cl-HCO3	Ca-Na-Cl-HCO3	Ca-Na-Cl-HCO3	Ca-Na-Cl-HCO3	Ca-Na-Cl-HCO3	Ca-Na-Cl-HCO3	Na-Ca-HCO3-Cl	Na-Ca-HCO3-Cl-(SO4)
ION-ION RATIOS											
Br*1000/Cl weight		12.7	23.5	12.5	16.3	19.5	24.2	86.0	21.2	22.7	23.0
Br*1000/Cl molal	mol/mol	5.6	10.4	5.6	7.2	8.6	10.7	38.2	9.4	10.1	10.2
Na/Cl molal	mol/mol	0.8	0.5	0.5	0.5	0.4	0.4	0.4	0.5	2.4	1.0
K/Na molal	mol/mol	0.249	0.245	0.196	0.161	0.211	0.226	0.175	0.204	0.213	0.176
SO4/Cl molal	mol/mol	0.109	0.050	0.045	0.038	0.033	0.033	0.052	0.036	0.292	0.245
Na/(Cl+SO4)	mol/mol	0.7	0.5	0.5	0.5	0.4	0.4	0.4	0.5	1.8	0.8
ISOTOPE RATIOS											
$\delta^{37}Cl$	pm SMOC	0.14	0.76	0.74	0.61	0.57	0.23	-0.08	-0.03	0.33	0.63
error $\delta^{37}Cl$	pm SMOC	0.10	0.10	0.10	0.10	0.10	0.16	0.10	0.11	0.10	0.10
$^{87}Sr/^{86}Sr$		0.728839	0.735001	0.733930	0.728697	0.731254	0.720505	0.721331	0.724700	0.720094	0.725861
error $^{87}Sr/^{86}Sr$		0.00005	0.00003	0.00005	0.00005	0.00005	0.00005	0.00005	0.00005	0.00003	0.00003

Table 5-2: Continued

Sample		IG_BH06_DG003	IG_BH06_PW014	IG_BH06_PW015	IG_BH06_AR045	IG_BH06_PW016	IG_BH06_AR049	IG_BH06_PW017	IG_BH06_PW018	IG_BH06_PW019	IG_BH06_PW020	IG_BH06_AR064
Hydroisotop Nr.		392249	390169	390170	392246	390171	392247	390172	390173	390174	390175	392248
Interval	m BHL	744.0	747.5	774.9	796.7	804.7	820.2	840.2	853.0	885.3	927.6	971.4
Ratio Exp.Water : Rock	g/g	0.112	0.103	0.100	0.093	0.100	0.103	0.103	0.101	0.098	0.097	0.089
Ratio TW:PW	g/g	197.3	78.6	78.5	97.5	77.7	79.7	62.3	82.2	62.3	71.8	65.1
MASTER VARIABLES												
pH (lab)	-log(H+)	7.4	7.8	7.8	7.3	7.9	7.5	7.8	7.7	7.6	7.8	7.6
Spec. Electr. Conductivity	µS/cm	427	440	502	1277	511	490	926	1200	1006	787	680
Acid Capacity (4.3)	mmol	1.30	1.03	1.24	0.80	1.22	1.20	1.06	1.00	0.85	0.86	0.96
Base Capacity (8.2)	mmol	-	-	-	-	-	-	-	-	-	-	-
Sample Temperature	°C	21.8	24.6	24.6	22.3	24.6	22.1	24.6	24.6	24.6	24.6	21.6
DOC	mg/l	27.8	7.3	8.28	14.6	6.96	12	11.4	9.11	7.58	7.29	10.9
TIC	mg/l	19.2	14.5	17.0	13.8	18.0	18.4	13.3	14.8	12.8	13.0	16.3
DISSOLVED CONSTITUENTS												
CATIONS	mg/l											
Sodium (Na^+)	mg/l	18.9	22	22.3	29.5	25.5	25.5	27.2	21.4	26	32.3	37.1
Potassium (K^+)	mg/l	10.8	10	8.6	11	8.7	4.75	5.2	7.3	7.7	10.5	10.4
Calcium (Ca^{2+})	mg/l	53.9	64.3	68.9	202.0	71.1	63.7	147.0	195.0	182.0	110.0	87.0
Magnesium (Mg^{2+})	mg/l	0.57	0.48	0.5	0.7	0.45	0.49	0.76	0.62	0.49	0.49	0.67
Strontium (Sr^{2+})	mg/l	0.56	< 0,1	< 0,1	1.61	< 0,1	0.874	< 0,1	1.6	< 0,1	< 0,1	0.872
Aluminium (Al^{3+})	mg/l	0.07	0.04	0.05	0.05	0.04	0.09	0.04	0.03	0.04	0.05	0.09
Silicon (Si^{4+})	mg/l	9.13	7.48	7.25	7.44	7.14	8.3	6.2	7.07	7.44	6.43	9.39
Boron (B)	mg/l	0.128	0.106	0.090	0.108	0.091	0.169	0.120	0.097	0.095	0.087	0.154
ANIONS												
Fluoride (F^-)	mg/l	< 0,1	< 0,1	< 0,1	0.32	< 0,1	0.68	0.72	0.48	0.67	< 0,1	0.68
Chloride (Cl^-)	mg/l	66.8	96.9	108	144	110	100	180	169	186	210	167
Bromide (Br^-)	mg/l	5.09	1.5	5.3	4.53	4.6	5.03	14.2	4.1	3.2	3.4	3.39
Nitrate (NO_3^-)	mg/l	< 0,2	< 0,2	< 0,2	0.7	< 0,2	1.1	< 0,2	0.49	0.82	< 0,2	1.1
Sulphate (SO_4^{2-})	mg/l	17.1	19.7	14.1	335	30.1	19.3	95.4	223	187	12.1	15.2
Total Alkalinity	meq/l	1.30	1.03	1.24	0.80	1.22	1.20	1.06	1.00	0.85	0.86	0.96
Total Alkalinity as HCO_3^-	mg/l	79.1	62.7	75.4	48.6	74.7	73.2	64.7	60.8	51.7	52.2	58.3
PARAMETERS CALCULATED FROM ANALYTICAL DATA												
Sum of Analysed Constituents	mg/l	253	278	303	778	325	295	535	684	646	431	382
Charge Balance:	%	3.32%	3.13%	0.29%	-0.76%	-0.95%	-0.77%	2.20%	1.91%	1.82%	0.90%	1.75%
WATER TYPE		Ca-Na-Cl-HCO3-(SO4)	Ca-Na-Cl-HCO3	Ca-Na-Cl-HCO3	Ca-(Na)-SO4-Cl	Ca-Na-Cl-HCO3-(SO4)	Ca-Na-Cl-HCO3	Ca-Na-Cl-SO4-(HCO3)	Ca-(Na)-Cl-SO4	Ca-(Na)-Cl-SO4	Ca-(Na)-Cl-(HCO3)	Ca-Na-Cl-(HCO3)
ION-ION RATIOS												
Br*1000/Cl weight		76.2	15.5	49.1	31.5	41.8	50.3	78.9	24.3	17.2	16.2	20.3
Br*1000/Cl molal	mol/mol	33.8	6.9	21.8	14.0	18.6	22.3	35.0	10.8	7.6	7.2	9.0
Na/Cl molal	mol/mol	0.4	0.4	0.3	0.3	0.4	0.4	0.2	0.2	0.2	0.2	0.3
K/Na molal	mol/mol	0.336	0.267	0.227	0.219	0.201	0.110	0.112	0.201	0.174	0.191	0.165
SO4/Cl molal	mol/mol	0.094	0.075	0.048	0.859	0.101	0.071	0.196	0.487	0.371	0.021	0.034
Na/(Cl+SO4)	mol/mol	0.4	0.3	0.3	0.2	0.3	0.4	0.2	0.1	0.2	0.2	0.3
ISOTOPE RATIOS												
$\delta^{37}Cl$	pm SMOC	0.74	0.10	0.48	0.96	0.09	0.69	0.18	0.13	0.63	-0.12	0.62
error $\delta^{37}Cl$	pm SMOC	0.10	0.10	0.10	0.10	0.14	0.10	0.24	0.10	0.10	0.10	0.10
$^{87}Sr/^{86}Sr$		0.730835	0.727862	0.723620	0.719688	0.722793	0.725499	0.731229	0.730014	0.739200	0.723781	0.722730
error $^{87}Sr/^{86}Sr$		0.00003	0.00005	0.00005	0.00003	0.00005	0.00003	0.00005	0.00005	0.00005	0.00005	0.00003

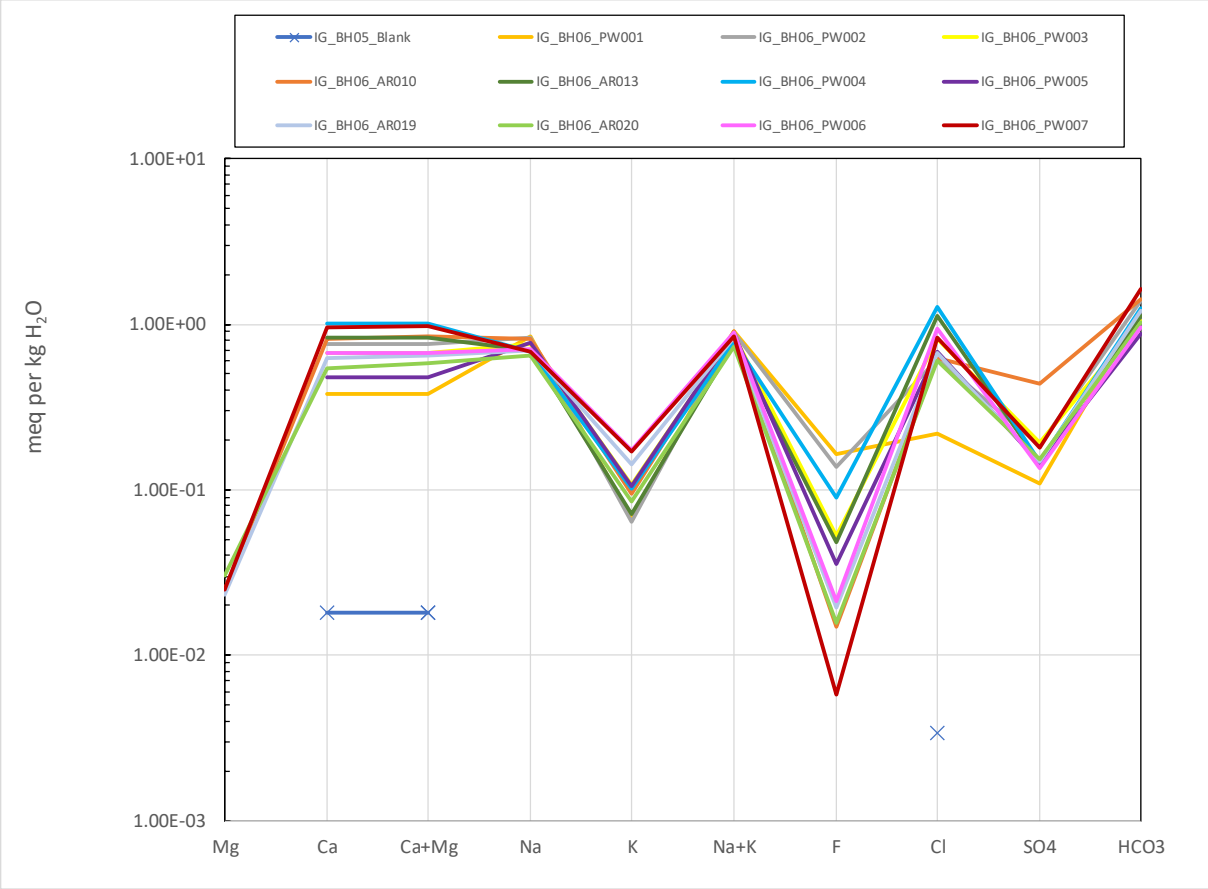


Figure 5-2: Schoeller diagram of experiment solutions from out-diffusion experiments.

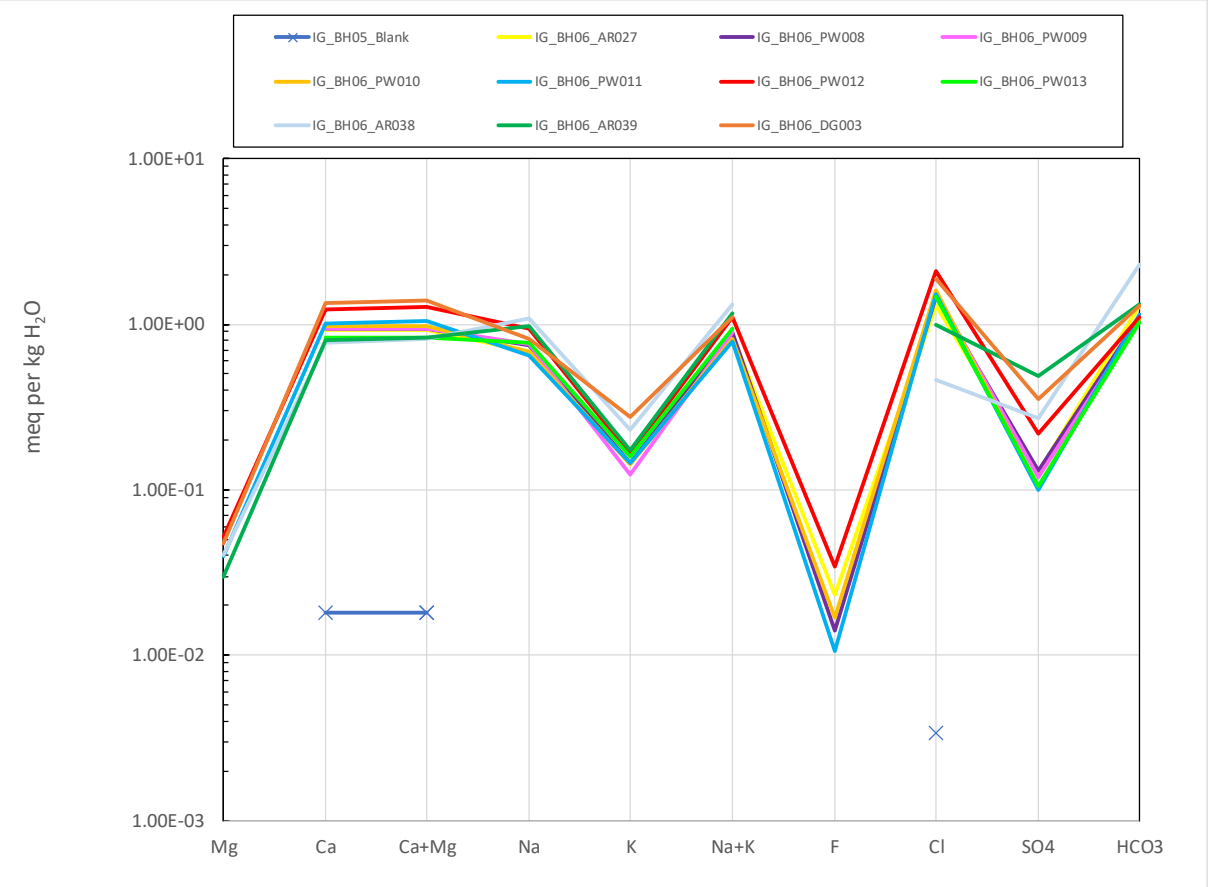


Figure 5-2 continued

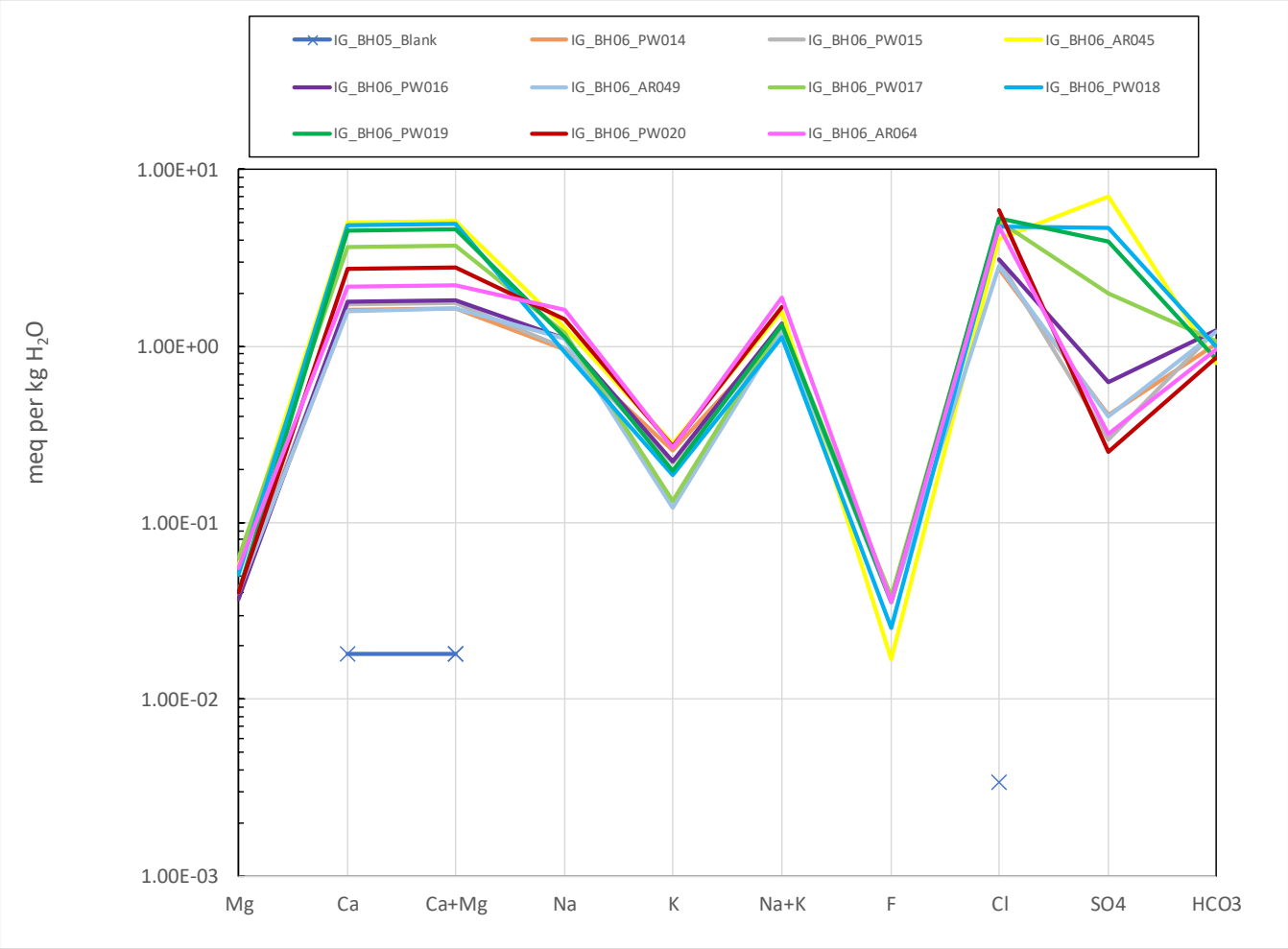


Figure 5-2 continued

6.0 RESULTS FROM ELEMENTAL TIME SERIES AND PORE DIFFUSION COEFFICIENT OF CHLORIDE

6.1 Elemental Elution Curves

Non-destructive out-diffusion experiments are performed based on the concept of chemical exchange between porewater residing in the rock matrix and a test solution of known composition surrounding the rock sample. The experimental setup is maintained until well-defined conditions between the two solution reservoirs are attained. Because of the closed system character of out-diffusion experiments, the target conditions to be achieved between the two solution reservoirs are equilibrium for any solutes for which the porewater is the only source, and which are only subjected to transport processes.

For the present study, improved analytical techniques allowed continuous monitoring of all major solute concentrations in the eluate solutions during out-diffusion. This allows definition of mineral reactions and – at a later stage – possible determination of solute-specific transport (e.g., ion-specific accessible porosity) in the matrix of crystalline rocks.

Porewater chloride and bromide concentrations are calculated based on the final concentrations in the out-diffusion test solutions and the water content of the individual core samples (Section 3). The approach to equilibrium was monitored by periodically taking sub-samples and analysing them for their Cl and Br concentrations. The criterion for attainment of equilibrium conditions is defined by a difference of less than 5 % in Cl and Br concentrations between the last sub-sample and the final test solution at the end of the experiment. This corresponds to the analytical uncertainty of the Cl and Br measurements. Sub-samples were collected as a function of time during all conducted out-diffusion experiments.

In order to verify the equilibrium conditions after a longer experiment time, the out-diffusion experiments were run for 253 to 324 days. Equilibrium with respect to Cl and Br was attained for almost all samples with respect to the above criteria after 29 – 95 days and 13 – 78 days, respectively (Figure 6-1).

The calculated Br*1000/Cl mass ratios (further expressed as Br/Cl ratio) of the individual out-diffusion experiments either increase or decrease within the first days or weeks of elution and are subsequently constant or are constant over the entire period of elution (Figure 6-1). This indicates that there is no significant influence of a diffusional fractionation between bromide and chloride at the end of the experiment.

Sodium shows a heterogeneous elution behaviour. For most samples, the Na-concentration in the individual test waters shows a steep increase in the first 7-14 days, followed by a flattening of the curve and a continuous increase, which becomes less with ongoing experimental time (Figure 6-1), but not reaching full equilibrium after the experimental time. Only the Na elution curve of samples IG_BH06_PW009, IG_BH06_PW010 and IG_BH06_PW015 show a clear diffusion like shape and equilibrium after 51 to 81 days.

Potassium, in contrast, reaches equilibrium in all conducted out-diffusion experiments. All samples except samples IG_BH06_PW002 and IG_BH06_AR010 show a sharp increase within the first 7 to 48 days of the experiments, followed by flattening and achievement of equilibrium after app 21 to 95 days (Figure 6-1).

Calcium shows heterogeneous elution behaviour in the individual out-diffusion experiments. Some samples reach equilibrium between 66 to 95 days and some samples show equilibrium for the last subsample and final sample after 120 to 324 days. Despite of a full equilibration of the conservative anions, Cl and Br, after a much shorter time, the experiments were extended to make sure that the samples were in equilibrium. As such, some samples did reach equilibrium with respect to Ca, whereas others show an increase in Ca concentration during the entire period of elution (Figure 6-1). This means that they are not in equilibrium with respect to Ca and suggests the Ca originates from 1) Ca-carbonates in the saussuritised plagioclases, and/or 2) interactions between the fluids and Ca-feldspars.

For most of the samples, the sulphate concentrations display a steady increase during the elution period and achievement of equilibrium for the last two or three subsamples after 75 to 123 days (Figure 6-1). For samples IG_BH06_PW007, AR013, AR019, AR020, AR045 and DG003 a steady increase during the entire elution period is observed. This is reasoned to be caused by the oxidation and elution of sulphide minerals present in the rock as accessories.

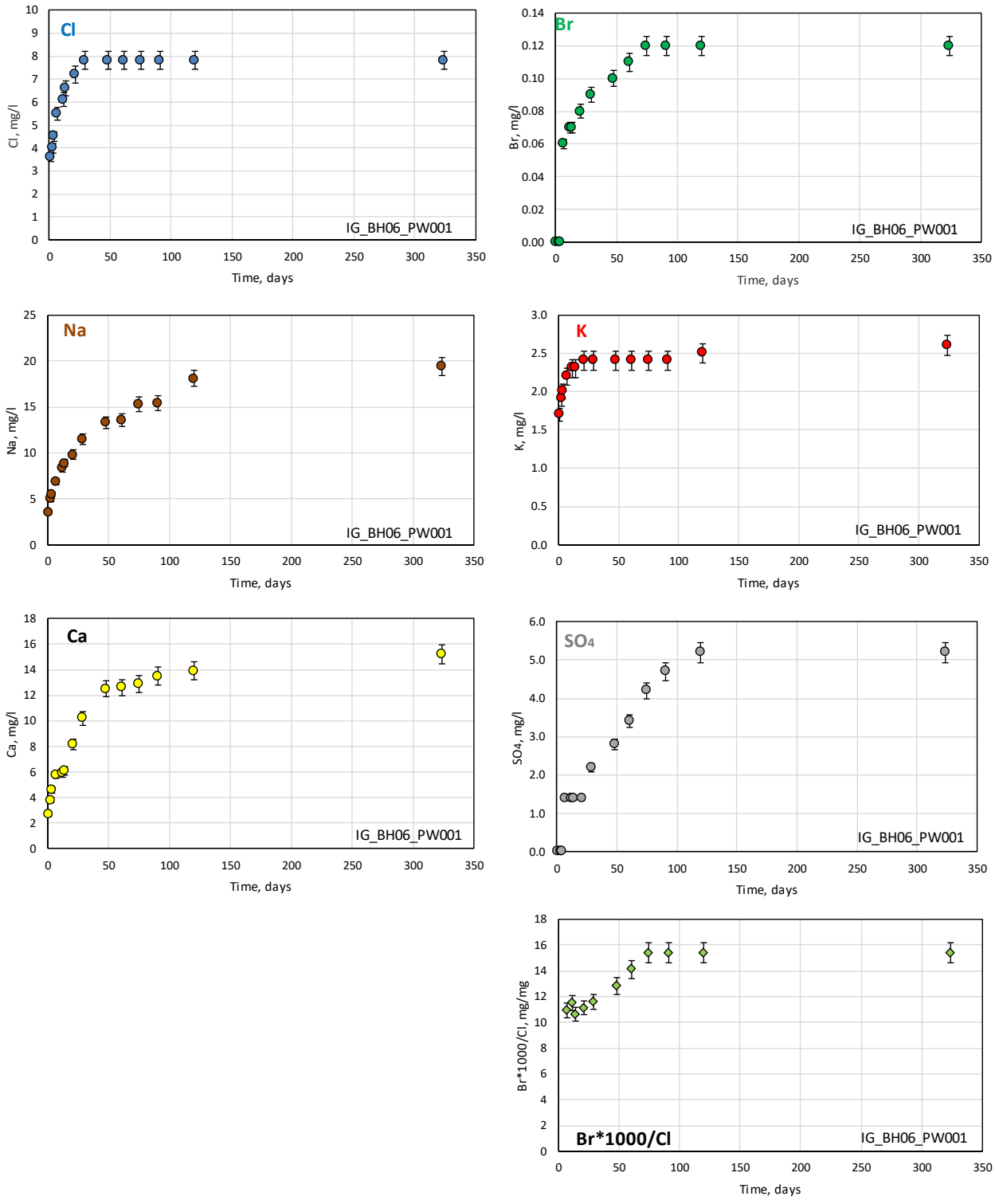


Figure 6-1: Elution curves of anions and cations set-up by the periodic sampling of the test solutions from out-diffusion experiments using core samples from borehole IG_BH06; the errors are the analytical uncertainty of ± 5 %.

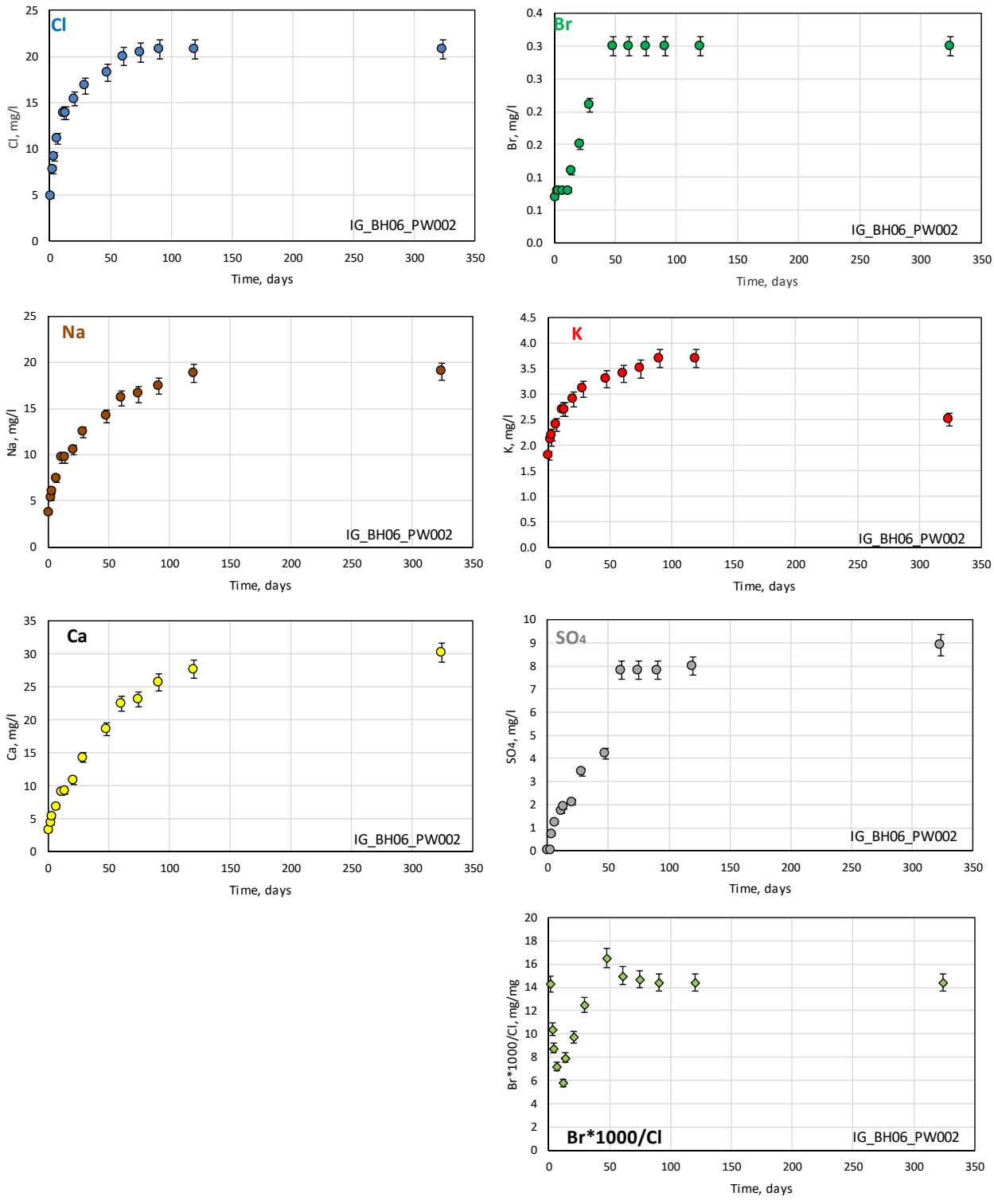


Figure 6-1 continued

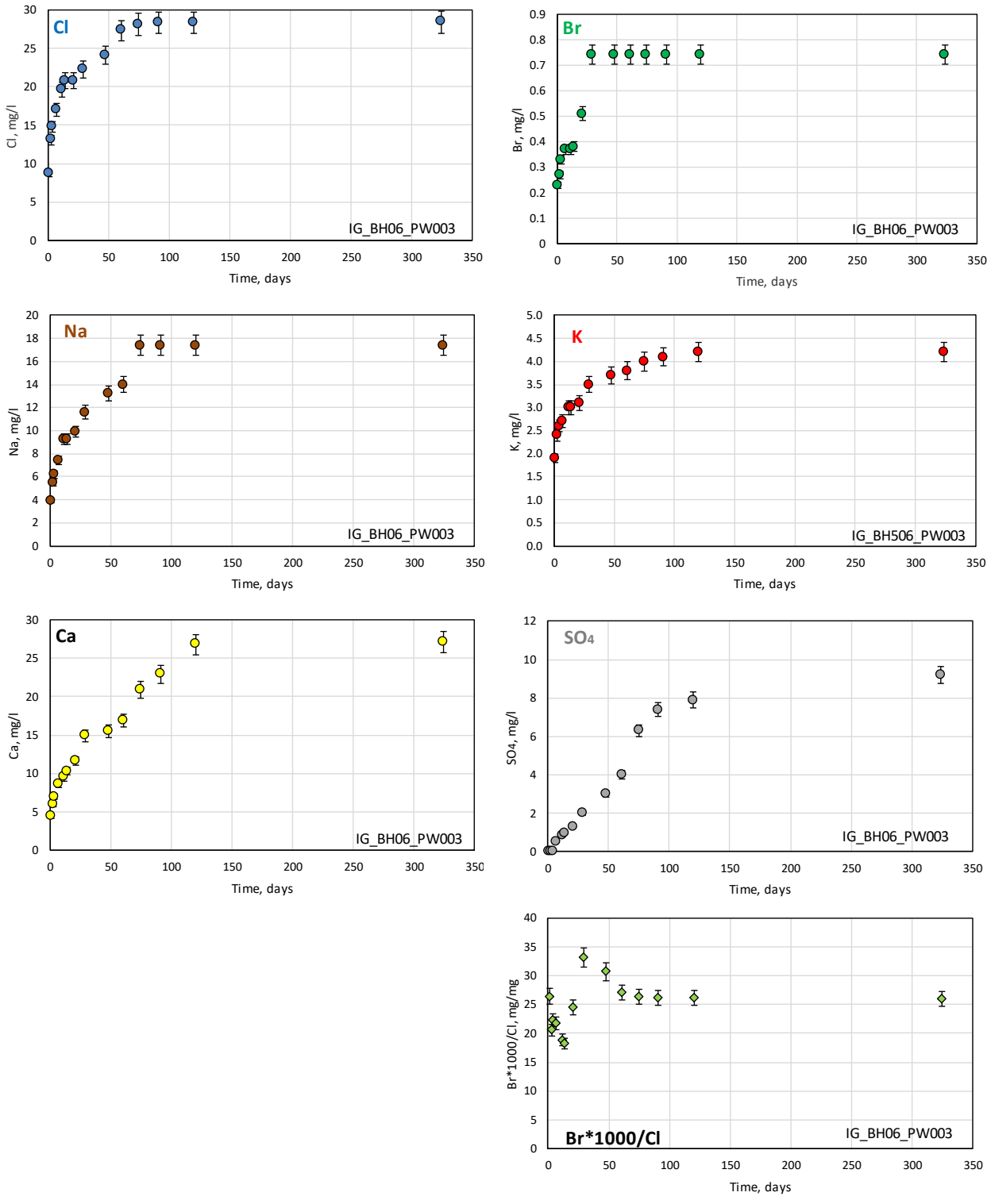


Figure 6-1 continued

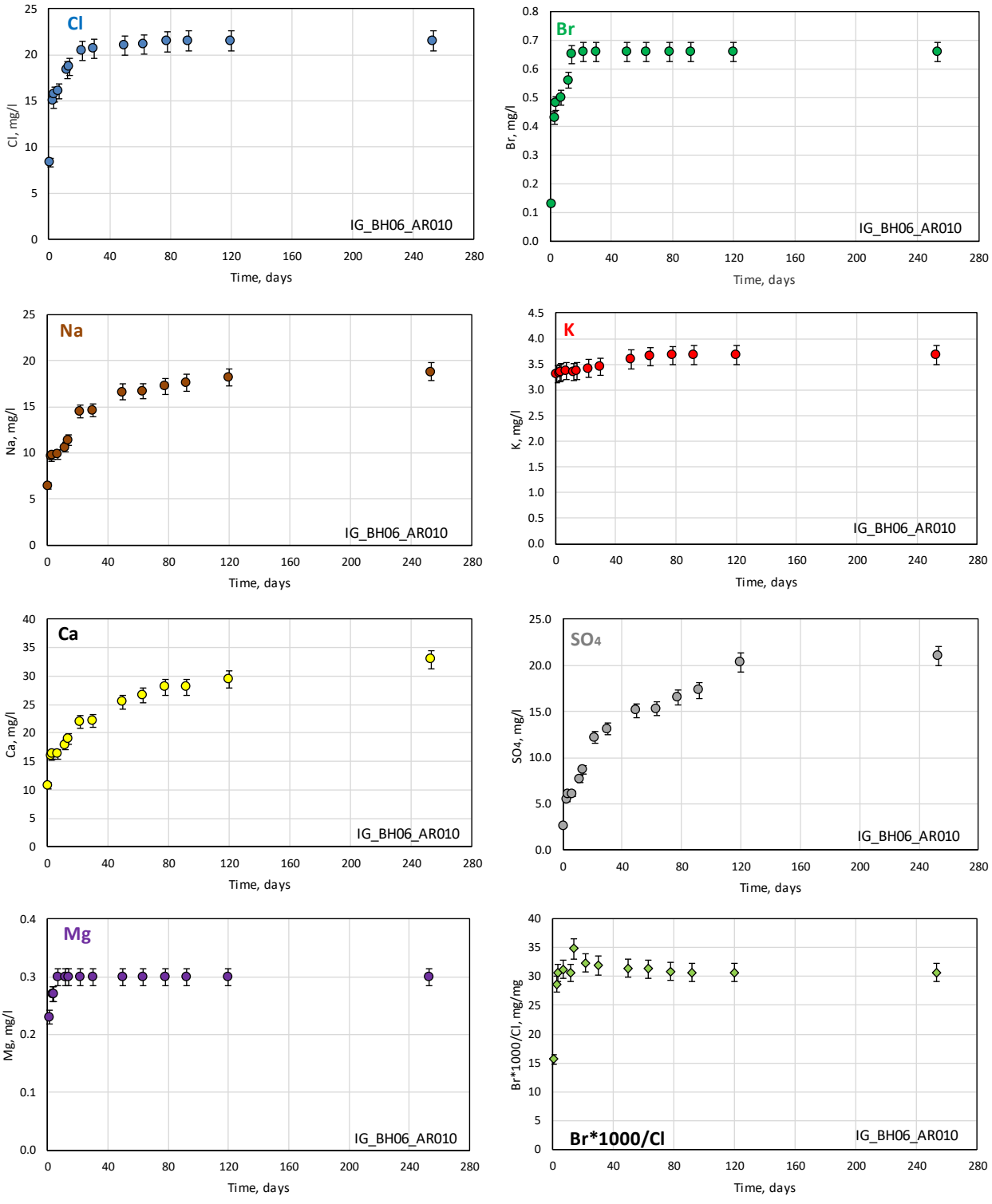


Figure 6-1 continued

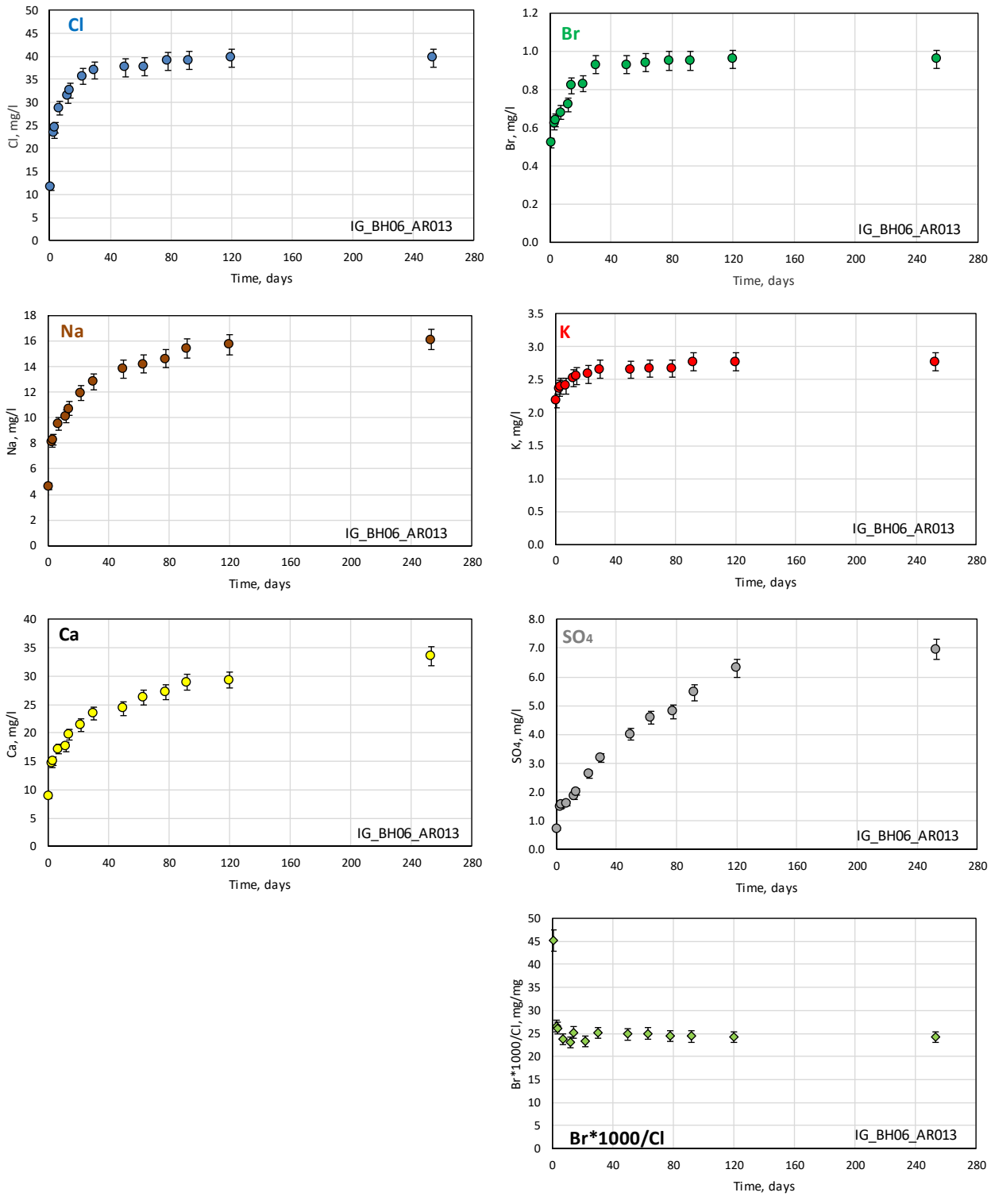


Figure 6-1 continued

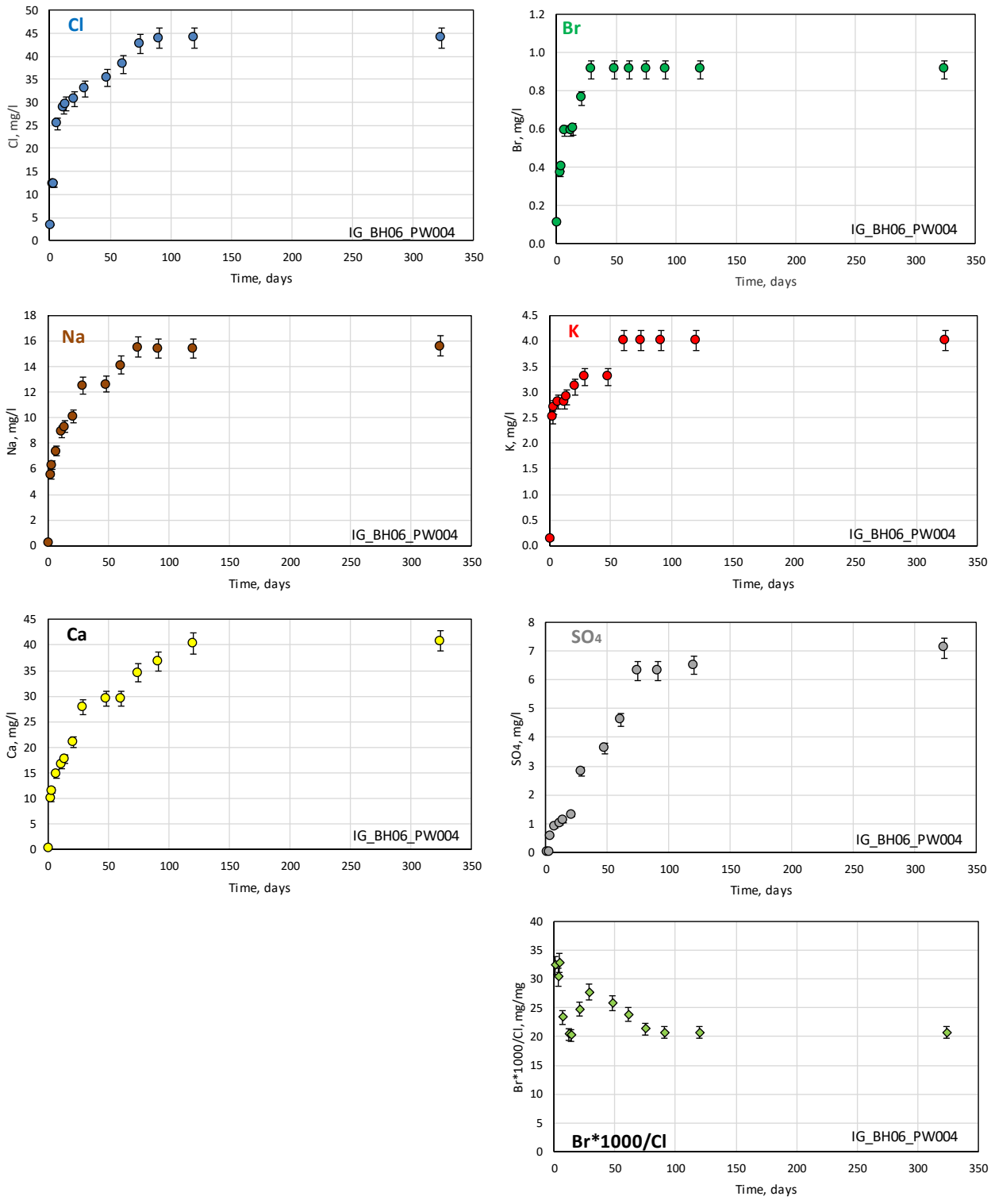


Figure 6-1 continued

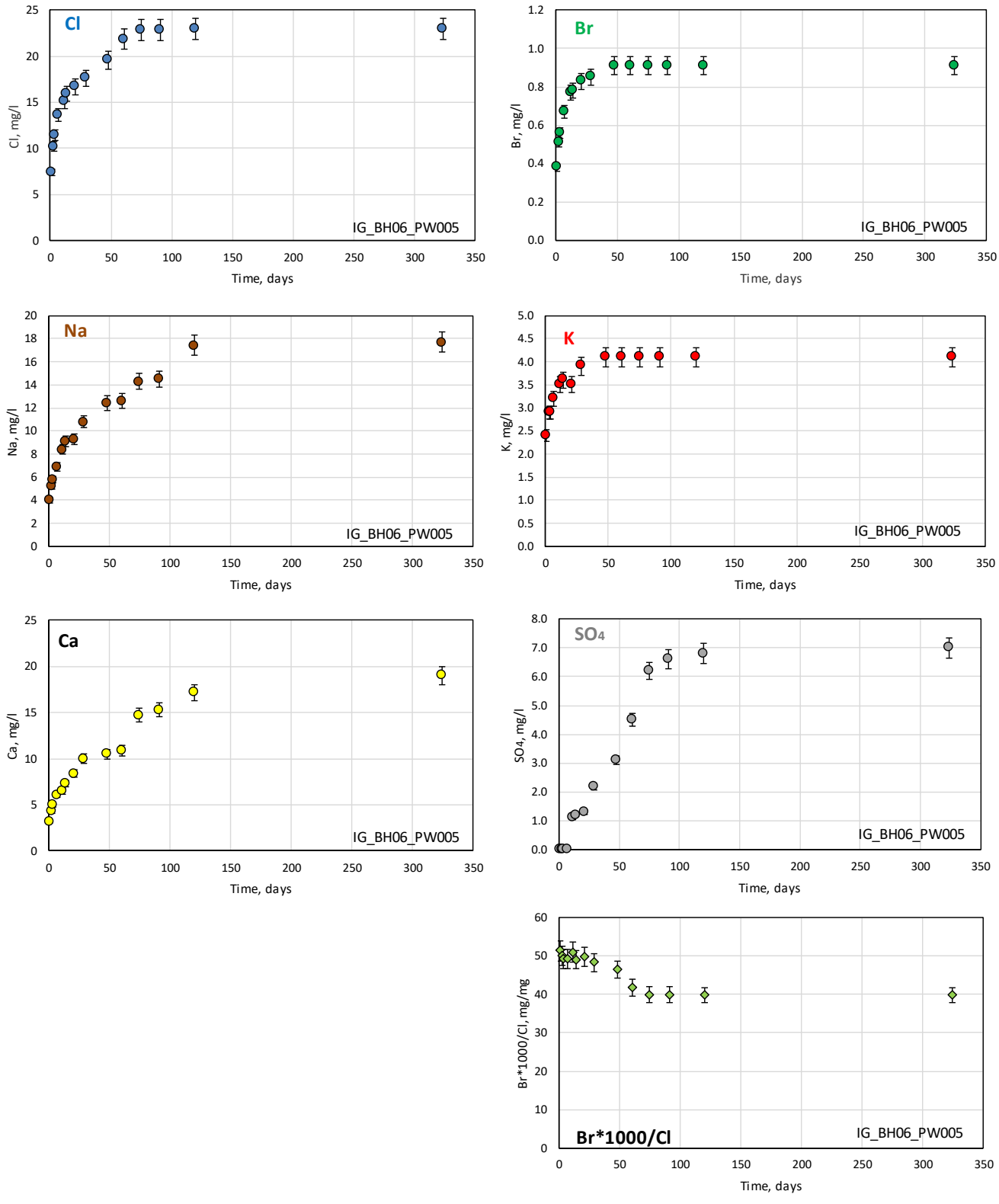


Figure 6-1 continued

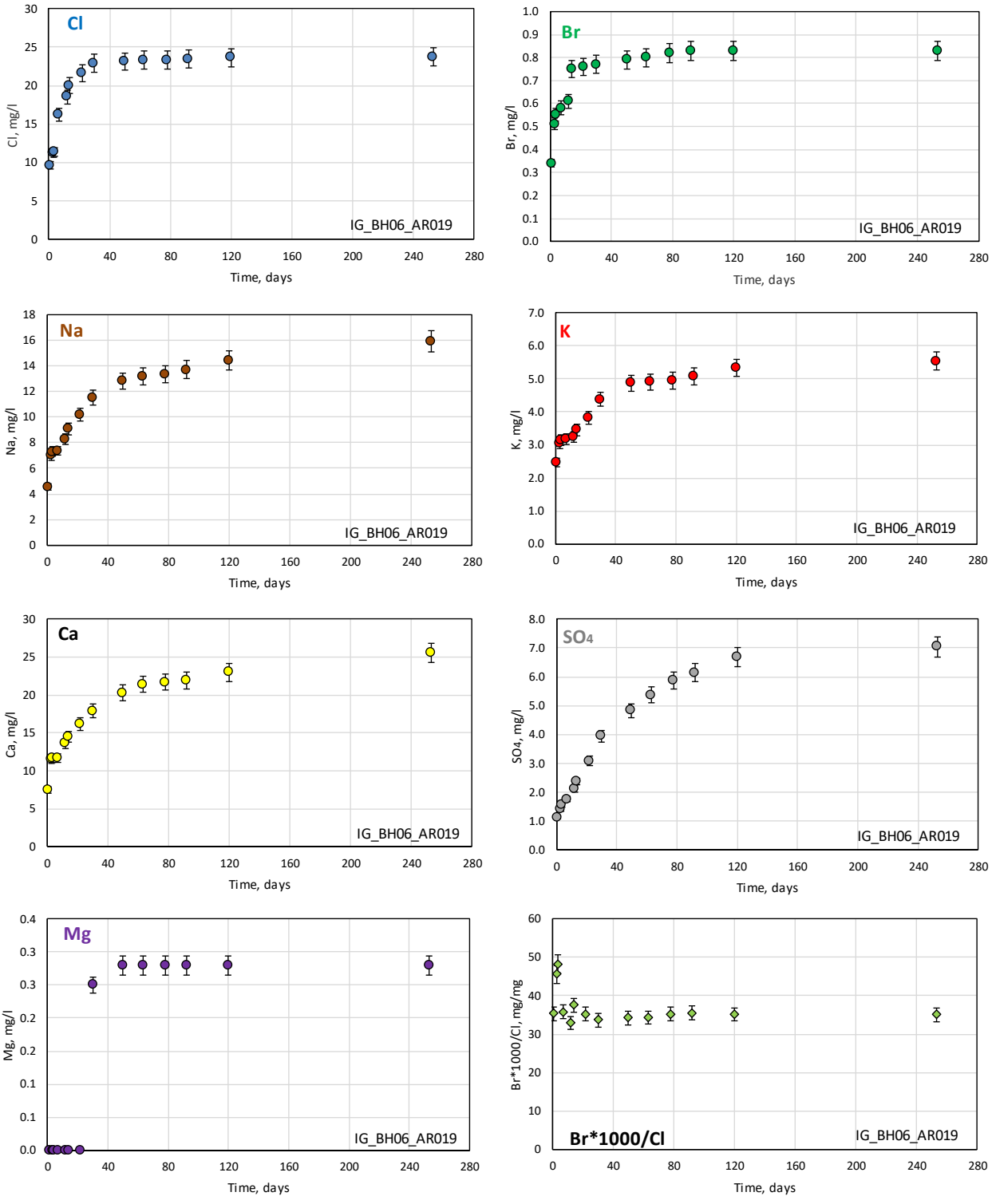


Figure 6-1 continued

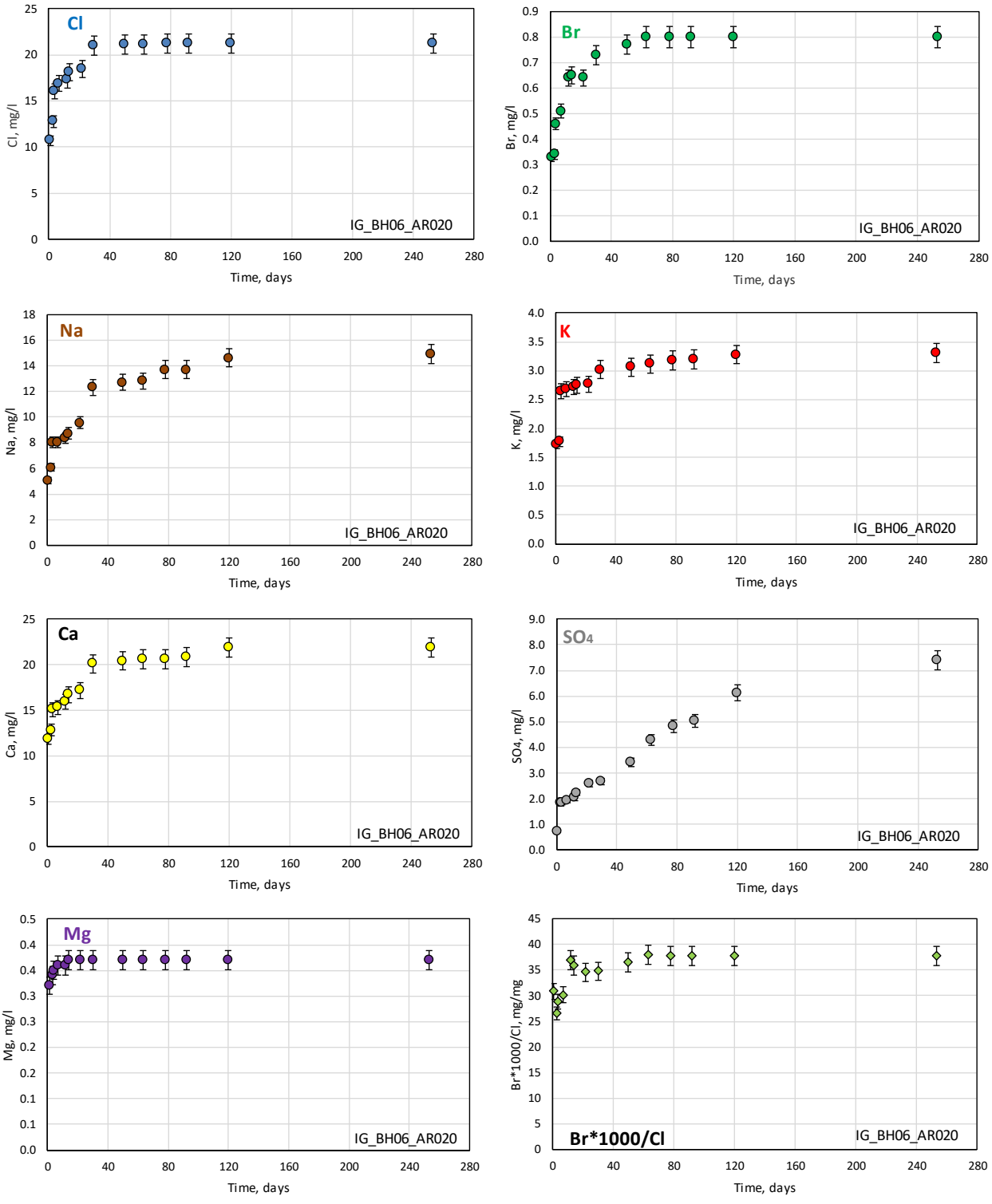


Figure 6-1 continued

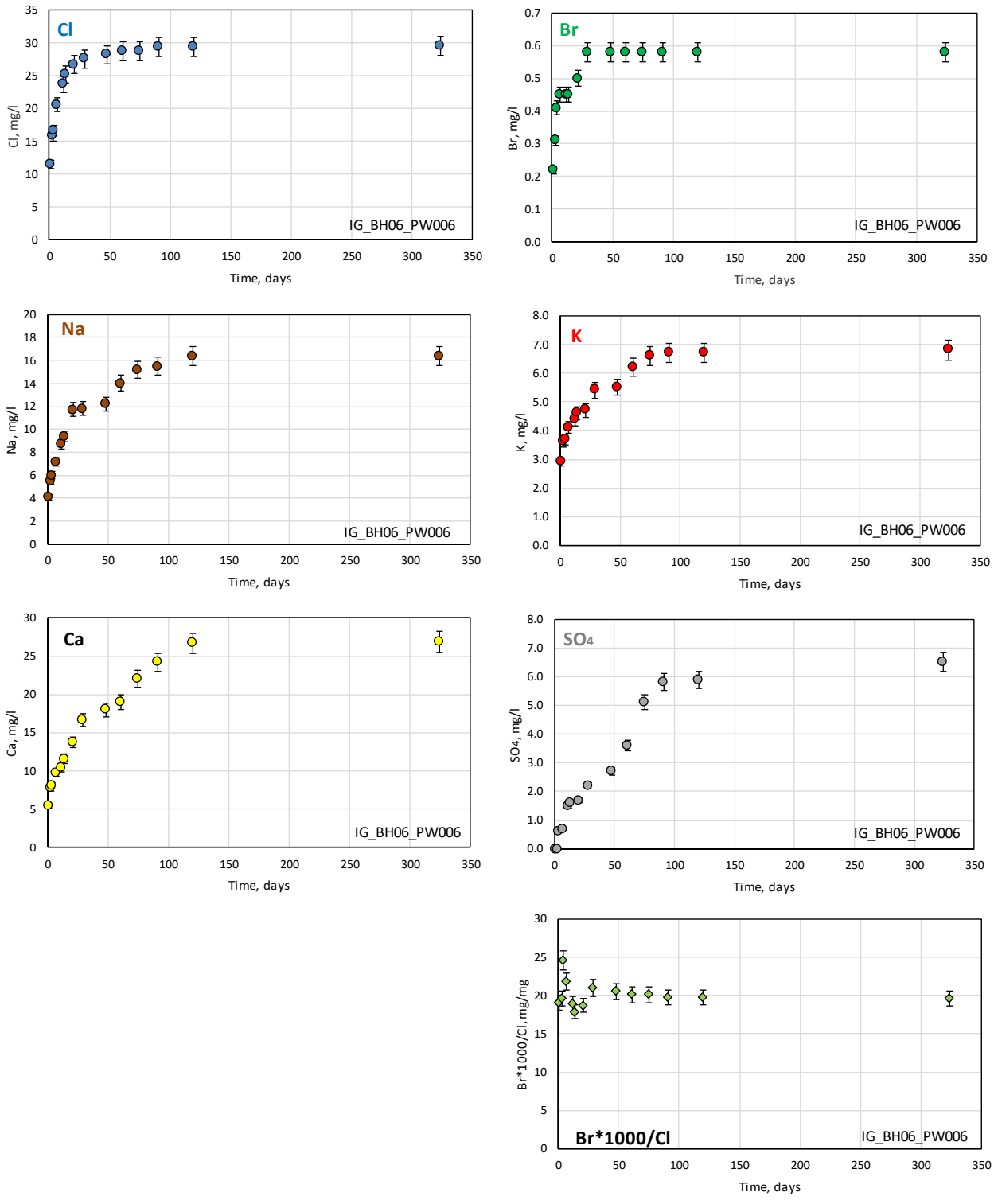


Figure 6-1 continued

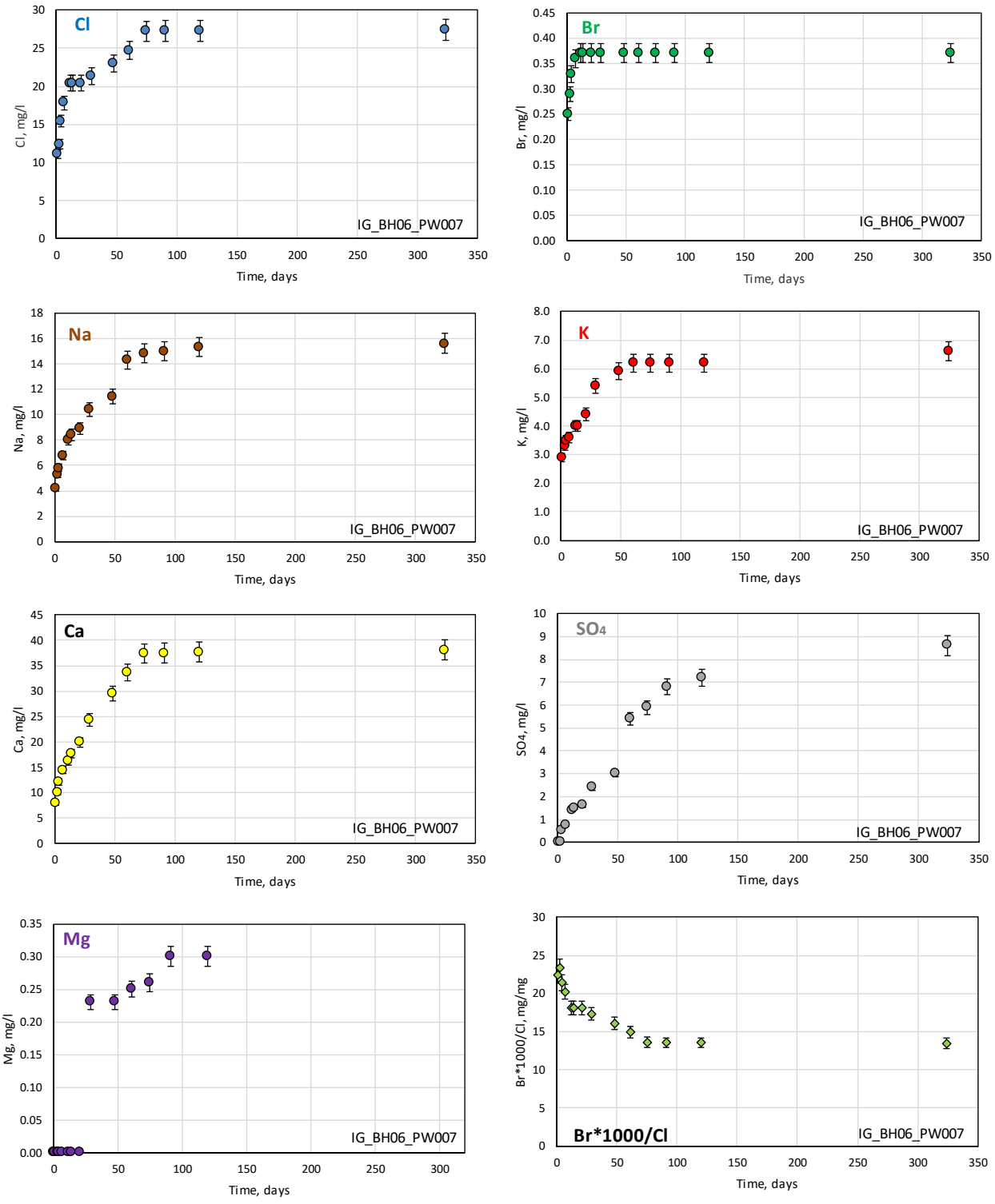


Figure 6-1 continued

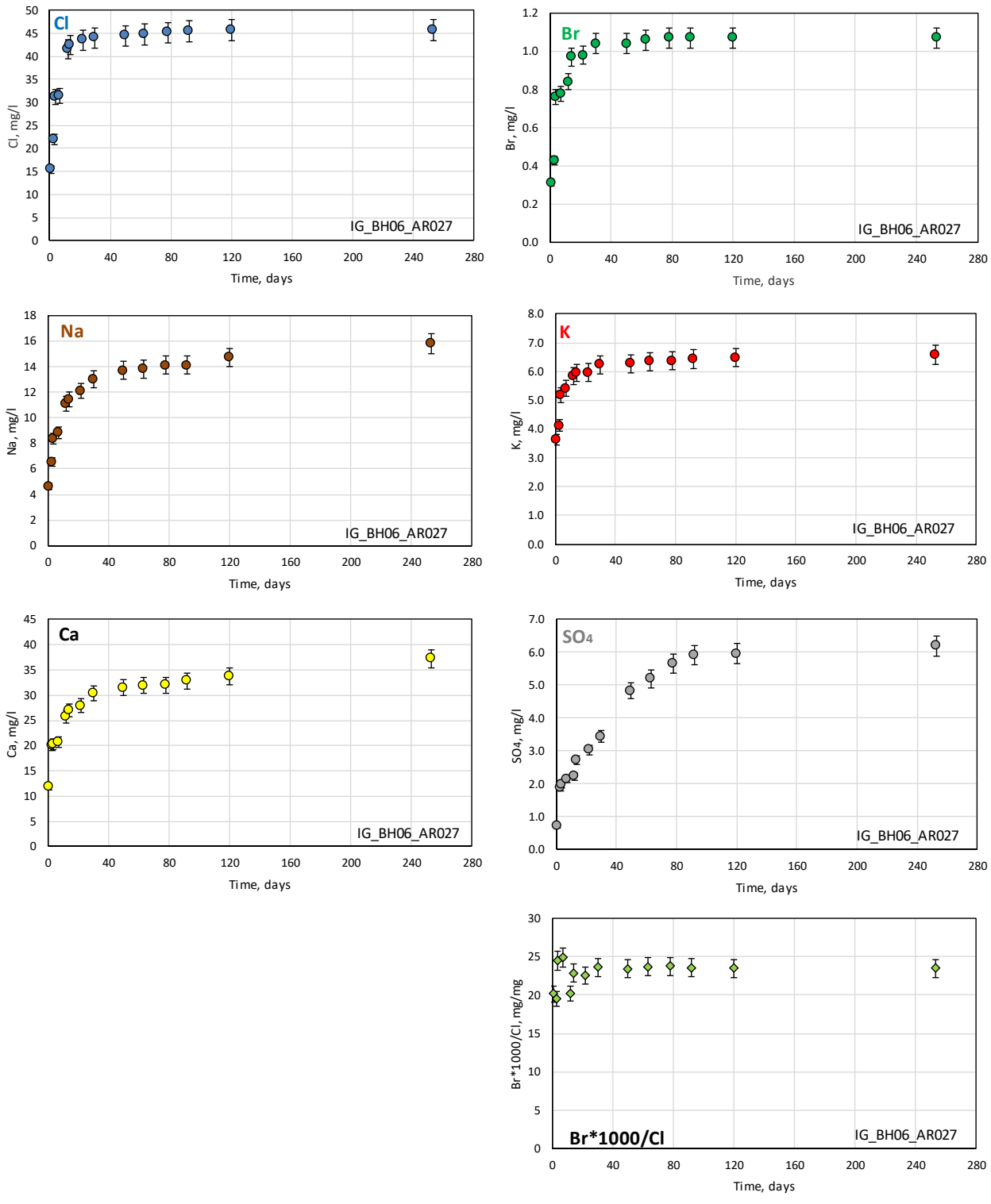


Figure 6-1 continued

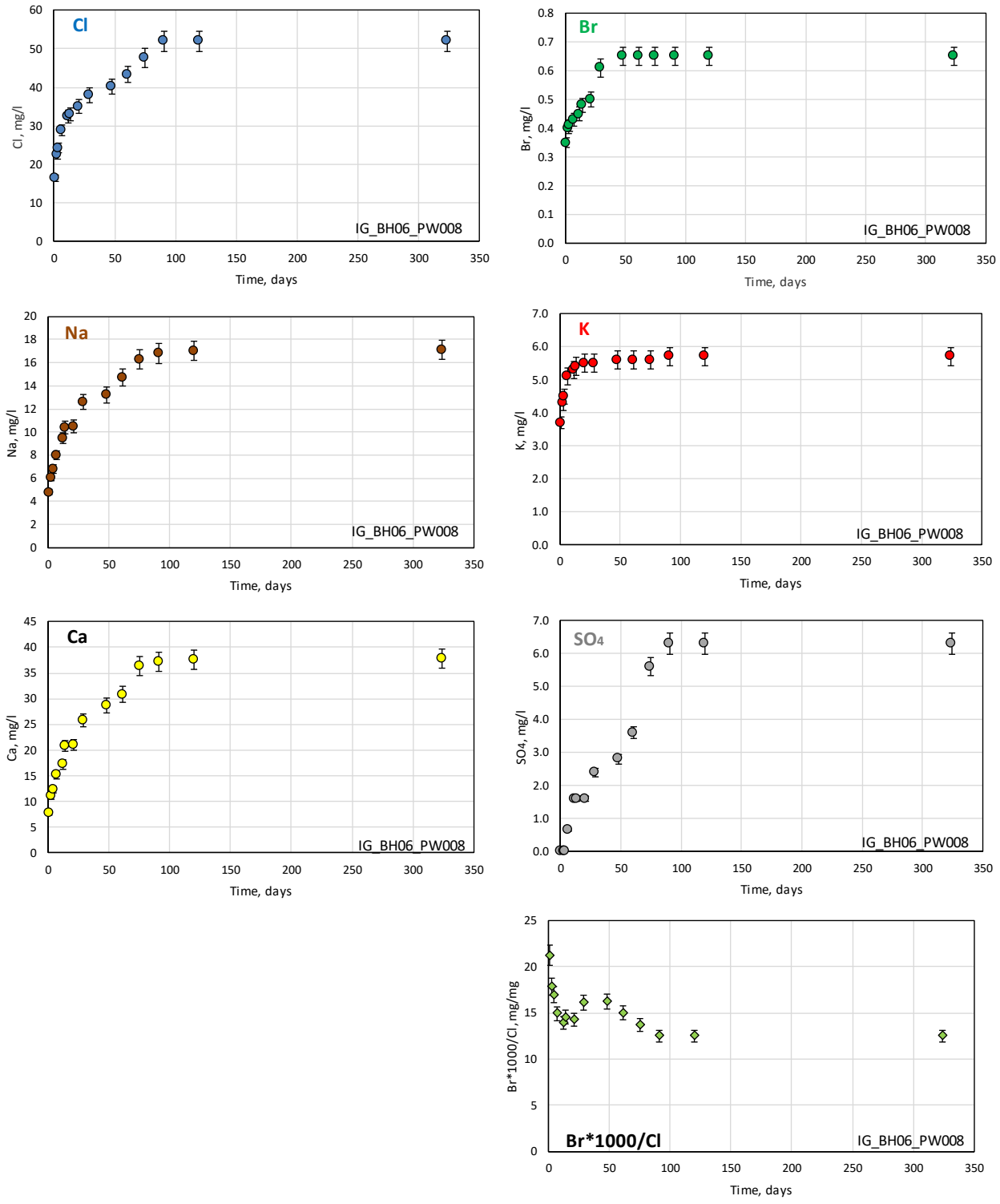


Figure 6-1 continued

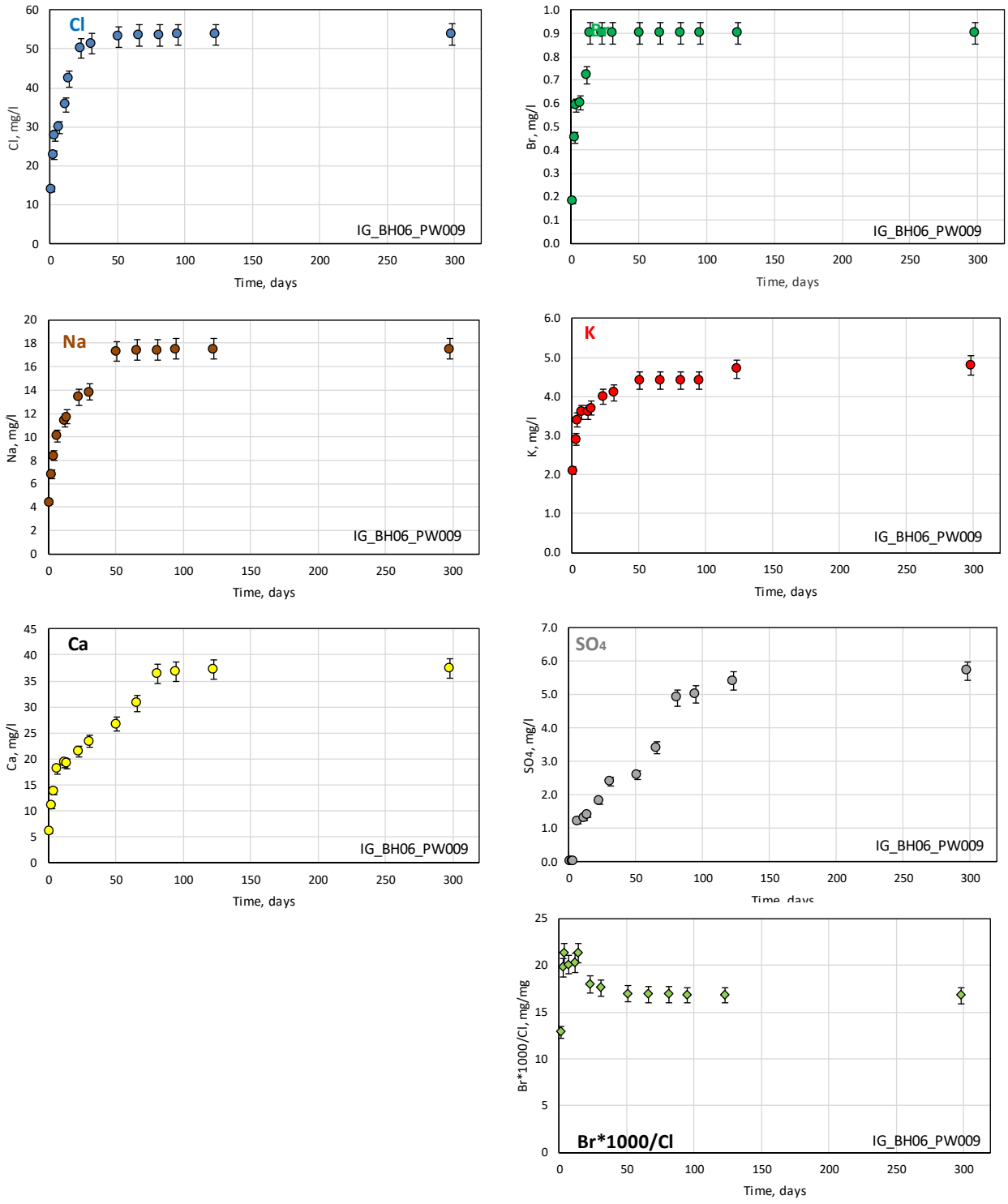


Figure 6-1 continued

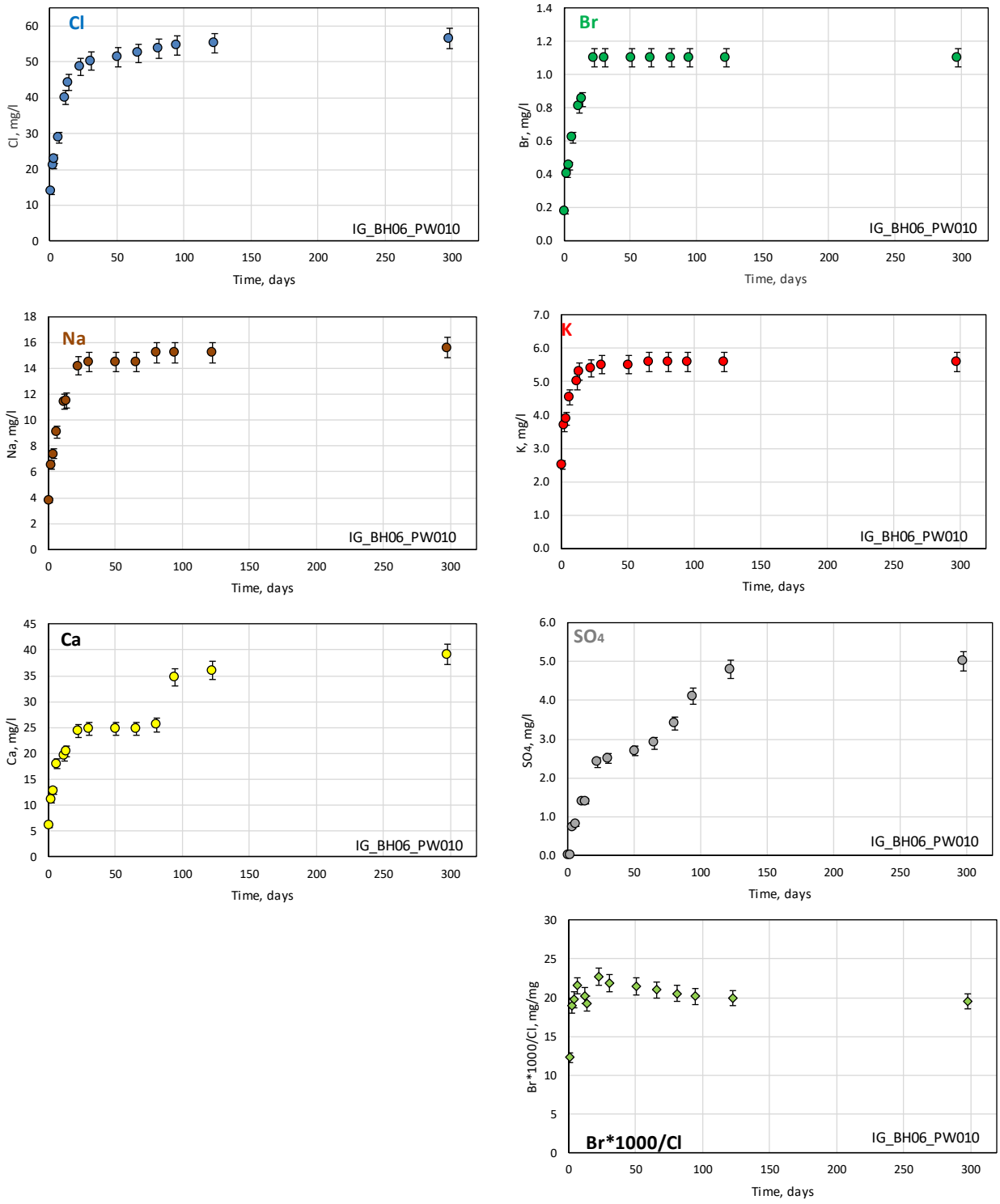


Figure 6-1 continued

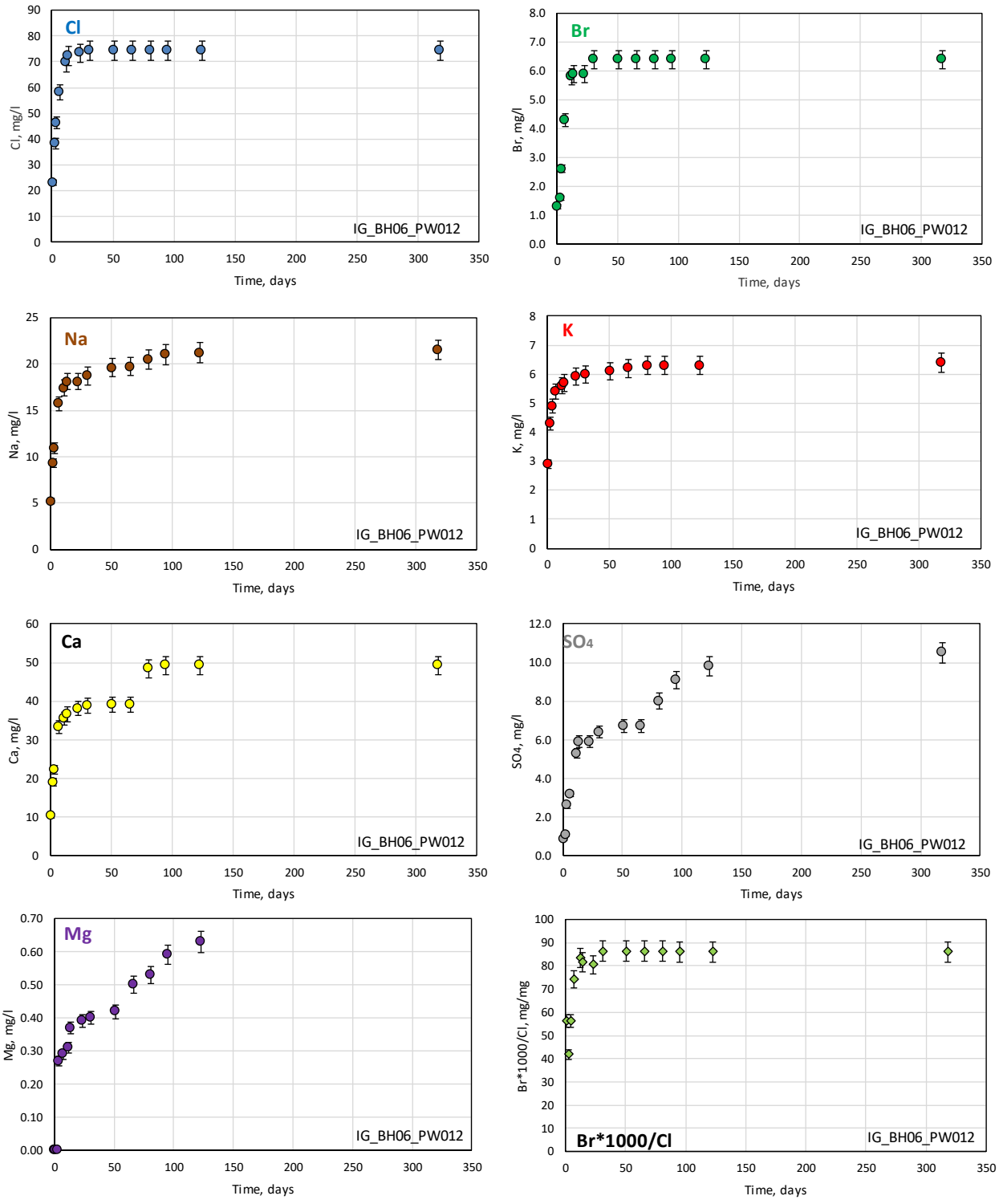


Figure 6-1 continued

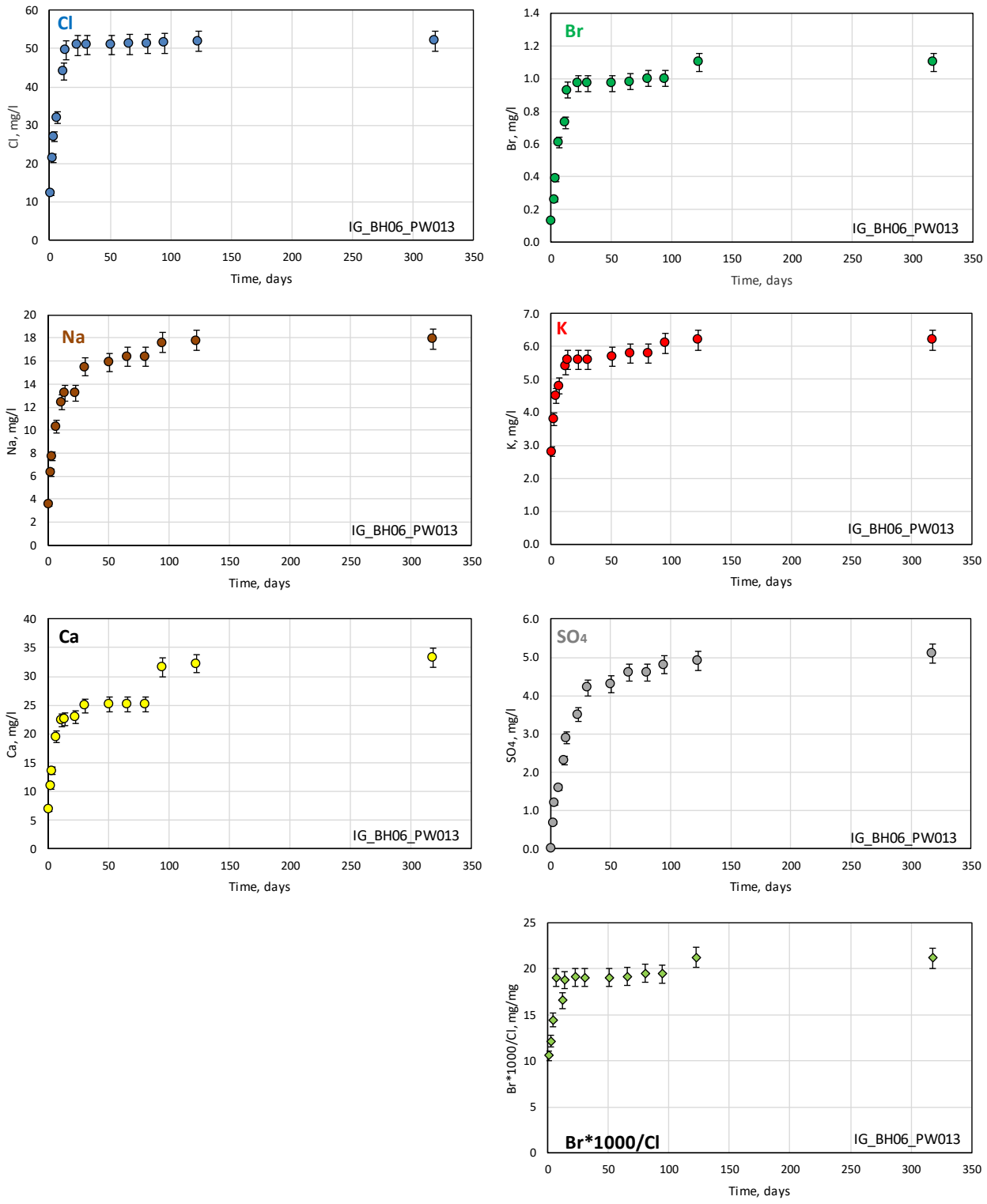


Figure 6-1 continued

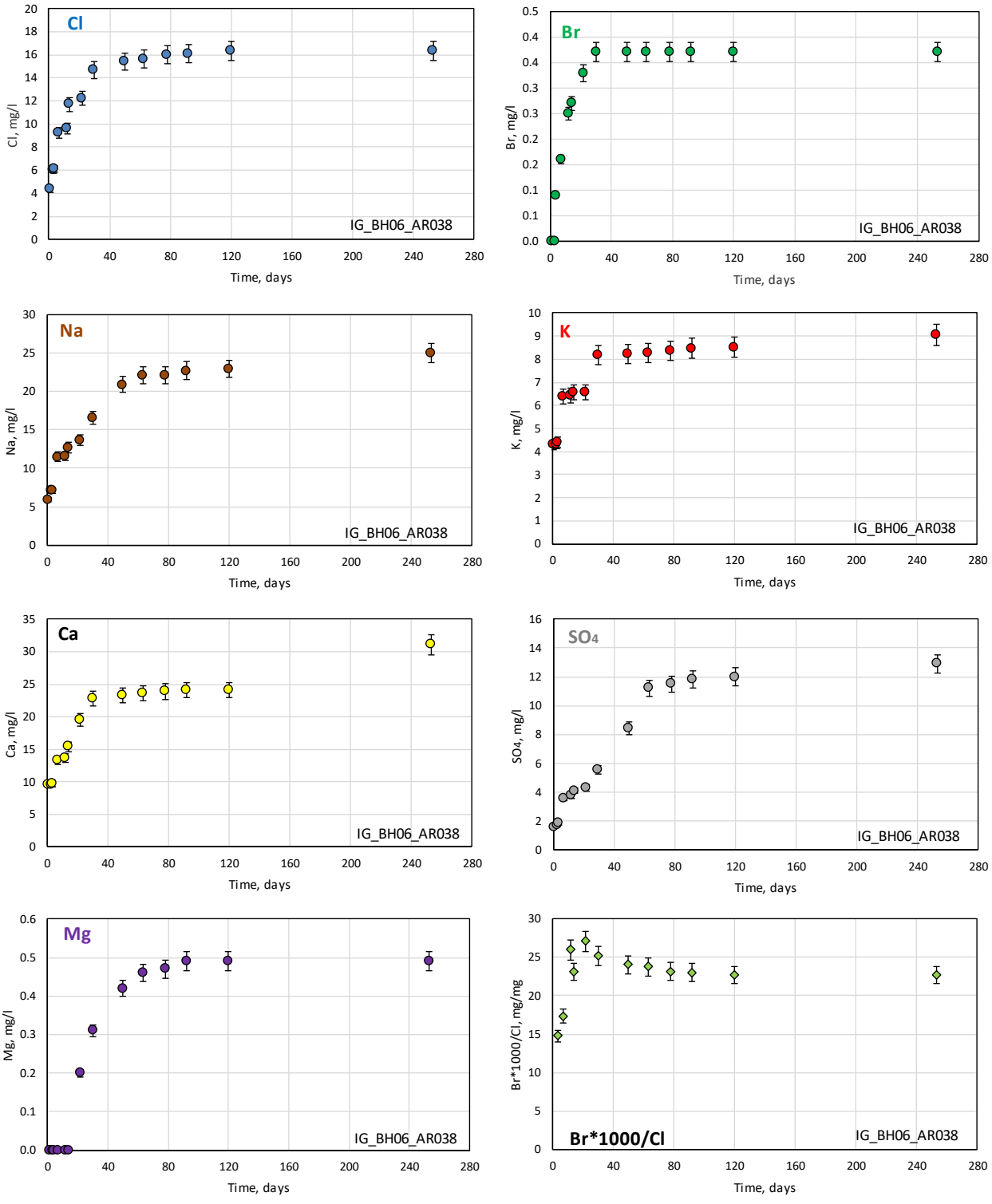


Figure 6-1 continued

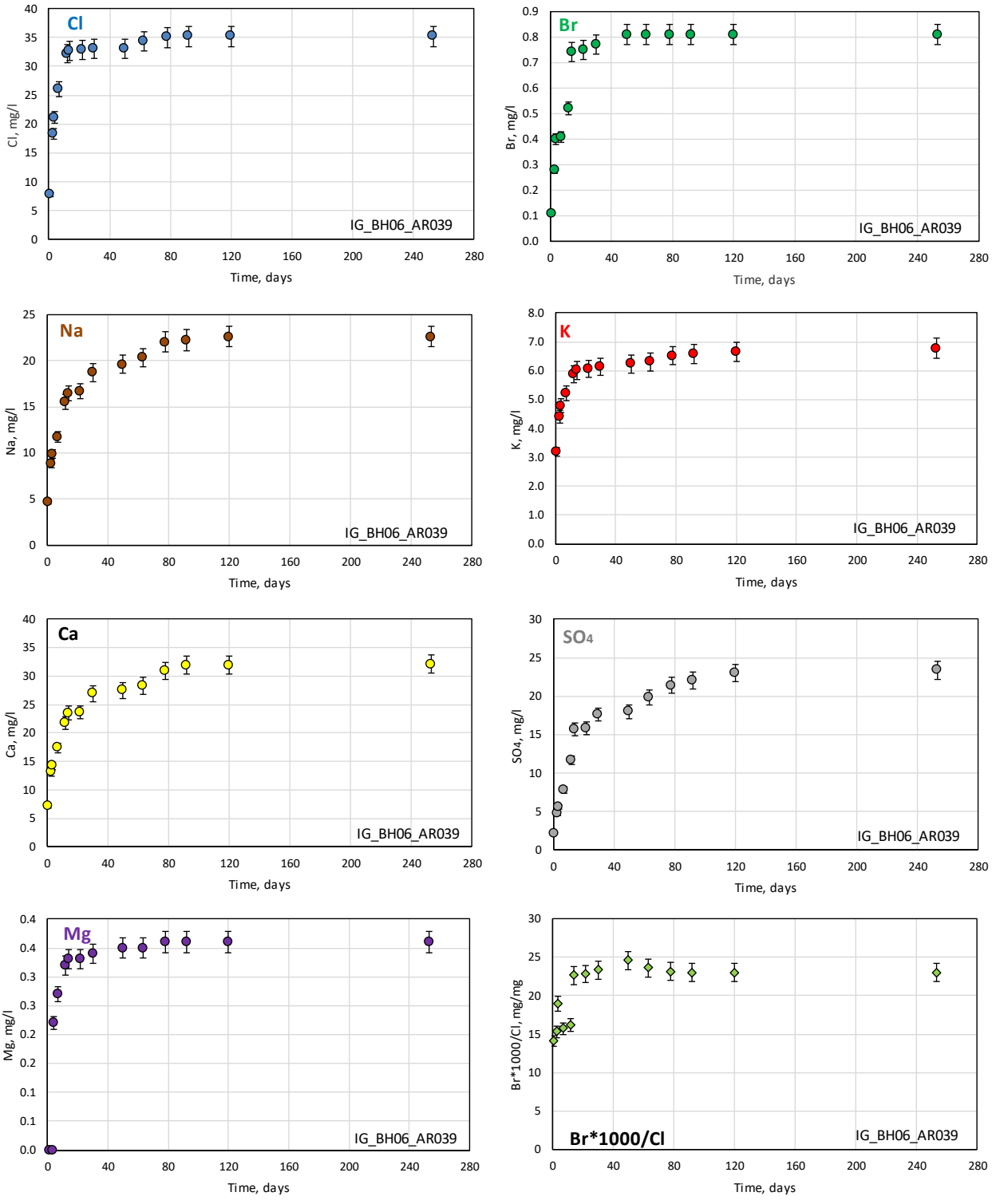


Figure 6-1 continued

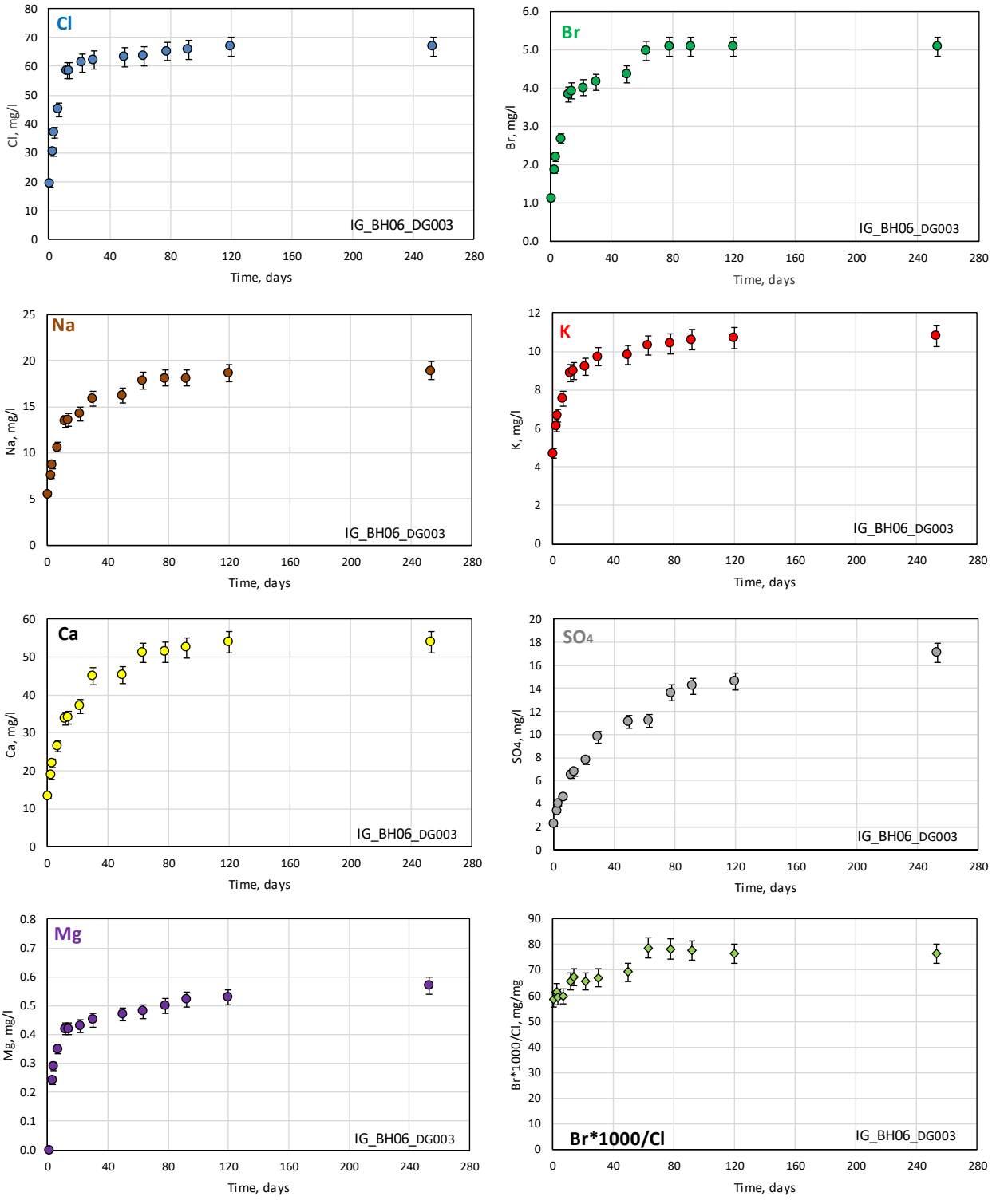


Figure 6-1 continued

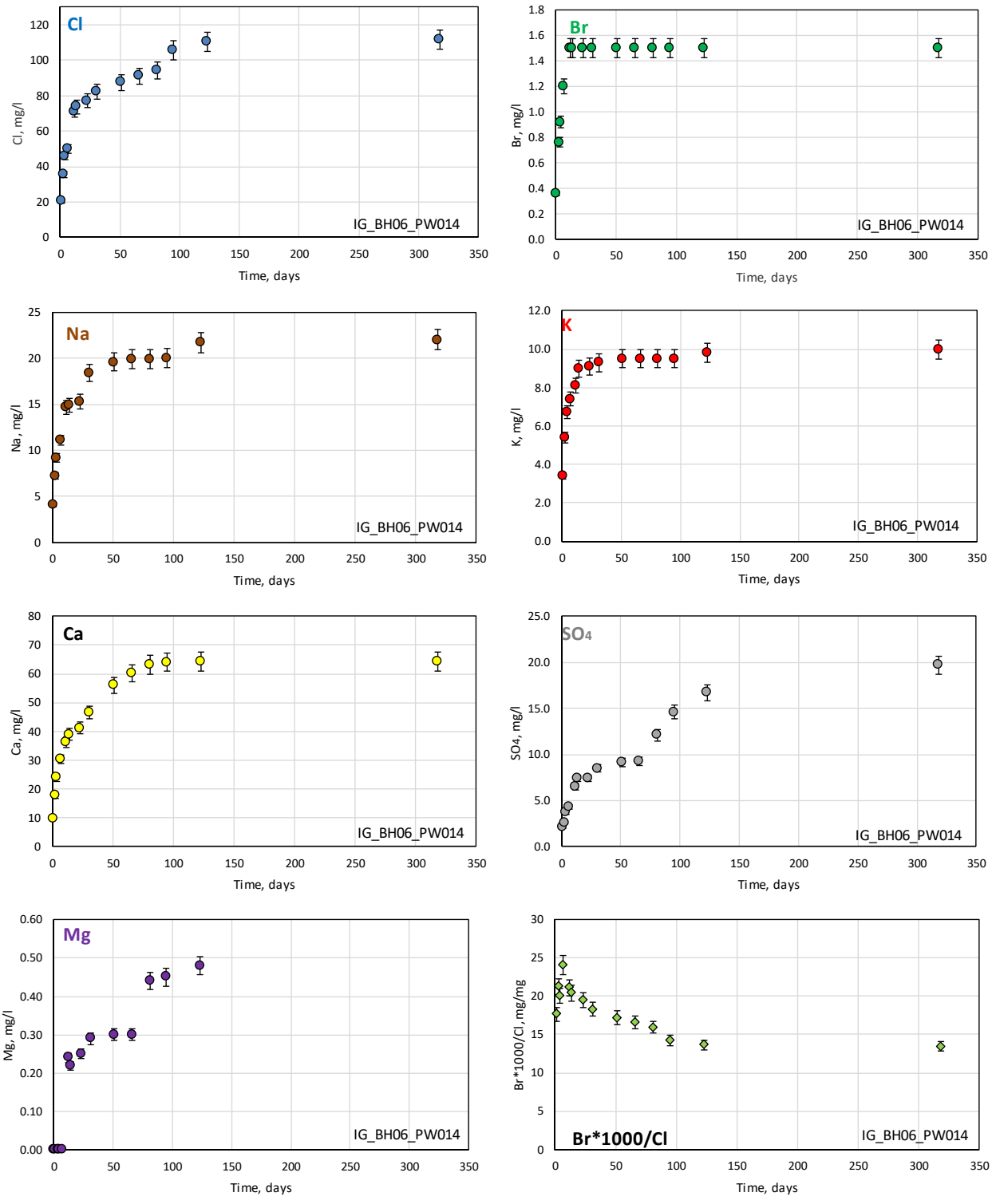


Figure 6-1 continued

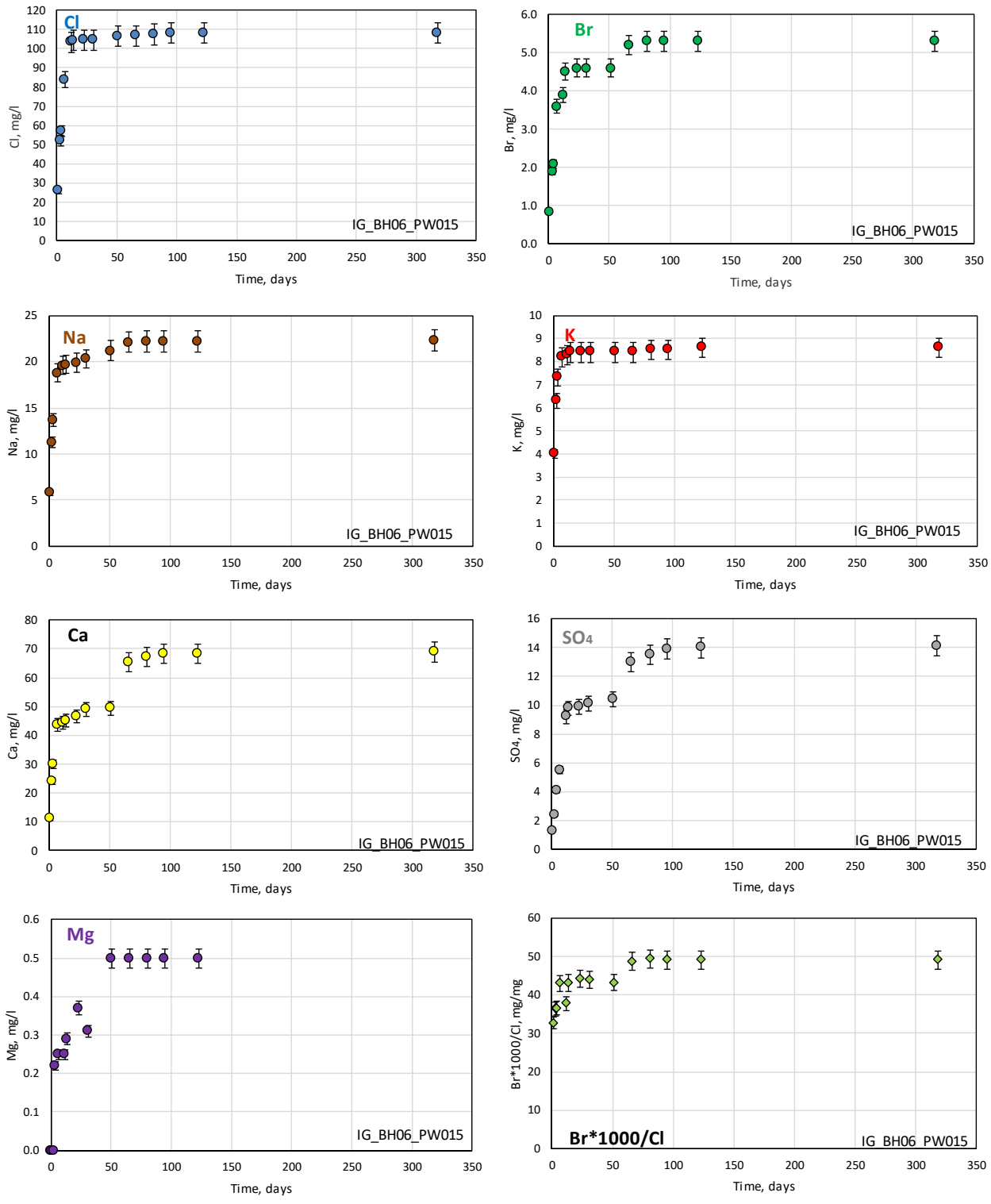


Figure 6-1 continued

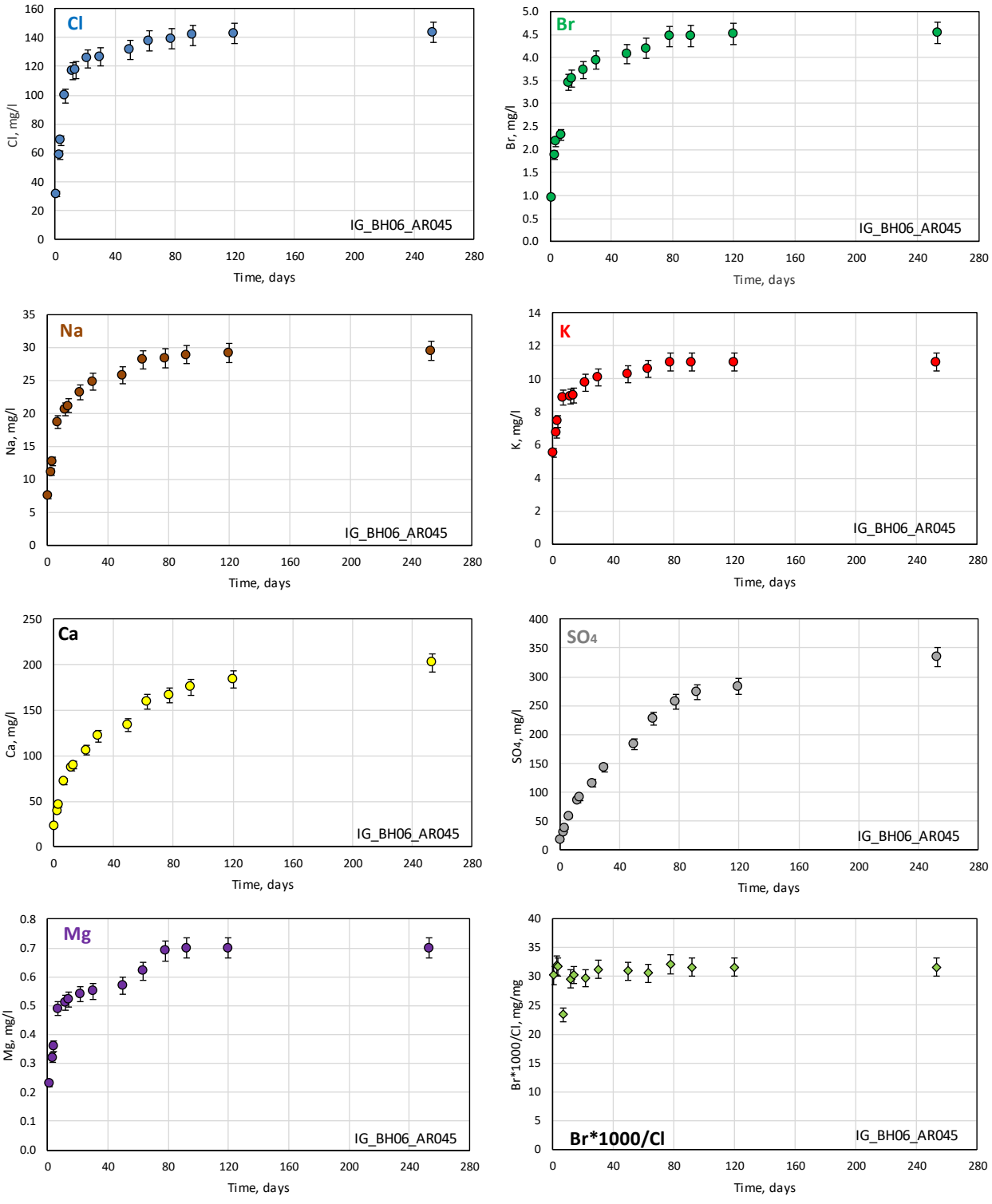


Figure 6-1 continued

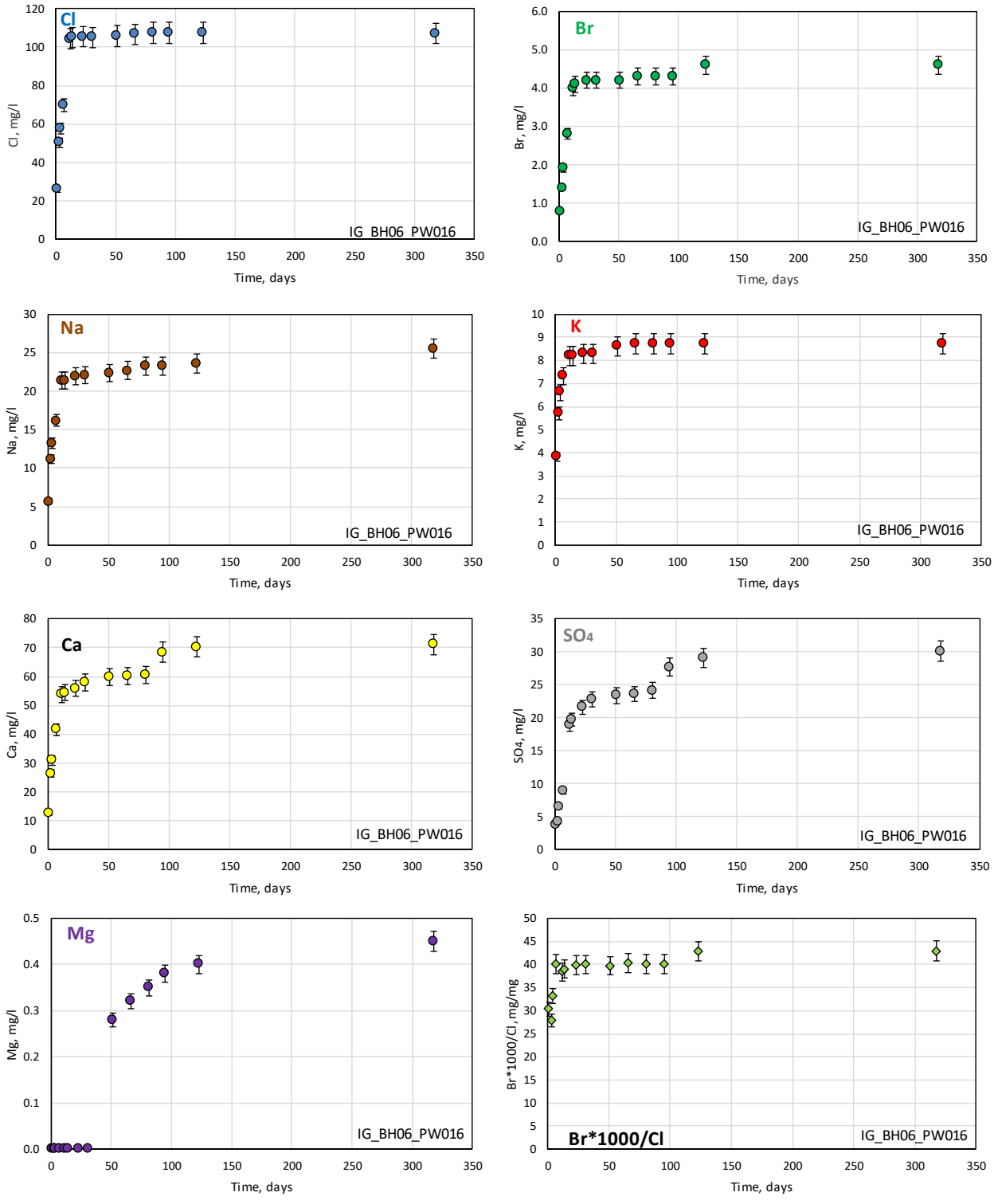


Figure 6-1 continued

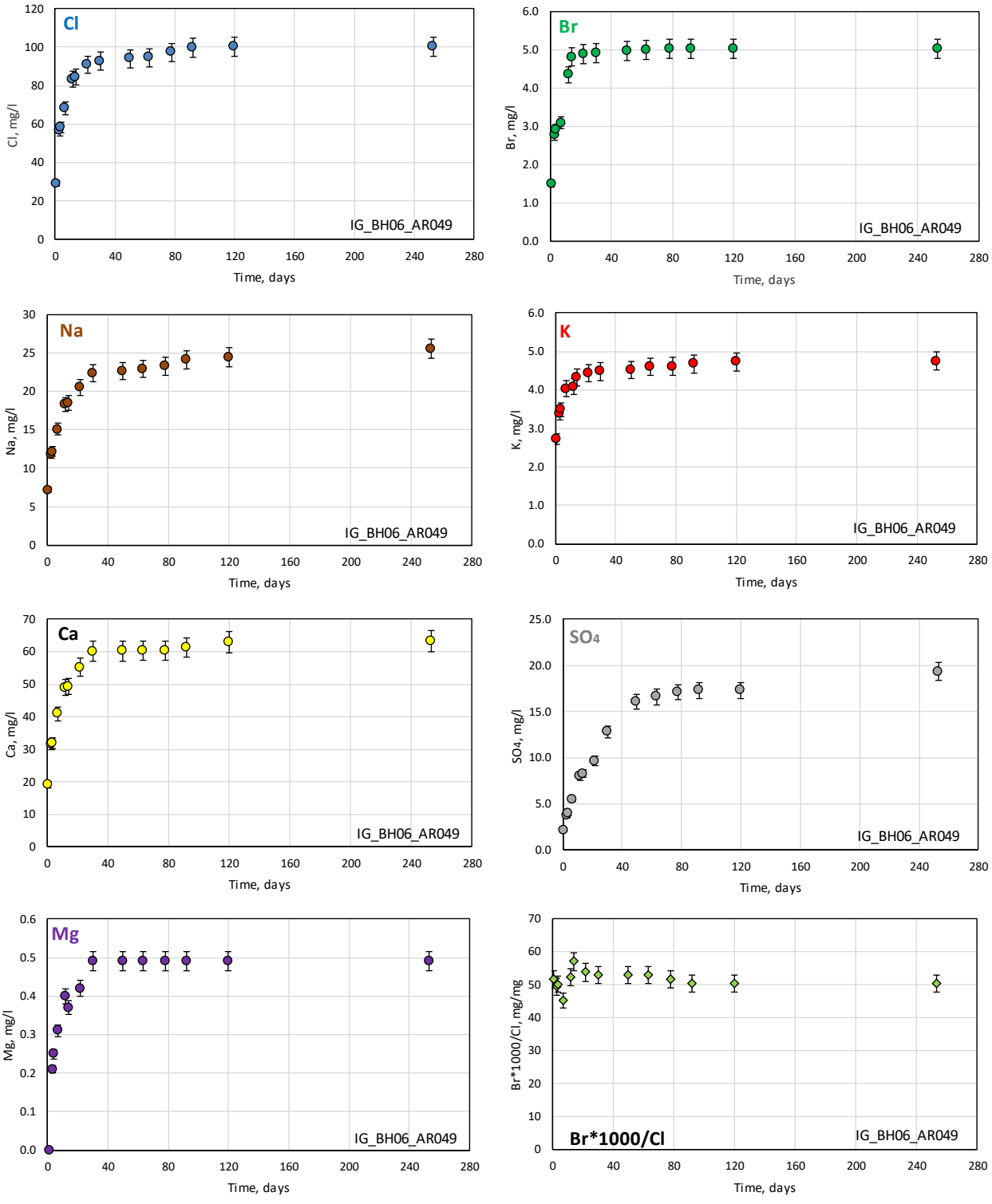


Figure 6-1 continued

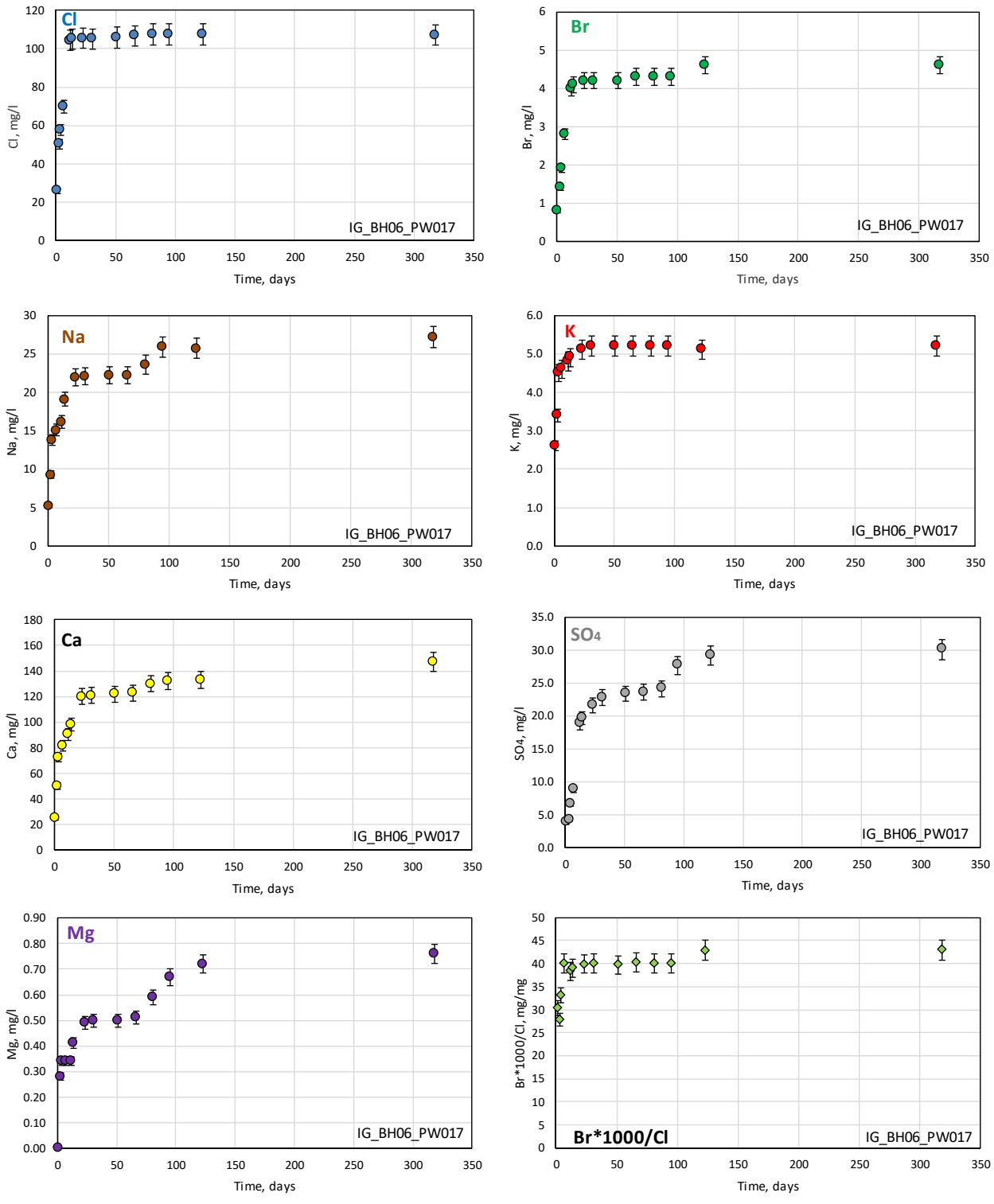


Figure 6-1 continued

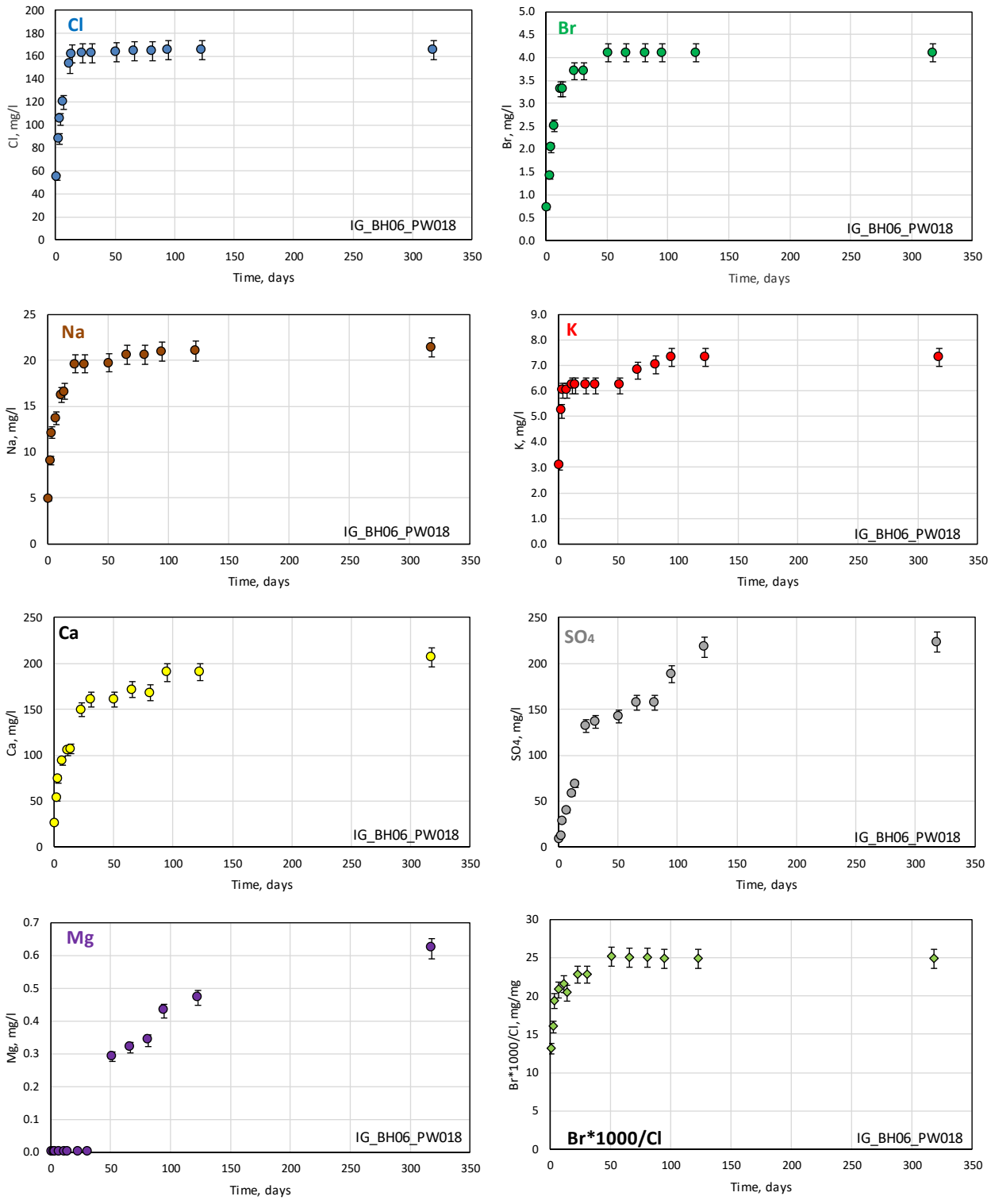


Figure 6-1 continued

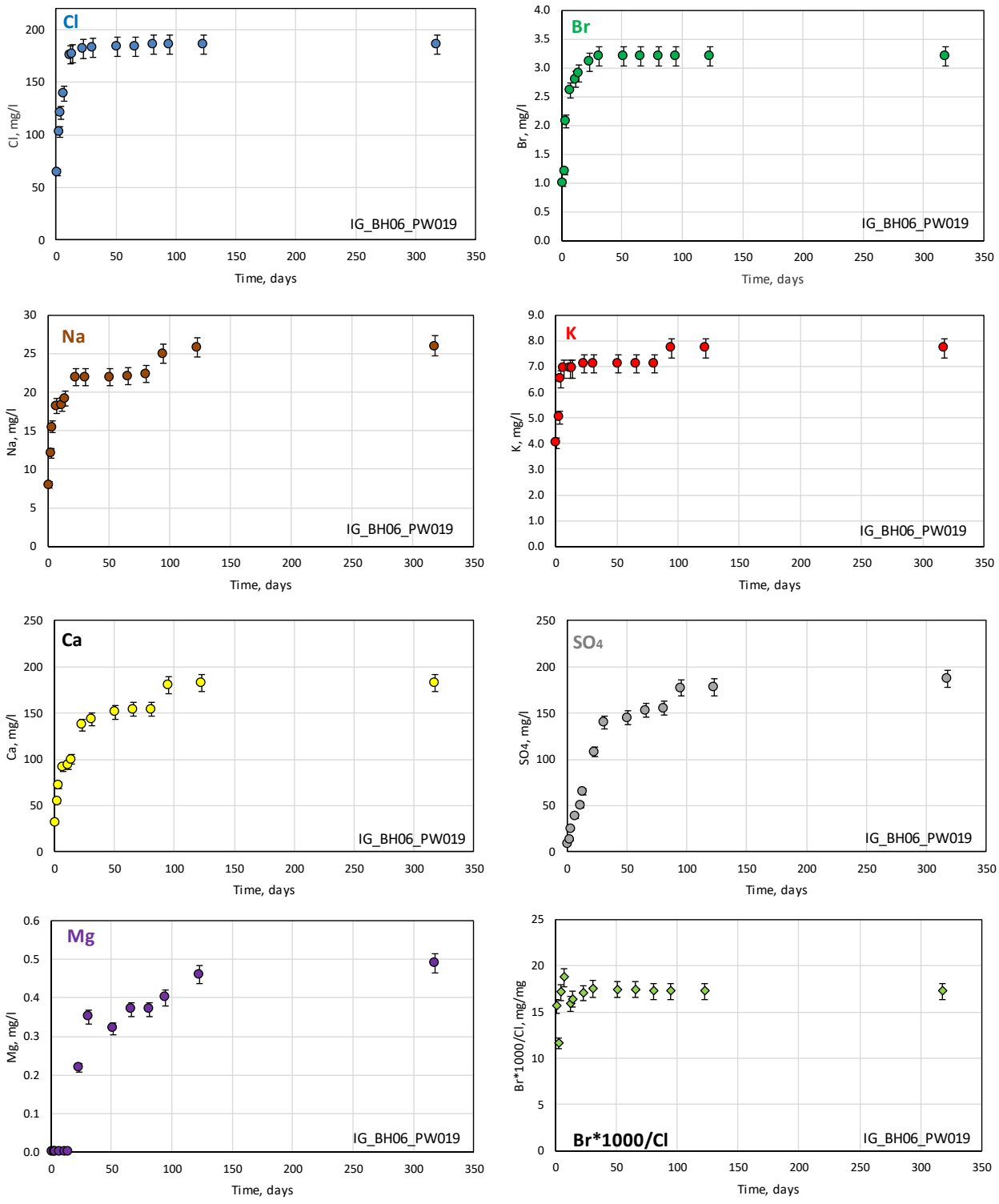


Figure 6-1 continued

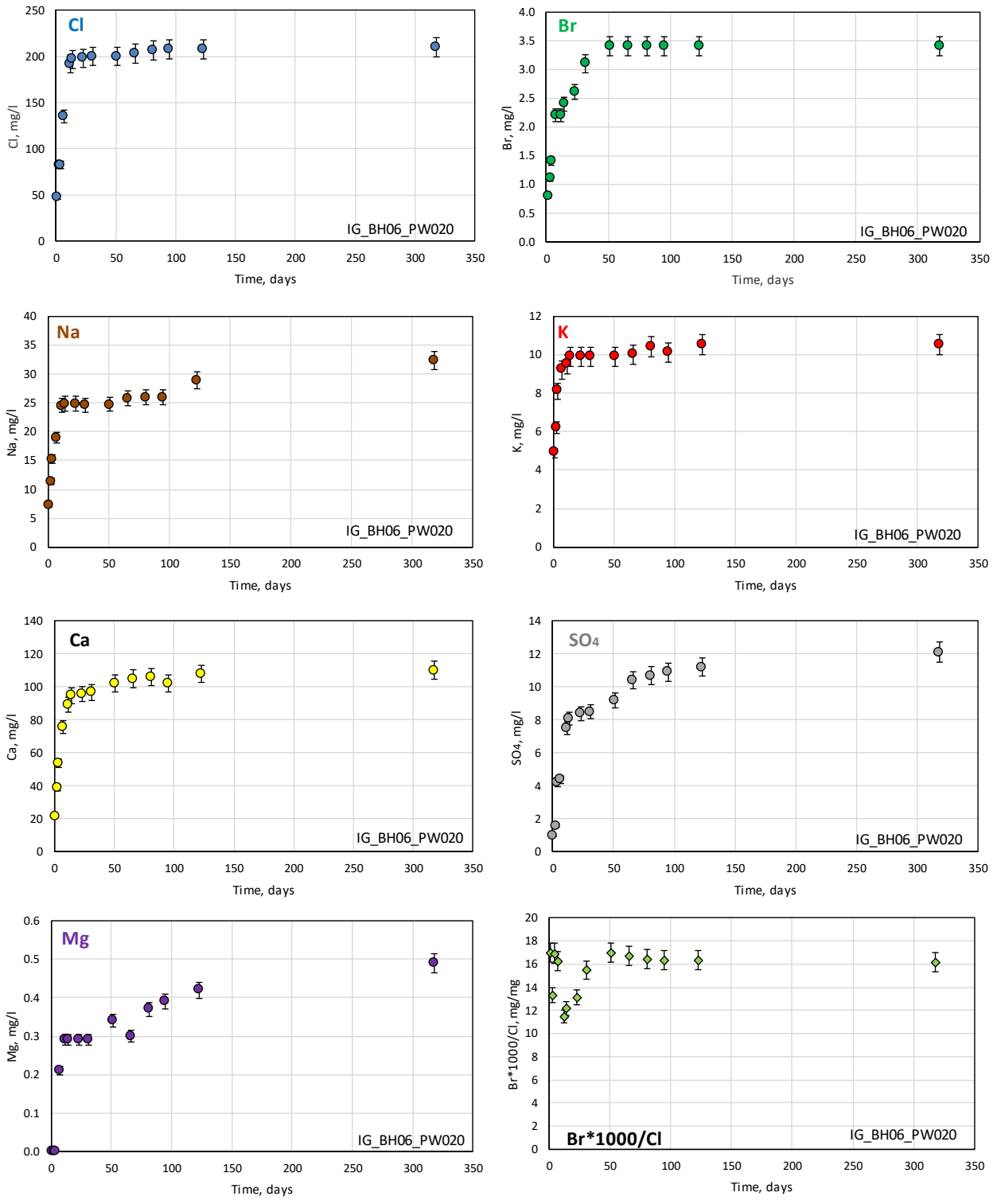


Figure 6-1 continued

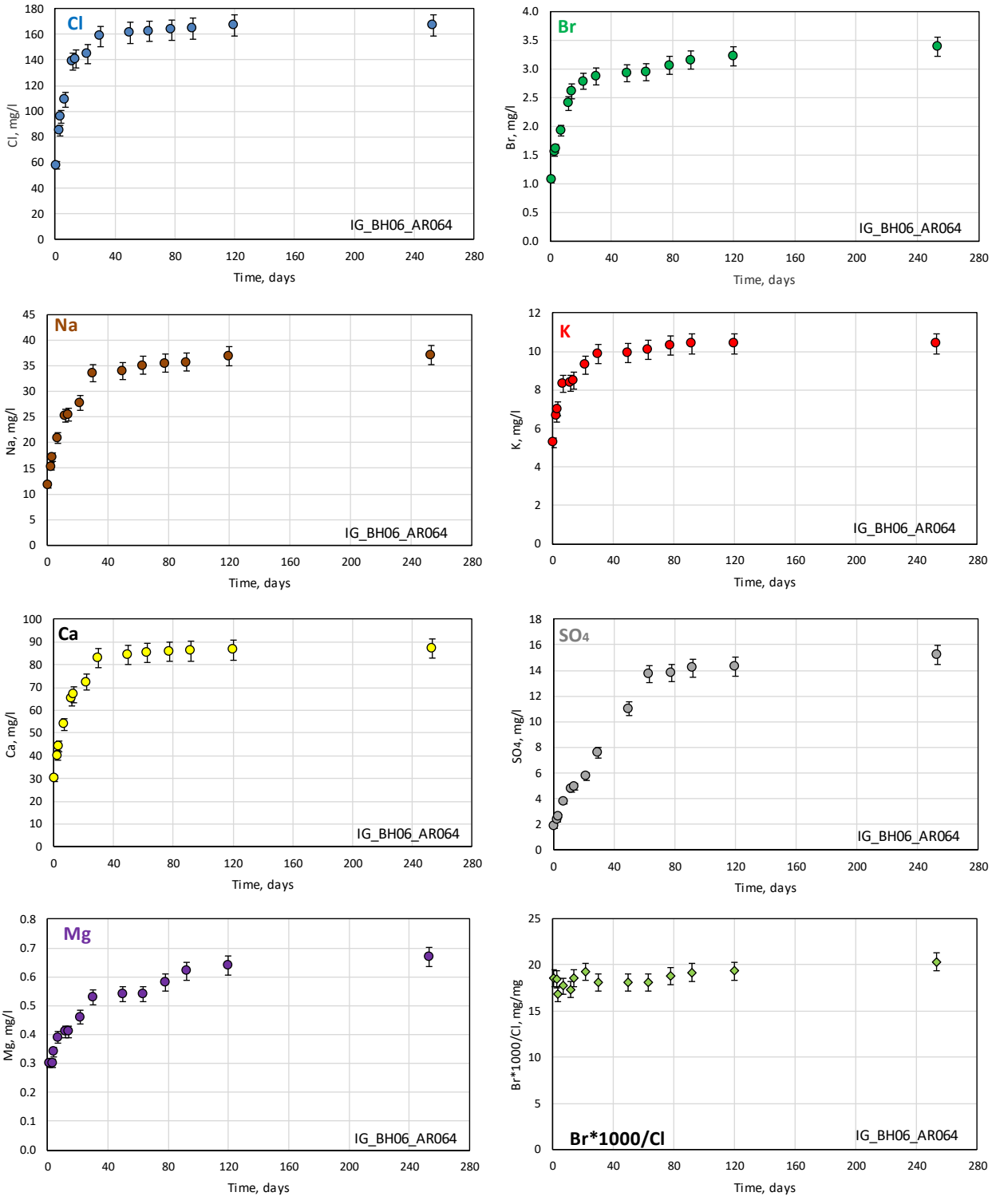


Figure 6-1 continued

6.2 Modelling of Pore Diffusion Coefficients

Chloride pore diffusion coefficients were derived by modelling the chloride breakthrough curves obtained from the out-diffusion experiments of all 31 samples from IG_BH06. The chloride breakthrough curves are deduced from the Cl contents in the small-sized sub-samples that were collected periodically during the out-diffusion experiments (Section 3.3.2, 6.1). The pore diffusion coefficient is obtained by fitting the observed data with an analytical solution for one-dimensional radial diffusion out of the cylinder into a well-mixed solution reservoir (Crank 1975). The applied model (T. Gimmi, RWI, University of Bern) is restricted to homogeneous hydraulic properties (porosity, diffusion coefficient) across the core cylinder, and cannot consider heterogeneous properties due to rock anisotropy or induced effects, such as a drilling disturbed zone and/or stress release (Meier et al., 2015).

The pore diffusion coefficient, D_p, of a solute in a geological media mainly depends on the shape and size of water conducting pores (constrictivity) and on the pathways given by the connected pore network (tortuosity, e.g., Ohlsson and Neretnieks 1995). It can be defined as

$$D_p = D_w \frac{\delta_D}{\tau^2} \qquad \text{eq. 8}$$

where D_P = pore-diffusion coefficient in m^2/s, D_W = diffusion coefficient in pure water in m^2/s, δ_D = constrictivity, τ = tortuosity, and the term δ_D/τ^2 is called the geometry factor.

In a first assumption the pore diffusion coefficient of a given species, D_P, can be converted to the effective diffusion coefficient of this species, D_e, according to

$$D_e = D_p \Phi_{WC} \qquad \text{eq. 9}$$

where D_e is the effective diffusion coefficient in m^2/s and Φ_{WC} the species-accessible porosity.

The shape of the Cl elution curves obtained for all core samples from IG_BH06 suggests a heterogeneous transport system from the rim to the centre of the core (Figure 6-2). The initial slopes are steeper (in the transient state) during the first five to ten days of out-diffusion than the more moderate slopes observed later in the experiments.

The quality of the D_P fits is controlled by the difference ($\Delta_{meas\text{-}mod}$) of the measured and modelled Cl concentration at equal time and shown graphically by logarithmic plots (Figure 6-2). To determine the lowest $\Delta_{meas\text{-}mod}$ values, a stepwise adjustment ($\pm 0.5*10^{-10} m^2/s$) of the single points was conducted and the $\Delta_{meas\text{-}mod}$ values were calculated for every measured point. The determination of the best fits per sampling point indicates a gradual decrease of the modelled pore diffusion coefficients as diffusion progresses deeper into the cores.

The modelled D_P values, which were determined at 45 °C, are additionally converted to 10 °C and 25°C by the Stoke-Einstein equation (Lide 1994). For the investigated core samples, the influence of the disturbed zone results in a pore diffusion coefficient that is a factor 1.8 to 5.7 higher than that of the inner core (Table 6-1, Figure 6-2).

The average pore diffusion coefficients (D_P) of the 31 crystalline core samples vary between 0.3 and $1.2*10^{-10}$ m^2/s (10 °C), resulting in effective diffusion coefficients (D_e) between 0.1 and $0.6*10^{-12}$ m^2/s (10 °C) (Table 6-1, Figure 6-2).

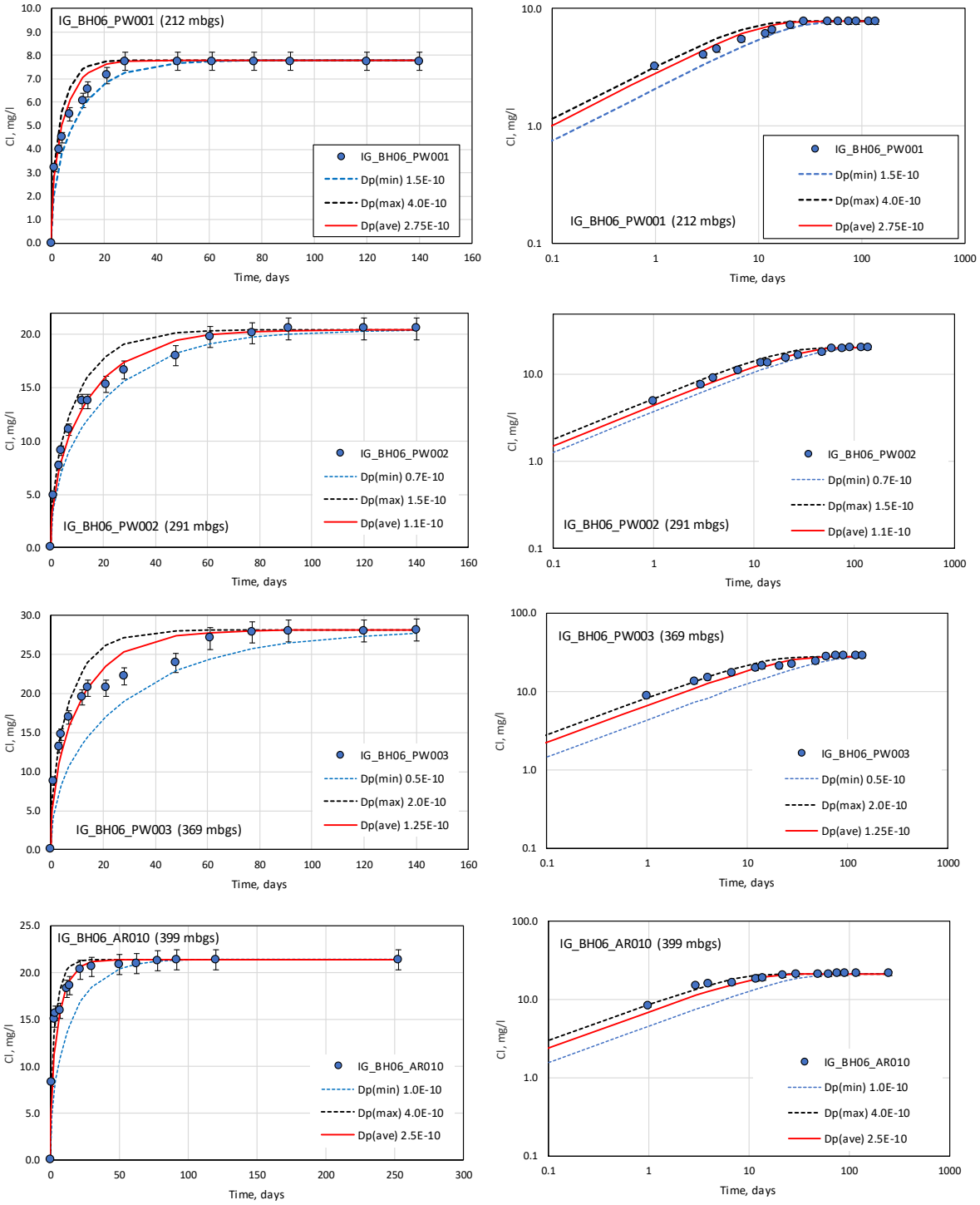


Figure 6-2: Maximum (Dp(max)) and minimum (Dp(min)) pore diffusion coefficients (45 °C) determined ba a best fit of Cl elution curves in linear and logarithmic time and concentration scale; the solid lines mark the average diffusion coefficients (45 °C, Dp (ave))

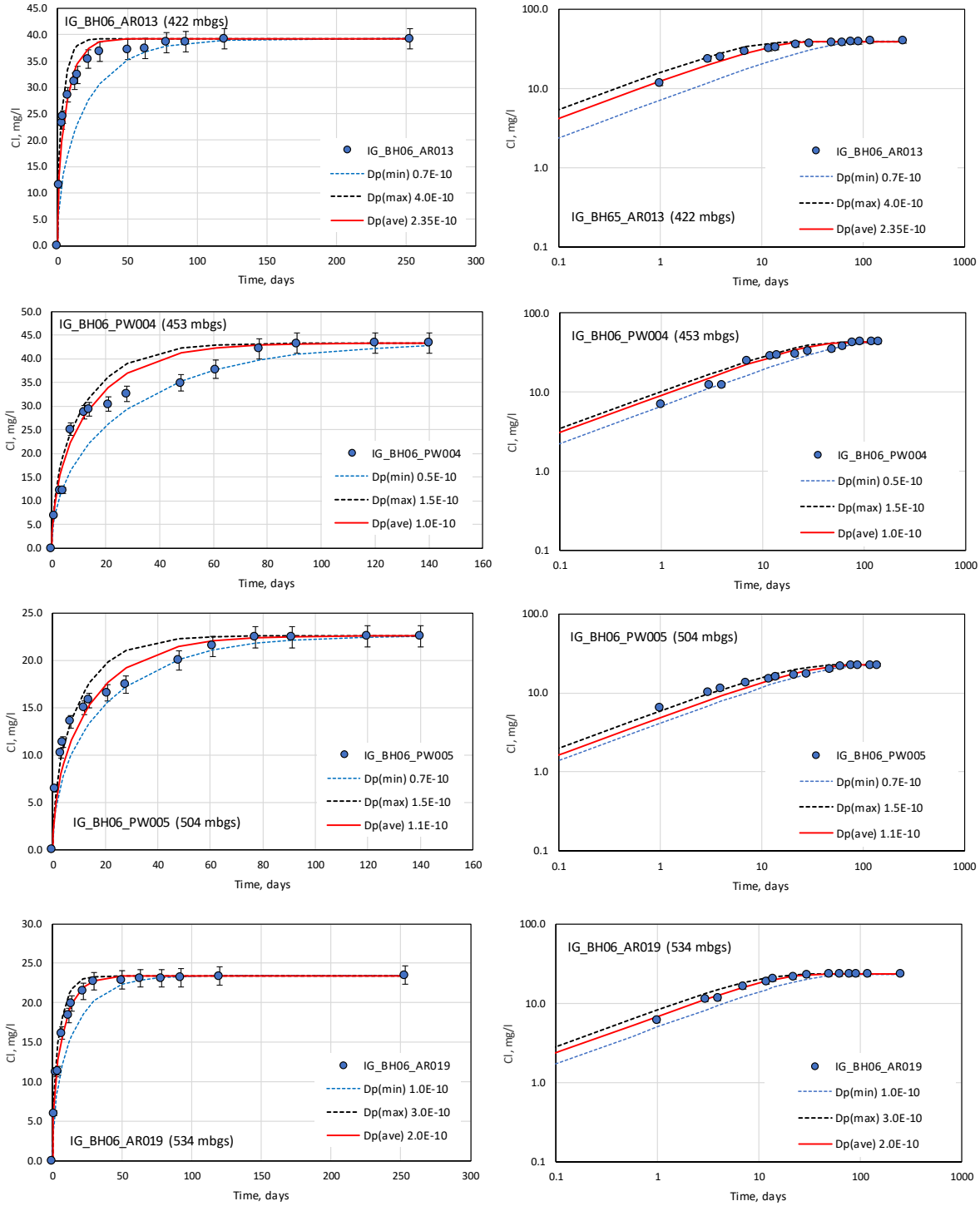


Figure 6-2 continued

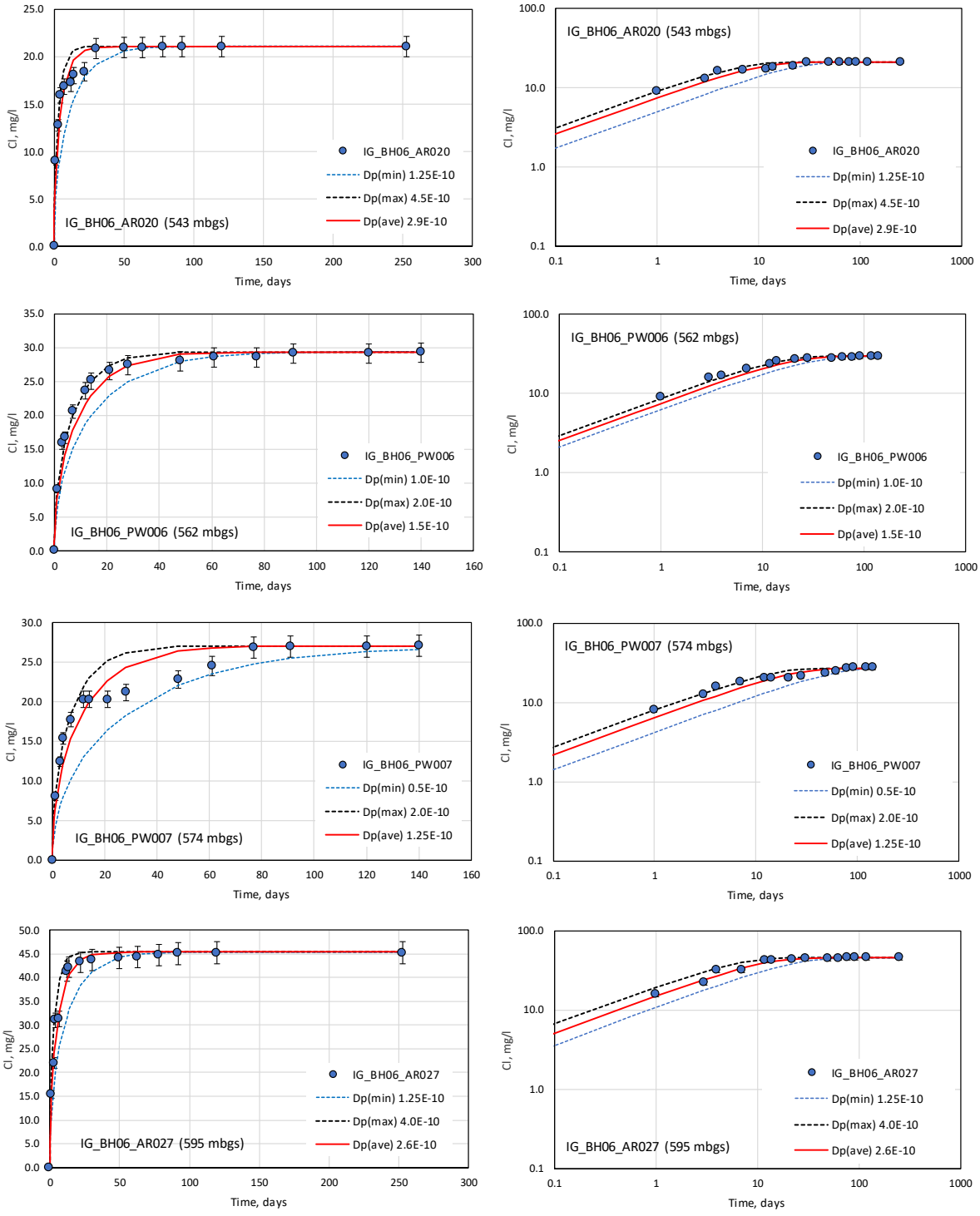


Figure 6-2 continued

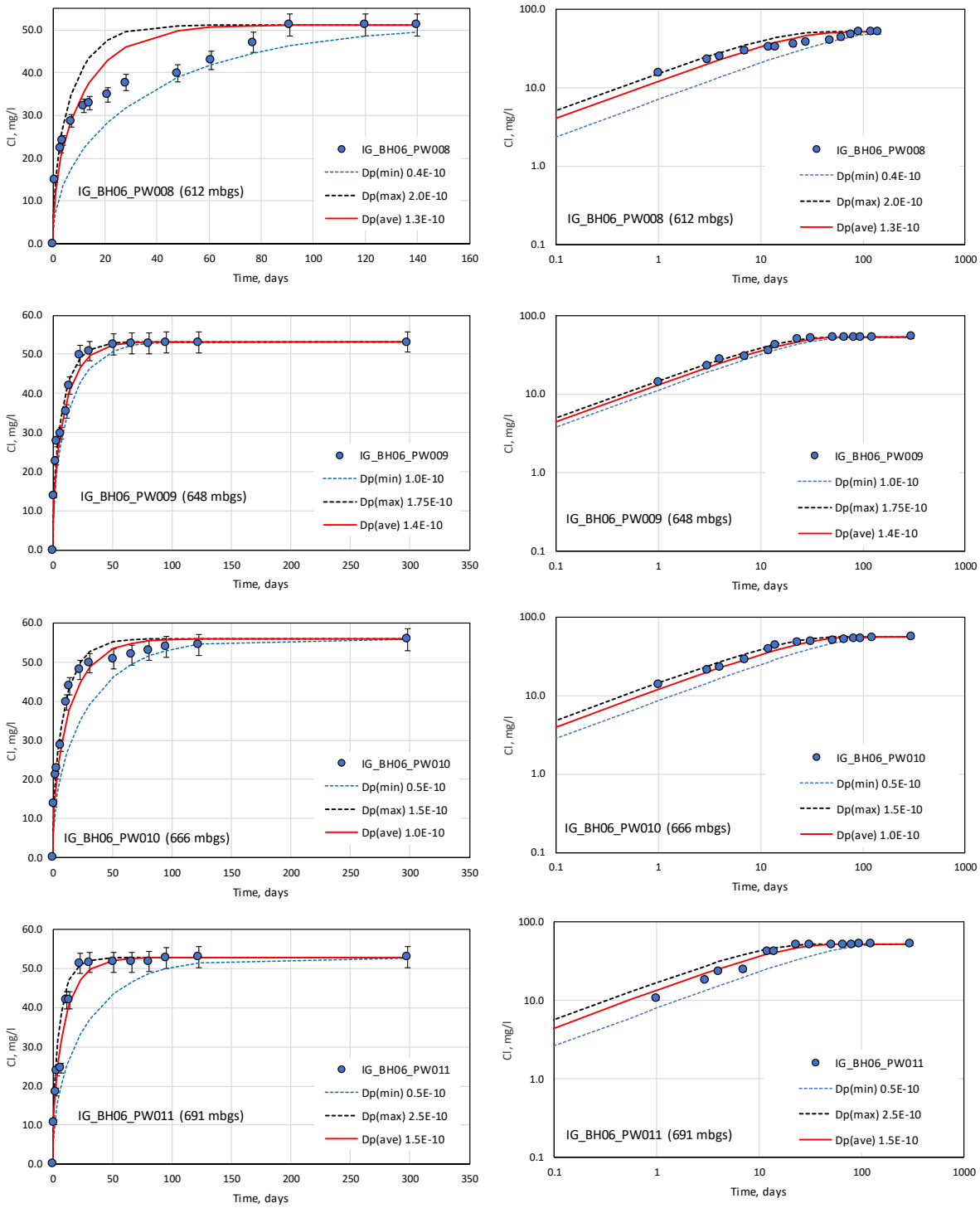


Figure 6-2 continued

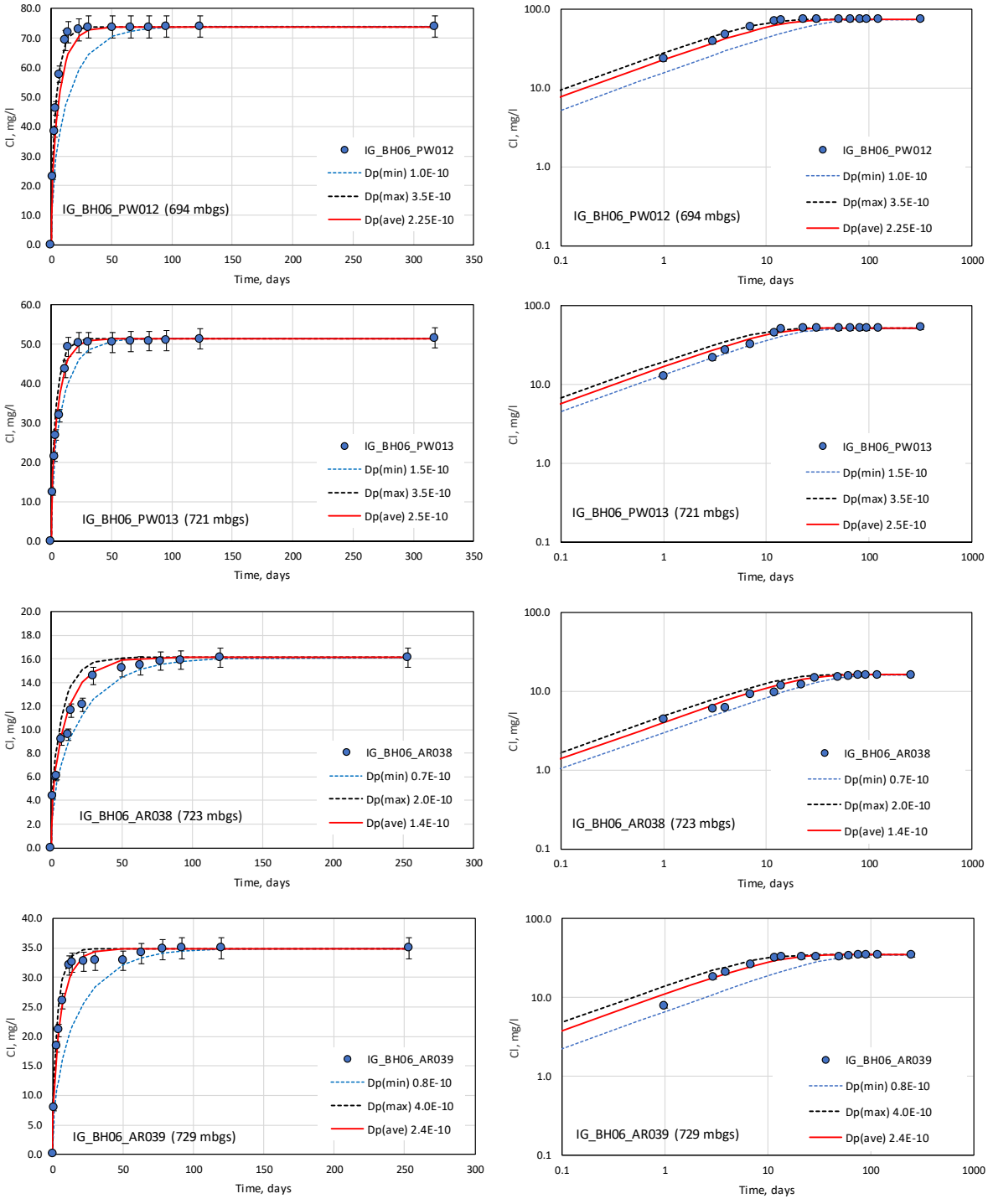


Figure 6-2 continued

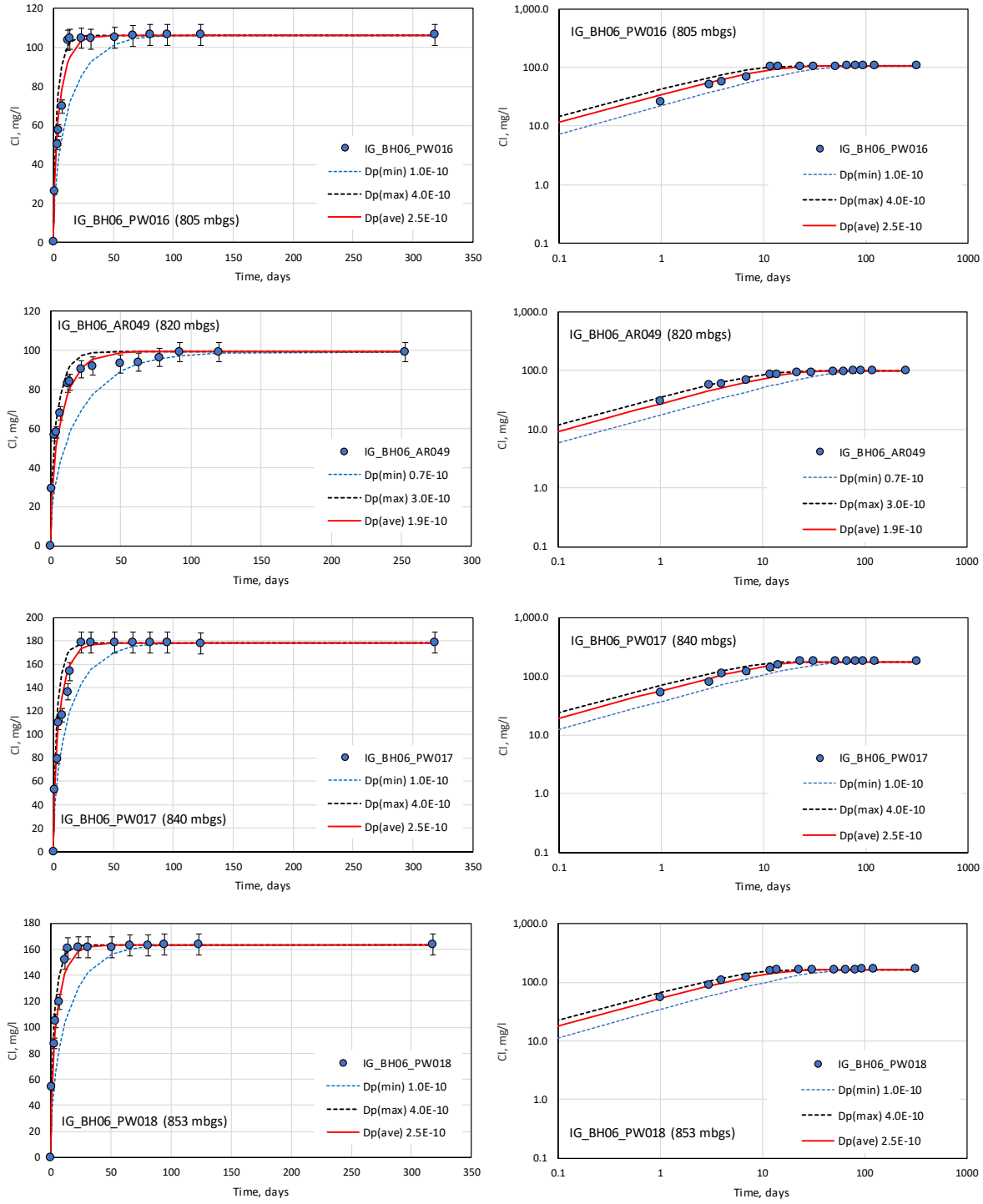


Figure 6-2 continued

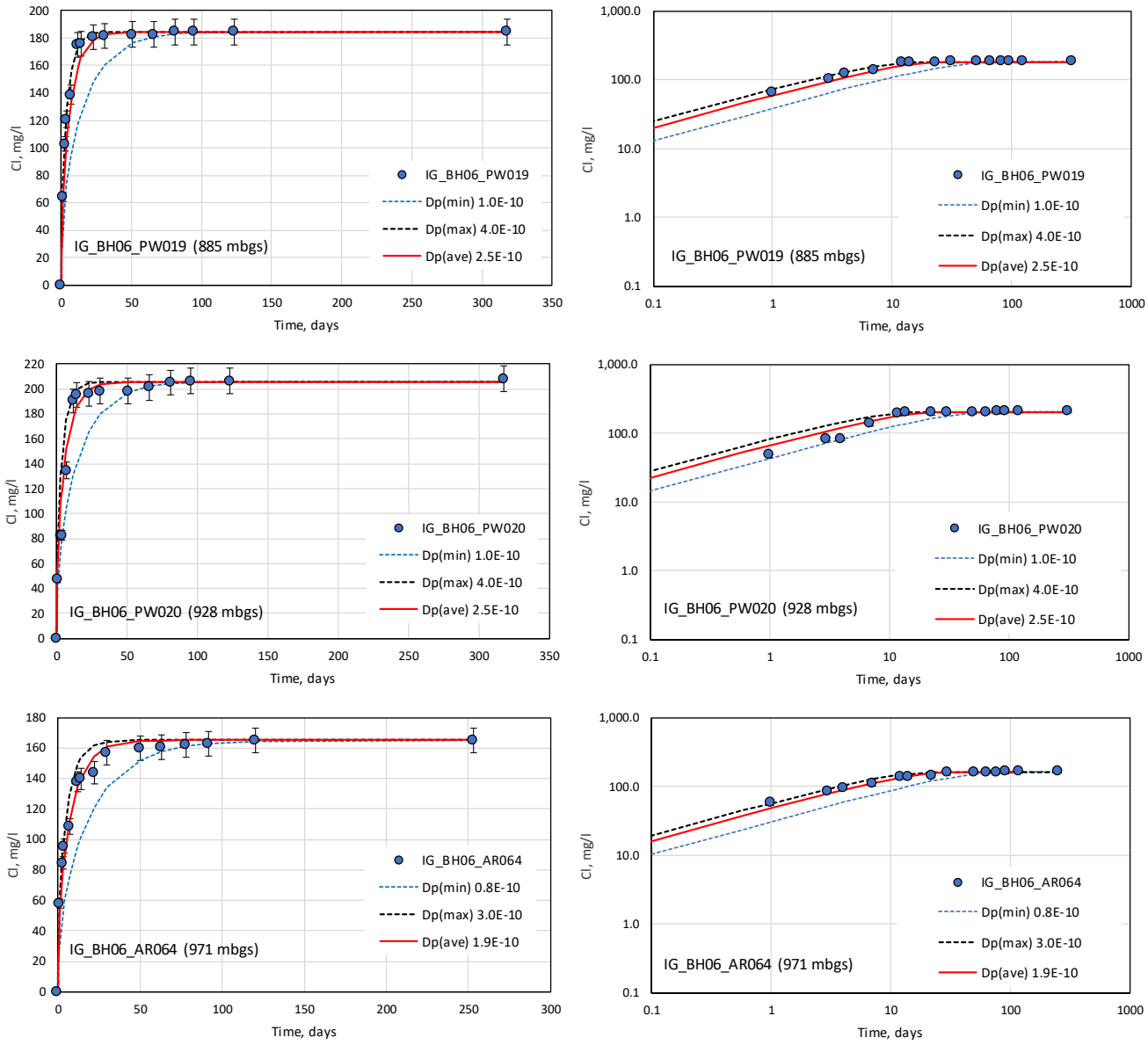


Figure 6-2 continued

Table 6-1: Minimum (min), maximum (max) and average (avg) pore and effective diffusion coefficients determined by 1-dimensional modelling of Cl elution curves of out-diffusion experiments on core samples from IG_BH06 at 45 °C and calculated by the Stoke-Einstein-equation for 10 °C and 25 °C; G / T = granodiorite / tonalite; A = amphibolite; T = feldspar phyric tonalite.

Sample	Depth	Lithology	WL-Porosity	D(P)*10^{-10} (45 °C)			D(P)*10^{-10} (10 °C)			D(e)*10^{-12} (10 °C)			D(P)*10^{-10} (25 °C)			D(e)*10^{-12} (25 °C)		
				max	min	avg	max	min	avg	max	min	avg	max	min	avg	max	min	avg
	mbgs		Vol.%	m^2/s			m^2/s			m^2/s			m^2/s			m^2/s		
IG_BH06_PW001	212.3	G / T	0.55	4.0	1.5	2.8	1.6	0.6	1.1	0.9	0.3	0.6	2.5	0.9	1.7	1.4	0.5	1.0
IG_BH06_PW002	291.5	G / T	0.47	1.5	0.7	1.1	0.6	0.3	0.4	0.3	0.1	0.2	0.9	0.4	0.7	0.4	0.2	0.3
IG_BH06_PW003	253.2	G / T	0.52	2.0	0.5	1.3	0.8	0.2	0.5	0.4	0.1	0.3	1.3	0.3	0.8	0.7	0.2	0.4
IG_BH06_AR010	398.7	T	0.20	4.0	1.0	2.5	1.6	0.4	1.0	0.3	0.1	0.2	2.5	0.6	1.6	0.5	0.1	0.3
IG_BH06_AR013	421.6	G / T	0.43	4.0	0.7	2.4	1.6	0.3	1.0	0.7	0.1	0.4	2.5	0.4	1.5	1.1	0.2	0.6
IG_BH06_PW004	453.2	G / T	0.45	1.5	0.5	1.0	0.6	0.2	0.4	0.3	0.1	0.2	0.9	0.3	0.6	0.4	0.1	0.3
IG_BH06_PW005	504.1	G / T	0.52	1.5	0.7	1.1	0.6	0.3	0.4	0.3	0.1	0.2	0.9	0.4	0.7	0.5	0.2	0.4
IG_BH06_AR019	534.0	G / T	0.42	3.0	1.0	2.0	1.2	0.4	0.8	0.5	0.2	0.3	1.9	0.6	1.3	0.8	0.3	0.5
IG_BH06_AR020	542.9	G / T	0.49	4.5	1.3	2.9	1.8	0.5	1.2	0.9	0.2	0.6	2.8	0.8	1.8	1.4	0.4	0.9
IG_BH06_PW006	562.4	G / T	0.52	2.0	1.0	1.5	0.8	0.4	0.6	0.4	0.2	0.3	1.3	0.6	0.9	0.6	0.3	0.5
IG_BH06_PW007	574.2	G / T	0.50	2.0	0.5	1.3	0.8	0.2	0.5	0.4	0.1	0.3	1.3	0.3	0.8	0.6	0.2	0.4
IG_BH06_AR027	595.0	G / T	0.49	4.0	1.3	2.6	1.6	0.5	1.1	0.8	0.2	0.5	2.5	0.8	1.6	1.2	0.4	0.8
IG_BH06_PW008	612.2	G / T	0.46	2.0	0.4	1.2	0.8	0.2	0.5	0.4	0.1	0.2	1.3	0.3	0.8	0.6	0.1	0.3
IG_BH06_PW009	647.9	G / T	0.39	1.8	1.0	1.4	0.7	0.4	0.6	0.3	0.2	0.2	1.1	0.6	0.9	0.4	0.2	0.3
IG_BH06_PW010	665.9	G / T	0.38	1.5	0.5	1.0	0.6	0.2	0.4	0.2	0.1	0.2	0.9	0.3	0.6	0.4	0.1	0.2
IG_BH06_PW011	691.0	G / T	0.36	2.5	0.5	1.5	1.0	0.2	0.6	0.4	0.1	0.2	1.6	0.3	0.9	0.6	0.1	0.3
IG_BH06_PW012	693.7	G / T	0.39	3.5	1.0	2.3	1.4	0.4	0.9	0.5	0.2	0.4	2.2	0.6	1.4	0.8	0.2	0.5
IG_BH06_PW013	720.5	G / T	0.36	3.5	1.5	2.5	1.4	0.6	1.0	0.5	0.2	0.4	2.2	0.9	1.6	0.8	0.3	0.6
IG_BH06_AR038	722.6	A	0.14	2.0	0.7	1.4	0.8	0.3	0.5	0.1	0.04	0.1	1.3	0.4	0.8	0.2	0.1	0.1
IG_BH06_AR039	728.8	T	0.20	4.0	0.8	2.4	1.6	0.3	1.0	0.3	0.1	0.2	2.5	0.5	1.5	0.5	0.1	0.3
IG_BH06_DG003	744.0	G / T	0.15	3.0	0.7	1.9	1.2	0.3	0.8	0.2	0.04	0.1	1.9	0.4	1.2	0.3	0.1	0.2
IG_BH06_PW014	747.5	G / T	0.35	1.0	0.3	0.7	0.4	0.1	0.3	0.1	0.04	0.1	0.6	0.2	0.4	0.2	0.1	0.1
IG_BH06_PW015	774.9	G / T	0.34	4.0	1.0	2.5	1.6	0.4	1.0	0.6	0.1	0.3	2.5	0.6	1.6	0.9	0.2	0.5
IG_BH06_AR045	796.7	G / T	0.26	4.0	0.8	2.4	1.6	0.3	1.0	0.4	0.1	0.3	2.5	0.5	1.5	0.6	0.1	0.4
IG_BH06_PW016	804.7	G / T	0.35	4.0	1.0	2.5	1.6	0.4	1.0	0.6	0.1	0.4	2.5	0.6	1.6	0.9	0.2	0.5
IG_BH06_AR049	820.2	G / T	0.34	3.0	0.7	1.9	1.2	0.3	0.8	0.4	0.1	0.3	1.9	0.4	1.2	0.6	0.1	0.4
IG_BH06_PW017	840.2	G / T	0.44	4.0	1.0	2.5	1.6	0.4	1.0	0.7	0.2	0.4	2.5	0.6	1.6	1.1	0.3	0.7
IG_BH06_PW018	853.0	G / T	0.33	4.0	1.0	2.5	1.6	0.4	1.0	0.5	0.1	0.3	2.5	0.6	1.6	0.8	0.2	0.5
IG_BH06_PW019	885.3	G / T	0.42	4.0	1.0	2.5	1.6	0.4	1.0	0.7	0.2	0.4	2.5	0.6	1.6	1.0	0.3	0.7
IG_BH06_PW020	927.6	G / T	0.36	4.0	1.0	2.5	1.6	0.4	1.0	0.6	0.1	0.4	2.5	0.6	1.6	0.9	0.2	0.6
IG_BH06_AR064	971.4	G / T	0.37	3.0	0.8	1.9	1.2	0.3	0.8	0.4	0.1	0.3	1.9	0.5	1.2	0.7	0.2	0.4

7.0 CHLORIDE, BROMIDE AND CHLORIDE ISOTOPES IN POREWATER OF CORE SAMPLES FROM BOREHOLE IG_BH06

Chloride and bromide concentrations of porewater were determined by aqueous extraction experiments (Section 3.2.1) and out-diffusion experiments (Section 3.2.2). Aqueous extraction experiments were conducted prior to the other longer-term experiments to obtain preliminary information about porewater salinities.

7.1 Porewater Chloride Concentrations Estimated by Aqueous Extraction Experiments

Aqueous extraction experiments were conducted on 19 core samples from different depth intervals. Approximate estimates of porewater Cl concentrations were calculated according to equation 3 (Section 3.2.1). During crushing of the rock samples, saline fluids from fluid inclusions in quartz and feldspar are released, which contribute to the Cl and Br inventory of the samples. This means that the chloride concentrations determined by aqueous extraction overestimate the actual porewater Cl concentrations.

Estimated porewater Cl concentrations for core samples from IG_BH06 determined by aqueous extractions vary between 3.53 and 25.8 g/kg H_2O (Table 7-2).

Based on the Cl-concentration range of porewater in core samples taken from IG_BH06 (1.72 – 20.6 g/kg H_2O = 0.10 - 0.76 mol), the salinity of isotope diffusive exchange experiment solutions was defined at 0.3 mol NaCl (see Section 8.0).

Table 7-1: Porewater Cl and Br concentrations and Br*1000/Cl mass ratios estimated using aqueous extraction experiments; the errors of porewater Cl and Br concentrations and Br*1000/Cl mass ratios are calculated by Gaussian error propagation (Appendix C).

Sample	Depth	Estimated $Cl_{PW(aq.ex.)}$	Br_{PW}	Br*1000/Cl
	mbgs*	mg/kgH_2O	mg/kgH_2O	mg/mg
IG_BH06_AQ001	212.9	4111	65	16
IG_BH06_AQ002	221.1	3534	79	22
IG_BH06_AQ003	370.3	4267	357	84
IG_BH06_AQ004	453.5	5428	190	35
IG_BH06_AQ005	504.4	4195	567	135
IG_BH06_AQ006	562.7	6022	156	26
IG_BH06_AQ007	574.4	5377	150	28
IG_BH06_AQ008	612.5	6184	137	22
IG_BH06_AQ009	648.2	5765	135	24
IG_BH06_AQ010	666.2	6554	188	29
IG_BH06_AQ011	694.0	5413	349	65
IG_BH06_AQ012	720.8	6883	165	24
IG_BH06_AQ013	747.8	9310	309	33
IG_BH06_AQ014	771.2	25777	679	26
IG_BH06_AQ015	804.9	7631	285	37
IG_BH06_AQ016	841.2	20931	1549	74
IG_BH06_AQ017	853.3	20737	510	25
IG_BH06_AQ018	885.6	17599	359	20
IG_BH06_AQ019	928.0	12549	263	21

* mbgs (downhole)

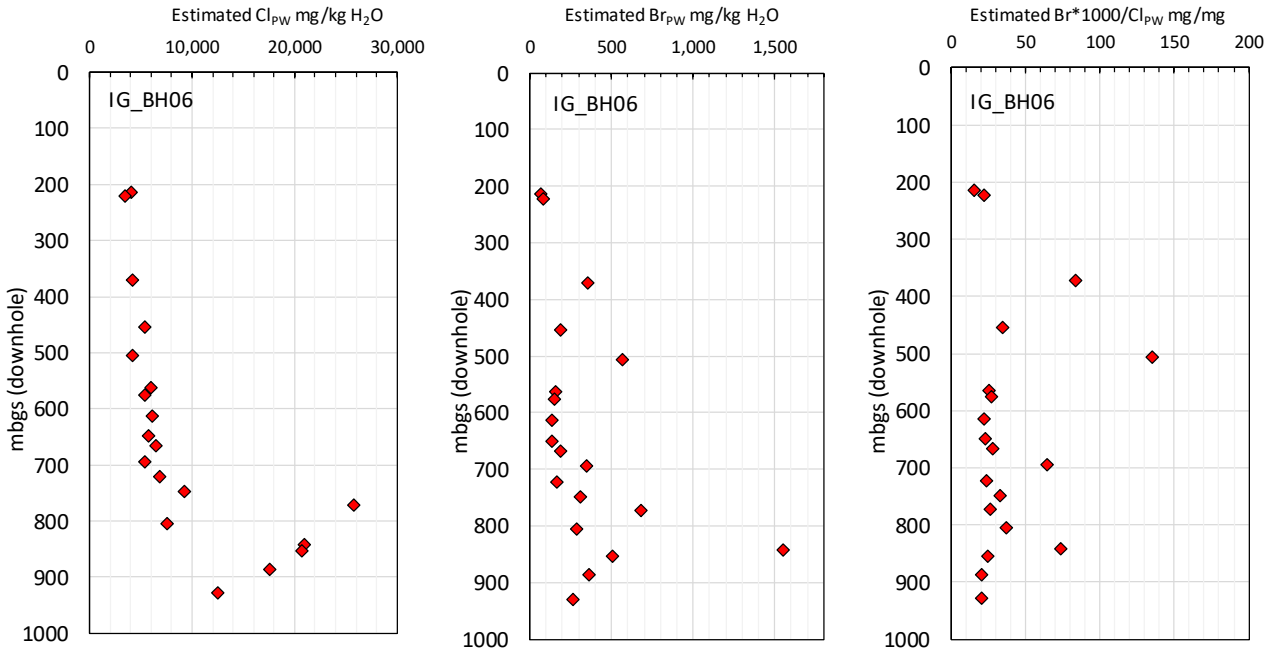


Figure 7-1: Borehole IG_BH06: Estimated porewater Cl and Br concentrations and Br*1000/Cl mass ratios versus depth by aqueous extraction experiments.

7.2 Porewater Chloride Concentrations and Bromide Concentrations and $\delta^{37}Cl$ Isotope Ratios Determined by Out-Diffusion Experiments

The conservative behaviour of chloride and bromide, the absence of Cl- and Br-bearing minerals in the rock, and the non-destructive character of the out-diffusion method, make the porewater the only source for dissolved Cl and Br in the experimental solutions. This allows calculation of the Cl and Br concentration in the porewaters by mass balance according to equation 4 (Section 3.3.2), given that equilibrium in the out-diffusion experiments is achieved. As shown by their chloride and bromide elution curves, this latter condition is fulfilled for all samples (Section 6.1).

The mass ratio of the two conservative elements, Cl and Br, can serve as a tracer of the origin of Cl and Br in porewater and fracture groundwater. The $\delta^{37}Cl$ ratio measured for the experiment solutions directly corresponds to the porewater Cl isotope signature. This is because the attained equilibrium in the out-diffusion experiment with respect to total Cl is also expected to result in equilibrium with respect to the Cl isotopes (Gimmi and Waber 2004).

Chloride concentrations of porewater taken between 212 and 971 mbgs (downhole) from IG_BH06 vary between 382 and 13,961 mg/kg H_2O (Table 7-2). Porewater bromide concentrations of the same respective samples from IG_BH06 vary between 6.9 and 1,411 mg/kg H_2O (Table 7-2). The Br*1000/Cl mass ratios (=Br/Cl ratio) of porewater from IG_BH06 vary between 1.5 and 308 (Table 7-2). In the bromide versus chloride diagram, porewaters extracted from borehole IG_BH06 cores plot significantly above the seawater dilution line (Br*1000/Cl mass ratio of seawater = 3.4, Figure 7-3).

The errors are calculated based on Gaussian error propagation (cf. Appendix C). In these calculations the mass and water content differences determined before and after the out-diffusion experiments are taken into account.

For several core samples, especially for those with low water contents, the high mass differences (cf. Table 4-3, Figure 4-2) lead to high errors of the porewater chloride and bromide concentrations and Br/Cl ratios. Porewater $\delta^{37}Cl$ isotope signatures vary between -0.12 ± 0.10 ‰ and 1.02 ± 0.10 ‰ SMOC along the depth profile between 212 and 971 mbgs (downhole) (Table 7-2). Porewater stable chlorine isotope signatures do not show a trend that correlates with porewater Cl concentrations (Table 7-2 and Figure 7-4). One porewater $\delta^{37}Cl$ result (IG_BH06_PW017) shows a larger (> 0.20 ‰) error than the others (Table 7-2). The errors are determined by the standard deviation of a triplicate measurement of the single samples.

Table 7-2: Porewater Cl and Br concentrations, Br*1000/Cl mass ratios and $\delta^{37}Cl$ isotope signatures. Cl concentrations are determined by out-diffusion experiments; the errors of porewater Cl and Br concentrations and Br*1000/Cl mass ratios are calculated by Gaussian error propagation (Appendix C); the errors of $\delta^{37}Cl$ values are the standard deviation of triplicate analyses; G / T = granodiorite / tonalite; A = amphibolite; T = feldspar phyric tonalite.

Sample	Depth mbgs*	Lithology	Cl_{PW} (o.d.) mg/kgH_2O	Br_{PW} mg/kgH_2O	Br*1000/Cl mg/mg	$\delta^{37}Cl$ ‰ SMOC
IG_BH06_PW001	212.3	G / T	382±30	117±9	308±34	-0.12±0.10
IG_BH06_PW002	291.5	G / T	1221±192	79±12	65±14	0.17±0.10
IG_BH06_PW003	253.2	G / T	1555±81	64±3	41±3	0.42±0.10
IG_BH06_AR010	398.7	T	2602±541	330±69	127±37	1.02±0.10
IG_BH06_AR013	421.6	G / T	2258±261	245±28	109±18	0.99±0.10
IG_BH06_PW004	453.2	G / T	2697±261	184±18	68±9	0.89±0.14
IG_BH06_PW005	504.1	G / T	1221±75	209±13	171±15	0.11±0.10
IG_BH06_AR019	534.0	G / T	1419±162	269±31	190±31	0.62±0.11
IG_BH06_AR020	542.9	G / T	1131±62	283±16	250±19	0.62±0.10
IG_BH06_PW006	562.4	G / T	1690±89	81±4	48±4	0.31±0.10
IG_BH06_PW007	574.2	G / T	1547±109	12±1	7.5±0.7	0.14±0.10
IG_BH06_AR027	595.0	G / T	2477±205	239±20	96±11	0.76±0.10
IG_BH06_PW008	612.2	G / T	2976±206	6.9±0.5	2.3±0.2	0.74±0.10
IG_BH06_PW009	647.9	G / T	3681±306	44±4	12±1	0.61±0.10
IG_BH06_PW010	665.9	G / T	3993±355	33±3	8.1±1.0	0.57±0.10
IG_BH06_PW011	691.0	G / T	4344±225	6.5±0.3	1.5±0.1	0.23±0.16
IG_BH06_PW012	693.7	G / T	5090±886	59±10	12±3	-0.08±0.10
IG_BH06_PW013	720.5	G / T	4121±436	30±3	7.3±1.1	-0.03±0.11
IG_BH06_AR038	722.6	A	3093±570	702±129	227±59	0.33±0.10
IG_BH06_AR039	728.8	T	4714±1095	817±190	173±57	0.63±0.10
IG_BH06_DG003	744.0	G / T	13091±3210	1411±346	108±37	0.74±0.10
IG_BH06_PW014	747.5	G / T	7618±697	75±7	10±1	0.10±0.10
IG_BH06_PW015	774.9	G / T	8519±1321	292±45	34±8	0.48±0.10
IG_BH06_AR045	796.7	G / T	14013±3033	1041±225	74±23	0.96±0.10
IG_BH06_PW016	804.7	G / T	8572±1874	109±24	13±4	0.09±0.14
IG_BH06_AR049	820.2	G / T	7986±1663	415±87	52±15	0.69±0.10
IG_BH06_PW017	840.2	G / T	11297±856	82±6	7.2±0.8	0.18±0.24
IG_BH06_PW018	853.0	G / T	13961±2086	454±68	33±7	0.13±0.10
IG_BH06_PW019	885.3	G / T	11689±2010	18±3	1.5±0.4	0.63±0.10
IG_BH06_PW020	927.6	G / T	15103±2737	180±33	12±3	-0.12±0.10
IG_BH06_AR064	971.4	G / T	10925±2009	406±75	37±10	0.62±0.10

* mbgs (downhole)

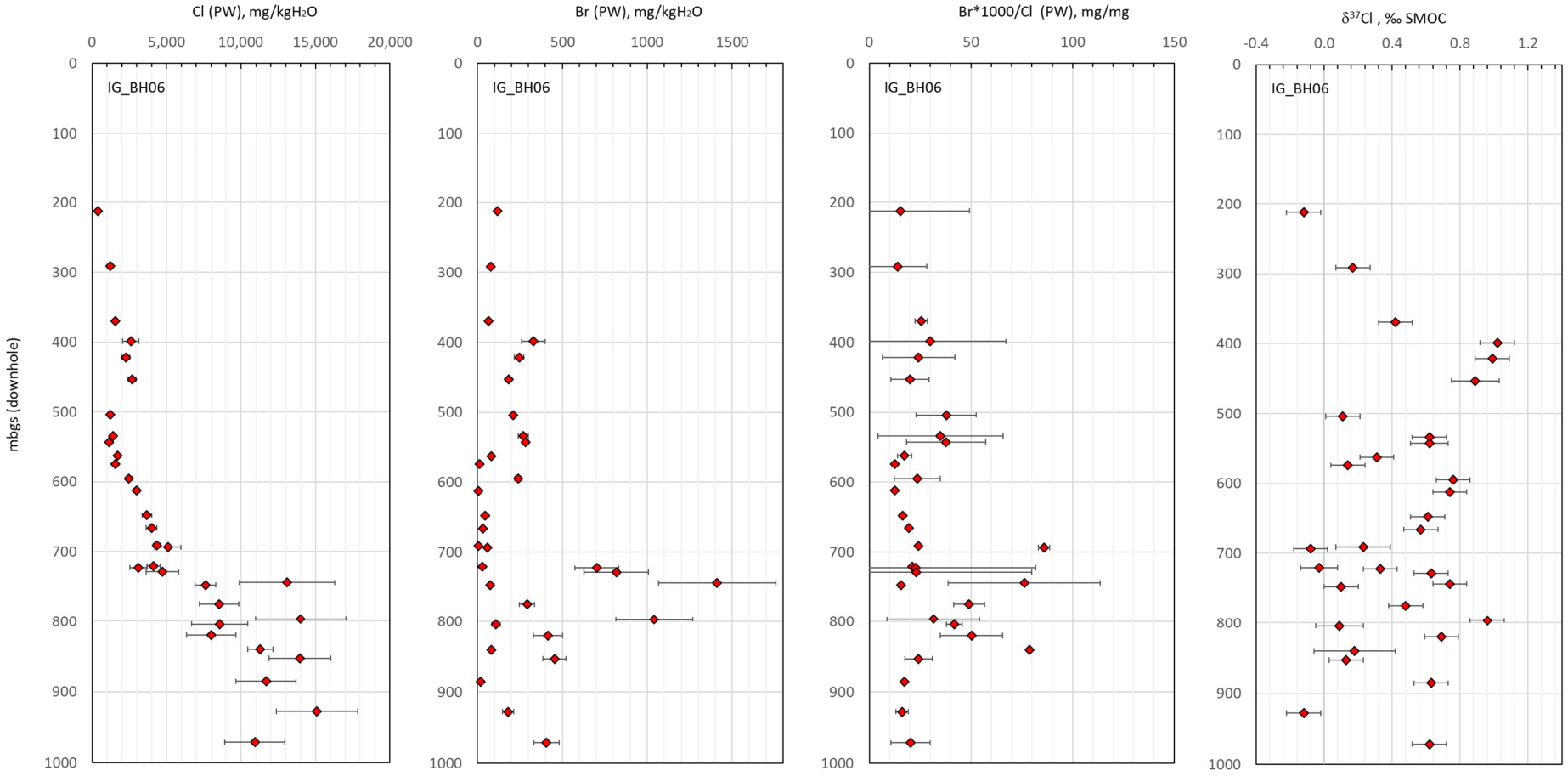


Figure 7-2: Porewater chloride, bromide, Br*1000/Cl mass ratios and $\delta^{37}Cl$ isotope signatures from cores from borehole IG_BH06 as function of depth.

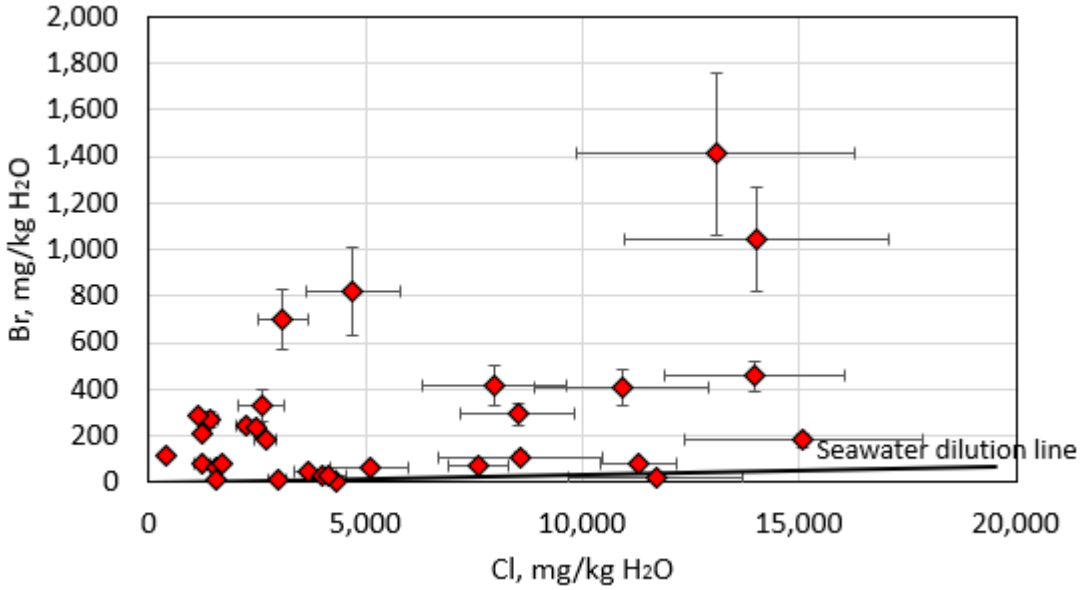


Figure 7-3: Porewater Cl versus Br concentrations determined by out-diffusion experiments on core samples from IG_BH06.

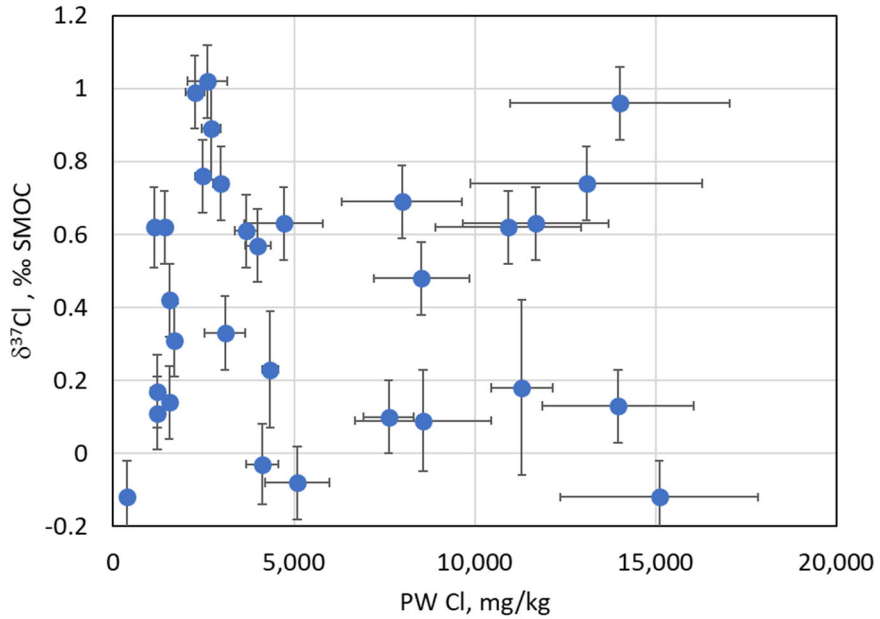


Figure 7-4: Porewater δ^{37}Cl isotope signatures versus porewater Cl concentrations.

8.0 $\delta^{18}O$ AND $\delta^{2}H$ OF POREWATER OF CORE SAMPLES FROM IG_BH06

Isotope diffusive exchange experiments have been carried out on 30 core samples (60 individual experiments) from IG_BH06. The $\delta^{18}O$ and $\delta^{2}H$ values of porewater are calculated according to Equation 7 (Section 3.2.3), expressed relative to the standard V-SMOW, and are listed in Table 8-1 and graphically shown in Figure 8-1 and Figure 8-2.

The calculated porewater isotope signatures, which are based on the isotope analyses of the test waters, are carefully evaluated for potential artefacts (mainly due to evaporation of test water during the experiment, test water storage and handling). Evaporation of porewater during storage and handling was minimized by careful handling of the core samples (Section 3.3.3). These processes might result in large discrepancies between the gravimetric water content and that calculated from isotope mass balance, and errors in the resulting (calculated) porewater isotopic signatures. Such differences were not observed in this study (Section 4.1.2). Some samples showed a higher (>0.5 wt.%) water content determined by isotope diffusive exchange than determined gravimetrically (cf. Section 4.1.2).

According to the quality check of the raw data, it was decided to qualify those data as reliable even though the water contents differ by >0.5 wt%. Evaporation within the experiment was monitored by keeping track of all individual weights before and after the experiments. Some of the experiments suffered evaporation > 2 % of the total water mass in the experiments (= mass of porewater determined gravimetrically + mass of test water) during the time of equilibration.

The maximum Cl concentration determined by aqueous extraction prior to set-up of the isotope diffusive exchange experiments is 25.8 g/kg H_2O, which relates to 0.80 mol $NaCl_{eq}$. However only four samples (IG_BH06_AQ014 and to a lower extent IG_BH06_AQ016, IG_BH06_AQ017 and IG_BH06_AQ018) showed such high Cl-concentrations. The other samples showed a maximum Cl-concentration of 12.5 g/kg H_2O, which relates to 0.39 mol $NaCl_{eq}$. Out-diffusion experiments showed an actual maximum Cl concentration of 15.1 g/kg H_2O, which relates to 0.47 mol $NaCl_{eq}$. Based on the aqueous extraction results, it was decided to adjust the salinity of the test solutions to 0.3 mol NaCl to prevent mass transfer from the test water reservoir to the rocks.

Stable oxygen and hydrogen isotope signatures of porewater extracted from IG_BH06 vary between -9.50 and 4.32 ‰ for $\delta^{18}O$ and -79.7 and -9.7 ‰ for $\delta^{2}H$ (Table 8-1, Figure 8-1).

Porewaters from IG_BH06 of core samples taken between 212 and 971 mbgs (downhole) plot slightly to the right of the global meteoric water line (GMWL) on the $\delta^{18}O$-$\delta^{2}H$ diagram (Figure 8-2).

The errors, which are calculated by Gaussian error propagation (cf. Appendix C) depend, inter alia, on the porewater to test water mass ratio (R(tw/pw)), which depends on the water content and mass of rocks in the experiments. The correlation of the R(tw/pw) with the porewater $\delta^{18}O$ and $\delta^{2}H$ errors indicates that the higher the ratio, the higher the determined error (Figure 8-3).

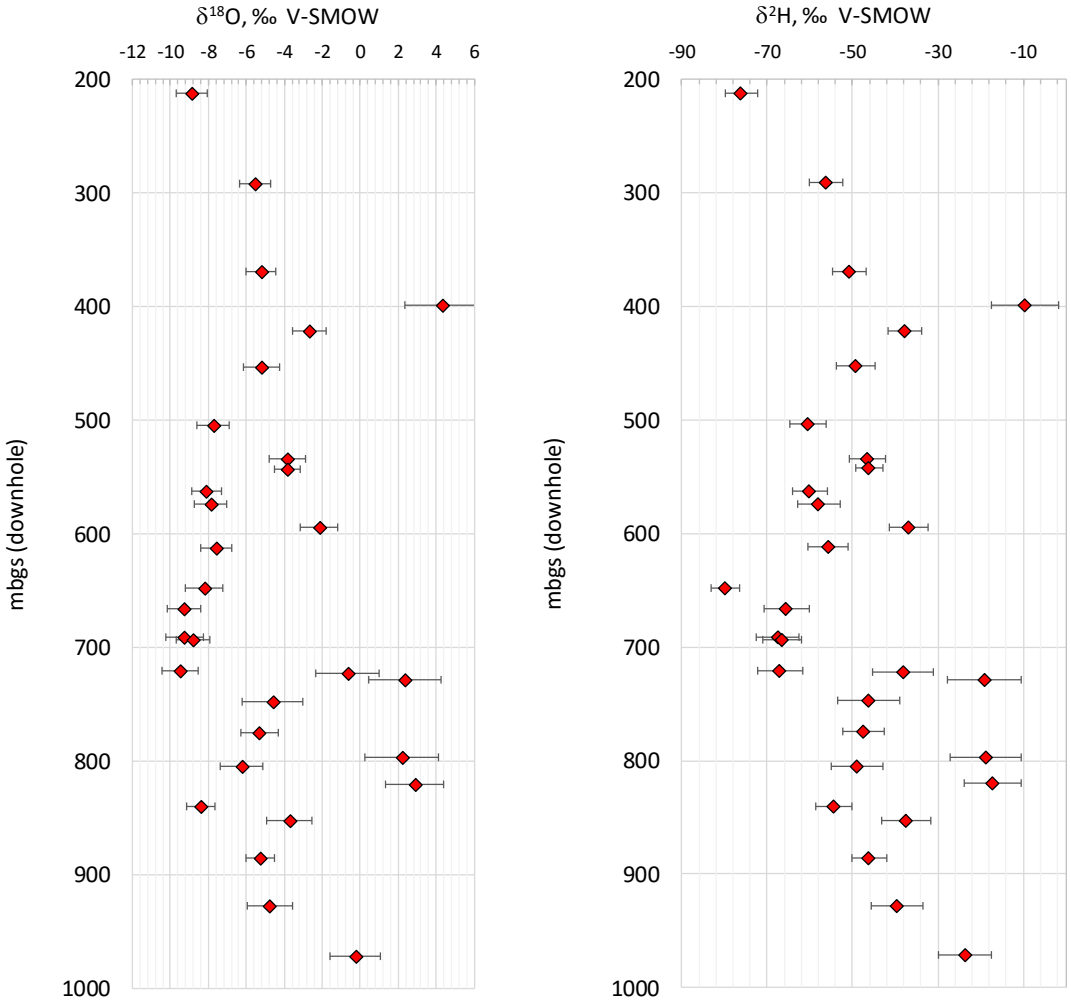


Figure 8-1: $\delta^{18}O$ and $\delta^{2}H$ porewater signatures as function of depth along borehole IG_BH06; errors are calculated by Gaussian error propagation (depth in mbgs (downhole)).

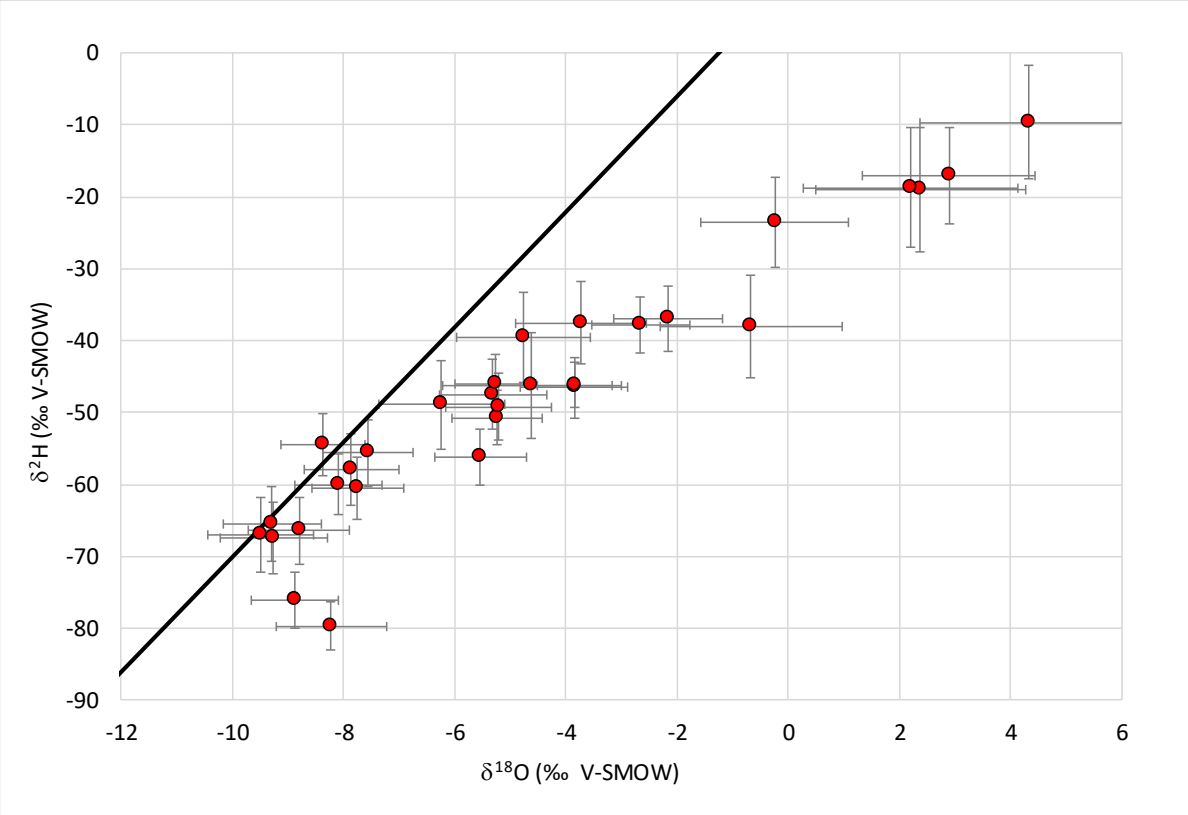


Figure 8-2: $\delta^{18}O$ versus $\delta^{2}H$ values of porewater; the black line marks the global meteoric water line; the errors of the stable isotope ratios are calculated by Gaussian error propagation.

Table 8-1: $\delta^{18}O$ and $\delta^{2}H$ values of porewater of core samples from borehole IG_BH06; the errors are calculated by Gaussian error propagation; G / T = granodiorite / tonalite; A = amphibolite; T = feldspar phyric tonalite.

Sample	Depth mbgs*	Lithology	$\delta^{18}O$ ‰ V-SMOW	Error $\delta^{18}O$ ‰ V-SMOW	$\delta^{2}H$ ‰ V-SMOW	Error $\delta^{2}H$ ‰ V-SMOW
IG_BH06_PW001	212.3	G / T	-8.87	0.79	-76.0	3.8
IG_BH06_PW002	291.5	G / T	-5.54	0.82	-56.2	3.9
IG_BH06_PW003	253.2	G / T	-5.23	0.81	-50.7	3.9
IG_BH06_PW004	453.2	G / T	-5.22	0.94	-49.2	4.7
IG_BH06_PW005	504.1	G / T	-7.75	0.83	-60.5	4.3
IG_BH06_PW006	562.4	G / T	-8.10	0.79	-60.0	4.2
IG_BH06_PW007	574.2	G / T	-7.86	0.86	-57.9	4.9
IG_BH06_PW008	612.2	G / T	-7.55	0.82	-55.6	4.7
IG_BH06_PW009	647.9	G / T	-8.22	0.99	-79.7	3.4
IG_BH06_PW010	665.9	G / T	-9.29	0.89	-65.4	5.2
IG_BH06_PW011	691.0	G / T	-9.25	0.97	-67.5	5.0
IG_BH06_PW012	693.7	G / T	-8.80	0.90	-66.4	4.6
IG_BH06_PW013	720.5	G / T	-9.50	0.95	-66.9	5.2
IG_BH06_PW014	747.5	G / T	-4.61	1.62	-46.2	7.3
IG_BH06_PW015	774.9	G / T	-5.32	0.97	-47.5	4.9
IG_BH06_PW016	804.7	G / T	-6.23	1.13	-48.9	6.1

Sample	Depth mbgs*	Lithology	$\delta^{18}O$ ‰ V-SMOW	Error $\delta^{18}O$ ‰ V-SMOW	$\delta^{2}H$ ‰ V-SMOW	Error $\delta^{2}H$ ‰ V-SMOW
IG_BH06_PW017	840.2	G / T	-8.38	0.76	-54.4	4.3
IG_BH06_PW018	853.0	G / T	-3.72	1.18	-37.5	5.7
IG_BH06_PW019	885.3	G / T	-5.26	0.73	-46.1	4.1
IG_BH06_PW020	927.6	G / T	-4.76	1.19	-39.5	6.2
IG_BH06_AR010	398.7	T	4.32	1.94	-9.7	8.0
IG_BH06_AR013	421.6	G / T	-2.66	0.88	-37.8	3.9
IG_BH06_AR019	534.0	G / T	-3.85	0.96	-46.6	4.3
IG_BH06_AR020	542.9	G / T	-3.84	0.68	-46.2	3.2
IG_BH06_AR027	595.0	G / T	-2.17	0.98	-36.9	4.6
IG_BH06_AR038	722.6	A	-0.67	1.64	-38.1	7.1
IG_BH06_AR039	728.8	T	2.38	1.90	-19.1	8.6
IG_BH06_AR045	796.7	G / T	2.20	1.94	-18.8	8.3
IG_BH06_AR049	820.2	G / T	2.89	1.54	-17.2	6.7
IG_BH06_AR064	971.4	G / T	-0.24	1.33	-23.6	6.3

*mbgs (downhole)

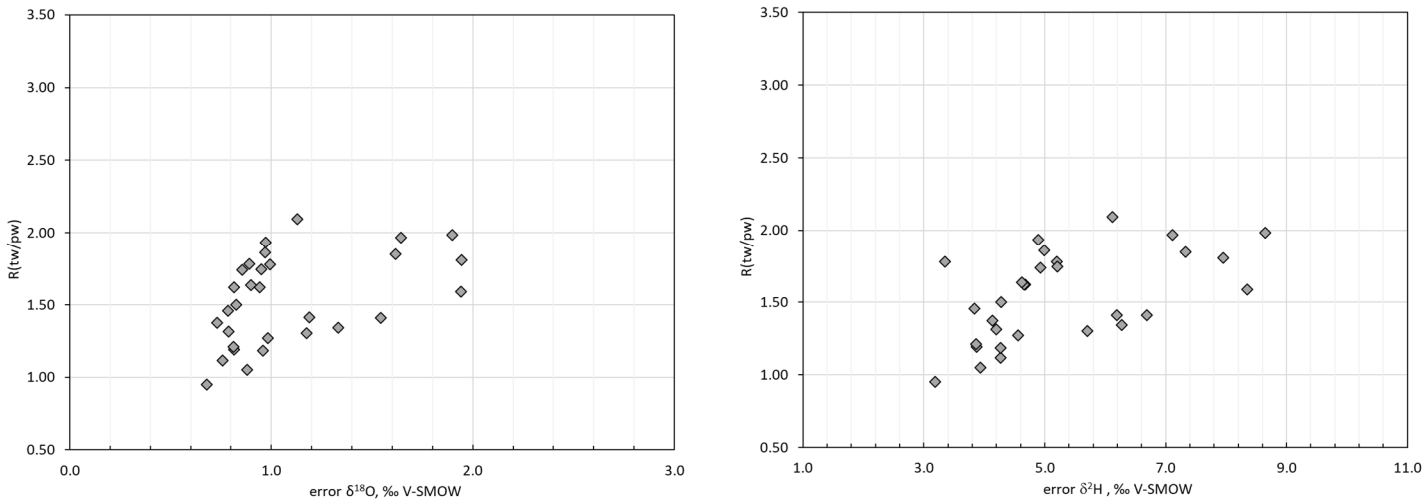


Figure 8-3: Errors of the determination of the $\delta^{18}O$ (left) and $\delta^{2}H$ (right) porewater isotope signatures versus the mass ratio of test water and porewater (R(tw/pw)).

9.0 RESULTS FROM DISSOLVED GASES IN MATRIX POREWATER OF CORE SAMPLES FROM IG_BH06

Gases dissolved in porewater were extracted, chemically and isotopically characterised, and quantified on ten core samples, where five were used for the analyses of noble gases and five for the analyses of non-inert gases. The experiments were conducted using intact core pieces of 20 – 24 cm length with masses between 1,504 and 1,784 g.

A detailed description of the sampling and analytical procedures and the derivation of the porewater gas concentrations is given in Section 2.2 and 3.3. The raw data of the gas-chromatographic and mass-spectrometric measurements, and the corresponding determination of the water contents, are given in Appendix B.

In the experimental set-up, gases dissolved in porewater migrate from the rock to the void volume. The closed system is set under vacuum, allowing an almost complete degassing of the porewater. Based on scoping calculations using diffusion as the transport mechanism, dissolved hydrocarbon gases and noble gases are estimated to be in equilibrium in the system porewater – void volume in time periods between 45 days (Helium) and 230 days (butane, Figure 9-1). The model calculations were performed using a code by T. Gimmi (RWI, University of Bern) with an analytical solution for radial diffusion out of the cylinder into a defined reservoir (Crank 1975). These approaches take only diffusive transport driven by the concentration gradient between pore water and void volume into account and, therefore, describe a maximal equilibration time. A faster degassing due to possible suction effects is not taken into account in these scoping calculations.

The core samples were allowed to equilibrate with the surrounding low-pressure atmosphere in the cylinders for 349 to 374 days (DG samples) and for 637 to 668 days (NG samples), respectively.

After the complete diffusive equilibration, the gas present in the void space of the cylinder is in equilibrium with the gas dissolved in matrix porewater. The efficiency of the diffusive release of gases from matrix porewater is given by the ratio of the connected pore volume, to the void space in the cylinder, which varies between 0.008 and 0.017 for the set-up experiments (Appendix B). The proportion of the water volume to the sum of pore volume and void volume is < 2 %. The remaining volume of gas in the porewater is thus also << 2 % of the total gas volume. Hence, the release of gases from the rock pore space to the void volume of the sampling cell water can be considered as quantitative.

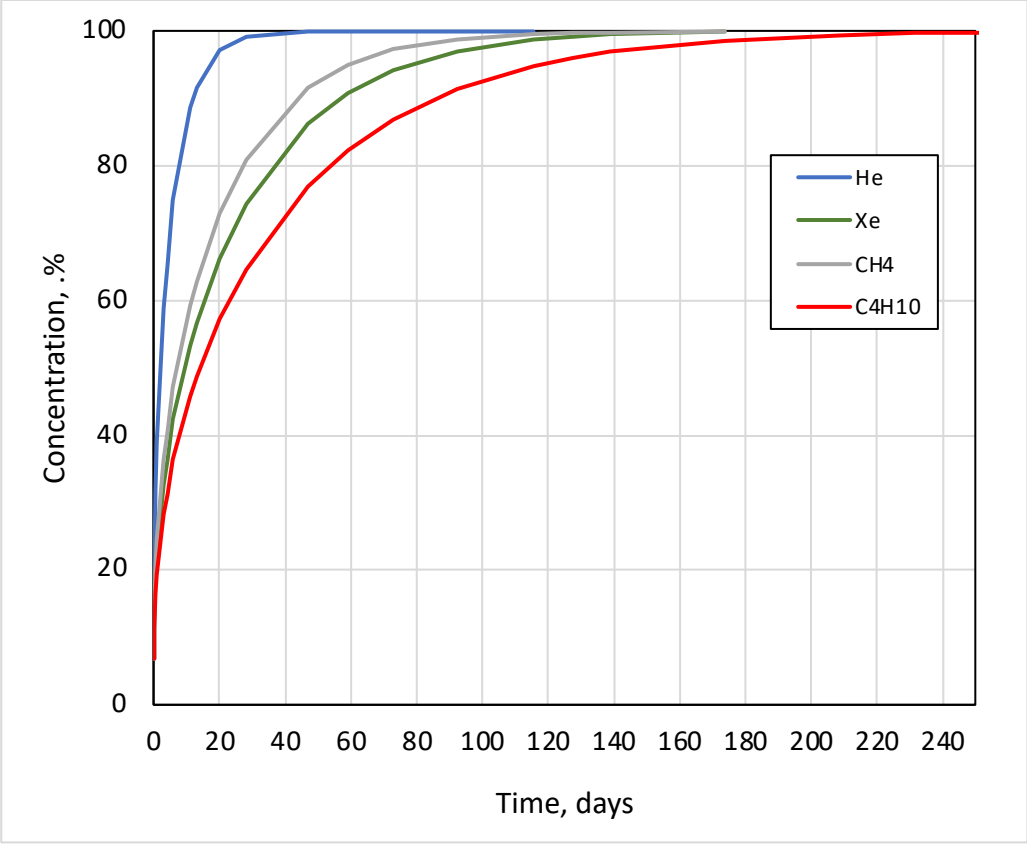


Figure 9-1: Diffusive equilibration of gases dissolved in porewater. The model calculations show that the equilibration time in days is sufficient to achieve equilibrium with respect to the analysed gases. The

diffusive exchange in the experiments of the non-inert gases and noble gases with the lowest (Butane, Xenon) and the highest diffusion coefficient in free water (Methane, Helium) were modelled ($D_{(He)}$ = 7.2*10^{-9} m^2/s, $D_{(Xe)}$ = 1.5*10^{-9} m^2/s, $D_{(CH_4)}$ = 1.9*10^{-9} m^2/s, $D_{(C_4H_{10})}$ = 9.6*10^{-10} m^2/s at 20°C, Jähne et al. 1987). The conversion of these diffusion coefficients in free water to pore diffusion coefficients of the single gases in the rock samples was done according to Equation 14 using an average geometry factor of 0.04 as estimated for chloride (cf. Section 6.2).

As for dissolved chemical compounds, the concentration of a dissolved gas in the porewater might be subjected to contamination during drilling and sampling. Such possible artefacts need to be explored before the interpretation of the gas data.

In situ gas concentrations of matrix porewater can be changed by the penetration of drilling fluid in the core triggered by stress release and by the drilling process (drilling disturbed zone). The evaluation of the influence of these disturbing processes done in different studies working with crystalline rocks show only a minor influence on the porewater characteristics (Eichinger et al., 2013, Meier et al., 2015, Eichinger & Iannotta, 2022).

For gases dissolved in pore water, exchange with the surrounding drilling fluid, and/or atmospheric air, might occur in the time period between the release of the core samples from the bedrock and the set-up of the experiments (closing of the gas tight cylinders). The time periods between drilling and recovery of the cores and experimental set-up were below 15 minutes. Modelling of the diffusive loss of He and CH_4 from the cores during the sampling done by Eichinger et al. (2013) show that within two hours only gas dissolved in matrix porewater that occurs in the rim (~2.5 mm) of the cores is affected. It thus appears that the diffusive loss of gases during sampling is within the error of the gas analyses and can be neglected.

9.1 Non-Inert Gases

Non-inert gases were extracted and evaluated from five core samples taken between 510 and 936 mbgs (downhole).

9.1.1 Concentrations of Reactive, Non-Inert Gases Dissolved in Porewater

The raw data of the reactive gas analyses are given in Appendix B and the porewater gas concentrations corrected for air contamination are given in Table 9-1.

The final pressures of the cylinders after equilibration varied between 33 and 917 mbars at 22 °C.

The sample IG_BH06_DG001 (showed a final pressure of 917 mbar, which is close to atmospheric). It could be assumed that for the cylinder (510.2 mbgs (downhole)) tightening of the lid was not sufficient, which lead to an intake of air. The gases of this sample were analysed, but the results are not reliable. Therefore, non-inert gases and their isotopes of the sample IG_BH06_NG001 (512.5 mbgs (downhole)) were analysed after the analyses of noble gases.

Due to the fact that the cores are naturally saturated, the partial pressure of water vapour was calculated according to Equation 10. The subtraction of the water vapour partial pressure, and the correlation to standard conditions, gives total gas pressures between 7.3 and 10.2 mbar STP, corresponding to 1.9 to 3.1 NmL of gas extracted from the porewater.

Oxygen was used as tracer for air contamination in the cylinders, based on the assumption that in situ porewater is oxygen free. The proportion of air contamination was calculated according to Equation 9. Oxygen concentrations vary between 0.3 and 1.5 Vol.% (18.4 Vol.% for the highly contaminated sample) corresponding to

an air contamination between 1.4 and 7.2 % (88 % for the highly contaminated sample) of the total gas volume. The concentrations of the gas species were corrected using the general air composition (Appendix B). These contaminations mainly concern the normal gases N_2 and CO_2. The calculations show that for N_2, 10 – 99 % of the detected nitrogen comes from the degassed porewater. Concentrations of hydrocarbons in air are low and air contamination has even less of an effect on those concentrations.

The extracted and corrected volumes of the individual gas species are converted to milliliters gas per liter porewater STP (NmL/L_{PW}, 0°C = 273 K, 1013 hPa) using the volume of porewater according to Equation 11.

9.1.1.1 Porewater Nitrogen-, Hydrogen- and Carbon Dioxide Concentrations

Nitrogen and hydrogen are the most abundant gas species dissolved in porewater of core samples taken between 512 m and 936 mbgs (downhole) from IG_BH06. The concentrations of nitrogen (N_2) vary between 383 NmL/L_{PW} and 740 NmL/L_{PW} (Table 9-1,Figure 9-2). Nitrogen concentrations are constant within analytical uncertainty at depths of 512 m and 621 mbgs (downhole) (383-727 NmL/L_{PW}) and are higher in the deeper intervals sampled at 802 and 936 mbgs (downhole) (564 – 740 NmL/LPW, Table 9-1, Figure 9-2). Hydrogen (H_2) concentrations vary between 12.3 and 114 NmL/L_{PW} and vary within the individual intervals (Table 9-1,Figure 9-2). Carbon dioxide (CO_2) concentrations are low and vary between <0.1 NmL/L_{PW} and 0.41 NmL/L_{PW} in the samples taken at 512 m and 936 mbgs (downhole), respectively (Table 9-1). They appear to decrease with increasing depth at the intervals between 512 m to 802 mbgs (downhole) and are higher in the deeper interval between 842 and 936 mbgs (downhole) (Figure 9-2).

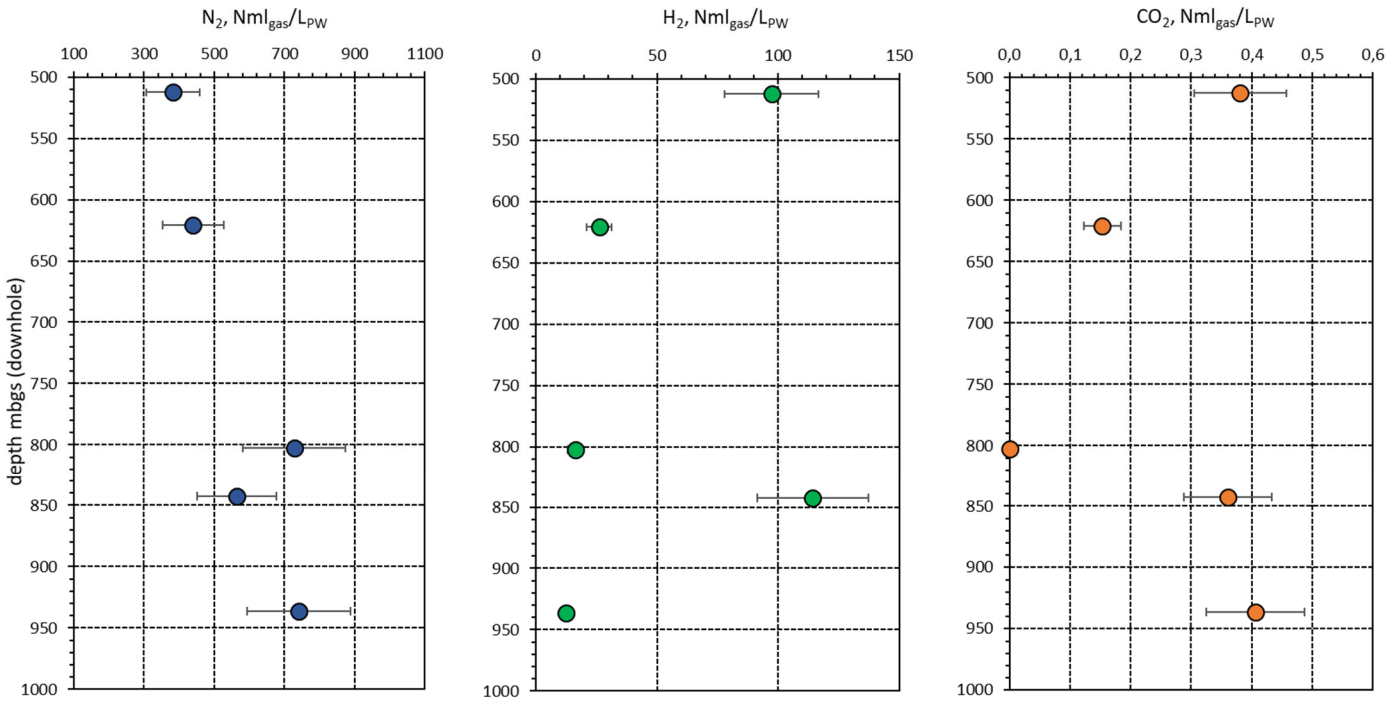


Figure 9-2: Porewater nitrogen (N_2, left), hydrogen (H_2, center) and carbon dioxide (CO_2, right) concentrations as function of depth along borehole IG_BH06; errors are ± 20% (depth in mbgs (downhole)).

9.1.1.2 Porewater Hydrocarbon Gas Concentrations

Methane concentrations dissolved in porewater of cores taken in intervals between 512 m and 936 mbgs (downhole) from IG_BH06 vary between 0.61 NmL/L_{PW} and 9.77 NmL/L_{PW} and are higher at 512 m than at 621 mbgs (downhole). At the sample taken at 802 mbgs (downhole), the lowest CH_4 porewater concentration was detected (Figure 9-3, Table 9-1). In the deep interval, a higher CH_4 concentration was detected at 843 m whereas the sample taken at 936 mbgs (downhole) shows slight lower CH_4-concentrations.

In all samples, higher saturated hydrocarbons up to butane could be detected. The concentrations of the individual hydrocarbon species vary between 0.001 NmL/L_{PW} and 0.18 NmL/L_{PW}, where ethane (C_2H_6) is the most abundant species in all samples (Table 9-1). The sum of the detected higher hydrocarbons varies between 0.026 NmL/L_{PW} and 0.21 NmL/L_{PW}. The sum of the gaseous higher hydrocarbons dissolved in porewater follows the same pattern with depth as that observed for methane (Table 9-1, Figure 9-3).

In all five samples, unsaturated hydrocarbons up to butene, with concentrations between <0.001 NmL/L_{PW} and 0.013 NmL/L_{PW}, were detected (Table 9-1). The sum of gaseous unsaturated hydrocarbons dissolved in porewater varies between 0.0028 NmL/L_{PW} and 0.029 NmL/L_{PW}. They become higher in the intervals n sampled at 512 m and 621 mbgs (downhole), and are relatively constant at the following intervals down to 936 mbgs (downhole) (Figure 9-3, Table 9-1).

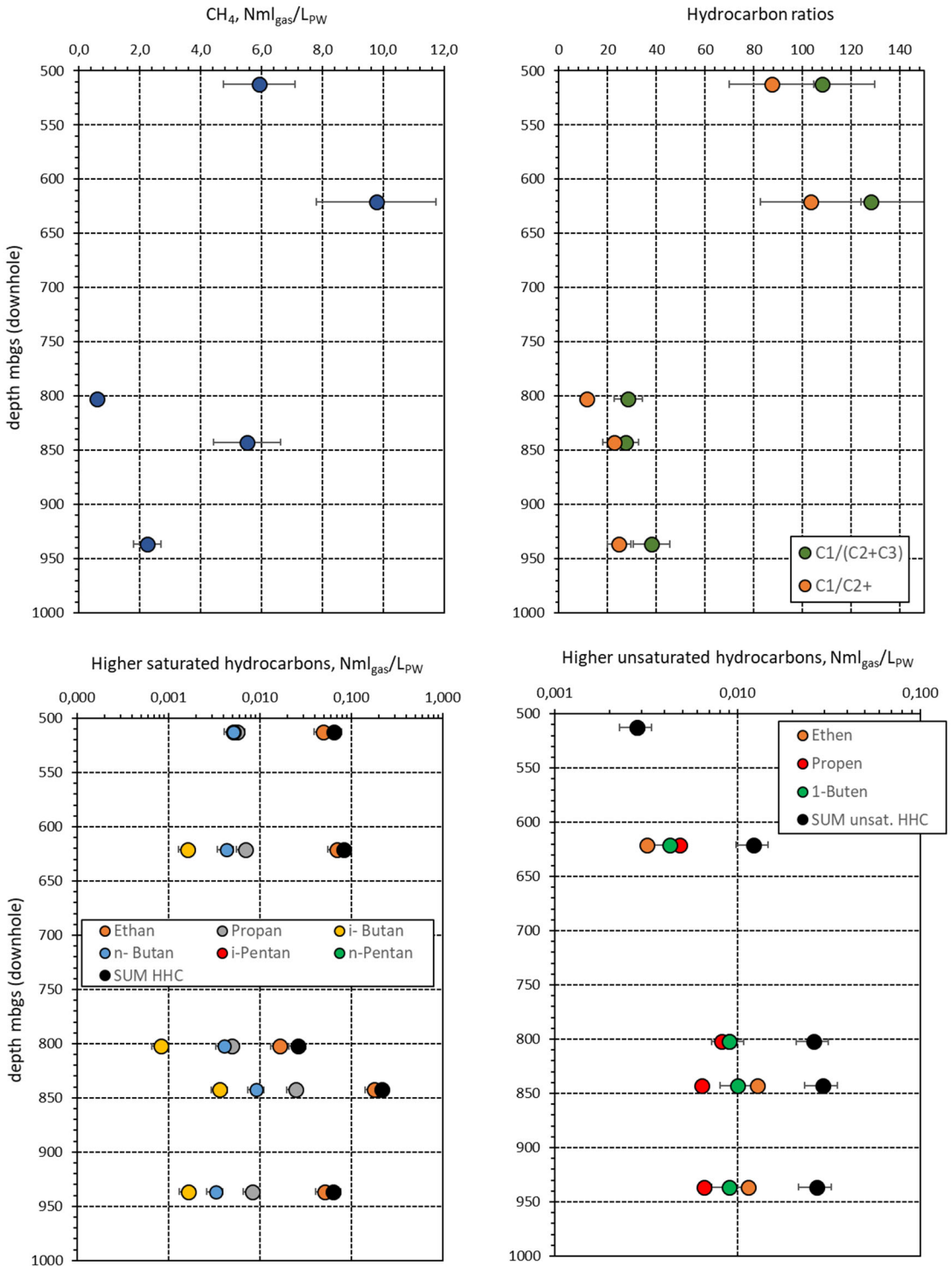


Figure 9-3: Porewater methane (CH_4, top, left), saturated (C_2-C_5, bottom left) and unsaturated (C_2-C_4, bottom right) higher hydrocarbon concentrations and hydrocarbon ratios (top, right) as function of depth along borehole IG_BH06; errors are ± 20%.

The volume ratios of methane over ethane plus propane ($C_1/(C_2+C_3)$) of hydrocarbons dissolved in porewater vary between 27 and 128 and are constant within the error range (108 – 128) at the depth intervals sampled at 512 and 621 mbgs (downhole). In the deeper zone between 802 and 936 mbgs (downhole) the $C_1/(C_2+C_3)$ ratios are lower than in the upper zone, at an almost constant level, 27 and 38, respectively (Table 9-1, Figure 9-3). The volume ratios of methane over the sum of all gaseous saturated hydrocarbons (C_1/C_{2+}) vary between 12 and 103 and show the same pattern as observed for the $C_1/(C_2+C_3)$ ratios.

Table 9-1: Concentrations of gases dissolved in porewater of core samples from borehole IG_BH06; the volumes in NmL/L$_{PW}$ are given normalised to standard conditions (273 K = 0°C, 1 bar); the errors are estimated to be ±20 %.

Sample		IG_BH06_ DG001**	IG_BH06_ NG001	IG_BH06_ DG002	IG_BH06_ DG004	IG_BH06_ DG005	IG_BH06_ DG006
Depth a.b.	**mbgs**	**510.2**	**512.5**	**620.9**	**802.4**	**842.7**	**936.4**
Water Content*	wt.%	0.18	0.22	0.21	0.18	0.23	0.18
Mass of PW	g	3.01	3.76	3.62	2.66	3.39	2.82
Hydrocarbons							
Methane (CH_4)	Nml/LPW	0.71	5.93	9.77	0.61	5.53	2.25
Ethane (C_2H_6)	Nml/LPW	0.009	0.049	0.069	0.016	0.177	0.051
Propane (C_3H_8)	Nml/LPW	<0.001	0.006	0.007	0.005	0.025	0.008
i- Butane (i-C_4H_{10})	Nml/LPW	<0.001	0.005	0.002	0.001	0.004	0.002
n- Butane (n-C_4H_{10})	Nml/LPW	<0.001	0.005	0.004	0.004	0.009	0.003
i-Pentane (i-C_5H_{12})	Nml/LPW	<0.001	<0.001	<0.001	<0.001	<0.001	<0.001
n-Pentane (n-C_5H_{12})	Nml/LPW	<0.001	<0.001	<0.001	<0.001	<0.001	<0.001
Ethene (C_2H_4)	Nml/LPW	<0.001	<0.001	0.003	0.009	0.013	0.011
Propene (C_3H_6)	Nml/LPW	<0.001	0.003	0.005	0.008	0.006	0.007
1-Butene (1-C_4H_8)	Nml/LPW	<0.001	<0.001	0.004	0.009	0.010	0.009
Normal gases	Nml/LPW						
Nitrogen (N_2)	Nml/LPW	891	383	440	727	564	740
Carbon dioxide (CO_2)	Nml/LPW	<0.1	0.38	0.15	<0.1	0.36	0.41
Hydrogen (H_2)	Nml/LPW	<0.1	97.3	26.2	16.4	114	12.3
Ratios							
$C_1/(C_2+C_3)$	ml/ml	82	108	128	28	27	38
C_1/C_{2+}	ml/ml	82	87	103	12	23	25

Depths in mbgs (downhole)

* mass of porewater determined on gas samples from weight measurements before out-gassing

** results are less reliable, because sample container was not tight and showed a final pressure of 917 mbar

9.1.2 Stable Isotope Signatures of Non-Inert Gases Dissolved in Porewater

Despite the low hydrocarbon concentrations dissolved and extracted from porewater of cores taken between 512 and 936 mbgs (downhole) stable carbon isotope signatures could be analysed for the gaseous hydrocarbons (C_1-C_4) for all samples. Hydrogen isotopes of methane could also be detected for all samples. Nitrogen isotopes on dissolved nitrogen could be analysed on three DG samples.

Stable nitrogen isotopes ($\delta^{15}N\text{-}N_2$) of nitrogen dissolved in porewater vary between 0.0 ‰ and -0.3 ‰-Air (Table 9-2, Figure 9-4).

Stable isotope signatures of methane dissolved in porewater vary between -49.8 ‰ and – 21.6 ‰ V-PDB for $\delta^{13}C$ and between -333 ‰ and -241 ‰ V-SMOW for $\delta^{2}H$.(Table 9-2, Figure 9-4). In the depth profile, stable carbon isotopes become generally more enriched with depth in the intervals between 512 and 936 mbgs (downhole), before they are more enriched in the deeper intervals between 843 and 936 mbgs (downhole). Stable hydrogen isotope signatures do not show such a unique pattern for the samples taken at the individual bedrock intervals but vary mainly in the two deep intervals (Figure 9-4).

Stable carbon isotope signatures ($\delta^{13}C\text{-}C_2H_6$, $\text{-}C_3H_8$,$\text{-i-}C_4H_{10}$, $\text{n-}C_4H_{10}$) of higher hydrocarbon dissolved in porewater vary between –30.9 ‰ and -15.9 ‰ V-PDB and show no general trends with depth (Table 9-2, Figure 9-5).

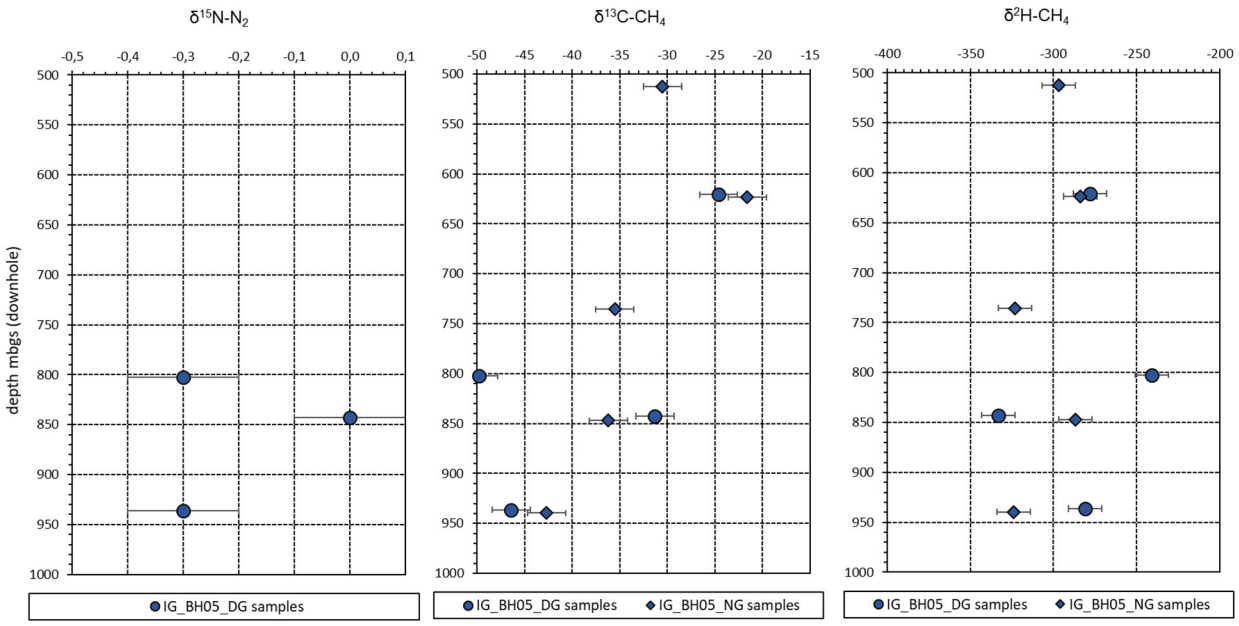


Figure 9-4: Stable isotope signatures of nitrogen ($\delta^{15}N\text{-}N_2$, left) and methane ($\delta^{13}C\text{-}CH_4$, center, $\delta^{2}H\text{-}CH_4$, right) dissolved in porewater as function of depth along borehole IG_BH06; errors are ± 0.1 ‰ for $\delta^{15}N\text{-}N_2$, ± 2.0 ‰ for $\delta^{13}C\text{-}CH_4$ and ± 10.0 ‰ for $\delta^{2}H\text{-}CH_4$.

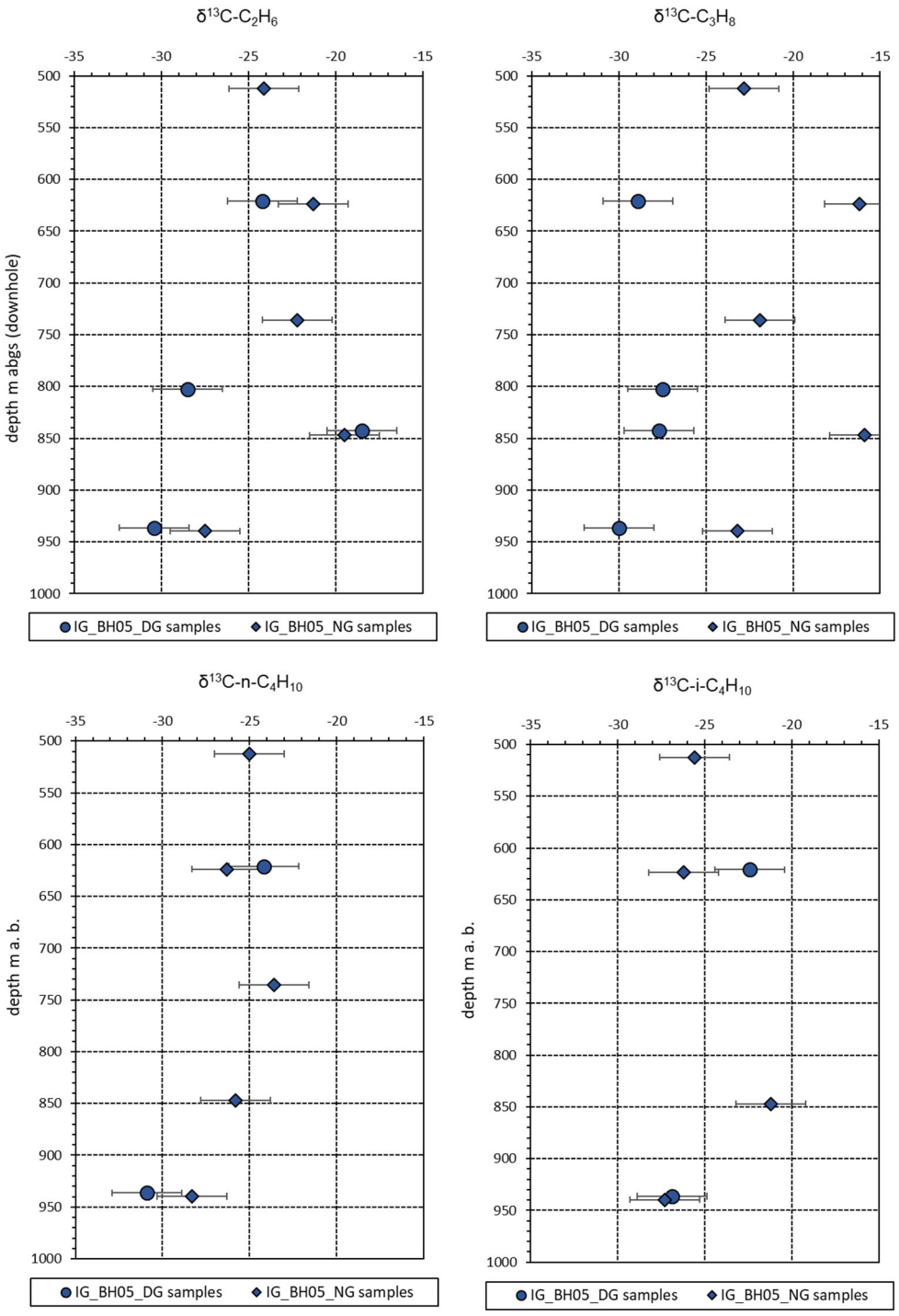


Figure 9-5: Stable carbon isotope signatures of higher hydrocarbons dissolved in porewater as function of depth along borehole IG_BH06; errors are ± 2.0 ‰

Stable isotope signatures of hydrocarbons give, in combination with their composition and their volume ratios, valuable information about their genesis and origin. Therefore, the hydrocarbon data from the porewaters of core samples from IG_BH06 are correlated to end-member signatures and ratios according to the recent literature. The

correlation of $\delta^{13}C$- and $\delta^{2}H$ isotope signatures of methane dissolved in porewater indicates, according to Whiticar (2020), that almost all samples taken between 512 m and 936 mbgs (downhole) are of a hydrothermal, crystalline origin (Figure 9-6).

The $\delta^{13}C$ pattern of the dissolved hydrocarbons of porewater from IG_BH06 show almost homogeneous patterns, with increasing carbon isotope signatures with increasing carbon numbers (Figure 9-7, Table 9-2). They show a similar pattern to hydrocarbons formed under thermogenic conditions, shown by Sherwood Lollar et al. (1994), but are more enriched than the literature data. The enrichment in ^{13}C in almost all hydrocarbons, compared to the literature data, agrees with the $\delta^{13}C$-, and $\delta^{2}H$-CH_4 isotopic signatures; these signatures are more enriched in ^{2}H and ^{13}C compared to methane from thermogenic and organic sources (Figure 9-6).

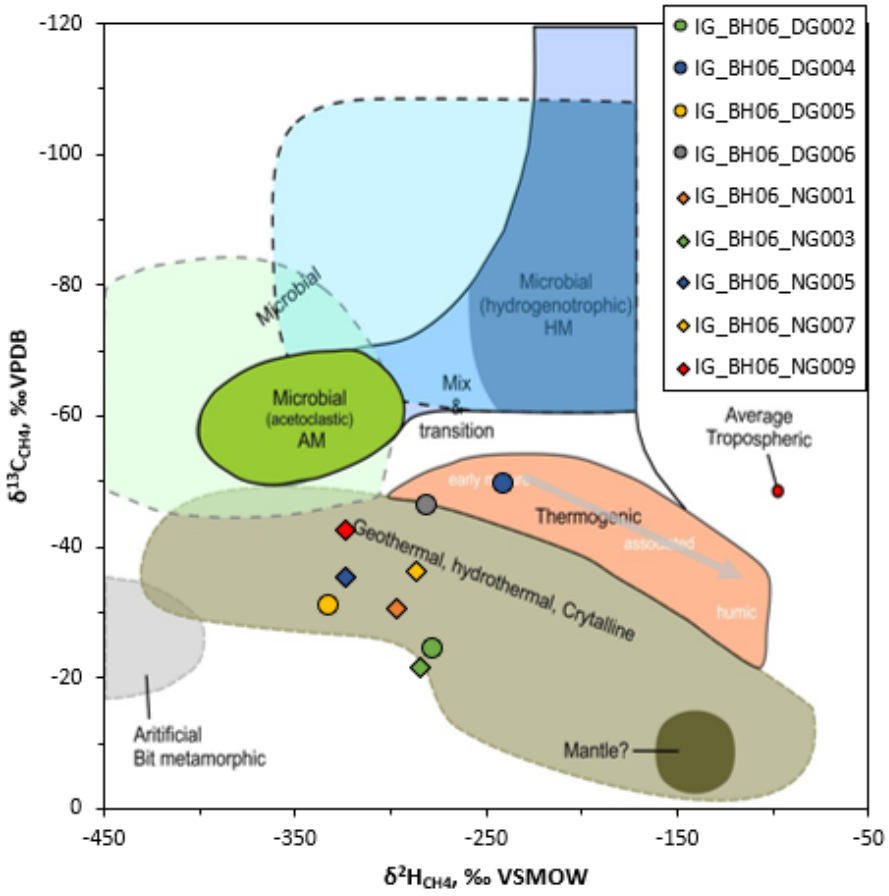


Figure 9-6: Isotopic classification of methane dissolved in porewater from core samples from borehole IG_BH06. The porewater results are compared to end-member signatures according to Whiticar (2020).

In the $\delta^{13}C$-CH_4 versus C_1/C_2+C_3 diagram, the porewater hydrocarbon data plot in the upper area of the thermogenic field with a mixing trend to an abiotic component according to Kietäväinen et al. (2017), indicating a thermogenic/abiotic origin of the dissolved hydrocarbons (Figure 9-8).

In summary, a coherent pattern of porewater methane and higher hydrocarbon concentrations, hydrocarbon ratios and stable isotopes is obtained, suggesting generally a hydrothermal crystalline origin for the dissolved hydrocarbons over the entire depth profile.

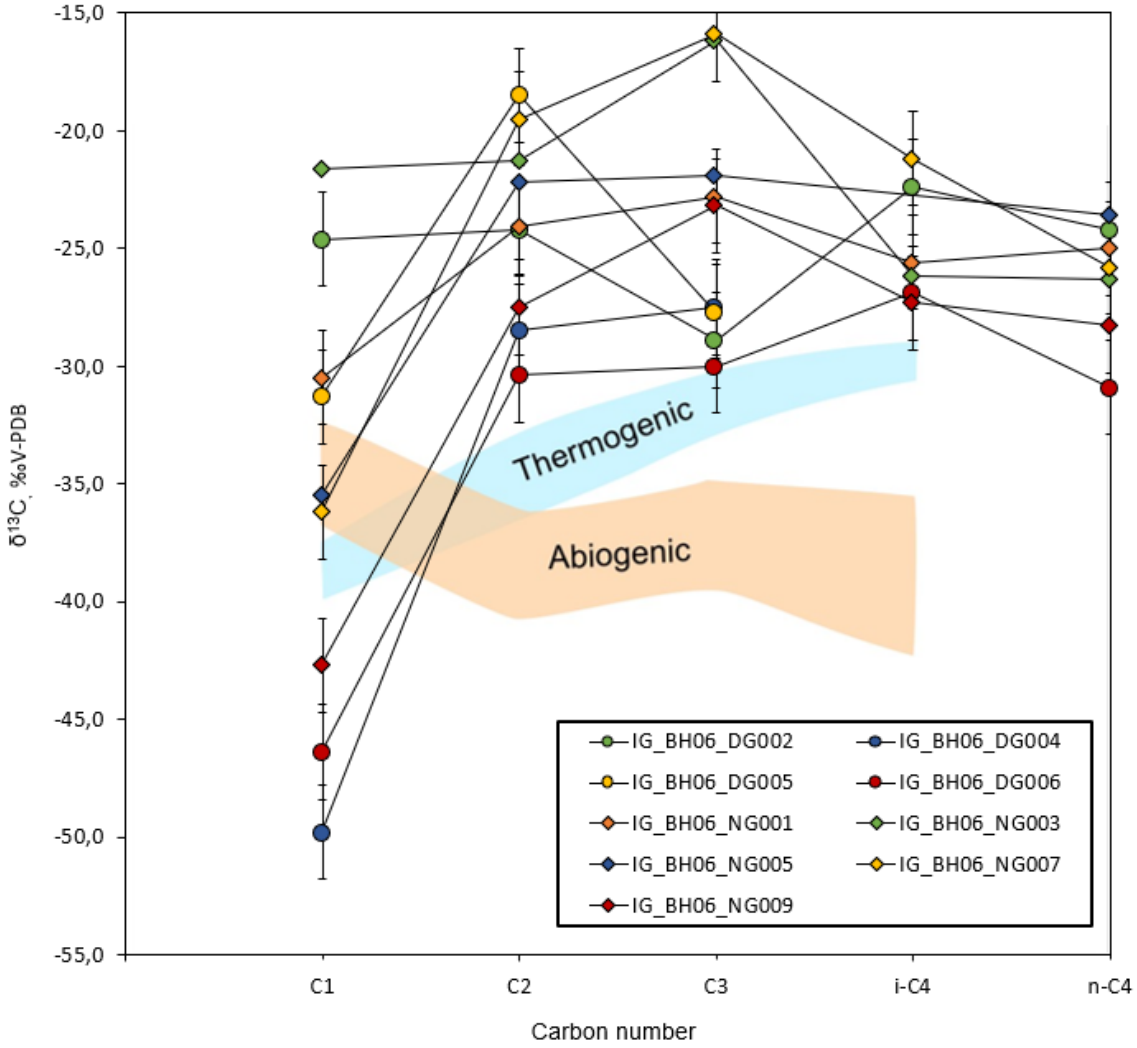


Figure 9-7: Carbon isotope signature patterns of hydrocarbons dissolved in porewater of cores from borehole IG_BH06 versus carbon numbers compared to patters of hydrocarbons produced by abiogenic processes (Sherwood Lollar et al. 2002) and thermogenic processes (Sherwood Lollar et al. 1994).

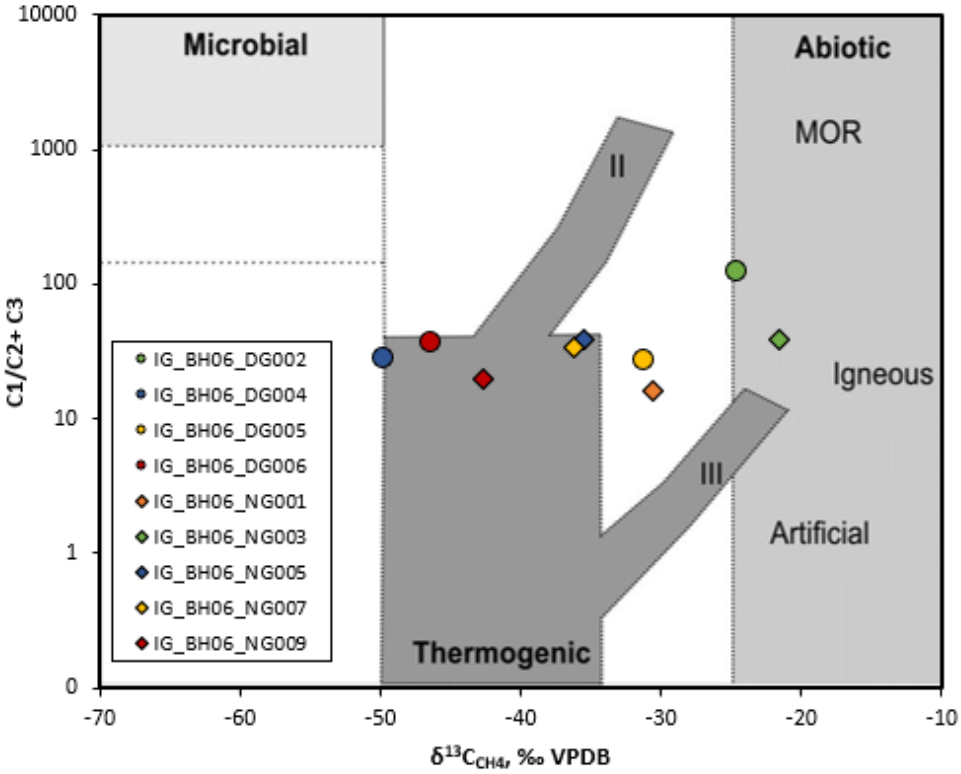


Figure 9-8: Carbon isotope signatures of methane versus the hydrocarbon ratio of methane over ethane plus propane (C_1/C_2+C_3) dissolved in porewater of cores from borehole IG_BH06 compared to end-member fields according to Faber (1987), Whiticar (1999) and Kietäväinen et al. (2017) and references therein.

Table 9-2: Stable isotope signatures of gases dissolved in porewater of core samples from borehole IG_BH06

Sample		IG_BH06_ DG001**	IG_BH06_ DG002	IG_BH06_ DG004	IG_BH06_ DG005	IG_BH06_ DG006
Depth	mbgs	510.2	620.9	802.4	842.7	936.4
$\delta^{15}N\text{-}N_2$	‰-Air	-0.4	n.b.	-0.3	0.0	-0.3
$\delta^{13}C\text{-}CH_4$	‰-PDB	-40.8	-24.6	-49.8	-31.3	-46.4
$\delta^{2}H\text{-}CH_4$	‰ V-SMOW	n.d.	-278	-241	-333	-281
$\delta^{13}C\text{-}C_2H_6$	‰-PDB	-28.2	-24.2	-28.5	-18.5	-30.4
$\delta^{13}C\text{-}C_3H_8$	‰-PDB	n.d.	-28.9	-27.5	-27.7	-30
$\delta^{13}C\text{-}i\text{-}C_4H_{10}$	‰-PDB	n.d.	-22.4	n.d.	n.d.	-26.9
$\delta^{13}C\text{-}n\text{-}C_4H_{10}$	‰-PDB	n.d.	-24.2	n.d.	n.d.	-30.9

Sample		IG_BH06_ NG001	IG_BH06_ NG003	IG_BH06_ NG005	IG_BH06_ NG007	IG_BH06_ NG009
Depth	mbgs	512.5	623.6	735.6	846.9	939.6
$\delta^{15}N\text{-}N_2$	‰-Air	n.a.	n.a.	n.a.	n.a.	n.a.
$\delta^{13}C\text{-}CH_4$	‰-PDB	-30.5	-21.6	-35.5	-36.2	-42.7
$\delta^{2}H\text{-}CH_4$	‰ V-SMOW	-297	-284	-323	-287	-324
$\delta^{13}C\text{-}C_2H_6$	‰-PDB	-24.1	-21.3	-22.2	-19.5	-27.5
$\delta^{13}C\text{-}C_3H_8$	‰-PDB	-22.8	-16.2	-21.9	-15.9	-23.2
$\delta^{13}C\text{-}i\text{-}C_4H_{10}$	‰-PDB	-25.6	-26.2	n.d.	-21.2	-27.3
$\delta^{13}C\text{-}n\text{-}C_4H_{10}$	‰-PDB	-25.0	-26.3	-23.6	-25.8	-28.3

Depths are in mbgs downhole

** results are less reliable, because sample container was not tight and showed a final pressure of 917 mbar

9.2 Noble Gases

Noble gases, like helium and argon, are continuously produced in rocks by radioactive decay of different elements in rock forming minerals (e.g., Porcelli et al. 2002). Noble gases are differentiated by either radiogenic or nucleogenic origin. Noble gas isotopes, which are directly produced by radioactive decay, such as ^{4}He and ^{40}Ar, are described as radiogenic. Those produced by nuclear reactions of α particles or by thermogenic neutrons, such as ^{3}He and ^{36}Ar, are described as nucleogenic noble gas isotopes. Helium produced in minerals is readily released to the surrounding porewater due to the strong activation energy during the production process (Lehmann et al. 2003; Tolstikhin et al. 2005). In contrast, in situ produced argon tends to remain in the minerals (K-Ar dating, e.g., Ballentine and Burnard 2002, Kelley 2002).

Once released to the porewater, noble gases are transported by diffusion from the rock matrix into adjacent fracture groundwater. The chemically inert character of noble gases as trace dissolved gases, and their continuous in situ production, make them a valuable tracer to investigate solute transport processes. Transport processes can be evaluated by comparing 1) the calculated noble gas production rates, 2) the measured noble gas concentrations in the rock, porewater and groundwater, and 3) the possible external input of noble gases into the system (Ballentine et al. 2002, Ozima & Podosek 2005).

Radiogenic and nucleogenic noble gases dissolved in matrix porewater and fracture groundwater in subsurface bedrock systems can either have a local source (i.e., in situ production in the rock matrix), or can be influenced by the ingress of noble gases produced via external sources (i.e., the mantle or the atmosphere) (Porcelli & Ballentine 2002). The different provenances of noble gases dissolved in porewater and fracture groundwater can be distinguished by comparing noble gas isotope ratios such as $^{3}He/^{4}He$ and $^{40}Ar/^{36}Ar$ ratios.

Noble gases (He, Ar) and noble gas isotopes ($^{3,4}He$, $^{20,22}Ne$, $^{36,40}Ar$, ^{84}Kr, ^{132}Xe) were extracted and analysed on five samples taken between 512 m and 940 mbgs (downhole) from IG_BH06.

The final pressures of the cylinders after equilibration varied between 33.6 and 36.8 mbars at temperatures of 22.7 to 23.3 °C. Due to the fact that the cores are naturally saturated, the partial pressure of water vapour was calculated according to Equation 10. The subtraction of the water vapour partial pressure, and the correlation to standard conditions, yields total gas pressures between 5.2 and 9.1 mbar STP, corresponding to 1.2 to 2.3 NmL of gas extracted from the porewater.

The individual noble gas concentrations were corrected for air contamination by the measurements of the $^{20,22}Ne$ concentrations. The calculations were carried out according to Equation 13. A correction for the $^{20,22}Ne$ concentration is feasible because the geogenic production rate is very low in the crust ($1.5*10^{-21}$ ccSTP/(g_{rock}*a) for ^{20}Ne and $5.2*10^{-22}$ ccSTP/(g_{rock}*a) for ^{22}Ne (Leya and Wieler 1999)).

The extracted $^{20,22}Ne$ concentrations vary between $6.20*10^{-7}$ and $8.28*10^{-7}$ NmL, which corresponds to an air contamination between 2.6 and 3.7 % of the total gas volume. The concentrations of the gas species were corrected using the general air composition (Appendix B).

The extracted and corrected volumes of the individual gas species are converted to milliliters gas per liter porewater STP (NmL/L_{PW}, 0°C = 273 K, 1013 hPa) using the volume of porewater according to Equation 11.

The concentrations of total helium and total argon dissolved in porewater vary between 2.49 and 4.58 NmL/L_{PW} for He and between 1.89 and 4.92 NmL/L_{PW} for Ar (Table 9-3). The porewater helium concentrations are almost constant within the error in the intervals sampled at 512 and 624 mbgs (downhole), and are higher at a constant level in the following intervals between 736 and 940 mbgs (downhole) (Figure 9-9). Total porewater argon concentrations increase between 512 and 736 mbgs (downhole), decrease slightly at 847 and 940 mbgs (downhole) (Figure 9-9).

^{84}Kr and ^{132}Xe concentrations, which were also determined, vary between 0.00048 and 0.00121 NmL/L_{PW} for ^{84}Kr and between 0.00008 and 0.00018 NmL/L_{PW} for ^{132}Xe (Table 9-3).

Porewater $^{40}Ar/^{36}Ar$ ratios vary between 342 and 664 in the sampled bedrock intervals (512 to 940 mbgs (downhole)) and are significantly higher than that of air (296), indicating a radiogenic accumulation over time (Table 9-3). The $^{40}Ar/^{36}Ar$ are constant in the intervals between 512 and 736 mbgs (downhole) and increase with increasing depth down to 940 mbgs (downhole) (Figure 9-10). Porewater $^{3}He/^{4}He$ ratios range between $2.86*10^{-8}$ and $3.23*10^{-8}$ and are constant in the sampled intervals (Table 9-3, Figure 9-10). The comparison with end-member $^{3}He/^{4}He$ ratios shows that the $^{3}He/^{4}He$ dissolved in porewater of core samples taken along the depth profile of IG_BH06 are low compared to air and mantle derived helium due to the accumulation of radiogenic ^{4}He (Figure 9-10, Figure 9-11). They are in the range of crustal derived helium (Figure 9-11, Osenbrück 1996). Proportions of mantle derived helium are not indicated.

Table 9-3: Noble gas concentrations and ratios dissolved in porewater of cores taken from borehole IG_BH06.

Sample		IG_BH06_ NG001	IG_BH06_ NG003	IG_BH06_ NG005	IG_BH06_ NG007	IG_BH06_ NG009
Depth	mbgs	512.5	623.6	735.6	846.9	939.6
Water Content	wt. %	0.22	0.20	0.09	0.20	0.17
Mass of PW	g	3.76	3.19	1.58	3.32	2.69
Helium	Nml/L_{PW}	3.46	2.49	4.14	4.51	4.58
Argon	Nml/L_{PW}	1.89	2.82	4.92	3.06	3.12
Krypton-84	Nml/L_{PW}	0.00050	0.00074	0.00121	0.00054	0.00048
Xenon-132	Nml/L_{PW}	0.00008	0.00012	0.00018	0.00008	0.00008
$^{40}Ar/^{36}Ar$		342	354	355	547	664
$^{3}He/^{4}He$		3.23E-08	2.86E-08	2.93E-08	3.14E-08	3.19E-08

Depths are in mbgs (downhole)

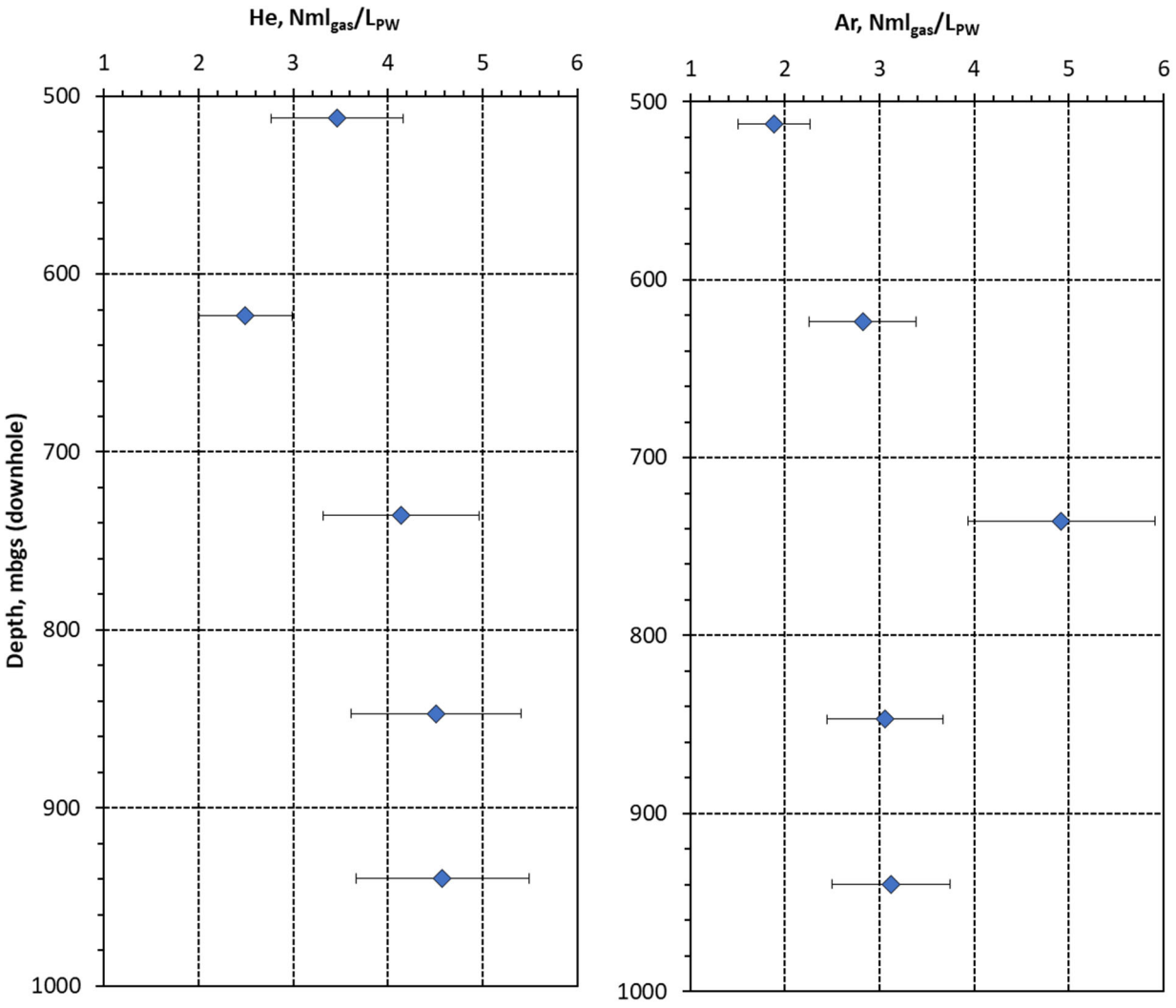


Figure 9-9: Helium (left) and argon concentrations of porewater as function of depth along borehole IG_BH06; errors are ± 20.0%

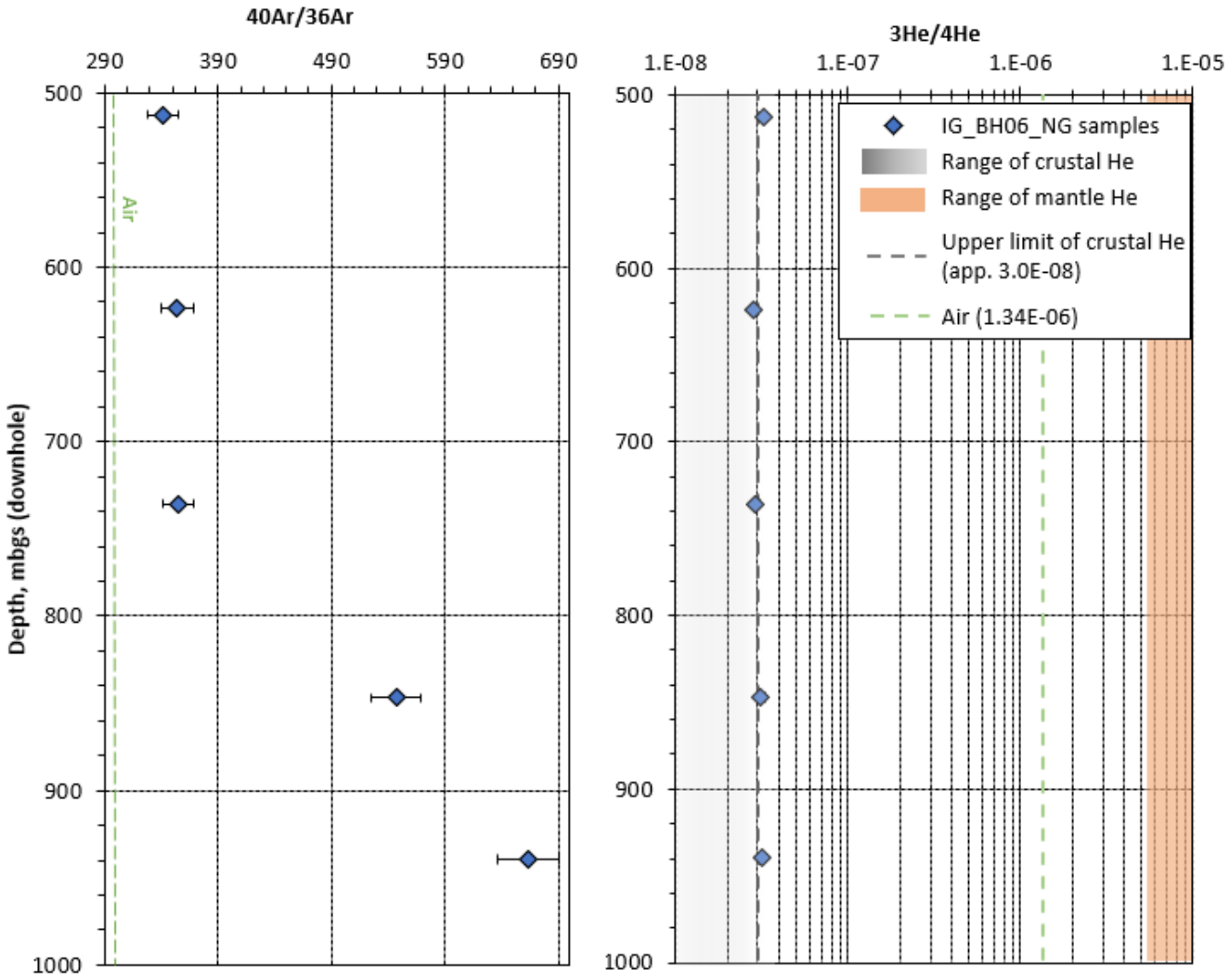


Figure 9-10: $^{40}Ar/^{36}Ar$ and $^{3}He/^{4}He$ isotope ratios dissolved in porewater as function of depth along borehole IG_BH06 compared to end-members of air and crustal and mantle He.

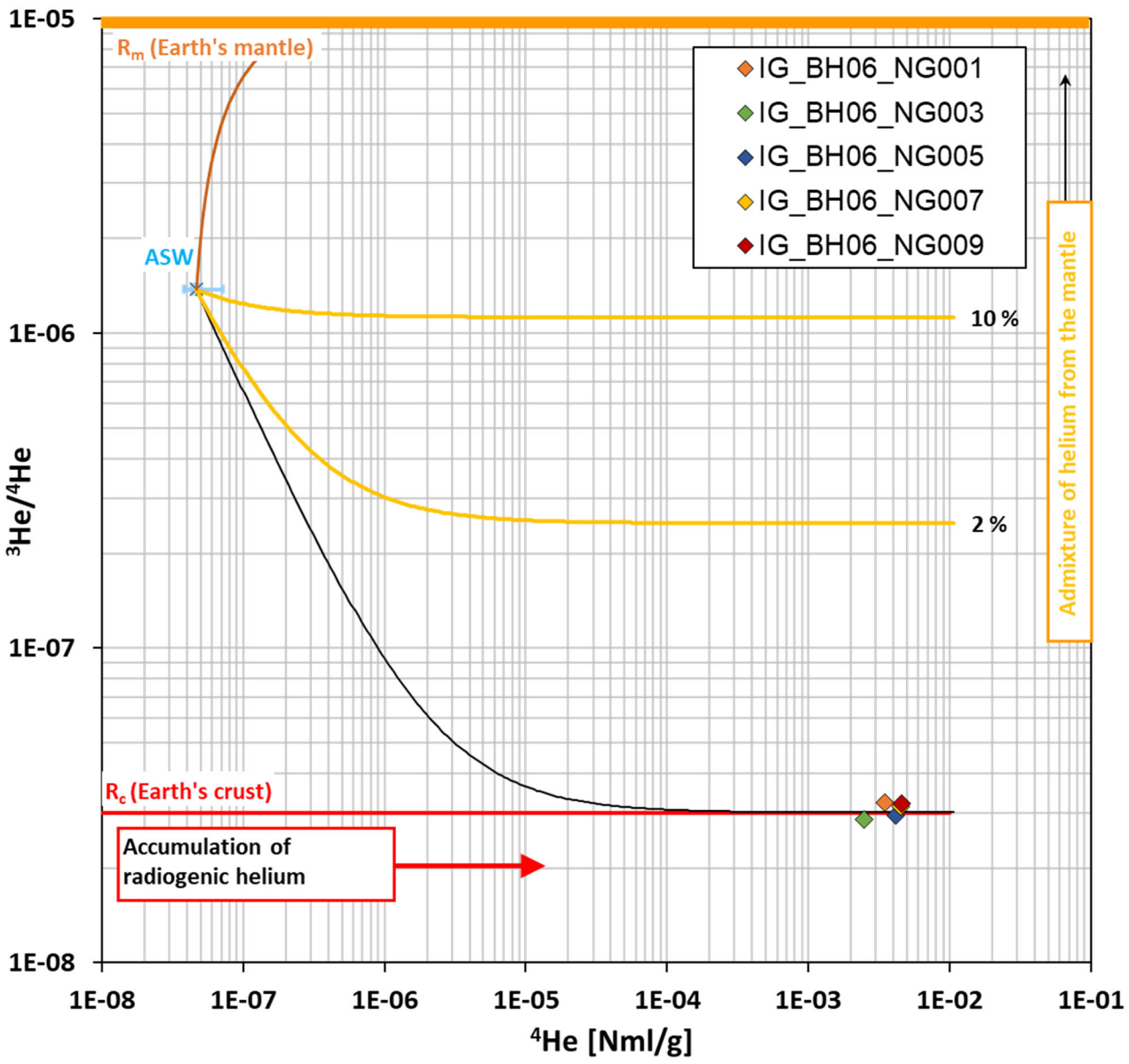


Figure 9-11: ^{3}He/^{4}He isotope ratios versus helium concentrations dissolved in porewater of cores taken from borehole IG_BH06 compared to end-member concentration of air saturated water (ASW), crust and mantle signature and potential mantle mixing paths (Osenbrück 1996)

10.0 REFERENCES

Ballentine, C.J., Burnard, P.G., 2002. Production, Release and Transport of Noble Gases in the Continental Crust. Reviews in Mineralogy & Geochemistry, 47, 481-529.

Ballentine, C.J., Burgess, R., Marty, B., 2002. Tracing Fluid Origin, Transport and Interaction in the crust. Reviews in Mineralogy & Geochemistry, 47, 539-608.

Blackburn, C.E. and Hinz, P., 1996. Gold and base metal potential of the northwest part of the Raleigh Lake greenstone belt, northwestern Ontario-Kenora Resident Geologist's District; in Summary of Field Work and Other Activities 1996, Ontario Geological Survey, Miscellaneous Paper 166, p.113-115.

Crank, J., 1975. The Mathematics of Diffusion; Oxford Science Publications; Oxford.

DesRoches, A., Sykes, M., Parmenter, A. and Sykes, E., 2018. Lineament Interpretation of the Revell Batholith and Surrounding Greenstone Belts (Nuclear Waste Management Organization. No. NWMO-TR-2018-19.

Eichinger, F.L., Waber, H.N., Smellie, J.A.T., 2006. Characterisation of Matrix Porewater at the Olkiluoto Investigation Site, Finland. Posiva Working Report 2006-103, Posiva OY, Olkiluoto Finland.

Eichinger, F., Hämmerli, J., Waber, H.N., Diamond, L.W., Smellie, J.A.T., 2013. Chemistry and Dissolved Gases of Matrix Porewater and Fluid Inclusions in Olkiluoto Bedrock from Drillhole ONK-PH9. Posiva Working Report 2011-63, Posiva Oy, Olkiluoto, Finland.

Eichinger, F., Iannotta, J., 2022. Characterisation of porewater of core samples from borehole KFR 121. SKB Report R-21-21, SKB, Stockholm, Sweden.

Ertl, S., Eichinger, F., Pichlmaier, J., Voropaev, A., 2024. A new method to determine d37Cl values of chloride in aquatic systems. Grundwasser.

Faber, E., Gerling, P., Dumke, I., 1987. Gaseous hydrocarbons of unknown origin found while drilling. Advances in Organic Geochemistry, 13, 875-879.

Friedrich, R., 2007. Grundwassercharakterisierung mit Umwelttracern: Erkundung des Grundwassers der Odenwald-Region sowie Implementierung eines neuen Edelgas-Massenspektrometersystems. Inaugural-Dissertation, Ruprecht-Karls-Universität, Heidelberg, Germany.

Golder, 2021. Phase 2 Initial Borehole Drilling and Testing at IG_BH04/05/06, Ignace Area – Borehole Characterization Plan for IG_BH06. NWMO Report Number: APM-PLAN-01332-0275

Golder and PGW (Paterson Grant and Watson Ltd.), 2017. Phase 2 Geoscientific Preliminary Assessment, Geological Mapping, Township of Ignace and Area, Ontario. NWMO Report Number: APM-REP-01332-0225.

Gimmi, T. and Waber, H.N., 2004. Modelling of Tracer Profiles in Pore Water of Argillaceous Rocks in the Benken Borehole: Stable Water Isotopes, Chloride, and Chlorine Isotopes; Nagra Tech. Rep. 2004-05, Nagra, Wettingen, Switzerland.

Jäckli, H., 1970. Kriterien zur Klassifikation von Grundwasservorkommen. Ecologae geol. Helv., 63 (2), 389-434.

Jähne, B., Heinz, G., Dietrich, W., 1987. Measurement of the Diffusion Coefficients of Sparingly Soluble Gases in Water. Journal of Geophysical Research, 92, C10, 10,767-10,776.

Kelley, S., 2002. K-Ar and Ar-Ar Dating. Reviews in Mineralogy & Geochemistry, 47, 785-810.

Kietäväinen, R., Ahonen, L., Niinikosi, P., Nykänen, H., Kukkonen, I.T., 2017. Abiotic and biotic controls on methane formation down to 2.5 km depth within the Precambrian Fennoscandian Shield. Geochimica et Cosmochimica Acta 202, 124-145.

Lehmann, B.E., Waber, H.N., Tolstikhin, I., Kamensky, I., Gannibal, M., Kalashnikov, E., Pevzner, B., 2003. Helium in solubility equilibrium with quartz and porefluids in rocks: A new approach in hydrology. Geophysical Research Letters, 30, 3, 28-1 – 28-4.

Leya, I., Wieler, R., 1999. Nucleogenic production of Ne isotopes in Earth's crust and upper mantle induced by alpha particles from the decay of U and Th. Journal of Geophysical Research, 104, 15439-15450.

Lide, D.R., 1994. CRC Handbook of chemistry and physics. 75th ed., CRC Press, Boca Raton, USA.

Meier, D.B., Waber, H.N., Gimmi, T., Eichinger, F., Diamond, L.W., 2015. Reconstruction of in situ porosity and porewater compositions of low-permeability crystalline rocks: Magnitude of artefacts induced by drilling and sample recovery. Journal of Contaminant Hydrology, 183, 55-71.

OGS (Ontario Geological Survey), 2011. 1:250 000 scale bedrock geology of Ontario, Ontario Geological Survey, Miscellaneous Release Data 126 - Revision 1.

Ohlsson, Y. and Neretnieks, I., 1995. Literature survey of matrix diffusion theory and of experiments and data including natural analogues; SKB Tech. Rep. 95-12, Svensk Kärnbränslehantering AB, Stockholm, Sweden.

Osenbrück, K., 1996. Alter und Dynamik tiefer Grundwässer: Eine neue Methode zur Analyse der Edelgase im Porenwasser in Gesteinen. Dissertation Ruprecht-Karls-Universität Heidelberg, Heidelberg, Germany.

Ozima, M., Podosek, F.A., 2005. Noble gas geochemistry. Cambridge University Press, Cambridge, UK.

Parmenter, A., Waffle, L. and DesRoches, A., 2020. An updated bedrock geology map and geological database for the northern portion of the Revell batholith (No. NWMO-TR-2020-08). Nuclear Waste Management Organization.

Porcelli, D., Ballentine, C.J., 2002. Models for the Distribution of Terrestrial Noble Gases and Evolution of the Atmosphere. Reviews in Mineralogy & Geochemistry, 47, 411-469.

Rogge, T., 1997. Eine molekular-diffusive Methode zur Bestimmung des Porenwassergehaltes und der Zusammensetzung von stabilen Isotopen im Porenwasser von Gestein; unveröffentlichte Diplomarbeit; Heidelberg.

Rübel, A.P., Sonntag, Ch., Lippmann, J., Pearson, F.J. and Gautschi, A., 2002. Solute transport in formations of very low permeability: Profiles of stable isotope and dissolved noble gas contents of pore water in the Opalinus Clay. Mont Terri, Switzerland; Geochim. Cosmochim. Acta, 66, 1311-1321.

Schmid, R., Douglas, Fettes D., Harte, B., Davis, E., Desmons, J., 2007. How to Name a Metamorphic Rock. Recommendations by the IUGS Subcomission on the Systematics of Metamorphic Rocks.

SGL (Sander Geophysics Limited), 2015. Phase 2 Geoscientific Preliminary Assessment, Acquisition, Processing and Interpretation of High-Resolution Airborne Geophysical Data, Township of Ignace, Ontario. Prepared for Nuclear Waste Management Organization (NWMO). NWMO Report Number: APM-REP-06145-0002.

Sherwood-Lollar, B. S., Weise, S. M., Frape, S. K., Barker, J. F., 1994. Isotopic constraints on the migration of hydrocarbon and helium gases southwestern Ontario. Bull. Can. Petrol. Geol. 42, 283-295.

Sherwood Lollar, B., Westgate, T.D., Ward, J.A., Slater, G.F., Lacrampe-Couloume, G., 2002. Abiogenic formation of alkanes in the Earth's crust as a minor source for global hydrocarbon reservoirs. Nature, 416, 522-524.

SRK (SRK Consulting, Inc.) and Golder, 2015. Phase 2 Geoscientific Preliminary Assessment, Observation of General Geological Features, Township of Ignace, Ontario. Prepared for Nuclear Waste Management Organization. NWMO Report Number: APM-REP-06145-0004.

Stone, D., 2009. Geology of the Bending Lake Area, Northwestern Ontario; in Summary of Field Work and Other Activities 2009. Ontario Geological Survey. Open File Report 6240.

Stone, D., 2010a. Geology of the Stormy Lake Area, Northwestern Ontario; in Summary of Field Work and Other Activities 2010. Ontario Geological Survey, Open File Report 6260.

Stone, D., 2010b. Precambrian geology of the central Wabigoon Subprovince area, northwestern Ontario. Ontario Geological Survey, Open File Report 5422.

Stone, D., Halle, J. and Chaloux, E., 1998. Geology of the Ignace and Pekagoning Lake Areas, Central Wabigoon Subprovince; in Summary of Field Work and Other Activities 1998, Ontario Geological Survey, Misc. Paper 169.

Stone, D., Davis, D.W., Hamilton, M.A. and Falcon, A., 2010. Interpretation of 2009 Geochronology in the Central Wabigoon Subprovince and Bending Lake Areas, Northwestern Ontario, in Summary of Field Work and Other Activities 2010, Ontario Geological Survey, Open File Report 6260.

Tolstikhin, I.N., Gannibal, M., Tarakanov, S., Pevzner, B., Lehmann, B., Ihly, B., Waber, H.N., 2005. Helium transfer from water into quartz crystals: A new approach for porewater dating. Earth and Planetary Science Letters, 238, 31-41.

Waber, H.N. and Smellie, J.A.T., 2005. SKB Site Investigations Forsmark – Borehole KFM06: Characterisation of porewater. Part I: Diffusion experiments; SKB P-Rep. P-05-196, Svensk Kärnbränslehantering AB, Stockholm, Sweden.

Waber, H.N. and Smellie, J.A.T., 2006. Oskarshamn site investigations. Borehole KLX03: Characterisation of porewater. Part 2: Rock properties and diffusion experiments; SKB P-Report P-06-77. Svensk Kärnbränslehantering AB, Stockholm, Sweden.

Whiticar, M.J., 1999. Carbon and hydrogen isotope systematics of bacterial formation and oxidation of methane. Chemical Geology, 161, 291-314.

Whiticar, M.J., 2020. The Biogeochemical Methane Cycle. In H. Wilkes (ed.), Hydrocarbons, Oils and Lipids: Diversity, Origin, Chemistry and Fate. Handbook of Hydrocarbon and Lipid Microbiology, Springer Nature, Switzerland.

WSP, 2024. Phase 2 Initial Borehole Drilling and Testing at IG_BH04/05/06, Ignace Area – Mineralogical and Geochemical Analysis of Core for IG_BH06 – (In preparation).

https://wsponlinecan.sharepoint.com/sites/ca-gld-20253946/externalsharing/wp04c shared files/ig_bh06 wp04c/13 final report ig_bh06 wp04c 09dec2024/20253946 ig_bh06 wp04c rpt_dec2024_r6a.docx

APPENDIX A

Core Logging Depth Correction and Photo Documentation

TECHNICAL MEMORANDUM

DATE August 4, 2024 **Reference No.** 20253946-6043-TM-001

TO File
WSP Canada Inc.

CC File

FROM George Schneider **EMAIL george.schneider@wsp.com**

ADDENDUM TO LABORATORY REPORT FROM HYDROISOTOP FOR WORK PACKAGE WP04C - BOREHOLE IG_BH06

This addendum corrects the depths (along borehole) of the samples for porewater extraction and analysis included in this report. The depth adjustment is the result of a correction applied to the core logging depths after reconciliation with the drilling depth records. Refer to the WP03 report for details and to the acQuire database for corrected depths.

Refer to Table 1 for the list of samples containing the original logged depths and the corrected depths after reconciliation between the core logging and drilling depths. This addendum shall always accompany the laboratory report when distributed to other parties.

Table 1: List of samples requiring depth correction

Sample ID	Test / Sample Type	Original Logged Depth (mbgs downhole)		Corrected Depth (mbgs downhole)	
		From	To	From	To
IG_BH06_AQ001	Aqueous Extraction	212.79	212.94	212.79	212.94
IG_BH06_AQ002	Aqueous Extraction	292.44	292.68	292.44	292.68
IG_BH06_AQ003	Aqueous Extraction	370.13	370.53	370.13	370.53
IG_BH06_AQ004	Aqueous Extraction	453.40	453.62	453.32	453.54
IG_BH06_AQ005	Aqueous Extraction	504.30	504.47	504.15	504.32
IG_BH06_AQ006	Aqueous Extraction	562.62	562.81	562.38	562.57
IG_BH06_AQ007	Aqueous Extraction	574.35	574.50	574.10	574.25
IG_BH06_AQ008	Aqueous Extraction	612.38	612.57	612.07	612.26
IG_BH06_AQ009	Aqueous Extraction	648.06	648.24	647.70	647.88
IG_BH06_AQ010	Aqueous Extraction	666.08	666.28	665.69	665.89
IG_BH06_AQ011	Aqueous Extraction	693.87	694.03	693.44	693.60
IG_BH06_AQ012	Aqueous Extraction	720.73	720.90	720.26	720.43
IG_BH06_AQ013	Aqueous Extraction	747.71	747.85	747.21	747.35
IG_BH06_AQ014	Aqueous Extraction	771.16	771.33	770.62	770.79

Sample ID	Test / Sample Type	Original Logged Depth (mbgs downhole)		Corrected Depth (mbgs downhole)	
		From	To	From	To
IG_BH06_AQ015	Aqueous Extraction	804.84	805.02	804.25	804.43
IG_BH06_AQ016	Aqueous Extraction	840.98	841.38	840.34	840.74
IG_BH06_AQ017	Aqueous Extraction	853.18	853.42	852.52	852.76
IG_BH06_AQ018	Aqueous Extraction	885.50	885.66	884.80	884.96
IG_BH06_AQ019	Aqueous Extraction	927.81	928.09	927.04	927.32
IG_BH06_AR010	Archive Sample	398.49	398.91	398.49	398.91
IG_BH06_AR013	Archive Sample	421.39	421.79	421.36	421.76
IG_BH06_AR019	Archive Sample	533.79	534.16	533.60	533.97
IG_BH06_AR020	Archive Sample	542.66	543.04	542.45	542.83
IG_BH06_AR027	Archive Sample	594.78	595.14	594.50	594.86
IG_BH06_AR038	Archive Sample	722.38	722.83	721.91	722.36
IG_BH06_AR039	Archive Sample	728.58	728.94	728.10	728.46
IG_BH06_AR045	Archive Sample	796.49	796.85	795.92	796.27
IG_BH06_AR049	Archive Sample	820.06	820.42	819.45	819.81
IG_BH06_AR064	Archive Sample	971.18	971.54	970.35	970.71
IG_BH06_DG001	Non-Inert Gas	510.09	510.29	509.93	510.13
IG_BH06_DG002	Non-Inert Gas	620.74	620.96	620.42	620.64
IG_BH06_DG003	Non-Inert Gas	743.92	744.13	743.42	743.63
IG_BH06_DG004	Non-Inert Gas	802.31	802.51	801.73	801.93
IG_BH06_DG005	Non-Inert Gas	842.56	842.76	841.92	842.12
IG_BH06_DG006	Non-Inert Gas	936.30	936.50	935.52	935.72
IG_BH06_NG001	Noble Gas	512.40	512.62	512.24	512.46
IG_BH06_NG003	Noble Gas	623.54	623.75	623.22	623.43
IG_BH06_NG005	Noble Gas	735.51	735.74	735.02	735.25
IG_BH06_NG007	Noble Gas	846.84	847.04	846.19	846.39
IG_BH06_NG009	Noble Gas	939.48	939.69	938.70	938.91
IG_BH06_PW001	Porewater	212.09	212.44	212.09	212.44
IG_BH06_PW002	Porewater	291.28	291.69	291.28	291.69
IG_BH06_PW003	Porewater	369.33	369.73	369.33	369.73
IG_BH06_PW004	Porewater	453.00	453.40	452.92	453.32
IG_BH06_PW005	Porewater	503.91	504.30	503.76	504.15
IG_BH06_PW006	Porewater	562.25	562.62	562.01	562.38
IG_BH06_PW007	Porewater	574.00	574.35	573.75	574.10

Sample ID	Test / Sample Type	Original Logged Depth (mbgs downhole)		Corrected Depth (mbgs downhole)	
		From	To	From	To
IG_BH06_PW008	Porewater	612.01	612.38	611.70	612.07
IG_BH06_PW009	Porewater	647.69	648.06	647.33	647.70
IG_BH06_PW010	Porewater	665.70	666.08	665.31	665.69
IG_BH06_PW011	Porewater	690.75	691.23	690.33	690.81
IG_BH06_PW012	Porewater	693.49	693.87	693.06	693.44
IG_BH06_PW013	Porewater	720.34	720.73	719.88	720.26
IG_BH06_PW014	Porewater	747.35	747.71	746.85	747.21
IG_BH06_PW015	Porewater	774.69	775.04	774.15	774.50
IG_BH06_PW016	Porewater	804.47	804.84	803.88	804.25
IG_BH06_PW017	Porewater	839.99	840.37	839.35	839.73
IG_BH06_PW018	Porewater	852.83	853.18	852.17	852.52
IG_BH06_PW019	Porewater	885.14	885.50	884.44	884.80
IG_BH06_PW020	Porewater	927.41	927.81	926.65	927.04

WSP Canada Inc.



George Schneider, M.Sc., P.Geo.

GWS/

Distribution: File

Attachments: N/A

c:\gws-work\1 - active\nwmo bh456\lab samples\ig_bh06 wp04c depth memo 04aug2024.docx

Figure A-1: On site documentation of core samples for porewater characterization sent to Hydroisotop (photos provided by Golder); Core samples are packed in the first evacuated and sealed plastic bag



IG_BH06_AQ001: 212.79-212.94 m



IG_BH06_AQ002: 292.44-292.68 m



IG_BH06_AQ003: 370.13-370.53 m



IG_BH06_AQ004: 453.40-453.62 m



IG_BH06_AQ005: 504.30-504.47 m



IG_BH06_AQ006: 562.62-562.81 m



IG_BH06_AQ007: 574.35-574.50 m



IG_BH06_AQ008: 612.38-612.57 m



IG_BH06_AQ009: 648.06-648.24 m



IG_BH06_AQ010: 666.08-666.28 m



IG_BH06_AQ011: 693.87-693.95 m



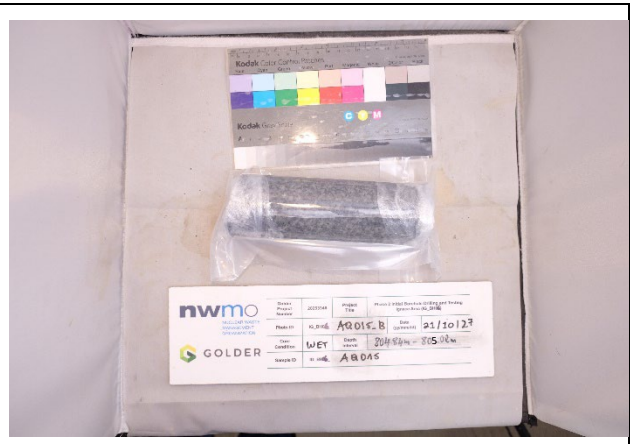
IG_BH06_AQ012: 720.73-720.90 m



IG_BH06_AQ013: 747.71-747.85 m



IG_BH06_AQ014: 771.16-771.22 m



IG_BH06_AQ015: 804.84-805.02 m



IG_BH06_AQ016: 840.98-841.38 m



IG_BH06_AQ017: 853.18-853.42 m



IG_BH06_AQ018: 885.50-885.66 m



IG_BH06_AQ019: 927.81-928.09 m



IG_BH06_PW001: 212.09-212.44 m



IG_BH06_PW002: 291.28-291.69 m



IG_BH06_PW003: 369.33-369.73 m



IG_BH06_PW004: 453.00-453.40 m



IG_BH06_PW005: 503.91-504.30 m



IG_BH06_PW006: 562.25-562.62 m



IG_BH06_PW007: 574.00-574.35 m



IG_BH06_PW008: 612.01-612.38 m



IG_BH06_PW009: 647.69-648.06 m

		
IG_BH06_PW010: 665.70-666.08 m	IG_BH06_PW011: 690.75-691.23 m	IG_BH06_PW012: 693.49-693.87 m
		
IG_BH06_PW013: 720.34-720.73 m	IG_BH06_PW014: 747.35-747.71 m	IG_BH06_PW015: 774.69-775.04 m



IG_BH06_PW016: 804.47-804.84 m



IG_BH06_PW017: 839.99-840.37 m



IG_BH06_PW018: 852.83-853.18 m



IG_BH06_PW019: 885.14-885.50 m



IG_BH06_PW020: 927.41-927.81 m



IG_BH06_AR010: 398.49-398.91 m



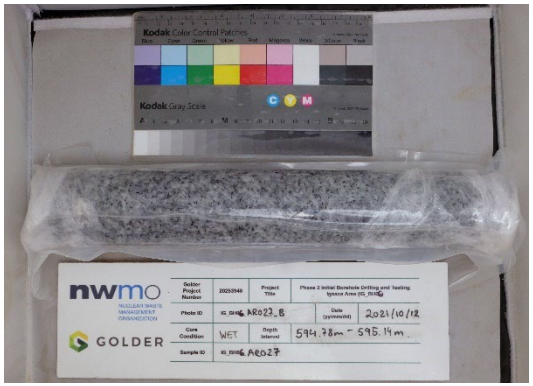
IG_BH06_AR013: 421.39-421.79 m



IG_BH06_AR019: 533.79-534.16 m



IG_BH06_AR020: 542.66-543.04 m



IG_BH06_AR027: 594.78-595.14 m



IG_BH06_AR038: 722.38-722.83 m



IG_BH06_AR039: 728.58-728.94 m



IG_BH06_AR045: 796.49-796.85 m



IG_BH06_AR049: 820.06-820.42 m



IG_BH06_AR064: 971.18-971.54 m



IG_BH06_DG003 743.92-744.13 m



IG_BH06_DG001: 510.09-510.29 m



IG_BH06_DG002: 620.74-620.96 m

		
IG_BH06_DG004: 802.31-802.51 m	IG_BH06_DG005: 842.56-842.76 m	IG_BH06_DG006: 936.30-936.50 m
		
IG_BH06_NG001: 512.40-512.62 m	IG_BH06_NG003: 623.54-623.65 m	IG_BH06_NG005: 735.51-735.74 m

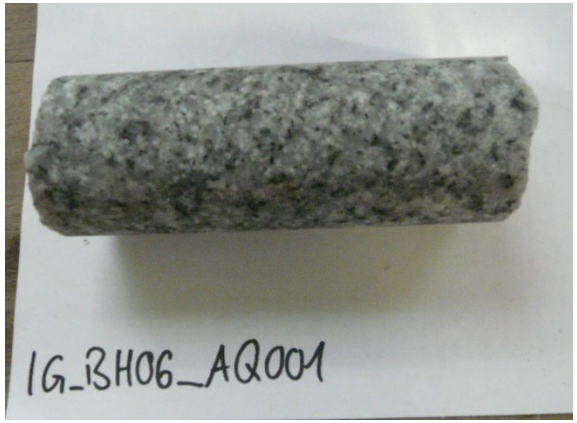


IG_BH06_NG007: 846.84-846.94 m

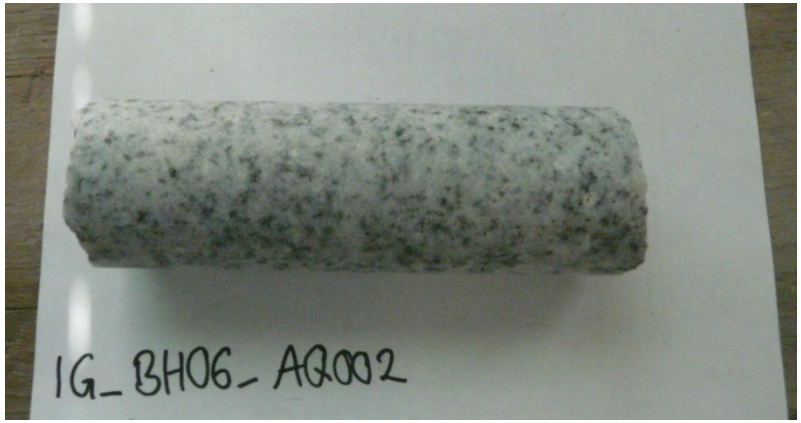


IG_BH06_NG009: 939.48-939.69 m

Figure A-2: Laboratory documentation of core samples for porewater characterization sent to Hydroisotop; photos were taken right after unpacking



IG_BH06_AQ001: 212.79-212.94 m



IG_BH06_AQ002: 292.44-292.68 m



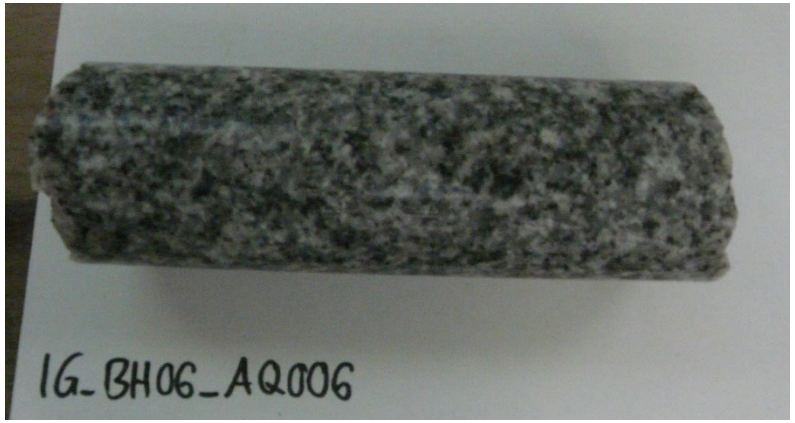
IG_BH06_AQ003: 370.13-370.53 m



IG_BH06_AQ004: 453.40-453.62 m



IG_BH06_AQ005: 504.30-504.47 m



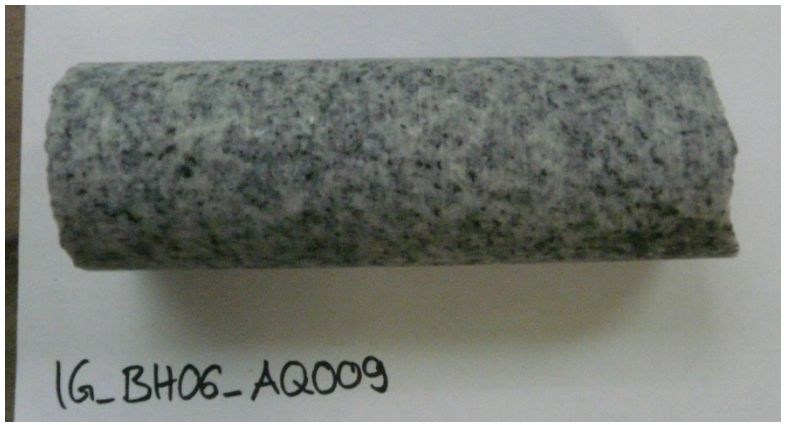
IG_BH06_AQ006: 562.62-562.81 m



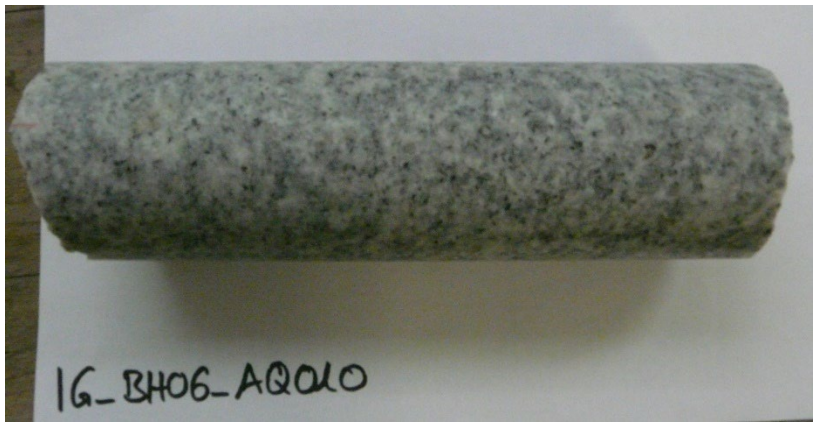
IG_BH06_AQ007: 574.35-574.50 m



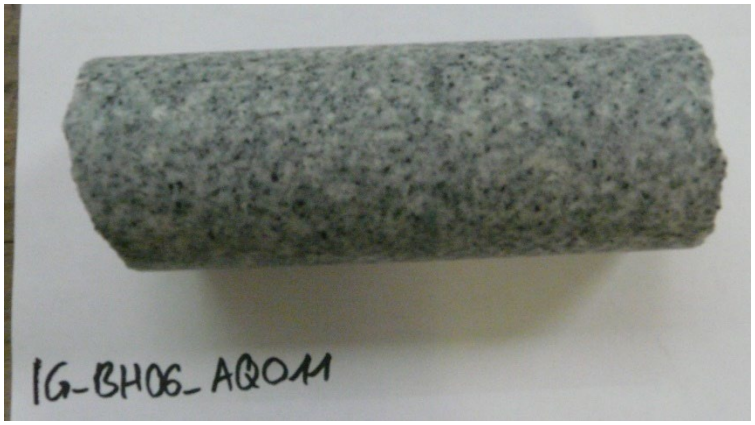
IG_BH06_AQ008: 612.38-612.57 m



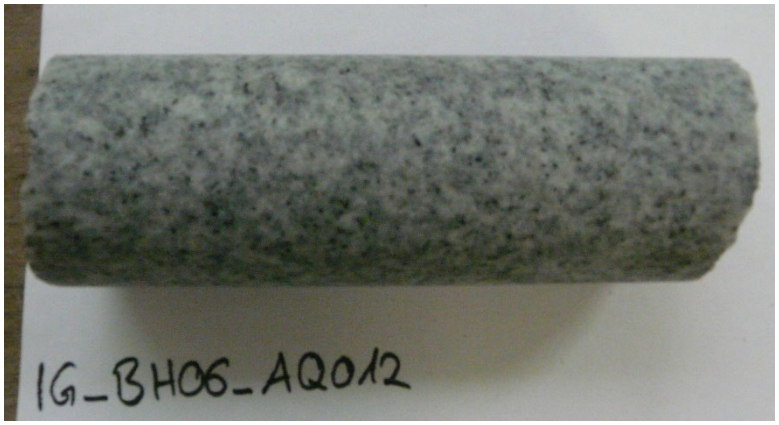
IG_BH06_AQ009: 648.06-648.24 m



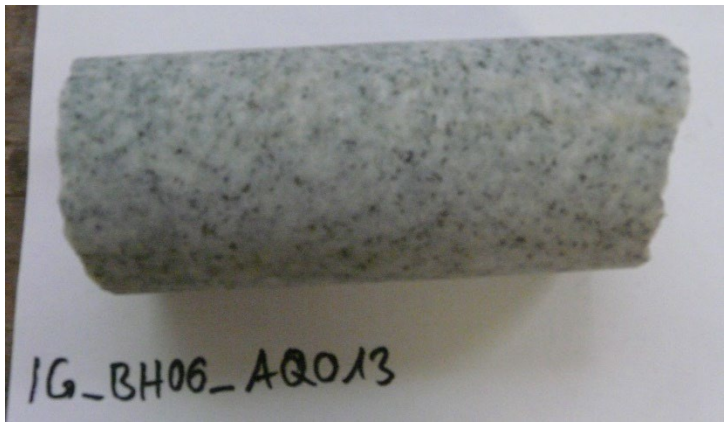
IG_BH06_AQ010: 666.08-666.28 m



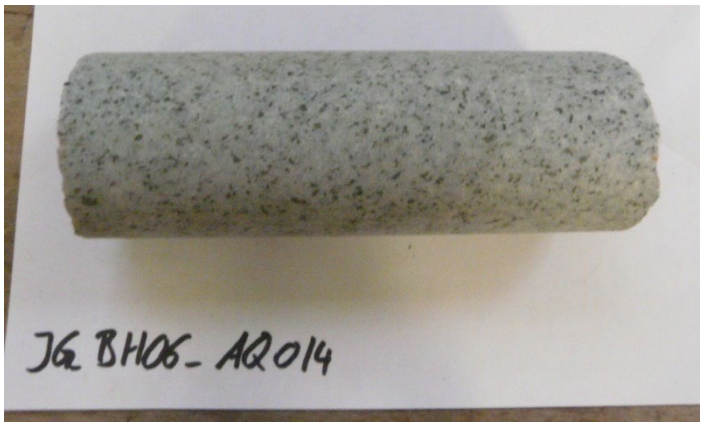
IG_BH06_AQ011: 693.87-693.95 m



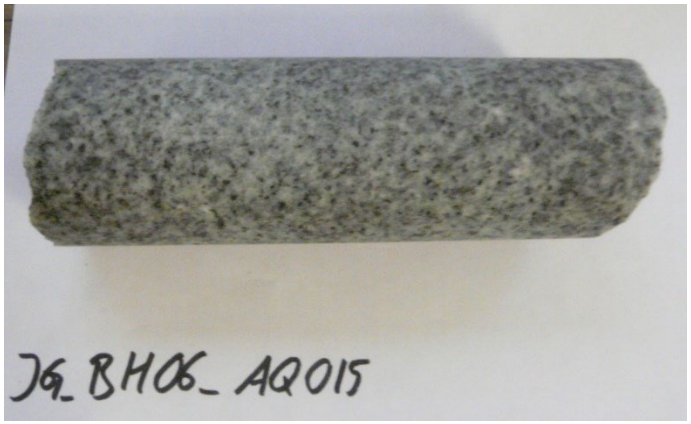
IG_BH06_AQ012: 720.73-720.90 m



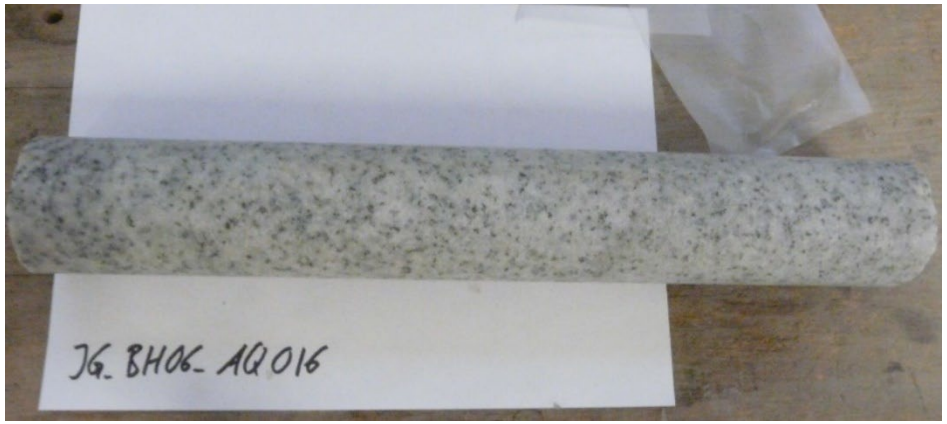
IG_BH06_AQ013: 747.71-747.85 m



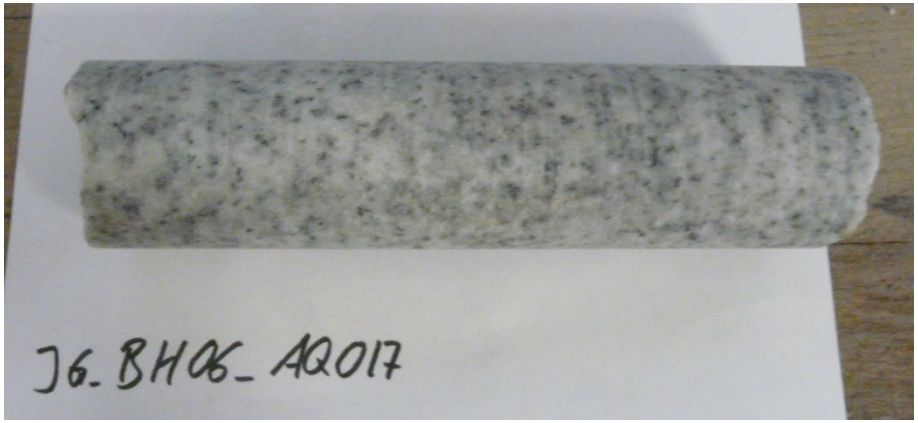
IG_BH06_AQ014: 771.16-771.22 m



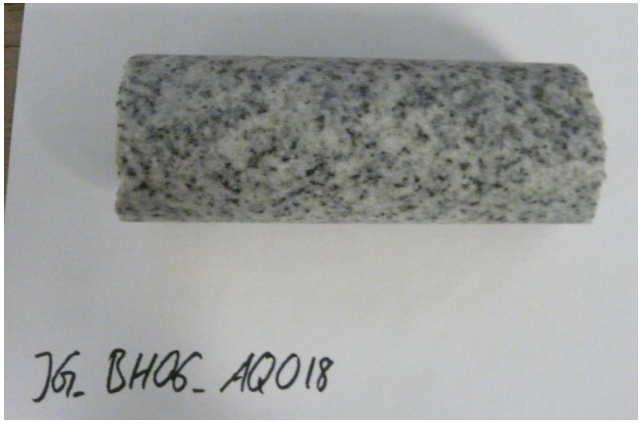
IG_BH06_AQ015: 804.84-805.02 m



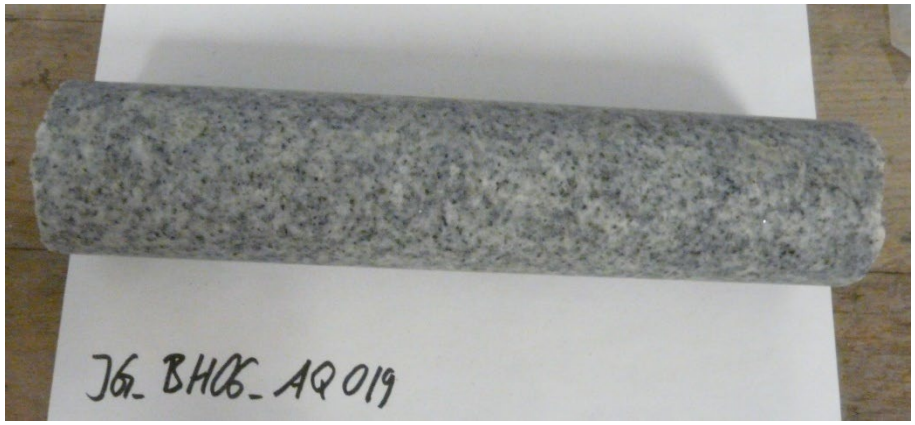
IG_BH06_AQ016: 840.98-841.38 m



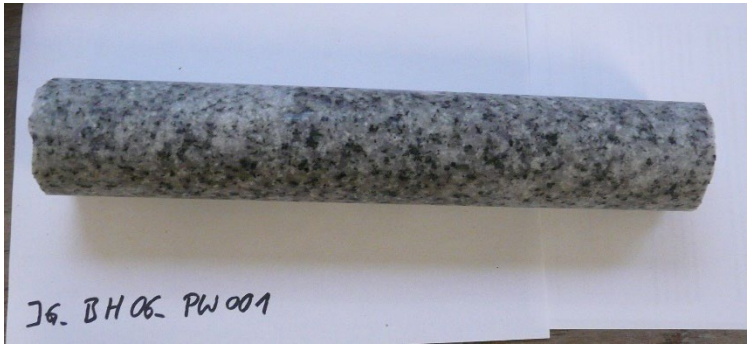
IG_BH06_AQ017: 853.18-853.42 m



IG_BH06_AQ018: 885.50-885.66 m



IG_BH06_AQ019: 927.81-928.09 m



IG_BH06_PW001: 212.09-212.44 m



IG_BH06_PW002: 291.28-291.69 m



IG_BH06_PW003: 369.33-369.73 m



IG_BH06_PW004: 453.00-453.40 m



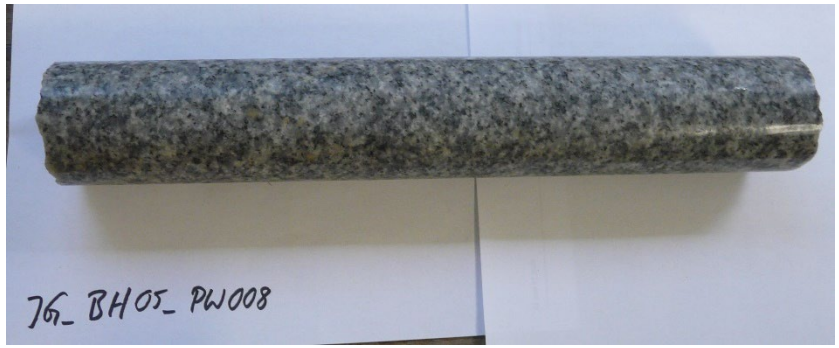
IG_BH06_PW005: 503.91-504.30 m



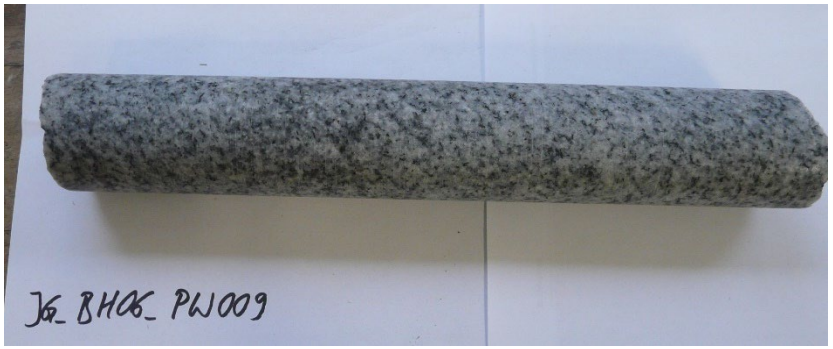
IG_BH06_PW006: 562.25-562.62 m



IG_BH06_PW007: 574.00-574.35 m



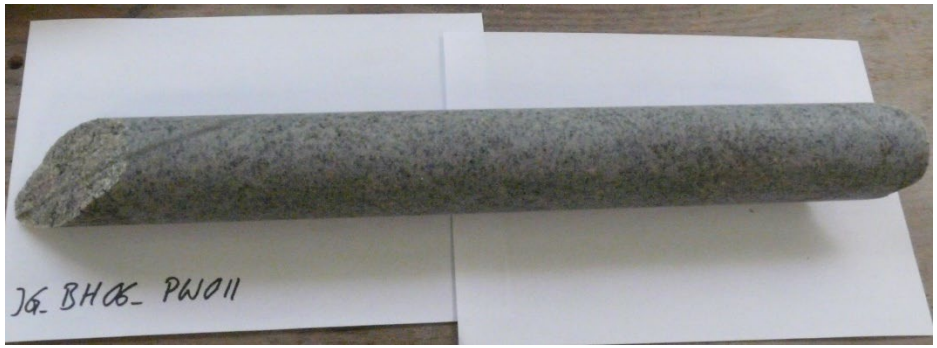
IG_BH06_PW008: 612.01-612.38 m



IG_BH06_PW009: 647.69-648.06 m



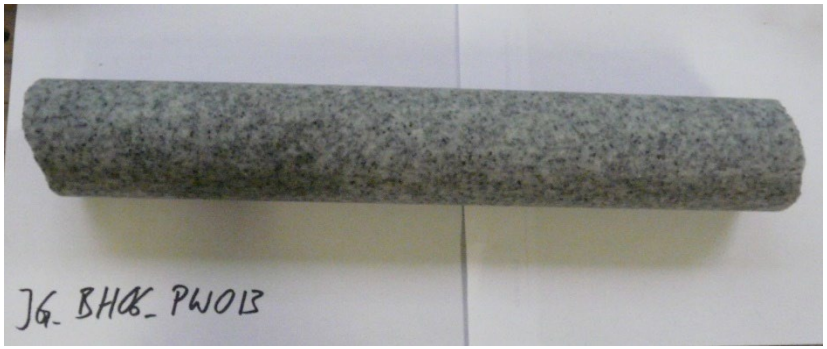
IG_BH06_PW010: 665.70-666.08 m



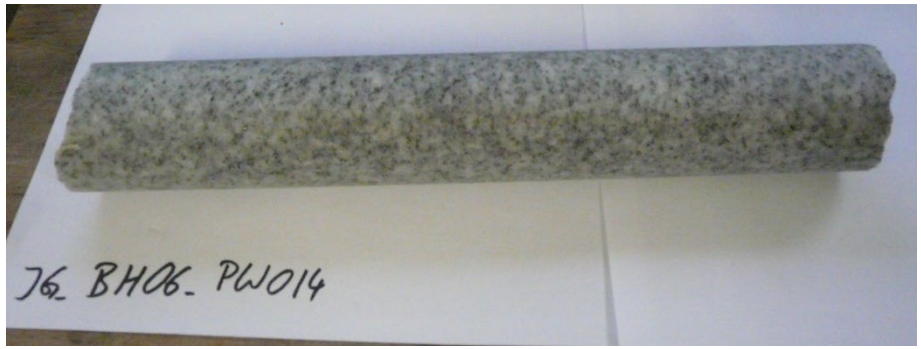
IG_BH06_PW011: 690.75-691.23 m



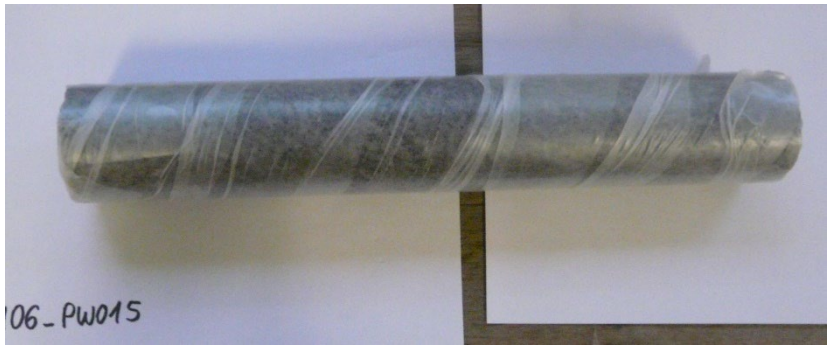
IG_BH06_PW012: 693.49-693.87 m



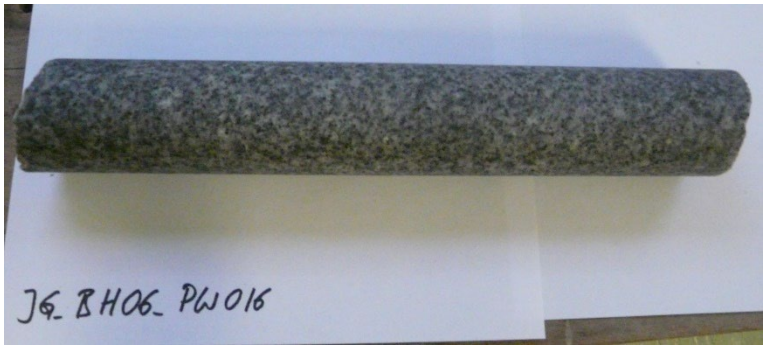
IG_BH06_PW013: 720.34-720.73 m



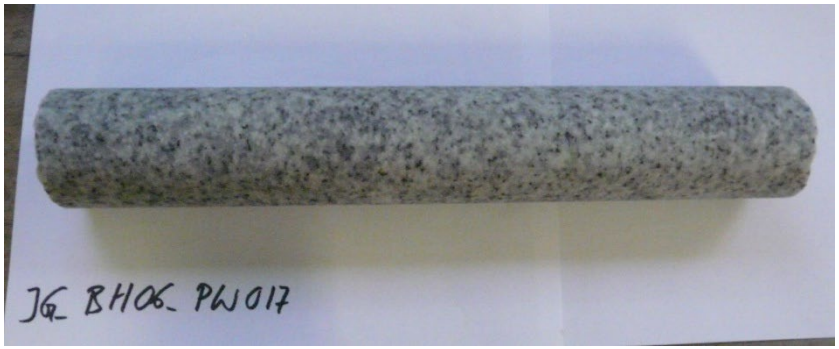
IG_BH06_PW014: 747.35-747.71 m



IG_BH06_PW015: 774.69-775.04 m



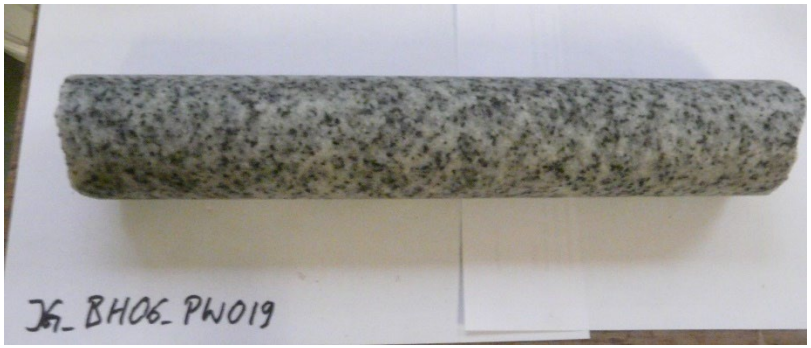
IG_BH06_PW016: 804.47-805.84 m



IG_BH06_PW017: 839.99-840.37 m



IG_BH06_PW018: 852.83-853.18 m



IG_BH06_PW019: 885.14-885.50 m



IG_BH06_PW020: 927.41-927.81 m



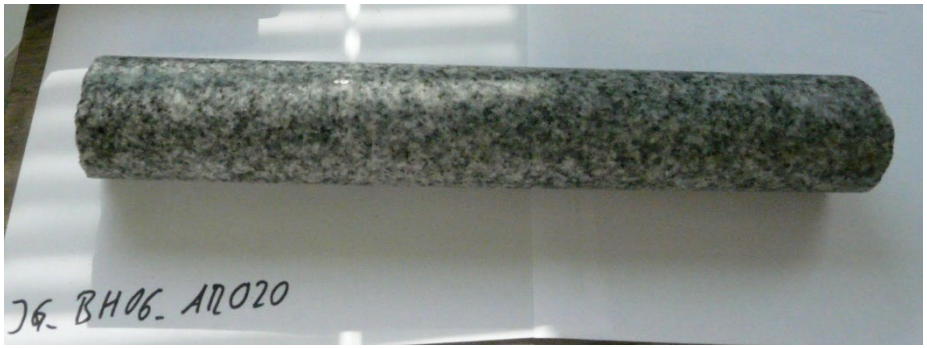
IG_BH06_AR010: 398.49-398.91 m



IG_BH06_AR013: 421.39-421.79 m



IG_BH06_AR019: 533.79-534.16 m



IG_BH06_AR020: 542.66-543.04 m



IG_BH06_AR027: 594.78-595.14 m



IG_BH06_AR038: 722.38-722.83 m



IG_BH06_AR039: 728.58-728.94 m



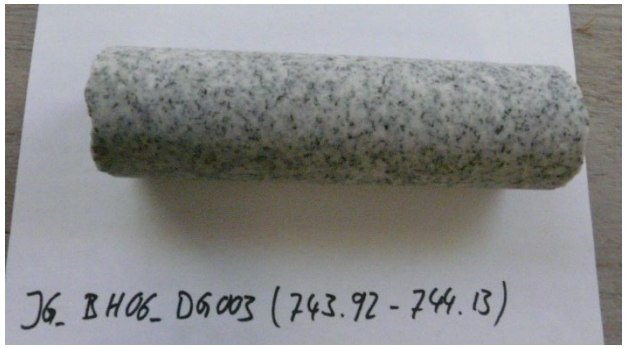
IG_BH06_AR045: 796.49-796.85 m



IG_BH06_AR049: 820.06-820.42 m



IG_BH06_AR064: 971.18-971.54 m



IG_BH06_DG003 743.92-744.13 m

APPENDIX B

Analytical Raw Data

APPENDIX B-1

Calculation of Water Content Values: Raw Data

Table B-1.1: Determination of gravimetric water content; sample weights, drying times and calculated water contents of core pieces used for aqueous extraction experiments

Sample	Date prepared	m (cryst.dish)	m (cryst+ rock)	28.10.2021	11.11.2021	25.11.2021	09.12.2021	23.12.2021	12.01.2022	26.01.2022			Sample	m(rock, wet)	m (rock, dry)
Drying times	days			7	21	35	49	63	83	97				g	g
IG_BH06_AQ001	21.10.2021	88.922	471.828	471.151	471.116	471.127	471.126						IG_BH06_AQ001	382.906	382.194
IG_BH06_AQ002	21.10.2021	90.813	639.511	638.528	638.479	638.483	638.471	638.454	638.431	638.43			IG_BH06_AQ002	548.698	547.617
IG_BH06_AQ003	21.10.2021	89.133	557.796	557.026	556.990	556.999	556.998						IG_BH06_AQ003	468.663	467.857
IG_BH06_AQ004	21.10.2021	90.911	521.784	521.231	521.195	521.196							IG_BH06_AQ004	430.873	430.284
IG_BH06_AQ005	21.10.2021	84.665	521.184	520.509	520.478	520.49	520.488						IG_BH06_AQ005	436.519	435.813
IG_BH06_AQ006	21.10.2021	87.330	555.078	554.339	554.297	554.304	554.302						IG_BH06_AQ006	467.748	466.967
IG_BH06_AQ007	21.10.2021	97.339	461.281	460.744	460.718	460.726	460.725						IG_BH06_AQ007	363.942	363.379
Sample	Date prepared	m (cryst.dish)	m (cryst+ rock)	24.11.2021	08.12.2021	15.12.2021	04.01.2022	18.01.2022	01.02.2022	16.02.2022					
Drying times	days			21	35	42	62	76	90	105					
IG_BH06_AQ008	03.11.2021	88.740	517.452	516.835	516.843	516.829	516.838	516.821	516.821				IG_BH06_AQ008	428.712	428.081
IG_BH06_AQ009	03.11.2021	86.348	492.560	492.031	492.045	492.034	492.041	492.025	492.027				IG_BH06_AQ009	406.212	405.677
IG_BH06_AQ010	03.11.2021	90.621	455.586	455.107	455.116	455.106	455.111	455.094	455.086	455.087			IG_BH06_AQ010	364.965	364.465
IG_BH06_AQ011	03.11.2021	88.970	458.827	458.369	458.384	458.377	458.384	458.368	458.369				IG_BH06_AQ011	369.857	369.398
IG_BH06_AQ012	03.11.2021	93.937	493.912	493.323	493.336	493.325	493.335	493.322	493.324				IG_BH06_AQ012	399.975	399.385
IG_BH06_AQ013	03.11.2021	88.905	419.733	419.365	419.372	419.363	419.368	419.358	419.356				IG_BH06_AQ013	330.828	330.451
			m(dry surf)	28.10.2021	11.11.2021	25.11.2021	09.12.2021	23.12.2021	12.01.2022						
Drying times	days			7	21	35	49	63	83						
IG_BH06_AQ001-A	21.10.2021		189.248	188.868	188.86	188.855	188.852	188.846	188.847				IG_BH06_AQ001-A	189.248	188.846
IG_BH06_AQ001-B	21.10.2021		140.611	140.330	140.324	140.315	140.313						IG_BH06_AQ001-B	140.611	140.313
IG_BH06_AQ002-A	21.10.2021		189.597	189.278	189.269	189.266	189.263	189.258	189.260				IG_BH06_AQ002-A	189.597	189.258
IG_BH06_AQ002-B	21.10.2021		217.817	217.425	217.412	217.409	217.407						IG_BH06_AQ002-B	217.817	217.407
IG_BH06_AQ003-A	21.10.2021		305.547	305.028	305.011	305.006	305.004						IG_BH06_AQ003-A	305.547	305.004
IG_BH06_AQ003-B	21.10.2021		250.922	250.494	250.468	250.46	250.457	250.452	250.454				IG_BH06_AQ003-B	250.922	250.452
IG_BH06_AQ004-A	21.10.2021		258.145	257.760	257.744	257.739	257.735	257.730	257.731				IG_BH06_AQ004-A	258.145	257.730
IG_BH06_AQ004-B	21.10.2021		213.685	213.374	213.359	213.352	213.346	213.340	213.342				IG_BH06_AQ004-B	213.685	213.340
IG_BH06_AQ005-A	21.10.2021		209.231	208.839	208.831	208.825	208.823						IG_BH06_AQ005-A	209.231	208.823
IG_BH06_AQ005-B	21.10.2021		227.437	227.026	227.019	227.014	227.011	227.004	227.006				IG_BH06_AQ005-B	227.437	227.004
IG_BH06_AQ006-A	21.10.2021		248.065	247.570	247.552	247.546	247.542	247.532	247.530				IG_BH06_AQ006-A	248.065	247.530
IG_BH06_AQ006-B	21.10.2021		237.024	236.577	236.559	236.551	236.547	236.539	236.537				IG_BH06_AQ006-B	237.024	236.537
IG_BH06_AQ007-A	21.10.2021		253.582	253.132	253.114	253.104	253.101	253.094	253.095				IG_BH06_AQ007-A	253.582	253.094
IG_BH06_AQ007-B	21.10.2021		183.527	183.207	183.195	183.188	183.184	183.180	183.179				IG_BH06_AQ007-B	183.527	183.179

Table B-1.1: Continued

			m(dry surf)	11.11.2021	25.11.2021	09.12.2021	23.12.2021	05.01.2022	18.01.2022	01.02.2022	16.02.2022		Sample	m(rock, wet)	m (rock, dry)
Drying times	**days**			8	22	36	50	63	76	90	105				
IG_BH06_AQ008-A	03.11.2021		240.901	240.503	240.49	240.483	240.476	240.474					IG_BH06_AQ008-A	240.901	240.474
IG_BH06_AQ008-B	03.11.2021		191.262	190.932	190.924	190.911	190.903	190.898	190.888	190.884	190.882		IG_BH06_AQ008-B	191.262	190.882
IG_BH06_AQ009-A	03.11.2021		223.275	222.974	222.968	222.962	222.955	222.955					IG_BH06_AQ009-A	223.275	222.955
IG_BH06_AQ009-B	03.11.2021		245.082	244.75	244.74	244.734	244.728	244.730					IG_BH06_AQ009-B	245.082	244.728
IG_BH06_AQ010-A	03.11.2021		235.961	235.64	235.626	235.619	235.612	235.614					IG_BH06_AQ010-A	235.961	235.612
IG_BH06_AQ010-B	03.11.2021		180.562	180.326	180.319	180.315	180.310	180.311					IG_BH06_AQ010-B	180.562	180.310
IG_BH06_AQ011-A	03.11.2021		199.990	199.745	199.741	199.734	199.729	199.731					IG_BH06_AQ011-A	199.990	199.729
IG_BH06_AQ011-B	03.11.2021		200.987	200.72	200.701	200.694	200.690	200.686	200.670	200.669			IG_BH06_AQ011-B	200.987	200.669
IG_BH06_AQ012-A	03.11.2021		211.840	211.522	211.516	211.510	211.506	211.506					IG_BH06_AQ012-A	211.840	211.506
IG_BH06_AQ012-B	03.11.2021		179.699	179.444	179.438	179.436							IG_BH06_AQ012-B	179.699	179.436
IG_BH06_AQ013-A	03.11.2021		144.421	144.259	144.25	144.245	144.238	144.238					IG_BH06_AQ013-A	144.421	144.238
IG_BH06_AQ013-B	03.11.2021		182.180	181.982	181.972	181.967	181.960	181.961					IG_BH06_AQ013-B	182.180	181.960

Sample	**Date prepared**	**m (cryst.dish)**	**m (cryst+ rock)**	**15.12.2021**	**12.01.2022**	**26.01.2022**	**08.02.2022**	**22.02.2022**	**08.03.2022**	**22.03.2022**					
Drying times	**days**			11	39	53	66	80	94	108					
IG_BH06_AQ014	04.12.2021	87.792	464.053	463.762	463.753	463.754	463.74	463.749	463.743	463.741			IG_BH06_AQ014	376.261	375.948
IG_BH06_AQ015	04.12.2021	83.84	522.973	522.575	522.565	522.566	522.551	522.56	522.552				IG_BH06_AQ015	439.133	438.711
IG_BH06_AQ016	04.12.2021	92.804	397.787	397.378	397.363	397.364	397.347	397.363					IG_BH06_AQ016	304.983	304.543
IG_BH06_AQ017	04.12.2021	91.200	513.66	513.208	513.192	513.193	513.177	513.188	513.182	513.177			IG_BH06_AQ017	422.460	421.977
IG_BH06_AQ018	04.12.2021	86.941	556.037	555.448	555.429	555.423	555.393	555.402	555.392				IG_BH06_AQ018	469.096	468.451
IG_BH06_AQ019	04.12.2021	81.571	363.182	362.861	362.854	362.859	362.846	362.855					IG_BH06_AQ019	281.611	281.275

			m(dry surf)	15.12.2021	05.01.2022	19.01.2022	03.02.2022	16.02.2022	02.03.2022	16.03.2022	31.03.2022				
Drying times	**days**			11	32	46	61	74	88	102	117				
IG_BH06_AQ014-A	04.12.2021		220.136	219.95	219.944	219.932	219.929	219.927					IG_BH06_AQ014-A	220.136	219.927
IG_BH06_AQ014-B	04.12.2021		251.894	251.695	251.675	251.664	251.662	251.660					IG_BH06_AQ014-B	251.894	251.660
IG_BH06_AQ015-A	04.12.2021		235.377	235.164	235.164								IG_BH06_AQ015-A	235.377	235.164
IG_BH06_AQ015-B	04.12.2021		243.307	243.17	243.169								IG_BH06_AQ015-B	243.307	243.169
IG_BH06_AQ016-A	04.12.2021		222.457	222.141	222.137	222.127	222.123	222.123					IG_BH06_AQ016-A	222.457	222.123
IG_BH06_AQ016-B	04.12.2021		278.934	278.55	278.541	278.531	278.527	278.517	278.510	278.508			IG_BH06_AQ016-B	278.934	278.508
IG_BH06_AQ017-A	04.12.2021		470.544	470.087	470.077	470.060	470.055	470.052	470.044	470.038	470.040		IG_BH06_AQ017-A	470.544	470.038
IG_BH06_AQ017-B	04.12.2021		206.448	206.212	206.203	206.164	206.158	206.153	206.149	206.148			IG_BH06_AQ017-B	206.448	206.148
IG_BH06_AQ018-A	04.12.2021		181.852	181.624	181.619	181.603	181.598	181.596					IG_BH06_AQ018-A	181.852	181.596
IG_BH06_AQ018-B	04.12.2021		240.019	239.715	239.708	239.695	239.691	239.686	239.680	239.679			IG_BH06_AQ018-B	240.019	239.679
IG_BH06_AQ019-A	04.12.2021		248.772	248.47	248.467	248.451	248.449	248.445	248.440	248.438			IG_BH06_AQ019-A	248.772	248.438
IG_BH06_AQ019-B	04.12.2021		333.295	332.896	332.895								IG_BH06_AQ019-B	333.295	332.895

Table B-1.2: Determination of gravimetric water content; sample weights, drying times and calculated water contents of rim core pieces of samples used for out-diffusion experiments

	Set-up date	m(dry surf)		15.11.2021	29.11.2021	13.12.2021	04.01.2022	19.01.2022	03.02.2022	16.02.2022	03.03.2022	17.03.2022	31.03.2022		Sample	m wet	m dry
Drying time (days)				7	21	35	57	72	87	100	115	129	143			g	g
IG_BH06_PW001-A	08.11.2021	204.163		203.792	203.783	203.774	203.777	203.767	203.764	203.761	203.757	203.755			IG_BH06_PW001-A	204.163	203.755
IG_BH06_PW001-B	08.11.2021	123.970		123.756	123.746	123.739	123.743	123.737							IG_BH06_PW001-B	123.970	123.737
IG_BH06_PW002-A	08.11.2021	402.012		401.352	401.332	401.317	401.325	401.307	401.305	401.301	401.290	401.294	401.296		IG_BH06_PW002-A	402.012	401.29
IG_BH06_PW002-B	08.11.2021	132.467		132.277	132.264	132.255	132.256								IG_BH06_PW002-B	132.467	132.255
IG_BH06_PW003-A	08.11.2021	294.034		293.477	293.463	293.450	293.458	293.443	293.441	293.437	293.428	293.431	293.430		IG_BH06_PW003-A	294.034	293.428
IG_BH06_PW003-B	08.11.2021	216.351		215.972	215.967	215.959	215.951	215.943	215.939	215.938					IG_BH06_PW003-B	216.351	215.938
IG_BH06_PW004-A	08.11.2021	265.522		265.127	265.113	265.103	265.106	265.094	265.092	265.083	265.075	265.073			IG_BH06_PW004-A	265.522	265.073
IG_BH06_PW004-B	08.11.2021	171.877		171.637	171.619	171.612	171.616	171.606	171.602	171.597	171.587	171.588			IG_BH06_PW004-B	171.877	171.587
IG_BH06_PW005-A	08.11.2021	311.563		311.024	311.013	311.004	311.012	310.999	310.996	310.995					IG_BH06_PW005-A	311.563	310.995
IG_BH06_PW005-B	08.11.2021	228.281		227.84	227.830	227.821	227.828	227.816	227.812	227.811					IG_BH06_PW005-B	228.281	227.811
IG_BH06_PW006-A	08.11.2021	229.293		228.859	228.843	228.833	228.838	228.828	228.826	228.817	228.808	228.810			IG_BH06_PW006-A	229.293	228.808
IG_BH06_PW006-B	08.11.2021	221.933		221.525	221.511	221.502	221.506	221.499	221.492	221.488	221.482	221.483			IG_BH06_PW006-B	221.933	221.482
IG_BH06_PW007-A	08.11.2021	189.634		189.302	189.277	189.264	189.262								IG_BH06_PW007-A	189.634	189.262
IG_BH06_PW007-B	08.11.2021	173.533		173.27	173.262	173.150	173.153	173.142	173.136	173.126	173.122	173.121			IG_BH06_PW007-B	173.533	173.121
IG_BH06_PW008-A	08.11.2021	202.920		202.574	202.543	202.533	202.529	202.516	202.506	202.506					IG_BH06_PW008-A	202.920	202.506
IG_BH06_PW008-B	08.11.2021	237.895		237.494	237.479	237.465	237.469	237.457	237.450	237.448					IG_BH06_PW008-B	237.895	237.448
IG_BH06_PW009-A	08.11.2021	257.477		257.144	257.136	257.128	257.132	257.122	257.119	257.118					IG_BH06_PW009-A	257.477	257.118
IG_BH06_PW009-B	08.11.2021	214.687		214.421	214.414	214.400	214.403	214.394	214.389	214.386	214.380	214.380			IG_BH06_PW009-B	214.687	214.38
IG_BH06_PW010-A	08.11.2021	267.202		266.872	266.859	266.849	266.856	266.845	266.840	266.836	266.829	266.832	266.830		IG_BH06_PW010-A	267.202	266.829
IG_BH06_PW010-B	08.11.2021	207.762		207.504	207.494	207.483	207.488	207.477	207.471	207.468	207.432	207.433			IG_BH06_PW010-B	207.762	207.432
IG_BH06_PW011-A	08.11.2021	334.129		333.792	333.779	333.775	333.777								IG_BH06_PW011-A	334.129	333.775
IG_BH06_PW011-B	08.11.2021	998.637		997.273	997.175	997.157	997.165	997.134	997.135	997.138	997.118	997.129			IG_BH06_PW011-B	998.637	997.118
IG_BH06_PW012-A	08.11.2021	297.375		297.002	296.992	296.983	296.988	296.974	296.963	296.949	296.938	296.941	296.942		IG_BH06_PW012-A	297.375	296.938
IG_BH06_PW012-B	08.11.2021	201.589		201.335	201.326	201.319	201.319								IG_BH06_PW012-B	201.589	201.319
IG_BH06_PW013-A	08.11.2021	200.758		200.525	200.521	200.514	200.516								IG_BH06_PW013-A	200.758	200.514
IG_BH06_PW013-B	08.11.2021	336.481		336.073	336.062	336.055	336.060	336.051	336.049	336.048					IG_BH06_PW013-B	336.481	336.048
IG_BH06_PW014-A	08.11.2021	154.315		154.175	154.166	154.158	154.154	154.155							IG_BH06_PW014-A	154.315	154.154
IG_BH06_PW014-B	08.11.2021	246.196		245.946	245.931	245.923	245.924								IG_BH06_PW014-B	246.196	245.923
	Set-up date	m(dry surf)		16.11.2021	30.11.2021	14.12.2021	28.12.2021	19.01.2022	03.02.2022	14.02.2022	28.02.2022	17.03.2022	31.03.2022		Sample	m wet	m dry
Drying time (days)				7	21	35	49	71	86	97	111	128	142			g	g
IG_BH06_PW015-A	09.11.2021	177.961		177.769	177.761	177.757	177.756								IG_BH06_PW015-A	177.961	177.756
IG_BH06_PW015-B	09.11.2021	162.565		162.412	162.406	162.402	162.391	162.383	162.377	162.377	162.365	162.357	162.355		IG_BH06_PW015-B	162.565	162.355
IG_BH06_PW016-A	09.11.2021	276.769		276.484	276.482										IG_BH06_PW016-A	276.769	276.482
IG_BH06_PW016-B	09.11.2021	214.060		213.833	213.828	213.825	219.823								IG_BH06_PW016-B	214.060	213.825
IG_BH06_PW017-A	09.11.2021	259.401		259.025	259.012	259.000	258.995	258.985	258.974	258.967	258.962	258.961			IG_BH06_PW017-A	259.401	258.961
IG_BH06_PW017-B	09.11.2021	199.229		198.959	198.948	198.939	198.935	198.927	198.923	198.923					IG_BH06_PW017-B	199.229	198.923

Table B-1.2: Continued

	Set-up date	m(dry surf)		15.12.2021	05.01.2022	19.01.2022	01.02.2022	16.02.2022						Sample	m wet	m dry
Drying time (days)				11	32	46	59	74							g	g
IG_BH06_PW018-A	04.12.2021	134.135		133.966	133.960	133.953	133.950	133.949						IG_BH06_PW018-A	134.135	133.949
IG_BH06_PW018-B	04.12.2021	185.486		185.304	185.288	185.281	185.278	185.276						IG_BH06_PW018-B	185.486	185.276
IG_BH06_PW019-A	04.12.2021	144.969		144.771	144.757	144.746	144.744							IG_BH06_PW019-A	144.969	144.744
IG_BH06_PW019-B	04.12.2021	169.721		169.497	169.479	169.463	169.459	169.457						IG_BH06_PW019-B	169.721	169.457
IG_BH06_PW020-A	04.12.2021	430.933		430.368	430.364	430.347	430.343	430.341						IG_BH06_PW020-A	430.933	430.341
IG_BH06_PW020-B	04.12.2021	243.933		243.642	243.637	243.623	243.620	243.620						IG_BH06_PW020-B	243.933	243.62

	Set-up date	m(dry surf)		23.03.2022	06.04.2022	20.04.2022	04.05.2022	18.05.2022	01.06.2022					Sample	m wet	m dry
Drying time (days)				9	23	37	51	65							g	g
IG_BH06_AR010-A	14.03.2022	222.230		222.093	222.091	222.082	222.086	222.089						IG_BH06_AR010-A	222.230	222.082
IG_BH06_AR010-B	14.03.2022	240.404		240.264	240.258	240.258	240.263	240.262						IG_BH06_AR010-B	240.404	240.258
IG_BH06_AR013-A	14.03.2022	166.039		165.806	165.800	165.786	165.786	165.787						IG_BH06_AR013-A	166.039	165.786
IG_BH06_AR013-B	14.03.2022	197.478		197.194	197.188	197.177	197.182	197.181						IG_BH06_AR013-B	197.478	197.177
IG_BH06_AR019-A	14.03.2022	151.167		150.961	150.956	150.943	150.946	150.944						IG_BH06_AR019-A	151.167	150.943
IG_BH06_AR019-B	14.03.2022	122.555		122.389	122.383	122.371	122.370							IG_BH06_AR019-B	122.555	122.37
IG_BH06_AR020-A	14.03.2022	156.354		156.088	156.080	156.072	156.074							IG_BH06_AR020-A	156.354	156.072
IG_BH06_AR020-B	14.03.2022	195.457		195.134	195.134	195.125	195.127	195.128						IG_BH06_AR020-B	195.457	195.125
IG_BH06_AR027-A	14.03.2022	177.513		177.257	177.249	177.237	177.234	177.235						IG_BH06_AR027-A	177.513	177.234
IG_BH06_AR027-B	14.03.2022	135.901		135.685	135.670	135.660	135.660							IG_BH06_AR027-B	135.901	135.66
IG_BH06_AR038-A	14.03.2022	432.989		432.815	432.795	432.772	432.778	432.778						IG_BH06_AR038-A	432.989	432.772
IG_BH06_AR038-B	14.03.2022	518.587		518.522	518.487	518.455	518.457	518.452	518.447					IG_BH06_AR038-B	518.587	518.447
IG_BH06_AR039-A	14.03.2022	225.143		224.998	224.998	224.987	224.995	224.993						IG_BH06_AR039-A	225.143	224.987
IG_BH06_AR039-B	14.03.2022	266.965		266.791	266.793	266.783	266.785							IG_BH06_AR039-B	266.965	266.783
IG_BH06_AR045-A	14.03.2022	240.111		239.929	239.925	239.917	239.92	239.921						IG_BH06_AR045-A	240.111	239.917
IG_BH06_AR045-B	14.03.2022	160.960		160.845	160.843	160.832	160.835	160.835						IG_BH06_AR045-B	160.960	160.832
IG_BH06_AR049-A	14.03.2022	178.466		178.288	178.282	178.272	178.276	178.274						IG_BH06_AR049-A	178.466	178.272
IG_BH06_AR049-B	14.03.2022	198.742		198.524	198.519	198.503	198.507	198.509						IG_BH06_AR049-B	198.742	198.503
IG_BH06_AR064-A	14.03.2022	170.920		170.712	170.708	170.696	170.697							IG_BH06_AR064-A	170.920	170.696
IG_BH06_AR064-B	14.03.2022	188.784		188.584	188.578	188.567	188.574	188.573						IG_BH06_AR064-B	188.784	188.567
IG_BH06_DG003-A	14.03.2022	159.390		159.326	159.316	159.308	159.294	159.295						IG_BH06_DG003-A	159.390	159.294
IG_BH06_DG003-B	14.03.2022	177.494		177.433	177.425	177.421	177.427	177.423						IG_BH06_DG003-B	177.494	177.421

Table B-1.3: Determination of gravimetric water content; sample weights, drying times and calculated water contents of core pieces used for isotope diffusive exchange experiments

Sample	Date start drying	Drying times (days	m (cryst.dish)	m (cryst+ rock)	25.01.2022	09.02.2022	23.02.2022	09.03.2022	23.03.2022	07.04.2022	21.04.2022	28.04.2022
IG_BH06_PW001 LAB	17.01.2022	101	87.819	455.058	454.485	454.460	454.467	454.461	454.451	454.554	454.458	454.462
IG_BH06_PW001 ICE	17.01.2022	80	87.508	458.342	457.746	457.727	457.730	457.723	457.714	457.715		
IG_BH06_PW002 LAB	17.01.2022	94	87.002	555.821	555.111	555.082	555.085	555.068	555.056	555.059	555.058	
IG_BH06_PW002 ICE	17.01.2022	65	93.902	566.826	566.120	566.094	566.099	566.080	566.080			
IG_BH06_PW003 LAB	17.01.2022	80	84.665	535.942	535.231	535.204	535.211	535.197	535.188	535.188		
IG_BH06_PW003 ICE	17.01.2022	101	90.365	536.300	535.615	535.587	535.594	535.579	535.575	535.568	535.585	535.581
IG_BH06_PW004 LAB	17.01.2022	65	97.337	530.135	529.633	529.602	529.604					
IG_BH06_PW004 ICE	17.01.2022	80	93.449	520.159	519.628	519.597	519.599	519.588	519.585	519.582		
IG_BH06_PW005 LAB	17.01.2022	80	89.518	468.417	467.869	467.845	467.855	467.846	467.836	467.835		
IG_BH06_PW005 ICE	17.01.2022	101	85.978	465.601	465.023	465.007	465.011	464.999	464.992	464.983	464.997	465.001
IG_BH06_PW006 LAB	17.01.2022	65	87.835	496.429	495.796	495.763	495.770	495.754	495.755			
IG_BH06_PW006 ICE	17.01.2022	94	85.350	491.411	490.757	490.729	490.737	490.729	490.717	490.725	490.726	
IG_BH06_PW007 LAB	17.01.2022	80	89.549	431.493	431.003	430.985	430.992	430.980	430.977	430.978		
IG_BH06_PW007 ICE	17.01.2022	65	87.328	430.327	429.826	429.809	429.817	429.809	429.808			
IG_BH06_PW008 LAB	17.01.2022	101	90.682	494.223	493.735	493.698	493.701	493.690	493.681	493.671	493.690	493.686
IG_BH06_PW008 ICE	17.01.2022	94	88.323	490.666	490.148	490.121	490.124	490.115	490.108	490.112	490.113	
IG_BH06_PW009 LAB	17.01.2022	94	90.907	490.304	489.837	489.816	489.822	489.804	489.800	489.817	489.815	
IG_BH06_PW009 ICE	17.01.2022	94	89.355	486.792	486.314	486.295	486.300	486.292	486.284	486.292	486.290	
IG_BH06_PW010 LAB	17.01.2022	101	89.129	488.278	487.817	487.794	487.798	487.790	487.780	487.777	487.788	487.786
IG_BH06_PW010 ICE	17.01.2022	80	85.209	481.871	481.394	481.375	481.377	481.367	481.363	481.361		

Sample	Date start drying	Drying times (days	m (cryst.dish)	m (cryst+ rock)	02.02.2022	16.02.2022	01.03.2022	15.03.2022	29.03.2022
IG_BH06_PW011 LAB	25.01.2022	49	87.555	495.587	495.115	495.114	495.102	495.101	
IG_BH06_PW011 ICE	25.01.2022	63	86.536	499.039	498.570	498.569	498.562	498.557	498.557
IG_BH06_PW012 LAB	25.01.2022	63	86.258	494.824	494.313	494.309	494.294	494.289	494.290
IG_BH06_PW012 ICE	25.01.2022	49	88.081	495.089	494.542	494.539	494.524	494.525	
IG_BH06_PW013 LAB	25.01.2022	49	86.038	489.088	488.595	488.592	488.579	488.577	
IG_BH06_PW013 ICE	25.01.2022	63	88.789	491.327	490.831	490.823	490.811	490.807	490.811
IG_BH06_PW014 LAB	25.01.2022	49	88.437	470.300	469.874	469.864	469.849	469.848	
IG_BH06_PW014 ICE	25.01.2022	63	88.435	490.462	489.972	489.958	489.944	489.941	489.943
IG_BH06_PW015 LAB	25.01.2022	63	88.244	549.426	549.007	549.005	548.992	548.988	548.993
IG_BH06_PW015 ICE	25.01.2022	63	88.633	544.664	544.194	544.190	544.176	544.171	544.175
IG_BH06_PW016 LAB	25.01.2022	49	84.289	459.028	458.618	458.613	458.600	458.599	
IG_BH06_PW016 ICE	25.01.2022	49	87.835	463.599	463.182	463.179	463.168	463.168	
IG_BH06_PW017 LAB	25.01.2022	63	92.192	541.216	540.451	540.439	540.421	540.415	540.416
IG_BH06_PW017 ICE	25.01.2022	63	83.814	534.418	533.640	533.627	533.610	533.606	533.607

Sample	mass dry	m rock wet	m rock dry
IG_BH06_PW001 LAB	454.451	367.239	366.632
IG_BH06_PW001 ICE	457.714	370.834	370.206
IG_BH06_PW002 LAB	555.056	468.819	468.054
IG_BH06_PW002 ICE	566.080	472.924	472.178
IG_BH06_PW003 LAB	535.188	451.277	450.523
IG_BH06_PW003 ICE	535.568	445.935	445.203
IG_BH06_PW004 LAB	529.602	432.798	432.265
IG_BH06_PW004 ICE	519.582	426.71	426.133
IG_BH06_PW005 LAB	467.835	378.899	378.317
IG_BH06_PW005 ICE	464.983	379.623	379.005
IG_BH06_PW006 LAB	495.754	408.594	407.919
IG_BH06_PW006 ICE	490.717	406.061	405.367
IG_BH06_PW007 LAB	430.977	341.944	341.428
IG_BH06_PW007 ICE	429.808	342.999	342.480
IG_BH06_PW008 LAB	493.671	403.541	402.989
IG_BH06_PW008 ICE	490.108	402.343	401.785
IG_BH06_PW009 LAB	489.800	399.397	398.893
IG_BH06_PW009 ICE	486.284	397.437	396.929
IG_BH06_PW010 LAB	487.777	399.149	398.648
IG_BH06_PW010 ICE	481.361	396.662	396.152

Sample	mass dry	m rock wet	m rock dry
IG_BH06_PW011 LAB	495.101	408.032	407.546
IG_BH06_PW011 ICE	498.557	412.503	412.021
IG_BH06_PW012 LAB	494.289	408.566	408.031
IG_BH06_PW012 ICE	494.524	407.008	406.443
IG_BH06_PW013 LAB	488.577	403.05	402.539
IG_BH06_PW013 ICE	490.807	402.538	402.018
IG_BH06_PW014 LAB	469.848	381.863	381.411
IG_BH06_PW014 ICE	489.941	402.027	401.506
IG_BH06_PW015 LAB	548.988	461.182	460.744
IG_BH06_PW015 ICE	544.171	456.031	455.538
IG_BH06_PW016 LAB	458.599	374.739	374.310
IG_BH06_PW016 ICE	463.168	375.764	375.333
IG_BH06_PW017 LAB	540.415	449.024	448.223
IG_BH06_PW017 ICE	533.606	450.604	449.792

Table B-1.3: Continued

Sample	Date start drying	Drying times (days	m (cryst.dish)	m (cryst+ rock)	16.02.2022	02.03.2022	15.03.2022	29.03.2022					Sample	mass dry	m rock wet	m rock dry
IG_BH06_PW018 LAB	08.02.2022	49	94.767	485.000	484.432	484.415	484.410	484.408					IG_BH06_PW018 LAB	484.408	390.233	389.641
IG_BH06_PW018 ICE	08.02.2022	49	87.608	481.460	480.920	480.907	480.902	480.900					IG_BH06_PW018 ICE	480.900	393.852	393.292
IG_BH06_PW019 LAB	08.02.2022	49	91.132	464.837	464.307	464.285	464.278	464.277					IG_BH06_PW019 LAB	464.277	373.705	373.145
IG_BH06_PW019 ICE	08.02.2022	49	91.796	475.786	475.282	475.263	475.256	475.255					IG_BH06_PW019 ICE	475.255	383.99	383.459
IG_BH06_PW020 LAB	08.02.2022	49	88.044	412.808	412.274	412.261	412.257	412.255					IG_BH06_PW020 LAB	412.255	324.764	324.211
IG_BH06_PW020 ICE	08.02.2022	49	89.342	405.038	404.546	404.535	404.530	404.529					IG_BH06_PW020 ICE	404.529	315.696	315.187
Sample	Date start drying	Drying times (days	m (cryst.dish)	m (cryst+ rock)	31.05.2022	14.06.2022	29.06.2022	13.07.2022	28.07.2022	10.08.2022	29.08.2022		Sample	mass dry	m rock wet	m rock dry
IG_BH06_AR010 LAB	24.05.2022	78	89.012	555.92	555.516	555.52	555.527	555.52	555.526	555.506			IG_BH06_AR010 LAB	555.506	466.908	466.494
IG_BH06_AR010 ICE	24.05.2022	21	90.403	554.684	554.268	554.269							IG_BH06_AR010 ICE	554.268	464.281	463.865
IG_BH06_AR013 LAB	24.05.2022	97	87.003	588.213	587.55	587.528	587.522	587.51	587.514	587.49	587.513		IG_BH06_AR013 LAB	587.490	501.21	500.487
IG_BH06_AR013 ICE	24.05.2022	65	84.292	586.729	586.05	586.033	586.037	586.023	586.025				IG_BH06_AR013 ICE	586.023	502.437	501.731
IG_BH06_AR019 LAB	24.05.2022	97	89.127	520.065	519.476	519.463	519.466	519.457	519.461	519.443	519.461		IG_BH06_AR019 LAB	519.443	430.938	430.316
IG_BH06_AR019 ICE	24.05.2022	78	91.200	521.876	521.269	521.254	521.257	521.244	521.255	521.232			IG_BH06_AR019 ICE	521.232	430.676	430.032
IG_BH06_AR020 LAB	24.05.2022	78	89.133	586.808	586.049	586.039	586.042	586.032	586.037	586.014			IG_BH06_AR020 LAB	586.014	497.675	496.881
IG_BH06_AR020 ICE	24.05.2022	78	91.516	590.308	589.554	589.548	589.553	589.541	589.547	589.523			IG_BH06_AR020 ICE	589.523	498.792	498.007
IG_BH06_AR027 LAB	24.05.2022	36	86.416	505.500	504.932	504.91	504.912						IG_BH06_AR027 LAB	504.910	419.084	418.494
IG_BH06_AR027 ICE	24.05.2022	36	90.683	509.005	508.437	508.414	508.414						IG_BH06_AR027 ICE	508.414	418.322	417.731
IG_BH06_AR038 LAB	24.05.2022	78	90.367	593.662	593.308	593.304	593.314	593.306	593.282	593.264			IG_BH06_AR038 LAB	593.264	503.295	502.897
IG_BH06_AR038 ICE	24.05.2022	78	87.507	591.002	590.655	590.649	590.658	590.649	590.652	590.638			IG_BH06_AR038 ICE	590.638	503.495	503.131
IG_BH06_AR039 LAB	24.05.2022	78	85.215	438.021	437.674	437.677	437.683	437.677	437.682	437.669			IG_BH06_AR039 LAB	437.669	352.806	352.454
IG_BH06_AR039 ICE	24.05.2022	78	84.665	436.227	435.831	435.828	435.838	435.829	435.835	435.823			IG_BH06_AR039 ICE	435.823	351.562	351.158
IG_BH06_AR045 LAB	24.05.2022	78	88.968	472.221	471.796	471.788	471.794	471.783	471.789	471.772			IG_BH06_AR045 LAB	471.772	383.253	382.804
IG_BH06_AR045 ICE	24.05.2022	78	87.818	470.74	470.27	470.257	470.266	470.257	470.262	470.245			IG_BH06_AR045 ICE	470.245	382.922	382.427
IG_BH06_AR049 LAB	24.05.2022	78	89.549	452.475	451.981	451.968	451.974	451.964	451.972	451.953			IG_BH06_AR049 LAB	451.953	362.926	362.404
IG_BH06_AR049 ICE	24.05.2022	78	90.911	454.045	453.536	453.523	453.528	453.519	453.525	453.504			IG_BH06_AR049 ICE	453.504	363.134	362.593
IG_BH06_AR064 LAB	24.05.2022	78	87.601	461.101	460.575	460.566	460.571	460.562	460.567	460.551			IG_BH06_AR064 LAB	460.551	373.500	372.950
IG_BH06_AR064 ICE	24.05.2022	78	89.358	462.023	461.474	461.471	461.476	461.466	461.472	461.456			IG_BH06_AR064 ICE	461.456	372.665	372.098

Table B-1.4: Determination of gravimetric water content; sample weights, drying times and calculated water contents of core pieces used for out-diffusion experiments

			before experiment (b.e.)		after experiment (a.e.)																	
Sample	Date start drying	Drying times (days)	m wet surface	m dry surface	m wet surf	m dry surf	05.10.2022	19.10.2022	31.10.2022	16.11.2022	30.11.2022	14.12.2022	03.01.2023	12.01.2023	25.01.2023	08.02.2023	22.02.2023	07.03.2023	21.03.2023	m (dry)	m(PW) b.e.	m(PW) a.e.
			g	g	g	g	g	g	g	g	g	g	g	g	g	g	g	g	g	g	g	g
Drying time (days)																						
IG_BH06_PW001	28.09.2022	174	1428.860	1428.845	1429.364	1429.050	1426.072	1426.009	1425.995	1425.970	1425.958	1425.940	1425.924	1425.933	1425.910	1425.889	1425.908	1425.906	1425.910	1425.889	2.956	3.161
IG_BH06_PW002	28.09.2022	106	1438.036	1438.025	1438.861	1438.610	1435.619	1435.564	1435.545	1435.527	1435.498	1435.489	1435.482	1435.482						1435.482	2.543	3.128
IG_BH06_PW003	28.09.2022	174	1453.468	1453.440	1453.653	1453.446	1450.775	1450.722	1450.710	1450.686	1450.672	1450.654	1450.637	1450.646	1450.620	1450.604	1450.621	1450.615	1450.616	1450.604	2.836	2.842
IG_BH06_PW004	28.09.2022	106	1451.726	1451.708	1452.180	1451.961	1449.418	1449.364	1449.337	1449.304	1449.288	1449.271	1449.252	1449.253						1449.252	2.456	2.709
IG_BH06_PW005	28.09.2022	106	1463.569	1463.528	1463.622	1463.453	1460.835	1460.770	1460.766	1460.744	1460.715	1460.710	1460.694	1460.694						1460.694	2.834	2.759
IG_BH06_PW006	28.09.2022	106	1452.990	1452.954	1453.103	1452.942	1450.320	1450.242	1450.230	1450.204	1450.177	1450.169	1450.147	1450.148						1450.147	2.807	2.795
IG_BH06_PW007	28.09.2022	106	1441.778	1441.750	1441.857	1441.640	1439.261	1439.149	1439.144	1439.121	1439.098	1439.087	1439.068	1439.067						1439.067	2.683	2.573
IG_BH06_PW008	28.09.2022	106	1452.143	1452.099	1452.194	1451.998	1449.753	1449.690	1449.666	1449.639	1449.611	1449.600	1449.580	1449.580						1449.580	2.519	2.418
IG_BH06_PW009	28.09.2022	106	1464.375	1464.366	1464.723	1464.534	1462.367	1462.330	1462.311	1462.291	1462.265	1462.260	1462.246	1462.248						1462.246	2.120	2.288
IG_BH06_PW010	28.09.2022	106	1472.497	1472.485	1472.868	1472.672	1470.512	1470.460	1470.448	1470.423	1470.409	1470.388	1470.376	1470.378						1470.376	2.109	2.296
IG_BH06_PW011	28.09.2022	106	1406.002	1405.997	1406.100	1406.011	1404.498	1404.222	1404.205	1404.188	1404.170	1404.163	1404.150	1404.152						1404.150	1.847	1.861
Sample	Date start drying	Drying times (days)	m wet surface	m dry surface	m wet surf	m dry surf	26.10.2022	09.11.2022	23.11.2022	07.12.2022	21.12.2022	04.01.2023	19.01.2023	02.02.2023	18.02.2023	02.03.2023	16.03.2023	30.03.2023				
			g	g	g	g	g	g	g	g	g	g	g	g	g	g	g	g				
IG_BH06_PW012	18.10.2022	36	1467.348	1467.328	1468.106	1467.915	1465.255	1465.225	1465.223											1465.223	2.105	2.692
IG_BH06_PW013	18.10.2022	36	1440.077	1440.071	1440.446	1440.305	1438.166	1438.121	1438.120											1438.120	1.951	2.185
IG_BH06_PW014	18.10.2022	123	1407.998	1407.996	1408.33	1408.170	1406.282	1406.232	1406.223	1406.192	1406.173	1406.168	1406.163	1406.146	1406.148					1406.146	1.850	2.024
IG_BH06_PW015	18.10.2022	78	1474.894	1474.833	1475.494	1475.255	1473.023	1473.000	1472.994	1472.971	1472.956	1472.958								1472.956	1.877	2.299
IG_BH06_PW016	18.10.2022	163	1479.106	1479.054	1480.152	1479.935	1477.252	1477.231	1477.217	1477.193	1477.181	1477.176	1477.172	1477.157	1477.162	1477.166	1477.156	1477.165		1477.156	1.898	2.779
IG_BH06_PW017	18.10.2022	123	1396.776	1396.768	1397.086	1396.920	1394.615	1394.555	1394.537	1394.507	1394.486	1394.482	1394.474	1394.462	1394.460					1394.460	2.308	2.460
IG_BH06_PW018	18.10.2022	78	1451.021	1451.005	1451.581	1451.380	1449.323	1449.288	1449.275	1449.247	1449.228	1449.227								1449.227	1.778	2.153
IG_BH06_PW019	18.10.2022	123	1440.235	1440.165	1441.001	1440.780	1438.065	1438.007	1437.991	1437.961	1437.940	1437.931	1437.925	1437.908	1437.909					1437.908	2.257	2.872
IG_BH06_PW020	18.10.2022	78	1465.050	1465.029	1465.826	1465.620	1463.162	1463.113	1463.103	1463.076	1463.053	1463.051								1463.051	1.978	2.569
Sample	Date start drying	Drying times (days)	m wet surface	m dry surface	m wet surf	m dry surf	01.12.2022	15.12.2022	03.01.2023	12.01.2023	25.01.2023	08.02.2023	21.02.2023	07.03.2023	21.03.2023							
			g	g	g	g	g	g	g	g	g	g	g	g	g							
IG_BH06_AR010	23.11.2022	118	1627.420	1627.420	1627.98	1627.895	1626.304	1626.289	1626.274	1626.278	1626.250	1626.237	1626.249	1626.252	1626.262					1626.237	1.183	1.658
IG_BH06_AR013	23.11.2022	90	1477.362	1477.362	1477.882	1477.687	1475.155	1475.089	1475.060	1475.056	1475.015	1475.003	1475.005							1475.003	2.359	2.684
IG_BH06_AR019	23.11.2022	104	1451.617	1451.617	1452.094	1451.930	1449.464	1449.400	1449.382	1449.374	1449.337	1449.321	1449.327	1449.325						1449.321	2.296	2.609
IG_BH06_AR020	23.11.2022	118	1425.077	1425.038	1425.146	1425.001	1422.559	1422.499	1422.476	1422.472	1422.438	1422.431	1422.441	1422.434	1422.442					1422.431	2.607	2.570
IG_BH06_AR027	23.11.2022	90	1454.975	1454.975	1455.43	1455.186	1452.509	1452.431	1452.381	1452.368	1452.334	1452.309	1452.308							1452.308	2.667	2.878
IG_BH06_AR038	23.11.2022	90	1602.754	1602.754	1603.089	1602.973	1602.313	1602.182	1602.116	1602.105	1602.061	1602.034	1602.033							1602.033	0.721	0.940
IG_BH06_AR039	23.11.2022	118	1431.104	1431.104	1431.916	1431.685	1430.120	1430.111	1430.105	1430.092	1430.067	1430.063	1430.060	1430.065	1430.065					1430.060	1.044	1.625
IG_BH06_AR045	23.11.2022	50	1417.982	1417.982	1418.839	1418.582	1416.676	1416.647	1416.633	1416.635										1416.633	1.349	1.949
IG_BH06_AR049	23.11.2022	90	1368.428	1368.428	1369.431	1369.149	1366.759	1366.718	1366.697	1366.691	1366.665	1366.657	1366.656							1366.656	1.772	2.493
IG_BH06_AR064	23.11.2022	104	1439.354	1439.354	1440.154	1439.961	1437.502	1437.460	1437.436	1437.418	1437.395	1437.390	1437.400	1437.391						1437.390	1.964	2.571
IG_BH06_DG003	23.11.2022	90	1216.271	1216.271	1217.415	1217.239	1215.679	1215.646	1215.632	1215.626	1215.593	1215.582	1215.581							1215.581	0.690	1.658

APPENDIX B-2

Determination of Bulk Wet and Dry Density: Raw Data

Table B-2.1: Determination of bulk wet and dry density; sample dimensions, weights and density results

Sample	m (core) wet	diameter core	height core	Volume core	bulk, wet density	bulk, dry density
	g	cm	cm	ccm	g/ccm	g/ccm
IG_BH06_AQ001	456.525	6.12	5.87	172.7	2.64	2.64
IG_BH06_AQ002	420.632	6.11	5.42	158.9	2.65	2.65
IG_BH06_AQ003	397.291	6.10	5.13	149.9	2.65	2.65
IG_BH06_AQ004	511.958	6.10	6.65	194.3	2.63	2.63
IG_BH06_AQ005	396.675	6.10	5.12	149.6	2.65	2.65
IG_BH06_AQ006	373.513	6.14	4.77	141.2	2.64	2.64
IG_BH06_AQ007	310.000	6.11	4.02	117.9	2.63	2.63
IG_BH06_AQ008	457.912	6.10	5.89	172.1	2.66	2.66
IG_BH06_AQ009	413.983	6.10	5.29	154.6	2.68	2.68
IG_BH06_AQ010	322.219	6.10	4.15	121.3	2.66	2.66
IG_BH06_AQ011	343.760	6.11	4.37	128.1	2.68	2.68
IG_BH06_AQ012	375.911	6.10	4.81	140.6	2.67	2.67
IG_BH06_AQ013	280.838	6.08	3.62	105.1	2.67	2.67
IG_BH06_AQ014	321.812	6.08	4.16	120.8	2.66	2.66
IG_BH06_AQ015	386.367	6.10	4.96	145.0	2.67	2.67
IG_BH06_AQ016	402.129	6.10	5.2	152.0	2.65	2.65
IG_BH06_AQ017	631.621	6.11	8.13	238.4	2.65	2.65
IG_BH06_AQ018	280.004	6.11	3.72	109.1	2.57	2.57
IG_BH06_AQ019	475.503	6.10	6.07	177.4	2.68	2.68

Table B-2.1: Continued

Sample	m (core a.e.) wet	m (core a.e.) dry	diameter core	height core	Volume core	bulk, wet density	bulk, dry density
	g	g	cm	cm	ccm	g/ccm	g/ccm
IG_BH06_PW001	1429.364	1429.050	6.09	18.42	536.6	2.66	2.66
IG_BH06_PW002	1438.861	1438.610	6.10	18.54	541.8	2.66	2.66
IG_BH06_PW003	1453.653	1453.446	6.09	18.71	545.0	2.67	2.67
IG_BH06_PW004	1452.180	1451.961	6.08	18.71	543.2	2.67	2.67
IG_BH06_PW005	1463.622	1463.453	6.09	18.75	546.2	2.68	2.68
IG_BH06_PW006	1453.103	1452.942	6.10	18.57	542.7	2.68	2.68
IG_BH06_PW007	1441.857	1441.640	6.09	18.35	534.5	2.70	2.70
IG_BH06_PW008	1452.194	1451.998	6.09	18.60	541.8	2.68	2.68
IG_BH06_PW009	1464.723	1464.534	6.08	18.74	544.1	2.69	2.69
IG_BH06_PW010	1472.868	1472.672	6.09	18.82	548.2	2.69	2.69
IG_BH06_PW011	1406.100	1406.011	6.09	17.71	515.9	2.73	2.73
IG_BH06_PW012	1468.106	1467.915	6.10	18.71	546.8	2.68	2.68
IG_BH06_PW013	1440.446	1440.305	6.08	18.47	536.2	2.69	2.69
IG_BH06_PW014	1408.330	1408.170	6.07	18.17	525.8	2.68	2.68
IG_BH06_PW015	1475.494	1475.255	6.08	18.80	545.8	2.70	2.70
IG_BH06_PW016	1480.152	1479.935	6.08	18.87	547.9	2.70	2.70
IG_BH06_PW017	1397.086	1396.920	6.09	18.01	524.6	2.66	2.66
IG_BH06_PW018	1451.581	1451.380	6.10	18.64	544.7	2.66	2.66
IG_BH06_PW019	1441.001	1440.780	6.11	18.55	543.9	2.65	2.65
IG_BH06_PW020	1465.826	1465.620	6.10	18.66	545.3	2.69	2.69
IG_BH06_AR010	1627.980	1627.895	6.11	20.58	603.4	2.70	2.70
IG_BH06_AR013	1477.882	1477.687	6.10	18.98	554.7	2.66	2.66
IG_BH06_AR019	1452.094	1451.930	6.10	18.66	545.3	2.66	2.66
IG_BH06_AR020	1425.146	1425.001	6.10	18.24	533.1	2.67	2.67
IG_BH06_AR027	1455.430	1455.186	6.09	18.73	545.6	2.67	2.67
IG_BH06_AR038	1603.089	1602.973	6.06	18.50	533.6	3.00	3.00
IG_BH06_AR039	1431.916	1431.685	6.08	18.33	532.2	2.69	2.69
IG_BH06_AR045	1418.839	1418.582	6.08	18.09	525.2	2.70	2.70
IG_BH06_AR049	1369.431	1369.149	6.10	17.87	522.2	2.62	2.62
IG_BH06_AR064	1440.154	1439.961	6.11	18.31	536.9	2.68	2.68
IG_BH06_DG003	1217.415	1217.239	6.06	15.72	453.4	2.69	2.68

APPENDIX B-3

Aqueous Extraction Experiments: Raw Data

Table B-3.1: Experimental data of aqueous extraction experiments

Sample	Depth	m (bottle)	m (bottle + rock)	m (rock)	m (H2O)	m (tot)	water:rock
	m a.b.	g	g	g	g	g	
IG_BH06_AQ001	212.9	14.511	158.172	143.661	54.720	212.892	0.38
IG_BH06_AQ002	292.6	15.069	122.105	107.036	65.227	187.332	0.61
IG_BH06_AQ003	370.3	15.025	149.799	134.774	50.667	200.466	0.38
IG_BH06_AQ004	453.5	15.003	161.273	146.270	50.413	211.686	0.34
IG_BH06_AQ005	504.4	15.029	158.49	143.461	49.329	207.819	0.34
IG_BH06_AQ006	562.7	15.013	169.699	154.686	61.896	231.595	0.40
IG_BH06_AQ007	574.4	15.079	165.1	150.021	50.417	215.517	0.34
IG_BH06_AQ008	612.5	15.096	146.092	130.996	65.064	211.156	0.50
IG_BH06_AQ009	648.2	15.062	142.653	127.591	73.553	216.206	0.58
IG_BH06_AQ010	666.2	15.025	149.677	134.652	67.367	217.044	0.50
IG_BH06_AQ011	694.0	15.093	150.55	135.457	67.574	218.124	0.50
IG_BH06_AQ012	720.8	14.946	143.349	128.403	75.866	219.215	0.59
IG_BH06_AQ013	747.8	15.050	137.57	122.520	68.922	206.492	0.56
IG_BH06_AQ014	771.2	32.652	136.165	103.513	120.193	256.358	1.16
IG_BH06_AQ015	804.9	32.772	161.375	128.603	141.207	302.582	1.10
IG_BH06_AQ016	841.2	32.609	117.964	85.355	127.158	245.122	1.49
IG_BH06_AQ017	853.3	32.935	134.652	101.717	119.171	253.823	1.17
IG_BH06_AQ018	885.6	32.721	159.516	126.795	157.142	316.658	1.24
IG_BH06_AQ019	928.0	32.530	148.635	116.105	124.532	273.167	1.07

APPENDIX B-4

Isotope Diffusive Exchange Experiments: Raw Data

Table B-4.1: Experimental data of isotope diffusive exchange experiments

Sample		Date Experiment Start	Date Experiment End	Weight container	Weight container and rock	Cryst. dish	Cryst Dish + H2O	Total weight container	Weight rock	Weight test solution	Total weight container after experiment	Weight test solution after experiment	Weight container and rock after experiment	Weight test solution after experiment	Weight rock after experiment	mass (PW)	mass TW+PW after exp.	Δ total weight before & after	Δ weight rock before & after	Δ weight test solution before & after	Δ weight rock and test solution	Δ weight rock and test solution - Δ total weight before and after	Δ weight rock and test solution	Δ water loss (total weight)	remaining water fraction
				g	g	g	g	g	g	g	g	g	g	g	g	g	g	g	g	g	g	g	% of TW	% of TW+PW	
PW001	LAB	08.11.2021	14.01.2022	516.564	885.041	13.235	15.063	900.095	368.477	1.828	900.066	15.074	884.988	1.839	368.424	0.607	2.446	-0.029	-0.053	0.011	-0.042	-0.013	2.3	1.2	0.99
PW002	LAB	08.11.2021	14.01.2022	517.100	986.332	13.843	15.675	1002.007	469.232	1.832	1001.977	15.643	986.331	1.800	469.231	0.765	2.565	-0.030	-0.001	-0.032	-0.033	-0.003	1.8	1.2	0.99
PW003	LAB	08.11.2021	14.01.2022	514.958	966.782	12.320	14.153	980.925	451.824	1.833	980.871	14.038	966.831	1.718	451.873	0.754	2.472	-0.054	0.049	-0.115	-0.066	-0.012	3.6	2.2	0.98
PW004	LAB	08.11.2021	14.01.2022	525.413	958.796	15.163	16.857	975.658	433.383	1.694	975.596	16.741	958.846	1.578	433.433	0.533	2.111	-0.062	0.050	-0.116	-0.066	-0.004	3.9	2.9	0.97
PW005	LAB	08.11.2021	14.01.2022	519.069	898.393	12.511	14.337	912.729	379.324	1.826	912.699	14.304	898.389	1.793	379.320	0.582	2.375	-0.030	-0.004	-0.033	-0.037	-0.007	2.0	1.3	0.99
PW006	LAB	08.11.2021	14.01.2022	516.989	926.338	14.806	16.632	942.978	409.349	1.826	942.953	16.598	926.355	1.792	409.366	0.675	2.467	-0.025	0.017	-0.034	-0.017	0.008	0.9	1.0	0.99
PW007	LAB	08.11.2021	14.01.2022	574.955	917.252	14.373	16.196	933.444	342.297	1.823	933.416	16.167	917.250	1.794	342.295	0.516	2.310	-0.028	-0.002	-0.029	-0.031	-0.003	1.7	1.2	0.99
PW008	LAB	08.11.2021	14.01.2022	575.939	979.764	14.098	15.881	995.644	403.825	1.783	995.625	15.887	979.737	1.789	403.798	0.552	2.341	-0.019	-0.027	0.006	-0.021	-0.002	1.2	0.8	0.99
PW009	LAB	08.11.2021	14.01.2022	517.682	917.847	13.878	15.712	933.573	400.165	1.834	933.542	15.657	917.879	1.779	400.197	0.504	2.283	-0.031	0.032	-0.055	-0.023	0.008	1.3	1.4	0.99
PW010	LAB	08.11.2021	14.01.2022	522.730	922.441	13.912	15.733	938.174	399.711	1.821	938.159	15.673	922.485	1.761	399.755	0.501	2.262	-0.015	0.044	-0.060	-0.016	-0.001	0.9	0.7	0.99
PW011	LAB	08.11.2021	21.01.2022	520.612	928.788	13.204	15.022	943.811	408.176	1.818	943.816	14.918	928.887	1.714	408.275	0.486	2.200	0.005	0.099	-0.104	-0.005	-0.010	0.3	-0.2	1.00
PW012	LAB	08.11.2021	21.01.2022	514.670	923.612	13.879	15.794	939.325	408.942	1.915	939.309	15.632	923.673	1.753	409.003	0.535	2.288	-0.016	0.061	-0.162	-0.101	-0.085	5.3	0.7	0.99
PW013	LAB	08.11.2021	21.01.2022	522.253	926.378	14.762	16.586	942.940	404.125	1.824	942.924	16.450	926.466	1.688	404.213	0.511	2.199	-0.016	0.088	-0.136	-0.048	-0.032	2.6	0.7	0.99
PW014	LAB	08.11.2021	21.01.2022	524.428	906.775	12.370	14.192	920.965	382.347	1.822	920.898	13.921	906.971	1.551	382.543	0.452	2.003	-0.067	0.196	-0.271	-0.075	-0.008	4.1	3.3	0.97
PW015	LAB	09.11.2021	21.01.2022	516.668	978.602	15.060	16.879	995.474	461.934	1.819	995.410	16.691	978.702	1.631	462.034	0.438	2.069	-0.064	0.100	-0.188	-0.088	-0.024	4.8	3.1	0.97
PW016	LAB	09.11.2021	21.01.2022	524.489	899.638	14.646	16.463	916.104	375.149	1.817	916.045	16.218	899.821	1.572	375.332	0.429	2.001	-0.059	0.183	-0.245	-0.062	-0.003	3.4	2.9	0.97
PW017	LAB	09.11.2021	21.01.2022	522.755	972.408	14.715	16.537	988.938	449.653	1.822	988.903	16.261	972.633	1.546	449.878	0.801	2.347	-0.035	0.225	-0.276	-0.051	-0.016	2.8	1.5	0.99
PW018	LAB	04.12.2021	08.02.2022	517.988	908.279	13.695	15.247	923.516	390.291	1.552	923.439	14.883	908.562	1.188	390.574	0.592	1.780	-0.077	0.283	-0.364	-0.081	-0.004	5.2	4.3	0.96
PW019	LAB	04.12.2021	08.02.2022	524.725	898.980	14.944	16.463	915.435	374.255	1.519	915.353	16.205	899.154	1.261	374.429	0.56	1.821	-0.082	0.174	-0.258	-0.084	-0.002	5.5	4.5	0.95
PW020	LAB	04.12.2021	08.02.2022	515.618	841.077	14.274	15.792	856.865	325.459	1.518	856.788	15.424	841.373	1.150	325.755	0.553	1.703	-0.077	0.296	-0.368	-0.072	0.005	4.7	4.5	0.95
AR010	LAB	14.03.2022	24.05.2022	523.470	990.576	12.515	14.048	1004.622	467.106	1.533	1004.614	13.743	990.851	1.228	467.381	0.414	1.642	-0.008	0.275	-0.305	-0.030	-0.022	2.0	0.5	1.00
AR013	LAB	14.03.2022	24.05.2022	516.344	1020.545	14.940	16.466	1036.999	504.201	1.526	1037.049	16.408	1020.624	1.468	504.280	0.723	2.191	0.050	0.079	-0.058	0.021	-0.029	-1.4	-2.3	1.02
AR019	LAB	14.03.2022	24.05.2022	526.432	958.012	12.863	14.395	972.402	431.580	1.532	972.454	14.307	958.126	1.444	431.694	0.622	2.066	0.052	0.114	-0.088	0.026	-0.026	-1.7	-2.5	1.03
AR020	LAB	14.03.2022	24.05.2022	518.000	1016.242	15.255	16.787	1033.018	498.242	1.532	1033.025	16.637	1016.370	1.382	498.370	0.794	2.176	0.007	0.128	-0.150	-0.022	-0.029	1.4	-0.3	1.00
AR027	LAB	14.03.2022	24.05.2022	522.046	941.666	13.925	15.450	957.112	419.620	1.525	957.118	15.274	941.820	1.349	419.774	0.59	1.939	0.006	0.154	-0.176	-0.022	-0.028	1.4	-0.3	1.00
AR038	LAB	14.03.2022	24.05.2022	522.421	1025.777	13.496	15.028	1040.804	503.356	1.532	1040.819	14.682	1026.114	1.186	503.693	0.398	1.584	0.015	0.337	-0.346	-0.009	-0.024	0.6	-0.9	1.01
AR039	LAB	14.03.2022	24.05.2022	517.227	869.989	15.063	16.592	886.578	352.762	1.529	886.592	16.217	870.349	1.154	353.122	0.352	1.506	0.014	0.360	-0.375	-0.015	-0.029	1.0	-0.9	1.01
AR045	LAB	14.03.2022	24.05.2022	524.900	908.146	13.844	15.368	923.511	383.246	1.524	923.518	15.035	908.460	1.191	383.560	0.449	1.640	0.007	0.314	-0.333	-0.019	-0.026	1.2	-0.4	1.00
AR049	LAB	14.03.2022	24.05.2022	524.775	887.686	15.034	16.555	904.242	362.911	1.521	904.245	16.262	887.963	1.228	363.188	0.522	1.750	0.003	0.277	-0.293	-0.016	-0.019	1.1	-0.2	1.00
AR064	LAB	14.03.2022	24.05.2022	515.050	888.530	15.272	16.795	905.323	373.480	1.523	905.330	16.473	888.834	1.201	373.784	0.55	1.751	0.007	0.304	-0.322	-0.018	-0.025	1.2	-0.4	1.00
PW001	ICE	08.11.2021	14.01.2022	575.890	947.229	14.028	15.851	963.078	371.339	1.823	963.050	15.852	947.197	1.824	371.307	0.628	2.452	-0.028	-0.032	0.001	-0.031	-0.003	1.7	1.1	0.99
PW002	ICE	08.11.2021	14.01.2022	523.023	997.488	13.403	15.230	1012.715	474.465	1.827	1012.684	15.194	997.492	1.791	474.469	0.746	2.537	-0.031	0.004	-0.036	-0.032	-0.001	1.8	1.2	0.99
PW003	ICE	08.11.2021	14.01.2022	515.295	961.617	13.940	15.756	977.375	446.322	1.816	977.313	15.640	961.668	1.700	446.373	0.732	2.432	-0.062	0.051	-0.116	-0.065	-0.003	3.6	2.5	0.97
PW004	ICE	08.11.2021	14.01.2022	517.383	945.552	15.033	16.838	962.397	428.169	1.805	962.336	16.680	945.641	1.647	428.258	0.577	2.224	-0.061	0.089	-0.158	-0.069	-0.008	3.8	2.7	0.97
PW005	ICE	08.11.2021	14.01.2022	521.651	901.626	12.856	14.676	916.297	379.975	1.820	916.278	14.644	901.637	1.788	379.986	0.618	2.406	-0.019	0.011	-0.032	-0.021	-0.002	1.2	0.8	0.99
PW006	ICE	08.11.2021	14.01.2022	525.750	932.036	14.997	16.814	948.859	406.286	1.817	948.834	16.756	932.078	1.759	406.328	0.694	2.453	-0.025	0.042	-0.058	-0.016	0.009	0.9	1.0	0.99
PW007	ICE	08.11.2021	14.01.2022	574.162	917.463	13.409	15.232	932.689	343.301	1.823	932.640	15.085	917.546	1.676	343.384	0.519	2.195	-0.049	0.083	-0.147	-0.064	-0.015	3.5	2.2	0.98
PW008	ICE	08.11.2021	14.01.2022	522.545	925.378	15.403	17.220	942.599	402.833	1.817	942.548	17.060	925.486	1.657	402.941	0.558	2.215	-0.051	0.108	-0.160	-0.052	-0.001	2.9	2.3	0.98
PW009	ICE	08.11.2021	14.01.2022	517.543	915.077	13.492	15.315	930.393	397.534	1.823	930.365	15.235	915.129	1.743	397.586	0.508	2.251	-0.028	0.052	-0.080	-0.028	0.000	1.5	1.2	0.99
PW010	ICE	08.11.2021	14.01.2022	522.633	919.766	13.902	15.723	935.496	397.133	1.821	935.482	15.662	919.822	1.760	397.189	0.510	2.270	-0.014	0.056	-0.061	-0.005	0.009	0.3	0.6	0.99
PW011	ICE	08.11.2021	21.01.2022	520.373	933.492	13.248	15.065	948.559	413.119	1.817	948.559	14.952	933.596	1.704	413.223	0.482	2.186	0.000	0.104	-0.113	-0.009	-0.009	0.5	0.0	1.00
PW012	ICE	08.11.2021	21.01.2022	521.837	929.712	15.241	17.055	946.772	407.875	1.814	946.764	16.966	929.797	1.725	407.960	0.565	2.290	-0.008	0.085	-0.089	-0.004	0.004	0.2	0.3	1.00
PW013	ICE	08.11.2021	21.01.2022	516.152	919.051	13.779	15.599	934.651	402.899	1.820	934.629	15.470	919.154	1.691	403.002	0.520	2.211	-0.022	0.103	-0.129	-0.026	-0.004	1.4	1.0	0.99
PW014	ICE	08.11.2021	21.01.2022	515.618	917.823	15.258	17.074	934.899	402.205	1.816	934.888	16.899	917.979	1.641	402.361	0.521	2.162	-0.011	0.156	-0.175	-0.019	-0.008	1.0	0.5	0.99
PW015	ICE	09.11.2021	21.01.2022	516.569	976.672	14.336	16.083	992.755	460.103	1.747	992.695	15.888	976.796	1.552	460.227	0.493	2.045	-0.060	0.124	-0.195	-0.071	-0.011	4.1	2.9	0.97
PW016	ICE	09.11.2021	21.01.2022	516.509	892.497	14.364	16.183	908.678	375.988	1.819	908.609	15.915	892.681	1.551	376.172	0.431	1.982	-0.069	0.184	-0.268	-0.084	-0.015	4.6	3.5	0.97
PW017	ICE	09.11.2021	21.01.2022	515.028	965.784	14.915	16.746	982.518	450.756	1.831	982.435	16.327	966.098	1.412	451.070	0.812	2.224	-0.083	0.314	-0.419	-0.105	-0.022	5.7	3.7	0.96
PW018	ICE	04.12.2021	08.02.2022	522.156	916.042	14.131	15.671	931.707	393.886	1.540	931.633	15.339	916.296	1.208	394.140	0.560	1.768	-0.074	0.254	-0.332	-0.078	-0.004	5.1	4.2	0.96
PW019	ICE	04.12.2021	08.02.2022	524.886	909.470	14.104	15.722	925.181	384.584	1.618	925.057	15.421	909.633	1.317	384.747	0.531	1.848	-0.124	0.163	-0.301	-0.138	-0.014	8.5	6.7	0.93
PW020	ICE	04.12.2021	08.02.2022	523.177	838.942	14.912	16.436	855.375	315.765	1.524	855.292	16.104	839.194	1.192	316.017	0.509	1.701	-0.083	0.252	-0.332	-0.080	0.003	5.2	4.9	0.95
AR010	ICE	14.03.2022	24.05.2022	518.156	982.447	13.409	14.942	997.384	464.291	1.533	997.399	14.611	982.770	1.202	464.614	0.416	1.618	0.015	0.323	-0.331	-0.008	-0.023	0.5	-0.9	1.01
AR013	ICE	14.03.2022	24.05.2022	524.392	1027.756	14.709	16.237	1043.974	503.364	1.528	1044.031	16.158	1027.851	1.449	503.459	0.706	2.155	0.057	0.095	-0.079	0.016	-0.041	-1.0	-2.6	1.03
AR019	ICE	14.03.2022	24.05.2022	523.393	954.249	14.752	16.277	970.526	430.856	1.525	970.571	16.185	954.366	1.433	430.973	0.644	2.077	0.045	0.117	-0.092	0.025	-0.020	-1.6	-2.2	1.02
AR020	ICE	14.03.2022	24.05.2022	516.438	1015.833	13.925	15.459	1031.282	499.395	1.534	1031.278	15.274	1015.985	1.349	499.547	0.785	2.134	-0.004	0.152	-0.185	-0.033	-0.029	2.2	0.2	1.00
AR027	ICE	14.03.2022	24.05.2022	523.548	942.216	14.907	16.418	958.630	418.668	1.511	958.638	16.228	942.384	1.321	418.836	0.591	1.912	0.008	0.168	-0.190	-0.022	-0.030	1.5	-0.4	1.00
AR038	ICE	14.03.2022	24.05.2022	523.913	1027.392	14.125	15.633	1043.027	503.479	1.508	1043.040	15.294	1027.727	1.169	503.814	0.364	1.533	0.013	0.335	-0.339	-0.004	-0.017	0.3	-0.8	1.01
AR039	ICE	14.03.2022	24.05.2022	521.181	872.652	12.379	13.890	886.544	351.471	1.511	886.555	13.514	873.019	1.135	351.838	0.404	1.539	0.011	0.367	-0.376	-0.009	-0.020	0.6	-0.7	1.01
AR045	ICE	14.03.2022	24.05.2022	517.561	902.373	14.649	16.175	918.539	384.812	1.526	918.548	15.785	902.740	1.136	385.179	0.495	1.631	0.009	0.367	-0.390	-0.023	-0.032	1.5	-0.6	1.01
AR049	ICE	14.03.2022	24.05.2022	523.207	886.426	13.689	15.197	901.620	363.219	1.508	901.625	14.865	886.737	1.176	363.530	0.541	1.717	0.005	0.311	-0.332	-0.021	-0.026	1.4	-0.3	1.00
AR064	ICE	14.03.2022	24.05.2022	514.835	887.642	15.163	16.658	904.299	372.807	1.495	904.309	16.294	887.988	1.131	373.153	0.567	1.698	0.010	0.346	-0.364	-0.018	-0.028	1.2	-0.6	1.01

Table B-4.2: Analytical raw data of isotope diffusive exchange experiments

Sample	Test water	Initial $\delta^{18}O$ TW	Initial $\delta^{2}H$ TW	Final $\delta^{18}O$ TW	Final $\delta^{2}H$ TW
		Permill VSMOW	Permill VSMOW	Permill VSMOW	Permill VSMOW
PW001	LAB	-10.30	-72.9	-9.94	-74.0
PW002	LAB	-10.30	-72.9	-8.98	-68.8
PW003	LAB	-10.30	-72.9	-8.83	-67.0
PW004	LAB	-10.30	-72.9	-9.01	-67.6
PW005	LAB	-10.30	-72.9	-9.65	-70.3
PW006	LAB	-10.30	-72.9	-9.72	-70.1
PW007	LAB	-10.30	-72.9	-9.70	-70.0
PW008	LAB	-10.30	-72.9	-9.58	-69.3
PW009	LAB	-10.30	-72.9	-9.86	-70.8
PW010	LAB	-10.30	-72.9	-10.07	-71.8
PW011	LAB	-10.30	-72.9	-10.08	-72.2
PW012	LAB	-10.30	-72.9	-9.96	-71.8
PW013	LAB	-10.30	-72.9	-10.13	-72.1
PW014	LAB	-10.30	-72.9	-9.46	-69.3
PW015	LAB	-10.30	-72.9	-9.08	-67.5
PW016	LAB	-10.30	-72.9	-9.47	-68.9
PW017	LAB	-10.30	-72.9	-9.79	-68.5
PW018	LAB	-10.19	-73.0	-8.81	-65.9
PW019	LAB	-10.19	-73.0	-8.70	-66.0
PW020	LAB	-10.19	-73.0	-9.04	-66.3
AR010	LAB	-10.16	-72.8	-7.52	-61.8
AR013	LAB	-10.16	-72.8	-7.97	-62.8
AR019	LAB	-10.16	-72.8	-8.53	-66.1
AR020	LAB	-10.16	-72.8	-7.96	-64.0
AR027	LAB	-10.16	-72.8	-8.01	-63.7
AR038	LAB	-10.16	-72.8	-8.47	-67.0
AR039	LAB	-10.16	-72.8	-7.97	-64.5
AR045	LAB	-10.16	-72.8	-8.09	-64.3
AR049	LAB	-10.16	-72.8	-7.39	-61.9
AR064	LAB	-10.16	-72.8	-7.98	-62.9
PW001	ICE	-31.74	-246.8	-25.91	-203.6
PW002	ICE	-31.74	-246.8	-24.38	-194.3
PW003	ICE	-31.74	-246.8	-24.07	-190.9
PW004	ICE	-31.74	-246.8	-25.40	-201.1
PW005	ICE	-31.74	-246.8	-25.61	-200.5
PW006	ICE	-31.74	-246.8	-25.51	-199.5
PW007	ICE	-31.74	-246.8	-25.88	-204.8
PW008	ICE	-31.74	-246.8	-25.54	-202.3
PW009	ICE	-31.74	-246.8	-26.73	-208.5
PW010	ICE	-31.74	-246.8	-26.71	-209.6
PW011	ICE	-31.74	-246.8	-27.08	-209.1
PW012	ICE	-31.74	-246.8	-26.32	-204.5
PW013	ICE	-31.74	-246.8	-27.08	-210.2
PW014	ICE	-31.74	-246.8	-27.57	-213.6
PW015	ICE	-31.74	-246.8	-25.10	-198.5
PW016	ICE	-31.74	-246.8	-26.53	-208.7
PW017	ICE	-31.74	-246.8	-25.51	-198.6
PW018	ICE	-31.71	-247.5	-25.64	-202.4
PW019	ICE	-31.71	-247.5	-23.91	-195.8
PW020	ICE	-31.71	-247.5	-26.11	-206.3
AR010	ICE	-31.59	-247.3	-25.07	-204.4
AR013	ICE	-31.59	-247.3	-23.17	-186.0
AR019	ICE	-31.59	-247.3	-24.39	-194.5
AR020	ICE	-31.59	-247.3	-21.91	-179.7
AR027	ICE	-31.59	-247.3	-23.62	-192.4
AR038	ICE	-31.59	-247.3	-26.00	-210.2
AR039	ICE	-31.59	-247.3	-25.63	-210.2
AR045	ICE	-31.59	-247.3	-25.92	-209.5
AR049	ICE	-31.59	-247.3	-24.21	-200.3
AR064	ICE	-31.59	-247.3	-24.61	-199.9

APPENDIX B-5

Out-diffusion Experiments: Raw Data

Table B-5.1: Experimental data of out-diffusion experiments

Sample		IG_BH05_Blank	IG_BH06_PW001	IG_BH06_PW002	IG_BH06_PW003	IG_BH06_PW004	IG_BH06_PW005	IG_BH06_PW006	IG_BH06_PW007	IG_BH06_PW008	IG_BH06_PW009	IG_BH06_PW010
Depth	m		212.3	291.5	253.2	453.2	504.1	562.4	574.2	612.2	647.9	665.9
start experiment		25.06.2021	08.11.2021	08.11.2021	08.11.2021	08.11.2021	08.11.2021	08.11.2021	08.11.2021	08.11.2021	04.12.2021	04.12.2021
Initial Rock Mass (as received, +/- mountain wet)	g		1428.860	1438.036	1453.468	1451.726	1463.569	1452.990	1441.778	1452.143	1464.375	1472.497
Initial Rock Mass (start experiment)	g		1428.845	1438.025	1453.440	1451.708	1463.528	1452.954	1441.750	1452.099	1464.366	1472.485
Final Rock Mass (resaturated)	g		1429.050	1438.610	1453.446	1451.961	1463.453	1452.942	1441.640	1451.998	1464.534	1472.672
Uptake of water	g		0.190	0.574	-0.022	0.235	-0.116	-0.048	-0.138	-0.145	0.159	0.175
Saturation	%		99.987	99.960	100.002	99.984	100.008	100.003	100.010	100.010	99.989	99.988
Core Diametre	cm		6.09	6.10	6.09	6.08	6.09	6.10	6.09	6.09	6.08	6.09
Core Length	cm		18.42	18.54	18.71	18.71	18.75	18.57	18.35	18.6	18.74	18.82
Volume of Rock Sample	cm3		536.55	541.83	545.00	543.21	546.17	542.70	534.52	541.80	544.08	548.21
Density (calculated from volume & mass)	g/cm3		2.66	2.65	2.67	2.67	2.68	2.68	2.70	2.68	2.69	2.69
Mass of Rock (calculated from volume and density)			1428.86	1438.04	1453.47	1451.73	1463.57	1452.99	1441.78	1452.14	1464.38	1472.50
Masses before experiment												
Mass cylinder	g	380.492	356.779	376.272	357.044	357.634	357.941	357.680	358.110	357.676	362.444	356.837
Mass cylinder + core	g		1785.628	1814.388	1810.511	1809.635	1821.573	1810.633	1799.870	1809.760	1826.345	1828.816
Mass cylinder + core + H2O	g	839.661	1930.081	1958.391	1961.544	1955.449	1965.608	1952.104	1941.811	1953.969	1967.203	1977.702
Mass tot start	g	839.661	1930.077	1958.317	1961.519	1955.158	1965.553	1952.100	1941.802	1953.966	1967.200	1977.739
Initial Water Mass	ml	459.169	144.453	144.003	151.033	145.814	144.035	141.471	141.941	144.209	140.858	148.886
Ratio Exp.Water : Rock			0.101	0.100	0.104	0.100	0.098	0.097	0.098	0.099	0.096	0.101
End Experiment		12.11.2021	28.09.2022	28.09.2022	28.09.2022	28.09.2022	28.09.2022	28.09.2022	28.09.2022	28.09.2022	28.09.2022	28.09.2022
Mass cylinder + core + H2O final	g		1921.775	1950.677	1953.917	1947.424	1956.705	1944.187	1934.007	1946.383	1959.066	1968.782
Final Water Mass (measured, not all recoverable)	ml	112.774	132.322	132.243	139.639	134.002	131.794	130.240	130.053	132.513	128.978	135.438
Time Experiment	days	140	324	324	324	324	324	324	324	324	298	298
Volume of samples for Cl-measurements												
sample A	ml	0.5	0.7	0.5	0.5	0.5	0.6	0.5	0.5	0.5	0.5	0.6
sample B	ml	0.5	0.6	0.5	0.5	0.5	0.6	0.5	0.5	0.5	0.5	0.6
sample C	ml	0.5	0.5	0.5	0.5	0.5	0.6	0.5	0.5	0.5	0.5	0.6
sample D	ml	0.5	0.5	0.5	0.5	0.5	0.5	0.5	0.5	0.5	0.5	0.5
sample E	ml	0.5	0.5	0.5	0.5	0.5	0.5	0.5	0.5	0.5	0.5	0.5
sample F	ml	0.5	0.5	0.5	0.5	0.5	0.5	0.5	0.5	0.5	0.5	0.5
sample G	ml	0.5	0.5	0.5	0.5	0.5	0.5	0.5	0.5	0.5	0.5	0.5
sample H	ml	0.5	0.5	0.5	0.5	0.5	0.5	0.5	0.5	0.5	0.5	0.5
sample I	ml	0.5	0.5	0.5	0.5	0.5	0.5	0.5	0.5	0.5	0.5	0.5
sample K	ml	0.5	0.5	0.5	0.5	0.5	0.5	0.5	0.5	0.5	0.5	0.5
sample L	ml	0.5	0.5	0.5	0.5	0.5	0.5	0.5	0.5	0.5	0.5	0.5
sample M	ml	0.5	0.5	0.5	0.5	0.5	0.5	0.5	0.5	0.5	0.5	0.5
sample N	ml	0.5	0.5	0.5	0.5	0.5	0.5	0.5	0.5	0.5	0.5	0.5
total volume subsamples		6.5	6.8	6.5	6.5	6.5	6.8	6.5	6.5	6.5	6.5	6.8
Volumen TS calculated cyl (ini-final)	ml		8.302	7.640	7.602	7.734	8.848	7.913	7.795	7.583	8.134	8.957
Difference V(ss) - V(calc)	ml		0.802	0.440	0.402	0.534	1.348	0.713	0.595	0.383	0.934	1.457
Difference % of TS	%		0.6	0.3	0.3	0.4	0.9	0.5	0.4	0.3	0.7	1.0

Table B-5.1: Continued

Sample		IG_BH06_PW011	IG_BH06_PW012	IG_BH06_PW013	IG_BH06_PW014	IG_BH06_PW015	IG_BH06_PW016	IG_BH06_PW017	IG_BH06_PW018	IG_BH06_PW019	IG_BH06_PW020
Depth	m	691.0	693.7	720.5	747.5	774.9	804.7	840.2	853.0	885.3	927.6
start experiment		04.12.2021	04.12.2021	04.12.2021	04.12.2021	04.12.2021	04.12.2021	04.12.2021	04.12.2021	04.12.2021	04.12.2021
Initial Rock Mass (as received, +/- mountain wet)	g	1406.002	1467.348	1440.077	1407.998	1474.894	1479.106	1396.776	1451.021	1440.235	1465.050
Initial Rock Mass (start experiment)	g	1406.997	1467.328	1440.071	1407.996	1474.833	1479.054	1396.768	1451.005	1440.165	1465.029
Final Rock Mass (resaturated)	g	1406.011	1467.915	1440.305	1408.170	1475.255	1479.935	1396.920	1451.380	1440.780	1465.620
Uptake of water	g	0.009	0.567	0.228	0.172	0.361	0.829	0.144	0.359	0.545	0.570
Saturation	%	99.999	99.961	99.984	99.988	99.976	99.944	99.990	99.975	99.962	99.961
Core Diametre	cm	6.09	6.1	6.08	6.07	6.08	6.08	6.09	6.1	6.11	6.1
Core Length	cm	17.71	18.71	18.47	18.17	18.80	18.87	18.01	18.64	18.55	18.66
Volume of Rock Sample	cm3	515.87	546.79	536.25	525.80	545.83	547.86	524.61	544.75	543.90	545.33
Density (calculated from volume & mass)	g/cm3	2.73	2.68	2.69	2.68	2.70	2.70	2.66	2.66	2.65	2.69
Mass of Rock (calculated from volume and density)		1406.00	1467.35	1440.08	1408.00	1474.89	1479.11	1396.78	1451.02	1440.24	1465.05
Masses before experiment											
Mass cylinder	g	382.385	380.863	379.313	380.756	361.451	382.821	361.316	380.761	380.760	380.901
Mass cylinder + core	g	1788.067	1847.421	1818.959	1788.279	1835.819	1860.992	1757.543	1831.774	1820.919	1845.933
Mass cylinder + core + H2O	g	1937.469	1990.508	1973.210	1933.665	1983.255	2008.464	1901.237	1977.838	1961.473	1987.893
Mass tot start	g	1937.541	1990.560	1973.309	1933.742	1980.572	2008.939	1901.257	1977.877	1961.523	1987.904
Initial Water Mass	ml	149.402	143.087	154.251	145.386	147.436	147.472	143.694	146.064	140.554	141.960
Ratio Exp.Water : Rock		0.106	0.098	0.107	0.103	0.100	0.100	0.103	0.101	0.098	0.097
End Experiment		28.09.2022	18.10.2022	18.10.2022	18.10.2022	18.10.2022	18.10.2022	18.10.2022	18.10.2022	18.10.2022	18.10.2022
Mass cylinder + core + H2O final	g	1929.483	1982.870	1965.583	1925.971	1972.399	2000.840	1892.420	1968.514	1952.548	1979.837
Final Water Mass (measured, not all recoverable)	ml	137.538	131.096	142.977	137.775	131.912	135.450	131.677	132.805	128.319	130.660
Time Experiment	days	298	318	318	318	318	318	318	318	318	318
Volume of samples for Cl-measurements											
sample A	ml	0.5	0.5	0.5	0.5	0.5	0.5	0.6	0.7	0.6	0.5
sample B	ml	0.5	0.5	0.5	0.5	0.5	0.5	0.6	0.6	0.6	0.5
sample C	ml	0.5	0.5	0.5	0.5	0.5	0.5	0.6	0.6	0.5	0.5
sample D	ml	0.5	0.5	0.5	0.5	0.5	0.5	0.5	0.6	0.5	0.5
sample E	ml	0.5	0.5	0.5	0.5	0.5	0.5	0.5	0.5	0.5	0.5
sample F	ml	0.5	0.5	0.5	0.5	0.5	0.5	0.5	0.5	0.5	0.5
sample G	ml	0.5	0.5	0.5	0.5	0.5	0.5	0.5	0.5	0.5	0.5
sample H	ml	0.5	0.5	0.5	0.5	0.5	0.5	0.5	0.5	0.5	0.5
sample I	ml	0.5	0.5	0.5	0.5	0.5	0.5	0.5	0.5	0.5	0.5
sample K	ml	0.5	0.5	0.5	0.5	0.5	0.5	0.5	0.5	0.5	0.5
sample L	ml	0.5	0.5	0.5	0.5	0.5	0.5	0.5	0.5	0.5	0.5
sample M	ml	0.5	0.5	0.5	0.5	0.5	0.5	0.5	0.5	0.5	0.5
sample N	ml	0.5	0.5	0.5	0.5	0.5	0.5	0.5	0.5	0.5	0.5
total volume subsamples		6.5	6.5	6.5	6.5	6.5	6.5	6.8	7.0	6.7	6.5
Volumen TS calculated cyl (ini-final)	ml	8.058	7.690	7.726	7.771	8.173	8.099	8.837	9.363	8.975	8.067
Difference V(ss) - V(calc)	ml	0.858	0.490	0.526	0.571	0.973	0.899	1.337	1.663	1.575	0.867
Difference % of TS	%	0.6	0.3	0.3	0.4	0.7	0.6	0.9	1.1	1.1	0.6

Table B-5.1: Continued

Sample		IG_BH06_AR010	IG_BH06_AR013	IG_BH06_AR019	IG_BH06_AR020	IG_BH06_AR027	IG_BH06_AR038	IG_BH06_AR039	IG_BH06_AR045	IG_BH06_AR049	IG_BH06_AR064	IG_BH06_DG003
Depth	m	398.7	421.6	534.0	542.9	595.0	722.6	728.8	796.7	820.2	971.4	744.0
start experiment		14.03.2022	14.03.2022	14.03.2022	14.03.2022	14.03.2022	14.03.2022	14.03.2022	14.03.2022	14.03.2022	14.03.2022	14.03.2022
Initial Rock Mass (as received, +/- mountain wet)	g	1627.420	1477.362	1451.617	1425.077	1454.975	1602.754	1431.104	1417.982	1368.428	1439.354	1216.271
Initial Rock Mass (start experiment)	g	1627.420	1477.362	1451.617	1425.038	1454.975	1602.754	1431.104	1417.982	1368.428	1439.354	1216.271
Final Rock Mass (resaturated)	g	1627.895	1477.687	1451.930	1425.001	1455.186	1602.973	1431.685	1418.582	1369.149	1439.961	1217.239
Uptake of water	g	0.475	0.325	0.313	-0.076	0.211	0.219	0.581	0.600	0.721	0.607	0.968
Saturation	%	99.971	99.978	99.978	100.005	99.986	99.986	99.959	99.958	99.947	99.958	99.920
Core Diametre	cm	6.11	6.10	6.1	6.1	6.09	6.06	6.08	6.08	6.1	6.11	6.06
Core Length	cm	20.58	18.98	18.66	18.24	18.73	18.50	18.33	18.09	17.87	18.31	15.72
Volume of Rock Sample	cm3	603.42	554.68	545.33	533.06	545.58	533.59	532.18	525.21	522.24	536.86	453.41
Density (calculated from volume & mass)	g/cm3	2.70	2.66	2.66	2.67	2.67	3.00	2.69	2.70	2.62	2.68	2.68
Mass of Rock (calculated from volume and density)		1627.42	1477.36	1451.62	1425.08	1454.98	1602.75	1431.10	1417.98	1368.43	1439.35	1216.27
Masses before experiment												
Mass cylinder	g	355.913	364.092	356.626	357.167	381.430	380.986	359.712	380.737	380.483	382.003	354.60
Mass cylinder + core	g	1983.363	1841.461	1808.247	1782.215	1836.538	1983.727	1790.825	1798.712	1748.951	1821.355	1570.876
Mass cylinder + core + H2O	g	2123.320	1975.803	1945.272	1920.263	1980.116	2122.471	1931.183	1930.295	1890.167	1949.272	1707.009
Mass tot start	g	2123.326	1975.810	1945.282	1920.272	1979.948	2122.477	1931.191	1930.292	1890.090	1949.275	1706.981
Initial Water Mass	ml	139.957	134.342	137.025	138.048	143.578	138.744	140.358	131.583	141.216	127.917	136.133
Ratio Exp.Water : Rock		0.086	0.091	0.094	0.097	0.099	0.087	0.098	0.093	0.103	0.089	0.112
End Experiment		22.11.2022	22.11.2022	22.11.2022	22.11.2022	22.11.2022	22.11.2022	22.11.2022	22.11.2022	22.11.2022	22.11.2022	22.11.2022
Mass cylinder + core + H2O final	g	2116.001	1968.404	1938.015	1912.670	1972.636	2115.208	1923.147	1922.971	1882.743	1941.861	1698.990
Final Water Mass (measured, not all recoverable)	ml	129.100	123.059	126.225	127.208	131.649	128.164	128.056	120.415	129.754	117.072	123.883
Time Experiment	days	253	253	253	253	253	253	253	253	253	253	253
Volume of samples for Cl-measurements												
sample A	ml	0.5	0.5	0.5	0.5	0.5	0.5	0.5	0.5	0.5	0.5	0.5
sample B	ml	0.5	0.5	0.5	0.5	0.5	0.5	0.5	0.5	0.5	0.5	0.5
sample C	ml	0.5	0.5	0.5	0.5	0.5	0.5	0.5	0.5	0.5	0.5	0.5
sample D	ml	0.5	0.5	0.5	0.5	0.5	0.5	0.5	0.5	0.5	0.5	0.5
sample E	ml	0.5	0.5	0.5	0.5	0.5	0.5	0.5	0.5	0.5	0.5	0.5
sample F	ml	0.5	0.5	0.5	0.5	0.5	0.5	0.5	0.5	0.5	0.5	0.5
sample G	ml	0.5	0.5	0.5	0.5	0.5	0.5	0.5	0.5	0.5	0.5	0.5
sample H	ml	0.5	0.5	0.5	0.5	0.5	0.5	0.5	0.5	0.5	0.5	0.5
sample I	ml	0.5	0.5	0.5	0.5	0.5	0.5	0.5	0.5	0.5	0.5	0.5
sample K	ml	0.5	0.5	0.5	0.5	0.5	0.5	0.5	0.5	0.5	0.5	0.5
sample L	ml	0.5	0.5	0.5	0.5	0.5	0.5	0.5	0.5	0.5	0.5	0.5
sample M	ml	0.5	0.5	0.5	0.5	0.5	0.5	0.5	0.5	0.5	0.5	0.5
sample N	ml	0.5	0.5	0.5	0.5	0.5	0.5	0.5	0.5	0.5	0.5	0.5
total volume subsamples		6.5	6.5	6.5	6.5	6.5	6.5	6.5	6.5	6.5	6.5	6.5
Volumen TS calculated cyl (ini-final)	ml	7.325	7.406	7.267	7.602	7.312	7.269	8.044	7.321	7.347	7.414	7.991
Difference V(ss) - V(calc)	ml	0.125	0.206	0.067	0.402	0.112	0.069	0.844	0.121	0.147	0.214	0.791
Difference % of TS	%	0.1	0.2	0.0	0.3	0.1	0.0	0.6	0.1	0.1	0.2	0.6

Table B-5.2: Chemical composition of time series samples taken during out-diffusion experiments

Sample			IG_BH06_PW001											IG_BH06_PW002										
Sub-samples	Time	Date	Na	K	Ca	Mg	Sr	F	Cl	SO4	NO3	Br	Br/Cl	Na	K	Ca	Mg	Sr	F	Cl	SO4	NO3	Br	Br/Cl
	days		mg/l	mg/l	mg/l	mg/l	mg/l	mg/l	mg/l	mg/l	mg/l	mg/l		mg/l	mg/l	mg/l	mg/l	mg/l	mg/l	mg/l	mg/l	mg/l	mg/l	
Preparation		08.11.2021																						
A	1	09.11.2021	3.5	1.7	2.7	<0.2	<0.1	0.19	3.6	<0,5	<0.2	<0.05		3.7	1.8	3.3	<0.2	<0.1	0.15	4.9	<0.5	<0.2	0.07	14
B	3	11.11.2021	5.0	1.9	3.8	<0.2	<0.1	0.16	4.0	<0,5	<0.2	<0.05		5.3	2.1	4.4	<0.2	<0.1	0.18	7.7	<0.5	<0.2	0.08	10
C	4	12.11.2021	5.5	2.0	4.6	<0.2	<0.1	0.35	4.5	<0,5	<0.2	<0.05		6.0	2.2	5.4	<0.2	<0.1	0.34	9.1	0.71	<0.2	0.08	9
D	7	15.11.2021	6.9	2.2	5.8	<0.2	<0.1	0.55	5.5	1.4	<0.2	0.06	11	7.4	2.4	6.9	<0.2	<0.1	0.51	11.1	1.2	<0.2	0.08	7
E	12	20.11.2021	8.4	2.3	5.9	<0.2	<0.1	0.58	6.1	1.4	<0.2	0.07	11	9.6	2.7	9.1	<0.2	<0.1	0.51	13.8	1.7	<0.2	0.08	6
F	14	22.11.2021	8.9	2.3	6.1	<0.2	<0.1	0.65	6.6	1.4	<0.2	0.07	11	9.6	2.7	9.3	<0.2	<0.1	0.55	13.8	1.9	<0.2	0.11	8
G	21	29.11.2021	9.8	2.4	8.2	<0.2	<0.1	0.81	7.2	1.4	<0.2	0.08	11	10.5	2.9	10.8	<0.2	<0.1	0.72	15.4	2.1	<0.2	0.15	10
H	29	07.12.2021	11.5	2.4	10.2	<0.2	<0.1	1.3	7.8	2.2	<0.2	0.09	12	12.4	3.1	14.3	<0.2	<0.1	1.0	16.8	3.4	<0.2	0.21	13
I	48	26.12.2021	13.3	2.4	12.5	<0.2	<0.1	1.5	7.8	2.8	<0.2	0.10	13	14.1	3.3	18.6	<0.2	<0.1	1.4	18.2	4.2	<0.2	0.30	16
K	61	08.01.2022	13.6	2.4	12.6	<0.2	<0.1	2.0	7.8	3.4	<0.2	0.11	14	16.1	3.4	22.5	<0.2	<0.1	2.1	20.0	7.8	<0.2	0.30	15
L	75	22.01.2022	15.3	2.4	12.9	<0.2	<0.1	2.4	7.8	4.2	<0.2	0.12	15	16.5	3.5	23.1	<0.2	<0.1	2.4	20.4	7.8	<0.2	0.30	15
M	91	07.02.2022	15.4	2.4	13.5	<0.2	<0.1	2.5	7.8	4.7	<0.2	0.12	15	17.4	3.7	25.7	<0.2	<0.1	2.5	20.8	7.8	<0.2	0.30	14
N	120	08.03.2022	18.1	2.5	13.9	<0.2	<0.1	3.0	7.8	5.2	<0.2	0.12	15	18.8	3.7	27.7	<0.2	<0.1	2.6	20.8	8.0	<0.2	0.30	14
FINAL	324	28.09.2022	19.4	2.6	15.2	<0.2	<0.1	3.1	7.8	5.2	<0.2	0.12	15	19.0	2.5	30.2	<0.2	<0.1	2.6	20.8	8.9	<0.2	0.30	14
Sample			**IG_BH06_PW003**											**IG_BH06_PW004**										
Sub-samples	**Time**	**Date**	**Na**	**K**	**Ca**	**Mg**	**Sr**	**F**	**Cl**	**SO4**	**NO3**	**Br**	**Br/Cl**	**Na**	**K**	**Ca**	**Mg**	**Sr**	**F**	**Cl**	**SO4**	**NO3**	**Br**	**Br/Cl**
	days		**mg/l**	**mg/l**	**mg/l**	**mg/l**	**mg/l**	**mg/l**	**mg/l**	**mg/l**	**mg/l**	**mg/l**		**mg/l**	**mg/l**	**mg/l**	**mg/l**	**mg/l**	**mg/l**	**mg/l**	**mg/l**	**mg/l**	**mg/l**	
Preparation		08.11.2021																						
A	1	09.11.2021	3.9	1.90	4.4	<0.2	<0.1	0.14	8.7	<0.5	<0.2	0.23	26	0.25	0.1	0.26	<0.2	<0.1	<0.1	3.4	<0.5	<0.2	0.11	32
B	3	11.11.2021	5.5	2.4	6.0	<0.2	<0.1	0.12	13.1	<0.5	<0.2	0.27	21	5.5	2.5	10.0	<0.2	<0.1	0.18	12.2	<0.5	<0.2	0.37	30
C	4	12.11.2021	6.2	2.6	7.0	<0.2	<0.1	0.19	14.8	<0.5	<0.2	0.33	22	6.3	2.7	11.6	<0.2	<0.1	0.18	12.2	0.57	<0.2	0.40	33
D	7	15.11.2021	7.4	2.7	8.6	<0.2	<0.1	0.29	17.0	0.55	<0.2	0.37	22	7.4	2.8	14.8	<0.2	<0.1	0.43	25.3	0.9	<0.2	0.59	23
E	12	20.11.2021	9.3	3.0	9.5	<0.2	<0.1	0.39	19.6	0.84	<0.2	0.37	19	8.9	2.8	16.6	<0.2	<0.1	0.75	28.9	1.0	<0.2	0.59	20
F	14	22.11.2021	9.3	3.0	10.3	<0.2	<0.1	0.39	20.8	0.95	<0.2	0.38	18	9.3	2.9	17.7	<0.2	<0.1	0.76	29.6	1.1	<0.2	0.60	20
G	21	29.11.2021	9.9	3.1	11.6	<0.2	<0.1	0.53	20.8	1.3	<0.2	0.51	25	10.1	3.1	21.0	<0.2	<0.1	0.87	30.7	1.3	<0.2	0.76	25
H	29	07.12.2021	11.6	3.5	14.9	<0.2	<0.1	0.55	22.3	2.0	<0.2	0.74	33	12.5	3.3	27.9	<0.2	<0.1	0.99	32.9	2.8	<0.2	0.91	28
I	48	26.12.2021	13.2	3.7	15.5	<0.2	<0.1	0.73	24.1	3.0	<0.2	0.74	31	12.6	3.3	29.5	<0.2	<0.1	1.2	35.3	3.6	<0.2	0.91	26
K	61	08.01.2022	14.0	3.8	16.9	<0.2	<0.1	0.81	27.3	4.0	<0.2	0.74	27	14.1	4.0	29.6	<0.2	<0.1	1.2	38.2	4.6	<0.2	0.91	24
L	75	22.01.2022	17.4	4.0	20.9	<0.2	<0.1	1.0	28.1	6.3	<0.2	0.74	26	15.5	4.0	34.6	<0.2	<0.1	1.6	42.7	6.3	<0.2	0.91	21
M	91	07.02.2022	17.4	4.1	22.9	<0.2	<0.1	1.0	28.3	7.4	<0.2	0.74	26	15.4	4.0	36.8	<0.2	<0.1	1.7	43.9	6.3	<0.2	0.91	21
N	120	08.03.2022	17.4	4.2	26.8	<0.2	<0.1	1.0	28.3	7.9	<0.2	0.74	26	15.4	4.0	40.3	<0.2	<0.1	1.7	44.0	6.5	<0.2	0.91	21
FINAL	324	28.09.2022	17.4	4.2	27.1	<0.2	<0.1	1.0	28.4	9.2	<0.2	0.74	26	15.6	4.0	40.8	<0.2	<0.1	1.7	44.0	7.1	<0.2	0.91	21
Sample			**IG_BH06_PW005**											**IG_BH06_PW006**										
Sub-samples	**Time**	**Date**	**Na**	**K**	**Ca**	**Mg**	**Sr**	**F**	**Cl**	**SO4**	**NO3**	**Br**	**Br/Cl**	**Na**	**K**	**Ca**	**Mg**	**Sr**	**F**	**Cl**	**SO4**	**NO3**	**Br**	**Br/Cl**
	days		**mg/l**	**mg/l**	**mg/l**	**mg/l**	**mg/l**	**mg/l**	**mg/l**	**mg/l**	**mg/l**	**mg/l**		**mg/l**	**mg/l**	**mg/l**	**mg/l**	**mg/l**	**mg/l**	**mg/l**	**mg/l**	**mg/l**	**mg/l**	
Preparation		08.11.2021																						
A	1	09.11.2021	4.0	2.4	3.2	<0.2	<0.1	<0.1	7.4	<0.5	<0.2	0.38	51	4.1	2.9	5.5	<0.2	<0.1	<0.1	11.5	<0,5	<0.2	0.22	19
B	3	11.11.2021	5.2	2.9	4.3	<0.2	<0.1	<0.1	10.2	<0.5	<0.2	0.51	50	5.5	3.6	7.8	<0.2	<0.1	<0.1	15.8	<0,5	<0.2	0.31	20
C	4	12.11.2021	5.8	2.9	5.0	<0.2	<0.1	<0.1	11.4	<0.5	<0.2	0.56	49	6.0	3.7	8.1	<0.2	<0.1	<0.1	16.7	0.6	<0.2	0.41	25
D	7	15.11.2021	6.9	3.2	6.1	<0.2	<0.1	0.11	13.6	<0.5	<0.2	0.67	49	7.2	4.1	9.8	<0.2	<0.1	<0.1	20.6	0.7	<0.2	0.45	22
E	12	20.11.2021	8.4	3.5	6.5	<0.2	<0.1	0.11	15.1	1.1	<0.2	0.77	51	8.7	4.4	10.4	<0.2	<0.1	<0.1	23.7	1.5	<0.2	0.45	19
F	14	22.11.2021	9.1	3.6	7.3	<0.2	<0.1	0.11	15.9	1.2	<0.2	0.78	49	9.4	4.6	11.6	<0.2	<0.1	<0.1	25.2	1.6	<0.2	0.45	18
G	21	29.11.2021	9.3	3.5	8.4	<0.2	<0.1	0.17	16.7	1.3	<0.2	0.83	50	11.7	4.7	13.7	<0.2	<0.1	0.11	26.7	1.7	<0.2	0.50	19
H	29	07.12.2021	10.8	3.9	10.0	<0.2	<0.1	0.25	17.6	2.2	<0.2	0.85	48	11.8	5.4	16.6	<0.2	<0.1	0.18	27.6	2.2	<0.2	0.58	21
I	48	26.12.2021	12.4	4.1	10.5	<0.2	<0.1	0.26	19.6	3.1	<0.2	0.91	46	12.2	5.5	18.0	<0.2	<0.1	0.22	28.2	2.7	<0.2	0.58	21
K	61	08.01.2022	12.6	4.1	10.9	<0.2	<0.1	0.38	21.8	4.5	<0.2	0.91	42	14.0	6.2	19.0	<0.2	<0.1	0.34	28.8	3.6	<0.2	0.58	20
L	75	22.01.2022	14.3	4.1	14.7	<0.2	<0.1	0.49	22.8	6.2	<0.2	0.91	40	15.2	6.6	22.0	<0.2	<0.1	0.38	28.8	5.1	<0.2	0.58	20
M	91	07.02.2022	14.5	4.1	15.3	<0.2	<0.1	0.53	22.8	6.6	<0.2	0.91	40	15.5	6.7	24.2	<0.2	<0.1	0.40	29.4	5.8	<0.2	0.58	20
N	120	08.03.2022	17.4	4.1	17.2	<0.2	<0.1	0.62	22.9	6.8	<0.2	0.91	40	16.4	6.7	26.7	<0.2	<0.1	0.40	29.4	5.9	<0.2	0.58	20
FINAL	324	28.09.2022	17.7	4.1	19.0	<0.2	<0.1	0.67	22.9	7.0	<0.2	0.91	40	16.4	6.8	26.9	<0.2	<0.1	0.40	29.5	6.5	<0.2	0.58	20

Table B-5.2: Continued

Sample			IG_BH06_PW007											IG_BH06_PW008									
Sub-samples	Time	Date	Na	K	Ca	Mg	Sr	F	Cl	SO4	NO3	Br	Br/Cl	Na	K	Ca	Mg	Sr	F	Cl	SO4	NO3	Br	Br/Cl
	days		mg/l	mg/l	mg/l	mg/l	mg/l	mg/l	mg/l	mg/l	mg/l	mg/l		mg/l	mg/l	mg/l	mg/l	mg/l	mg/l	mg/l	mg/l	mg/l	mg/l	
Preparation		08.11.2021																					
A	1	09.11.2021	4.2	2.9	8.0	<0.2	<0.1	<0,1	11.1	<0.5	<0.2	0.25	23	4.8	3.7	7.8	<0.2	<0.1	<0.1	16.5	<0,5	<0.2	0.35	21
B	3	11.11.2021	5.3	3.3	10.1	<0.2	<0.1	<0,1	12.4	<0.5	<0.2	0.29	23	6.1	4.3	11.0	<0.2	<0.1	<0.1	22.4	<0,5	<0.2	0.40	18
C	4	12.11.2021	5.8	3.5	12.1	<0.2	<0.1	<0,1	15.4	0.54	<0.2	0.33	21	6.8	4.5	12.3	<0.2	<0.1	<0.1	24.2	<0,5	<0.2	0.41	17
D	7	15.11.2021	6.8	3.6	14.5	<0.2	<0.1	<0,1	17.8	0.73	<0.2	0.36	20	8.0	5.1	15.2	<0.2	<0.1	<0.1	28.8	0.65	<0.2	0.43	15
E	12	20.11.2021	8.0	4.0	16.2	<0.2	<0.1	<0,1	20.4	1.4	<0.2	0.37	18	9.5	5.3	17.2	<0.2	<0.1	<0.1	32.4	1.6	<0.2	0.45	14
F	14	22.11.2021	8.4	4.0	17.7	<0.2	<0.1	<0,1	20.4	1.5	<0.2	0.37	18	10.4	5.4	20.9	<0.2	<0.1	<0.1	33.0	1.6	<0.2	0.48	15
G	21	29.11.2021	8.9	4.4	19.9	<0.2	<0.1	<0,1	20.4	1.6	<0.2	0.37	18	10.5	5.5	21.0	<0.2	<0.1	<0.1	35.0	1.6	<0.2	0.50	14
H	29	07.12.2021	10.4	5.4	24.4	<0.2	<0.1	<0,1	21.3	2.4	<0.2	0.37	17	12.6	5.5	25.8	<0.2	<0.1	0.14	37.9	2.4	<0.2	0.61	16
I	48	26.12.2021	11.4	5.9	29.5	0.23	<0.1	<0,1	23.0	3.0	<0.2	0.37	16	13.2	5.6	28.7	<0.2	<0.1	0.17	40.2	2.8	<0.2	0.65	16
K	61	08.01.2022	14.3	6.2	33.7	0.23	<0.1	<0,1	24.7	5.4	<0.2	0.37	15	14.7	5.6	30.8	<0.2	<0.1	0.21	43.3	3.6	<0.2	0.65	15
L	75	22.01.2022	14.8	6.2	37.3	0.25	<0.1	<0,1	27.2	5.9	<0.2	0.37	14	16.3	5.6	36.4	<0.2	<0.1	0.26	47.6	5.6	<0.2	0.65	14
M	91	07.02.2022	15.0	6.2	37.5	0.26	<0.1	0.11	27.3	6.8	<0.2	0.37	14	16.8	5.7	37.2	<0.2	<0.1	0.27	51.9	6.3	<0.2	0.65	13
N	120	08.03.2022	15.3	6.2	37.7	0.30	<0.1	0.11	27.3	7.2	<0.2	0.37	14	17.0	5.7	37.6	<0.2	<0.1	0.27	51.9	6.3	<0.2	0.65	13
FINAL	324	28.09.2022	15.6	6.6	38.1	0.30	<0.1	0.11	27.4	8.6	<0.2	0.37	14	17.1	5.7	37.8	<0.2	<0.1	0.27	51.9	6.3	<0.2	0.65	13
Sample			IG_BH06_PW009											IG_BH06_PW010									
Sub-samples	Time	Date	Na	K	Ca	Mg	Sr	F	Cl	SO4	NO3	Br	Br/Cl	Na	K	Ca	Mg	Sr	F	Cl	SO4	NO3	Br	Br/Cl
	days		mg/l	mg/l	mg/l	mg/l	mg/l	mg/l	mg/l	mg/l	mg/l	mg/l		mg/l	mg/l	mg/l	mg/l	mg/l	mg/l	mg/l	mg/l	mg/l	mg/l	
Preparation		04.12.2021																					
A	1	05.12.2021	4.4	2.1	6.1	<0.2	<0.1	<0,1	14	<0.5	<0.2	0.18	13	3.8	2.5	6.1	<0.2	<0.1	<0.1	13.8	<0,5	<0.2	0.17	12
B	3	07.12.2021	6.8	2.9	11.0	<0.2	<0.1	<0,1	22.8	<0.5	<0.2	0.45	20	6.5	3.7	11.0	<0.2	<0.1	<0.1	21.1	<0,5	<0.2	0.40	19
C	4	08.12.2021	8.4	3.4	13.8	<0.2	<0.1	<0,1	27.8	<0.5	<0.2	0.59	21	7.4	3.9	12.7	<0.2	<0.1	<0.1	22.8	0.73	<0.2	0.45	20
D	7	11.12.2021	10.1	3.6	18.1	<0.2	<0.1	<0,1	29.9	1.2	<0.2	0.60	20	9.1	4.5	18.0	<0.2	<0.1	<0.1	28.8	0.80	<0.2	0.62	22
E	12	16.12.2021	11.4	3.6	19.3	<0.2	<0.1	<0,1	35.6	1.3	<0.2	0.72	20	11.4	5.0	19.6	<0.2	<0.1	<0.1	40.0	1.4	<0.2	0.81	20
F	14	18.12.2021	11.7	3.7	19.1	<0.2	<0.1	<0,1	42.3	1.4	<0.2	0.90	21	11.5	5.3	20.5	<0.2	<0.1	<0.1	44.2	1.4	<0.2	0.85	19
G	23	27.12.2021	13.4	4.0	21.4	<0.2	<0.1	<0,1	50.2	1.8	<0.2	0.90	18	14.2	5.4	24.3	<0.2	<0.1	0.17	48.5	2.4	<0.2	1.1	23
H	31	04.01.2022	13.8	4.1	23.4	<0.2	<0.1	<0,1	51.3	2.4	<0.2	0.90	18	14.5	5.5	24.7	<0.2	<0.1	0.19	50.2	2.5	<0.2	1.1	22
I	51	24.01.2022	17.3	4.4	26.7	<0.2	<0.1	<0,1	53.1	2.6	<0.2	0.90	17	14.5	5.5	24.7	<0.2	<0.1	0.19	51.3	2.7	<0.2	1.1	21
K	66	08.02.2022	17.4	4.4	30.7	<0.2	<0.1	<0,1	53.4	3.4	<0.2	0.90	17	14.5	5.6	24.7	<0.2	<0.1	0.19	52.4	2.9	<0.2	1.1	21
L	81	23.02.2022	17.4	4.4	36.4	<0.2	<0.1	<0,1	53.4	4.9	<0.2	0.90	17	15.2	5.6	25.5	<0.2	<0.1	0.22	53.6	3.4	<0.2	1.1	21
M	95	09.03.2022	17.5	4.4	36.8	<0.2	<0.1	<0,1	53.6	5.0	<0.2	0.90	17	15.2	5.6	34.7	<0.2	<0.1	0.26	54.6	4.1	<0.2	1.1	20
N	123	06.04.2022	17.5	4.7	37.2	<0.2	<0.1	<0,1	53.6	5.4	<0.2	0.90	17	15.2	5.6	36.0	<0.2	<0.1	0.29	55.1	4.8	<0.2	1.1	20
FINAL	298	28.09.2022	17.5	4.8	37.4	<0.2	<0.1	<0,1	53.7	5.7	<0.2	0.90	17	15.6	5.6	39.1	<0.2	<0.1	0.32	56.5	5.0	<0.2	1.1	19
Sample			IG_BH06_PW011																					
Sub-samples	Time	Date	Na	K	Ca	Mg	Sr	F	Cl	SO4	NO3	Br	Br/Cl											
	days		mg/l	mg/l	mg/l	mg/l	mg/l	mg/l	mg/l	mg/l	mg/l	mg/l												
Preparation		04.12.2021																						
A	1	05.12.2021	2.8	2.1	6.8	<0.2	<0.1	<0.1	10.7	<0.5	<0.2	0.15	14											
B	3	07.12.2021	4.7	3.0	12.2	<0.2	<0.1	<0.1	18.5	<0.5	<0.2	0.35	19											
C	4	08.12.2021	5.8	3.7	15.8	<0.2	<0.1	<0.1	23.8	0.74	<0.2	0.52	22											
D	7	11.12.2021	6.8	4.0	19.4	<0.2	<0.1	<0.1	24.6	0.84	<0.2	0.59	24											
E	12	16.12.2021	9.7	4.6	21.7	<0.2	<0.1	0.12	42.2	1.3	<0.2	1.1	26											
F	14	18.12.2021	9.7	5.0	23.3	0.24	<0.1	0.12	42.2	1.4	<0.2	1.1	26											
G	23	27.12.2021	12.1	5.3	31.7	0.33	<0.1	0.12	51.8	2.1	<0.2	1.3	25											
H	31	04.01.2022	12.2	5.5	32.0	0.34	<0.1	0.13	52.0	2.4	<0.2	1.3	25											
I	51	24.01.2022	13.8	5.6	32.2	0.34	<0.1	0.15	52.1	2.6	<0.2	1.3	25											
K	66	08.02.2022	14.0	5.7	33.0	0.40	<0.1	0.16	52.1	3.1	<0.2	1.3	25											
L	81	23.02.2022	14.0	5.7	33.4	0.46	<0.1	0.16	52.3	3.2	<0.2	1.3	25											
M	95	09.03.2022	14.0	5.7	38.8	0.41	<0.1	0.18	53.2	3.9	<0.2	1.3	24											
N	123	06.04.2022	14.5	5.7	40.0	0.47	<0.1	0.18	53.4	4.4	<0.2	1.3	24											
FINAL	298	28.09.2022	14.8	5.7	40.3	0.48	<0.1	0.20	53.4	4.8	<0.2	1.3	24											

Table B-5.2: Continued

Sample			IG_BH06_PW012											IG_BH06_PW013										
Sub-samples	Time	Date	Na	K	Ca	Mg	Sr	F	Cl	SO4	NO3	Br	Br/Cl	Na	K	Ca	Mg	Sr	F	Cl	SO4	NO3	Br	Br/Cl
	days		mg/l	mg/l	mg/l	mg/l	mg/l	mg/l	mg/l	mg/l	mg/l	mg/l		mg/l	mg/l	mg/l	mg/l	mg/l	mg/l	mg/l	mg/l	mg/l	mg/l	
Preparation		04.12.2021																						
A	1	05.12.2021	5.2	2.9	10.4	<0.2	<0.1	<0,1	23.1	0.87	<0.2	1.3	56	3.6	2.8	6.9	<0.2	<0.1	<0.1	12.3	<0,5	<0.2	0.13	11
B	3	07.12.2021	9.3	4.3	19.0	<0.2	<0.1	<0,1	38.3	1.1	<0.2	1.6	42	6.3	3.8	11.0	<0.2	<0.1	<0.1	21.4	0.69	<0.2	0.26	12
C	4	08.12.2021	10.9	4.9	22.3	<0.2	<0.1	<0,1	46.3	2.6	<0.2	2.6	56	7.7	4.5	13.6	<0.2	<0.1	<0.1	27.0	1.2	<0.2	0.39	14
D	7	11.12.2021	15.7	5.4	33.4	0.27	<0.1	0.14	58.0	3.2	<0.2	4.3	74	10.3	4.8	19.5	<0.2	<0.1	<0.1	32.0	1.6	<0.2	0.61	19
E	12	16.12.2021	17.4	5.6	35.5	0.29	<0.1	0.16	69.7	5.3	<0.2	5.8	83	12.4	5.4	22.3	<0.2	<0.1	<0.1	44.1	2.3	<0.2	0.73	17
F	14	18.12.2021	18.1	5.7	36.6	0.31	<0.1	0.18	72.3	5.9	<0.2	5.9	82	13.2	5.6	22.6	<0.2	<0.1	<0.1	49.6	2.9	<0.2	0.93	19
G	23	27.12.2021	18.1	5.9	38.1	0.37	<0.1	0.18	73.3	5.9	<0.2	5.9	80	13.2	5.6	22.9	<0.2	<0.1	<0.1	50.8	3.5	<0.2	0.97	19
H	31	04.01.2022	18.7	6.0	38.9	0.39	<0.1	0.18	74.2	6.4	<0.2	6.4	86	15.5	5.6	24.9	<0.2	<0.1	<0.1	50.9	4.2	<0.2	0.97	19
I	51	24.01.2022	19.6	6.1	39.0	0.40	<0.1	0.20	74.2	6.7	<0.2	6.4	86	15.9	5.7	25.1	<0.2	<0.1	<0.1	50.9	4.3	<0.2	0.97	19
K	66	08.02.2022	19.7	6.2	39.1	0.42	<0.1	0.22	74.2	6.7	<0.2	6.4	86	16.4	5.8	25.1	<0.2	<0.1	<0.1	51.1	4.6	<0.2	0.98	19
L	81	23.02.2022	20.5	6.3	48.4	0.50	<0.1	0.41	74.2	8.0	<0.2	6.4	86	16.4	5.8	25.2	<0.2	<0.1	<0.1	51.2	4.6	<0.2	1.0	20
M	95	09.03.2022	21.0	6.3	49.2	0.53	<0.1	0.54	74.4	9.1	<0.2	6.4	86	17.6	6.1	31.6	<0.2	<0.1	<0.1	51.4	4.8	<0.2	1.0	19
N	123	06.04.2022	21.2	6.3	49.2	0.59	<0.1	0.64	74.4	9.8	<0.2	6.4	86	17.8	6.2	32.2	<0.2	<0.1	<0.1	51.8	4.9	<0.2	1.1	21
FINAL	318	18.10.2022	21.5	6.4	49.2	0.63	<0.1	0.65	74.4	10.5	<0.2	6.4	86	17.9	6.2	33.2	<0.2	<0.1	<0.1	52.0	5.1	<0.2	1.1	21
Sample			IG_BH06_PW014											IG_BH06_PW015										
Sub-samples	Time	Date	Na	K	Ca	Mg	Sr	F	Cl	SO4	NO3	Br	Br/Cl	Na	K	Ca	Mg	Sr	F	Cl	SO4	NO3	Br	Br/Cl
	days		mg/l	mg/l	mg/l	mg/l	mg/l	mg/l	mg/l	mg/l	mg/l	mg/l		mg/l	mg/l	mg/l	mg/l	mg/l	mg/l	mg/l	mg/l	mg/l	mg/l	
Preparation		04.12.2021																						
A	1	05.12.2021	4.1	3.4	9.7	<0.2	<0.1	<0.1	20.4	2.1	<0.2	0.36	18	5.8	4.0	11.1	<0.2	<0.1	<0.1	26.0	1.3	<0.2	0.85	33
B	3	07.12.2021	7.2	5.4	17.7	<0.2	<0.1	<0.1	35.8	2.6	<0.2	0.76	21	11.3	6.3	24.1	<0.2	<0.1	<0.1	52.2	2.4	<0.2	1.9	36
C	4	08.12.2021	9.2	6.7	24.0	<0.2	<0.1	<0.1	45.9	3.7	<0.2	0.92	20	13.7	7.3	29.9	<0.2	<0.1	<0.1	57.2	4.1	<0.2	2.1	37
D	7	11.12.2021	11.1	7.4	30.5	<0.2	<0.1	<0.1	49.9	4.3	<0.2	1.2	24	18.8	8.2	43.6	0.22	<0.1	<0.1	83.8	5.5	<0.2	3.6	43
E	12	16.12.2021	14.7	8.1	36.4	<0.2	<0.1	<0.1	71.1	6.5	<0.2	1.5	21	19.6	8.3	44.5	0.25	<0.1	<0.1	103	9.2	<0.2	3.9	38
F	14	18.12.2021	14.9	9.0	39.0	0.24	<0.1	<0.1	73.6	7.4	<0.2	1.5	20	19.7	8.4	45.2	0.25	<0.1	<0.1	104	9.8	<0.2	4.5	43
G	23	27.12.2021	15.3	9.1	41.2	0.22	<0.1	<0.1	76.9	7.4	<0.2	1.5	20	19.9	8.4	46.6	0.29	<0.1	<0.1	104	9.9	<0.2	4.6	44
H	31	04.01.2022	18.4	9.3	46.6	0.25	<0.1	<0.1	82.1	8.5	<0.2	1.5	18	20.3	8.4	49.1	0.37	<0.1	<0.1	105	10.1	<0.2	4.6	44
I	51	24.01.2022	19.6	9.5	56.1	0.29	<0.1	<0.1	87.3	9.1	<0.2	1.5	17	21.2	8.4	49.4	0.31	<0.1	<0.1	107	10.4	<0.2	4.6	43
K	66	08.02.2022	19.9	9.5	60.3	0.3	<0.1	<0.1	90.9	9.3	<0.2	1.5	17	22.1	8.4	65.3	0.50	<0.1	<0.1	107	13.0	<0.2	5.2	49
L	81	23.02.2022	19.9	9.5	63.2	0.3	<0.1	<0.1	94.1	12.1	<0.2	1.5	16	22.2	8.5	67.3	0.50	<0.1	<0.1	108	13.5	<0.2	5.3	49
M	95	09.03.2022	20.0	9.5	64.0	0.44	<0.1	<0.1	105	14.6	<0.2	1.5	14	22.2	8.5	68.4	0.50	<0.1	<0.1	108	13.9	<0.2	5.3	49
N	123	06.04.2022	21.7	9.8	64.3	0.45	<0.1	<0.1	110	16.7	<0.2	1.5	14	22.2	8.6	68.4	0.50	<0.1	<0.1	108	14.0	<0.2	5.3	49
FINAL	318	18.10.2022	22.0	10.0	64.3	0.48	<0.1	<0.1	112	19.7	<0.2	1.5	13	22.3	8.6	68.9	0.50	<0.1	<0.1	108	14.1	<0.2	5.3	49
Sample			IG_BH06_PW016																					
Sub-samples	Time	Date	Na	K	Ca	Mg	Sr	F	Cl	SO4	NO3	Br	Br/Cl											
	days		mg/l	mg/l	mg/l	mg/l	mg/l	mg/l	mg/l	mg/l	mg/l	mg/l												
Preparation		04.12.2021																						
A	1	05.12.2021	5.7	3.8	12.7	<0.2	<0.1	<0.1	26.0	3.8	<0.2	0.79	30											
B	3	07.12.2021	11.2	5.7	26.4	<0.2	<0.1	<0.1	50.2	4.2	<0.2	1.4	28											
C	4	08.12.2021	13.2	6.6	31.0	<0.2	<0.1	<0.1	57.6	6.6	<0.2	1.9	33											
D	7	11.12.2021	16.2	7.3	41.7	<0.2	<0.1	<0.1	69.9	8.9	<0.2	2.8	40											
E	12	16.12.2021	21.4	8.2	53.8	<0.2	<0.1	<0.1	104	18.9	<0.2	4.0	38											
F	14	18.12.2021	21.4	8.2	54.5	<0.2	<0.1	<0.1	105	19.7	<0.2	4.1	39											
G	23	27.12.2021	21.9	8.3	55.9	<0.2	<0.1	<0.1	105	21.6	<0.2	4.2	40											
H	31	04.01.2022	22.1	8.3	58.1	<0.2	<0.1	<0.1	105	22.8	<0.2	4.2	40											
I	51	24.01.2022	22.3	8.6	59.9	0.28	<0.1	<0.1	106	23.4	<0.2	4.2	40											
K	66	08.02.2022	22.7	8.7	60.3	0.32	<0.1	<0.1	107	23.6	<0.2	4.3	40											
L	81	23.02.2022	23.3	8.7	60.6	0.35	<0.1	<0.1	107	24.1	<0.2	4.3	40											
M	95	09.03.2022	23.3	8.7	68.5	0.38	<0.1	<0.1	107	27.7	<0.2	4.3	40											
N	123	06.04.2022	23.6	8.7	70.3	0.40	<0.1	<0.1	107	29.1	<0.2	4.6	43											
FINAL	318	18.10.2022	25.5	8.7	71.1	0.45	<0.1	<0.1	107	30.1	<0.2	4.6	43											

Table B-5.2: Continued

Sample			IG_BH06_PW017											IG_BH06_PW018									
Sub-samples	Time	Date	Na	K	Ca	Mg	Sr	F	Cl	SO4	NO3	Br	Br/Cl	Na	K	Ca	Mg	Sr	F	Cl	SO4	NO3	Br	Br/Cl
	days		mg/l	mg/l	mg/l	mg/l	mg/l	mg/l	mg/l	mg/l	mg/l	mg/l		mg/l	mg/l	mg/l	mg/l	mg/l	mg/l	mg/l	mg/l	mg/l	mg/l	
Preparation		04.12.2021																					
A	1	05.12.2021	5.2	2.6	25.2	<0.2	<0.1	<0.1	52.7	4.6	<0.2	2.2	42	4.9	3.04	26.1	<0.2	<0.1	<0.1	54.2	8.9	<0.2	0.71	13
B	3	07.12.2021	9.3	3.4	49.8	0.28	<0.1	<0.1	78.8	5.8	<0.2	4.6	58	9.1	5.2	53.3	<0.2	<0.1	<0.1	87.8	12.1	<0.2	1.4	16
C	4	08.12.2021	13.8	4.5	72.6	0.34	<0.1	0.22	110	13.6	<0.2	6.5	59	12.1	6.0	73.7	<0.2	<0.1	0.11	105	28.6	<0.2	2.0	19
D	7	11.12.2021	15.1	4.6	81.8	0.34	<0.1	0.22	117	17.1	<0.2	8.0	68	13.7	6.0	93.5	<0.2	<0.1	0.11	120	39.2	<0.2	2.5	21
E	12	16.12.2021	16.1	4.8	90.4	0.34	<0.1	0.33	137	21.8	<0.2	9.7	71	16.2	6.2	105	<0.2	<0.1	0.18	153	58.4	<0.2	3.3	22
F	14	18.12.2021	19.1	4.9	97.9	0.41	<0.1	0.65	155	32.3	<0.2	12.9	83	16.6	6.2	107	<0.2	<0.1	0.18	162	68.5	<0.2	3.3	20
G	23	27.12.2021	22.0	5.1	120	0.49	<0.1	0.66	180	50.6	<0.2	13.9	77	19.6	6.2	150	<0.2	<0.1	0.27	163	132	<0.2	3.7	23
H	31	04.01.2022	22.1	5.2	121	0.50	<0.1	0.71	180	50.6	<0.2	14.2	79	19.6	6.2	161	<0.2	<0.1	0.28	163	137	<0.2	3.7	23
I	51	24.01.2022	22.2	5.2	122	0.50	<0.1	0.72	180	56.2	<0.2	14.2	79	19.7	6.2	161	0.29	<0.1	0.33	163	142	<0.2	4.1	25
K	66	08.02.2022	22.2	5.2	123	0.51	<0.1	0.72	180	70.1	<0.2	14.2	79	20.6	6.8	171	0.32	<0.1	0.39	164	157	<0.2	4.1	25
L	81	23.02.2022	23.6	5.2	130	0.59	<0.1	0.72	180	72.0	<0.2	14.2	79	20.6	7.0	168	0.34	<0.1	0.46	164	157	<0.2	4.1	25
M	95	09.03.2022	25.9	5.2	132	0.67	<0.1	0.72	180	81.3	<0.2	14.2	79	20.9	7.3	190	0.43	1.2	0.48	165	188	0.41	4.1	25
N	123	06.04.2022	25.7	5.1	133	0.72	<0.1	0.72	179	89.9	<0.2	14.2	79	21.0	7.3	191	0.47	1.5	0.48	165	218	0.47	4.1	25
FINAL	318	18.10.2022	27.2	5.2	147	0.76	<0.1	0.72	180	95.4	<0.2	14.2	79	21.4	7.3	207	0.62	1.6	0.48	165	223	0.49	4.1	25
Sample			IG_BH06_PW019											IG_BH06_PW020									
Sub-samples	Time	Date	Na	K	Ca	Mg	Sr	F	Cl	SO4	NO3	Br	Br/Cl	Na	K	Ca	Mg	Sr	F	Cl	SO4	NO3	Br	Br/Cl
	days		mg/l	mg/l	mg/l	mg/l	mg/l	mg/l	mg/l	mg/l	mg/l	mg/l		mg/l	mg/l	mg/l	mg/l	mg/l	mg/l	mg/l	mg/l	mg/l	mg/l	
Preparation		04.12.2021																					
A	1	05.12.2021	8.0	4.0	31.5	<0.2	<0.1	<0.1	64.1	8.7	<0.2	1.0	16	7.3	4.9	21.9	<0.2	<0.1	<0.1	47.1	1.0	<0.2	0.8	17
B	3	07.12.2021	12.1	5.0	54.6	<0.2	<0.1	<0.1	103	12.9	<0.2	1.2	12	11.4	6.2	38.8	<0.2	<0.1	<0.1	82.6	1.6	<0.2	1.1	13
C	4	08.12.2021	15.5	6.5	71.8	<0.2	<0.1	0.12	121	25.2	<0.2	2.1	17	15.2	8.1	53.9	<0.2	<0.1	<0.1	82.6	4.2	<0.2	1.4	17
D	7	11.12.2021	18.2	6.9	91.4	<0.2	<0.1	0.19	139	38.7	<0.2	2.6	19	18.9	9.2	75.7	0.21	<0.1	<0.1	135	4.4	<0.2	2.2	16
E	12	16.12.2021	18.4	6.9	93.3	<0.2	<0.1	0.28	176	50.5	<0.2	2.8	16	24.5	9.5	89.3	0.29	<0.1	<0.1	192	7.5	<0.2	2.2	11
F	14	18.12.2021	19.2	6.9	100	<0.2	<0.1	0.36	177	64.9	<0.2	2.9	16	24.8	9.9	94.8	0.29	<0.1	<0.1	197	8.1	<0.2	2.4	12
G	23	27.12.2021	22.0	7.1	137	0.22	<0.1	0.47	182	108	<0.2	3.1	17	24.8	9.9	95.7	0.29	<0.1	<0.1	198	8.4	<0.2	2.6	13
H	31	04.01.2022	22.0	7.1	143	0.35	<0.1	0.51	183	140	<0.2	3.2	17	24.6	9.9	96.8	0.29	<0.1	<0.1	200	8.5	<0.2	3.1	16
I	51	24.01.2022	22.0	7.1	151	0.32	<0.1	0.63	184	145	<0.2	3.2	17	24.7	9.9	102	0.34	<0.1	<0.1	200	9.2	<0.2	3.4	17
K	66	08.02.2022	22.1	7.1	154	0.37	<0.1	0.64	184	153	<0.2	3.2	17	25.8	10.0	105	0.30	<0.1	<0.1	203	10.4	<0.2	3.4	17
L	81	23.02.2022	22.4	7.1	154	0.37	<0.1	0.65	186	155	<0.2	3.2	17	26.0	10.4	106	0.37	<0.1	<0.1	207	10.7	<0.2	3.4	16
M	95	09.03.2022	25.0	7.7	180	0.40	<0.1	0.66	186	177	0.78	3.2	17	26.0	10.1	102	0.39	<0.1	<0.1	208	10.9	<0.2	3.4	16
N	123	06.04.2022	25.8	7.7	182	0.46	<0.1	0.67	186	178	0.81	3.2	17	28.9	10.5	108	0.42	<0.1	<0.1	208	11.2	<0.2	3.4	16
FINAL	318	18.10.2022	26.0	7.7	182	0.49	<0.1	0.67	186	187	0.82	3.2	17	32.3	10.5	110	0.49	<0.1	<0.1	210	12.1	<0.2	3.4	16
Sample			IG_BH06_AR010											IG_BH06_AR013									
Sub-samples	Time	Date	Na	K	Ca	Mg	Sr	F	Cl	SO4	NO3	Br	Br/Cl	Na	K	Ca	Mg	Sr	F	Cl	SO4	NO3	Br	Br/Cl
	days		mg/l	mg/l	mg/l	mg/l	mg/l	mg/l	mg/l	mg/l	mg/l	mg/l		mg/l	mg/l	mg/l	mg/l	mg/l	mg/l	mg/l	mg/l	mg/l	mg/l	
Preparation		14.03.2022																					
A	1	15.03.2022	6.46	3.30	10.8	0.23	<0.1	<0.1	8.33	2.56	1.11	0.13	16	4.65	2.18	8.92	<0.2	<0.1	<0.1	11.5	0.73	0.34	0.52	45
B	3	17.03.2022	9.60	3.33	16.0	0.27	<0.1	<0.1	15.0	5.49	1.19	0.43	29	8.13	2.37	14.6	<0.2	<0.1	0.19	23.3	1.48	0.34	0.62	27
C	4	18.03.2022	9.76	3.35	16.3	0.27	<0.1	0.13	15.7	6.02	1.19	0.48	31	8.26	2.40	15.0	<0.2	<0.1	0.22	24.5	1.55	0.35	0.64	26
D	7	21.03.2022	9.83	3.37	16.3	0.30	<0.1	0.15	16.0	6.07	1.21	0.50	31	9.51	2.41	17.1	<0.2	<0.1	0.34	28.7	1.60	0.35	0.68	24
E	12	26.03.2022	10.6	3.35	17.9	0.30	<0.1	0.17	18.3	7.70	1.22	0.56	31	10.1	2.52	17.6	<0.2	<0.1	0.37	31.3	1.85	0.34	0.72	23
F	14	28.03.2022	11.4	3.37	19.0	0.30	<0.1	0.21	18.7	8.72	1.22	0.65	35	10.7	2.55	19.7	<0.2	<0.1	0.44	32.6	2.00	0.35	0.82	25
G	22	05.04.2022	14.5	3.42	21.9	0.30	<0.1	0.21	20.4	12.2	1.37	0.66	32	11.9	2.58	21.4	<0.2	<0.1	0.53	35.6	2.63	0.35	0.83	23
H	30	13.04.2022	14.6	3.45	22.1	0.30	<0.1	0.21	20.7	13.1	1.42	0.66	32	12.8	2.66	23.4	<0.2	<0.1	0.55	37.0	3.18	0.35	0.93	25
I	50	03.05.2022	16.6	3.60	25.4	0.30	<0.1	0.23	21.0	15.1	1.45	0.66	31	13.8	2.65	24.3	<0.2	<0.1	0.69	37.5	4.01	0.35	0.93	25
K	63	16.05.2022	16.7	3.65	26.6	0.30	<0.1	0.25	21.1	15.3	1.45	0.66	31	14.2	2.67	26.3	<0.2	<0.1	0.73	37.7	4.58	0.35	0.94	25
L	78	31.05.2022	17.2	3.67	28.1	0.30	<0.1	0.28	21.4	16.5	1.85	0.66	31	14.6	2.67	27.2	<0.2	<0.1	0.83	38.9	4.79	0.35	0.95	24
M	92	14.06.2022	17.6	3.68	28.1	0.30	<0.1	0.28	21.5	17.3	1.89	0.66	31	15.4	2.77	28.9	<0.2	<0.1	0.89	39.0	5.46	0.35	0.95	24
N	120	12.07.2022	18.2	3.68	29.4	0.30	<0.1	0.28	21.5	20.3	1.90	0.66	31	15.7	2.77	29.3	<0.2	<0.1	0.91	39.6	6.30	0.35	0.96	24
FINAL	253	22.11.2022	18.8	3.68	32.9	0.30	<0.1	0.28	21.5	21.0	1.92	0.66	31	16.1	2.77	33.5	<0.2	<0.1	0.92	39.6	6.96	0.35	0.96	24

Table B-5.2: Continued

Sample			IG_BH06_AR019											IG_BH06_AR020										
Sub-samples	Time	Date	Na	K	Ca	Mg	Sr	F	Cl	SO4	NO3	Br	Br/Cl	Na	K	Ca	Mg	Sr	F	Cl	SO4	NO3	Br	Br/Cl
	days		mg/l	mg/l	mg/l	mg/l	mg/l	mg/l	mg/l	mg/l	mg/l	mg/l		mg/l	mg/l	mg/l	mg/l	mg/l	mg/l	mg/l	mg/l	mg/l	mg/l	
Preparation		14.03.2022																						
A	1	15.03.2022	4.56	2.47	7.51	<0.2	<0.1	<0.1	9.63	1.14	<0.2	0.34	35	5.02	1.73	11.8	0.32	<0.1	0.13	10.7	0.73	0.23	0.33	31
B	3	17.03.2022	7.00	3.04	11.6	<0.2	<0.1	<0.1	11.2	1.41	<0.2	0.51	46	6.05	1.77	12.8	0.34	<0.1	0.15	12.8	1.83	0.25	0.34	27
C	4	18.03.2022	7.29	3.14	11.7	<0.2	<0.1	<0.1	11.4	1.57	<0.2	0.55	48	8.04	2.65	15.1	0.35	<0.1	0.16	16.0	1.84	0.28	0.46	29
D	7	21.03.2022	7.36	3.19	11.7	<0.2	<0.1	<0.1	16.2	1.76	<0.2	0.58	36	8.05	2.68	15.3	0.36	<0.1	0.16	16.9	1.92	0.29	0.51	30
E	12	26.03.2022	8.26	3.23	13.6	<0.2	<0.1	<0.1	18.5	2.13	<0.2	0.61	33	8.36	2.72	15.9	0.36	<0.1	0.17	17.3	2.04	0.31	0.64	37
F	14	28.03.2022	9.07	3.46	14.5	<0.2	<0.1	<0.1	20.0	2.37	<0.2	0.75	38	8.72	2.75	16.7	0.37	<0.1	0.18	18.1	2.23	0.32	0.65	36
G	22	05.04.2022	10.2	3.82	16.2	<0.2	<0.1	<0.1	21.6	3.09	<0.2	0.76	35	9.55	2.77	17.2	0.37	<0.1	0.19	18.5	2.58	0.34	0.64	35
H	30	13.04.2022	11.5	4.38	17.9	0.25	<0.1	0.26	22.9	3.95	0.42	0.77	34	12.3	3.02	20.1	0.37	<0.1	0.29	21.0	2.67	0.39	0.73	35
I	50	03.05.2022	12.8	4.87	20.3	0.28	<0.1	0.30	23.1	4.84	0.42	0.79	34	12.7	3.06	20.4	0.37	<0.1	0.30	21.1	3.41	0.39	0.77	36
K	63	16.05.2022	13.2	4.91	21.4	0.28	<0.1	0.37	23.3	5.37	0.42	0.80	34	12.8	3.12	20.6	0.37	<0.1	0.30	21.1	4.30	0.40	0.80	38
L	78	31.05.2022	13.3	4.95	21.7	0.28	<0.1	0.37	23.3	5.86	0.42	0.82	35	13.7	3.18	20.6	0.37	<0.1	0.30	21.2	4.82	0.41	0.80	38
M	92	14.06.2022	13.7	5.08	21.9	0.28	<0.1	0.37	23.4	6.14	0.43	0.83	35	13.7	3.20	20.8	0.37	<0.1	0.30	21.2	5.03	0.44	0.80	38
N	120	12.07.2022	14.4	5.34	23.0	0.28	<0.1	0.37	23.6	6.68	0.43	0.83	35	14.6	3.28	21.9	0.37	<0.1	0.30	21.2	6.13	0.44	0.80	38
FINAL	253	22.11.2022	15.9	5.54	25.6	0.28	<0.1	0.37	23.7	7.05	0.43	0.83	35	14.9	3.31	21.9	0.37	<0.1	0.30	21.2	7.41	0.44	0.80	38
Sample			IG_BH06_AR027																					
Sub-samples	Time	Date	Na	K	Ca	Mg	Sr	F	Cl	SO4	NO3	Br	Br/Cl											
	days		mg/l	mg/l	mg/l	mg/l	mg/l	mg/l	mg/l	mg/l	mg/l	mg/l												
Preparation		14.03.2022																						
A	1	15.03.2022	4.63	3.64	11.8	<0.2	<0.1	<0.1	15.4	0.71	<0.2	0.31	20											
B	3	17.03.2022	6.52	4.12	20.1	<0.2	<0.1	<0.1	22.0	1.89	<0.2	0.43	20											
C	4	18.03.2022	8.39	5.17	20.3	<0.2	<0.1	<0.1	31.1	1.98	<0.2	0.76	24											
D	7	21.03.2022	8.83	5.41	20.7	<0.2	<0.1	<0.1	31.4	2.14	<0.2	0.78	25											
E	12	26.03.2022	11.1	5.83	25.7	<0.2	<0.1	0.11	41.6	2.23	<0.2	0.84	20											
F	14	28.03.2022	11.4	5.96	27.0	<0.2	<0.1	0.15	42.4	2.72	<0.2	0.97	23											
G	22	05.04.2022	12.1	5.97	27.9	<0.2	<0.1	0.23	43.5	3.03	<0.2	0.98	23											
H	30	13.04.2022	13.0	6.24	30.4	<0.2	<0.1	0.28	44.0	3.44	0.29	1.04	24											
I	50	03.05.2022	13.7	6.28	31.5	<0.2	<0.1	0.33	44.4	4.82	0.31	1.04	23											
K	63	16.05.2022	13.8	6.35	31.9	<0.2	0.10	0.38	44.7	5.19	0.33	1.06	24											
L	78	31.05.2022	14.1	6.37	32.0	<0.2	0.10	0.38	45.1	5.65	0.48	1.07	24											
M	92	14.06.2022	14.1	6.43	32.8	<0.2	0.11	0.39	45.4	5.92	0.54	1.07	24											
N	120	12.07.2022	14.7	6.48	33.7	<0.2	0.12	0.42	45.6	5.96	0.57	1.07	23											
FINAL	253	22.11.2022	15.8	6.58	37.2	<0.2	0.20	0.44	45.6	6.19	0.59	1.07	23											
Sample			IG_BH06_AR038											IG_BH06_AR039										
Sub-samples	Time	Date	Na	K	Ca	Mg	Sr	F	Cl	SO4	NO3	Br	Br/Cl	Na	K	Ca	Mg	Sr	F	Cl	SO4	NO3	Br	Br/Cl
	days		mg/l	mg/l	mg/l	mg/l	mg/l	mg/l	mg/l	mg/l	mg/l	mg/l		mg/l	mg/l	mg/l	mg/l	mg/l	mg/l	mg/l	mg/l	mg/l	mg/l	
Preparation		14.03.2022																						
A	1	15.03.2022	5.91	4.30	9.50	<0.2	<0.1	<0.1	4.34	1.59	<0.2	<0,05		4.72	3.19	7.13	<0.2	<0.1	<0.1	7.81	2.18	<0.2	0.11	14
B	3	17.03.2022	7.10	4.33	9.63	<0.2	<0.1	<0.1	6.00	1.72	<0.2	<0,05		8.85	4.41	13.1	<0.2	<0.1	<0.1	18.3	4.78	<0.2	0.28	15
C	4	18.03.2022	7.13	4.41	9.77	<0.2	<0.1	<0.1	6.10	1.85	<0.2	0.09	15	9.90	4.79	14.2	0.22	<0.1	<0.1	21.1	5.62	<0.2	0.40	19
D	7	21.03.2022	11.5	6.39	13.3	<0.2	<0.1	<0.1	9.22	3.59	<0.2	0.16	17	11.7	5.20	17.4	0.27	<0.1	<0.1	26.1	7.79	<0.2	0.41	16
E	12	26.03.2022	11.6	6.44	13.6	<0.2	<0.1	<0.1	9.63	3.78	<0.2	0.25	26	15.5	5.87	21.8	0.32	0.12	<0.1	32.2	11.7	<0.2	0.52	16
F	14	28.03.2022	12.7	6.55	15.4	<0.2	<0.1	<0.1	11.7	4.12	<0.2	0.27	23	16.4	6.01	23.5	0.33	0.14	<0.1	32.7	15.7	<0.2	0.74	23
G	22	05.04.2022	13.6	6.58	19.6	0.20	<0,1	<0.1	12.2	4.28	<0.2	0.33	27	16.7	6.06	23.6	0.33	0.15	<0.1	32.9	15.8	0.21	0.75	23
H	30	13.04.2022	16.6	8.17	22.8	0.31	0.15	<0.1	14.7	5.58	<0.2	0.37	25	18.7	6.13	26.9	0.34	0.17	<0.1	33.0	17.6	0.22	0.77	23
I	50	03.05.2022	20.9	8.22	23.3	0.42	0.23	<0.1	15.4	8.43	<0.2	0.37	24	19.6	6.24	27.5	0.35	0.22	<0.1	33.0	18.0	0.30	0.81	25
K	63	16.05.2022	22.1	8.28	23.6	0.46	0.25	<0.1	15.6	11.2	<0.2	0.37	24	20.3	6.31	28.3	0.35	0.22	<0.1	34.3	19.8	0.32	0.81	24
L	78	31.05.2022	22.1	8.35	23.9	0.47	0.29	<0.1	16.0	11.5	<0.2	0.37	23	22.0	6.52	30.9	0.36	0.23	<0.1	35.0	21.4	0.34	0.81	23
M	92	14.06.2022	22.7	8.47	24.1	0.49	0.32	<0.1	16.1	11.8	<0.2	0.37	23	22.2	6.58	31.9	0.36	0.24	<0.1	35.2	22.0	0.34	0.81	23
N	120	12.07.2022	22.9	8.52	24.1	0.49	0.34	<0.1	16.3	12.0	<0.2	0.37	23	22.6	6.65	31.9	0.36	0.24	<0.1	35.2	23.0	0.34	0.81	23
FINAL	253	22.11.2022	25.0	9.06	31.1	0.49	0.34	<0.1	16.3	12.9	<0.2	0.37	23	22.6	6.78	32.1	0.36	0.29	<0.1	35.2	23.4	0.34	0.81	23

Table B-5.2: Continued

Sample			IG_BH06_AR045											IG_BH06_AR049										
Sub-samples	Time	Date	Na	K	Ca	Mg	Sr	F	Cl	SO4	NO3	Br	Br/Cl	Na	K	Ca	Mg	Sr	F	Cl	SO4	NO3	Br	Br/Cl
	days		mg/l	mg/l	mg/l	mg/l	mg/l	mg/l	mg/l	mg/l	mg/l	mg/l		mg/l	mg/l	mg/l	mg/l	mg/l	mg/l	mg/l	mg/l	mg/l	mg/l	
Preparation		14.03.2022																						
A	1	15.03.2022	7.48	5.52	23.1	0.23	0.15	<0.1	31.5	16.8	<0.2	0.95	30	7.20	2.72	19.0	<0.2	0.14	<0.1	29.1	2.12	0.41	1.50	52
B	3	17.03.2022	11.1	6.75	39.5	0.32	0.26	<0.1	58.6	31.1	<0.2	1.87	32	11.9	3.38	31.5	0.21	0.25	0.15	56.5	3.75	0.53	2.79	49
C	4	18.03.2022	12.7	7.43	45.7	0.36	0.30	0.18	68.6	37.9	<0.2	2.17	32	12.2	3.49	31.8	0.25	0.26	0.18	58.2	3.93	0.58	2.92	50
D	7	21.03.2022	18.7	8.85	71.4	0.49	0.38	0.20	99.4	58.7	0.28	2.32	23	15.1	4.03	40.9	0.31	0.30	0.25	68.3	5.46	0.84	3.09	45
E	12	26.03.2022	20.6	8.92	87.3	0.51	0.52	0.23	117	86.4	0.37	3.45	30	18.3	4.09	49.0	0.40	0.34	0.26	83.3	7.99	1.01	4.35	52
F	14	28.03.2022	21.1	8.98	89.8	0.52	0.55	0.23	117	90.8	0.39	3.54	30	18.5	4.32	49.3	0.37	0.40	0.26	84.4	8.27	1.03	4.81	57
G	22	05.04.2022	23.2	9.77	105.8	0.54	0.59	0.24	125	116	0.45	3.72	30	20.5	4.44	55.2	0.42	0.46	0.28	90.9	9.65	1.05	4.89	54
H	30	13.04.2022	24.8	10.1	121.5	0.55	0.72	0.29	126	142	0.45	3.94	31	22.3	4.48	60.1	0.49	0.56	0.32	92.7	12.8	1.06	4.91	53
I	50	03.05.2022	25.8	10.3	133.4	0.57	0.83	0.29	132	183	0.49	4.07	31	22.6	4.52	60.2	0.49	0.56	0.46	93.9	16.1	1.07	4.97	53
K	63	16.05.2022	28.1	10.6	159.1	0.62	0.85	0.29	138	227	0.57	4.20	31	22.9	4.60	60.3	0.49	0.56	0.52	94.6	16.6	1.08	5.01	53
L	78	31.05.2022	28.3	11.0	166.1	0.69	0.91	0.31	139	257	0.61	4.46	32	23.3	4.61	60.3	0.49	0.60	0.55	97.2	17.1	1.10	5.03	52
M	92	14.06.2022	28.9	11.0	175.1	0.70	0.95	0.32	142	274	0.64	4.47	32	24.1	4.68	61.3	0.49	0.62	0.61	99.9	17.3	1.10	5.03	50
N	120	12.07.2022	29.2	11.0	184.1	0.70	0.98	0.32	143	283	0.69	4.51	32	24.4	4.73	62.9	0.49	0.62	0.67	100	17.3	1.10	5.03	50
FINAL	253	22.11.2022	29.5	11.0	202	0.70	0.98	0.32	144	335	0.70	4.53	32	25.5	4.75	63.3	0.49	0.62	0.68	100	19.3	1.10	5.03	50
Sample			IG_BH06_AR064											IG_BH06_DG003										
Sub-samples	Time	Date	Na	K	Ca	Mg	Sr	F	Cl	SO4	NO3	Br	Br/Cl	Na	K	Ca	Mg	Sr	F	Cl	SO4	NO3	Br	Br/Cl
	days		mg/l	mg/l	mg/l	mg/l	mg/l	mg/l	mg/l	mg/l	mg/l	mg/l		mg/l	mg/l	mg/l	mg/l	mg/l	mg/l	mg/l	mg/l	mg/l	mg/l	
Preparation		14.03.2022																						
A	1	15.03.2022	11.7	5.26	30.1	0.30	0.20	<0,1	57.6	1.83	0.20	1.07	19	5.53	4.70	13.3	<0,2	<0,1	<0.1	19.2	2.22	<0.2	1.12	58
B	3	17.03.2022	15.4	6.66	40.1	0.30	0.24	<0,1	84.6	2.32	0.29	1.56	18	7.58	6.12	18.8	0.24	<0,1	<0.1	30.2	3.40	<0.2	1.86	62
C	4	18.03.2022	17.1	7.01	44.2	0.34	0.27	<0,1	95.7	2.65	0.41	1.61	17	8.74	6.65	22.0	0.29	<0,1	<0.1	37.0	4.03	<0.2	2.20	59
D	7	21.03.2022	20.8	8.32	53.8	0.39	0.30	<0,1	109	3.78	0.44	1.93	18	10.6	7.54	26.5	0.35	0.13	<0.1	44.9	4.60	<0.2	2.68	60
E	12	26.03.2022	25.2	8.37	64.9	0.41	0.39	0.20	139	4.75	0.45	2.40	17	13.4	8.86	33.8	0.42	0.21	<0.1	58.5	6.52	<0.2	3.84	66
F	14	28.03.2022	25.5	8.48	66.8	0.41	0.40	0.25	141	4.96	0.52	2.61	19	13.6	8.98	34.0	0.42	0.22	<0.1	58.5	6.73	<0.2	3.93	67
G	22	05.04.2022	27.7	9.30	72.3	0.46	0.42	0.28	145	5.72	0.55	2.78	19	14.2	9.2	37.0	0.43	0.28	<0.1	61.2	7.77	<0.2	4.01	66
H	30	13.04.2022	33.5	9.87	82.9	0.53	0.46	0.33	158	7.58	0.68	2.87	18	15.9	9.72	44.9	0.45	0.29	<0.1	62.1	9.79	<0.2	4.16	67
I	50	03.05.2022	33.9	9.90	84.4	0.54	0.48	0.37	161	11.0	0.70	2.92	18	16.2	9.81	45.2	0.47	0.29	<0.1	63.1	11.1	<0.2	4.36	69
K	63	16.05.2022	35.0	10.1	85.2	0.54	0.50	0.41	162	13.7	0.74	2.94	18	17.8	10.3	51.1	0.48	0.32	<0.1	63.5	11.2	<0.2	4.98	78
L	78	31.05.2022	35.5	10.3	85.8	0.58	0.50	0.52	163	13.8	0.85	3.06	19	18.1	10.4	51.3	0.50	0.34	<0.1	65.1	13.6	<0.2	5.09	78
M	92	14.06.2022	35.7	10.4	86.0	0.62	0.51	0.59	164	14.2	0.97	3.15	19	18.1	10.6	52.4	0.52	0.35	<0.1	65.6	14.2	<0.2	5.09	78
N	120	12.07.2022	36.9	10.4	86.4	0.64	0.51	0.66	167	14.3	1.1	3.22	19	18.6	10.7	53.9	0.53	0.37	<0.1	66.8	14.6	<0.2	5.09	76
FINAL	253	22.11.2022	37.1	10.4	87.0	0.67	0.51	0.68	167	15.2	1.1	3.39	20	18.9	10.8	53.9	0.57	0.56	<0.1	66.8	17.1	<0.2	5.09	76

APPENDIX B-6

Out-gassing Experiments: Raw Data

Table B-6.1: Analytical detection limits and analytical errors of gases determined by GC-FID and GC-WLD

Gas species	Analytical method	Detection Limit	Analytical error
Hydrocarbons		vpm	%
Methane (CH_4)	GC-FID	1.0	3
Ethane (C_2H_6)	GC-FID	1.0	5
Propane (C_3H_8)	GC-FID	1.0	5
i-Butane (i-C_4H_{10})	GC-FID	1.0	5
n-Butane (n-C_4H_{10})	GC-FID	1.0	5
i-Pentane (i-C_5H_{12})	GC-FID	1.0	5
n-Butane (n-C_5H_{12})	GC-FID	1.0	5
Ethene (C_2H_4)	GC-FID	1.0	5
Propene (C_3H_6)	GC-FID	1.0	5
Butene (C_4H_8)	GC-FID	1.0	5
Normal Gases		Vol. %	%
Nitrogen (N_2)	GC-WLD	0.01	2
Oxygen (O_2)	GC-WLD	0.01	2
Carbon dioxide (CO_2)	GC-WLD	0.01	3
Argon (Ar)	GC-WLD	0.01	5
Helium (He)	GC-WLD	0.01	5
Hydrogen (H_2)	GC-WLD	0.01	3

Table B-6.2: Composition of air used for correction (Ozima & Podosek, 2002)

Gas species		Unit	Conc. In air
Oxygen	O_2	%	20.94
Nitrogen	N_2	%	78.08
Carbon dioxide	CO_2	%	0.038
Methane	CH_4	%	0.000176
Helium	He	%	0.000524
Argon	Ar	%	0.934
Krypton	Kr	%	0.000114
Neon	Ne	%	0.00182
Xenon	Xe	%	8.70E-06
Atomic abundances of NG isotopes			
^{36}Ar		%	0.3364
^{40}Ar		%	99.6
^{3}He		%	0.000138
^{4}He		%	99.999862
^{84}Kr		%	57
^{20}Ne		%	90.5
^{22}Ne		%	9.23
^{132}Xe		%	26.9

Table B-6.3: Raw Data of gas chromatographic measurements

Labor-Nr.		**378520**	**378525**	**378521**	**378522**	**378523**	**378524**
		IG_BH06_ DG001	**IG_BH06_ NG001**	**IG_BH06_ DG002**	**IG_BH06_ DG004**	**IG_BH06_ DG005**	**IG_BH06_ DG006**
Depth	**mbgs**	**510,2**	**512,5**	**620,9**	**802,4**	**842,7**	**936,4**
Sampling date		**08.10.2021**	**09.10.2021**	**19.10.2021**	**26.10.2021**	**29.10.2021**	**02.11.2021**
Sampling time		**22:37**	**07:23**	**04:35**	**22:30**	**11:40**	**11:54**
Temperatur Lab	°C	22	22	22	22	22	22
Final Pressure	mbar	917	36	35	33	36	34
Void Volume	ml	257		221	212	298	303
Helium	Vol. %	< 0.01	5	4,2	3,6	22,4	3,7
Argon	Vol. %	0,9	1,5	2,2	2,8	2,2	3,3
Oxygen	Vol. %	18,4	1,5	0,7	0,7	0,3	0,3
Nitrogen	Vol. %	79	73,2	84,9	91,3	62,8	91,3
Carbon dioxide	Vol. %	< 0.01	0,07	0,03	< 0.01	0,04	0,05
Hydrogen	Vol. %	< 0.01	17,2	4,9	2	12,5	1,5
Methane	vpm	84	10478	18300	740	6050	2740
Ethane	vpm	1	87	130	20	194	62
Propane	vpm	< 1	10	13	6	27	10
i-Butane	vpm	< 1	9	3	1	4	2
n-Butane	vpm	< 1	9	8	5	10	4
i-Pentane	vpm	< 1	< 1	< 1	< 1	< 1	< 1
n-Pentane	vpm	< 1	< 1	< 1	< 1	< 1	< 1
Ethene	vpm	< 1	< 1	6	11	14	14
Propene	vpm	< 1	5	9	10	7	8
1-Butene	vpm	-		8	11	11	11
SUM	Vol.%	98,3	99,5	98,8	100,5	100,9	100,4
Ratios							
C1/(C2+)		84	87	103	12	23	25
N2/Ar		88	49	39	33	29	28

Table B-6.4: Experimental data of out-gassing experiments (non-inert (DG) gases)

Sample		**IG_BH06_ DG001**	**IG_BH06_ NG001**	**IG_BH06_ DG002**	**IG_BH06_ DG004**	**IG_BH06_ DG005**	**IG_BH06_ DG006**
Depth a.b.	**mbgs**	**510,2**	**512,5**	**620,9**	**802,4**	**842,7**	**936,4**
Lab Nr.		**378520**	**378525**	**378521**	**378522**	**378523**	**378524**
Temperature measurement	°C	22	22	22	22	22	23
	K	295	295	295	295	295	296
Pressure (start)	mbar	0	0	0	0	0	0
Temperature set-up	°C	16	16	16	16	16	17
	K	289	289	289	289	289	290
Pressure (start) corrected STP	mbar	0,0	0,0	0,0	0,0	0,0	0,0
He Volume (start)	ml	0,00	0,00	0,00	0,00	0,00	0,00
Pressure (end)	mbar	917	36	35	33	36	34
Water vapour pressure (22°C)	mbar	24,8	24,8	24,8	24,8	24,8	24,8
Pressure end (without P(WV))		892,2	11,2	10,2	8,2	11,2	9,2
Volume corrected for WV	ml	229,5	2,5	2,2	2,4	3,4	2,5
Air contamination	%	87,9	7,2	3,3	3,3	1,4	1,4
Pressure end corrected for air cont.	**mbar**	**108,3**	**10,4**	**9,9**	**7,9**	**11,0**	**9,1**
Pressure end corr STP	**mbar**	**100,2**	**9,6**	**9,1**	**7,3**	**10,2**	**8,4**
Void Volume	ml	257	221	212	298	303	276
Water content	wt.%	0,18	0,22	0,21	0,18	0,23	0,18
PW volume	ml	3,01	3,76	3,62	2,66	3,39	2,82
Ratio V(PW):V(void)		0,0117	0,0170	0,0171	0,0090	0,0112	0,0102
% of PW of tot Vol	%	1,2	1,7	1,7	0,9	1,1	1,0
Gas volume corrected WV, air	ml	27,9	2,3	2,1	2,4	3,3	2,5
Gas volume corrected STP	ml	25,8	2,1	1,9	2,2	3,1	2,3

Table B-6.5: Noble gas analyses; Inlet parameter and analytical raw data

						Inlet Parameters			
Sample	**Sample ID**	**date (meas.)**	**T (°C)**	**T(K)**	**ΔT (K)**	**P(mbar)**	**Δp (mbar)**	**V (cc)**	**ΔV (cc)**
IG_BH06_NG001	HI_378525	08.08.2023	23,01	296,16	0,1	33,55	0,067	36,316	0,04
IG_BH06_NG003	HI_378526	08.08.2023	22,72	295,87	0,1	34,96	0,070	36,316	0,04
IG_BH06_NG005	HI_378527	07.08.2023	22,86	296,01	0,1	34,26	0,069	36,316	0,04
IG_BH06_NG007	HI_378528	03.08.2023	23,32	296,47	0,1	33,78	0,068	36,316	0,04
IG_BH06_NG009	HI_378529	01.08.2023	22,80	295,95	0,1	36,80	0,074	36,316	0,04

		Isotopes abs. amounts [ccSTP]							
Sample	**Sample ID**	^{3}He	err abs.	^{4}He	err abs.	^{20}Ne	err abs.	^{22}Ne	err abs.
IG_BH06_NG001	HI_378525	4,19E-10	6,86E-12	1,30E-02	8,34E-05	6,67E-07	3,13E-09	6,93E-08	4,78E-10
IG_BH06_NG003	HI_378526	1,46E-10	3,55E-12	5,09E-03	3,35E-05	5,63E-07	2,67E-09	5,77E-08	4,63E-10
IG_BH06_NG005	HI_378527	1,85E-10	3,79E-12	6,29E-03	4,13E-05	7,51E-07	3,52E-09	7,72E-08	5,04E-10
IG_BH06_NG007	HI_378528	4,31E-10	6,94E-12	1,37E-02	8,87E-05	5,72E-07	2,70E-09	5,89E-08	4,49E-10
IG_BH06_NG009	HI_378529	2,24E-10	4,25E-12	7,02E-03	4,57E-05	5,62E-07	2,66E-09	5,82E-08	4,43E-10

		Isotopes abs. amounts [ccSTP]							
Sample	**Sample ID**	^{36}Ar	err abs.	^{40} Ar	err abs.	^{84}Kr	err abs.	^{132}Xe	err abs.
IG_BH06_NG001	HI_378525	2,19E-05	9,49E-07	7,42E-03	2,24E-05	1,90E-06	2,59E-08	2,87E-07	2,97E-09
IG_BH06_NG003	HI_378526	1,73E-05	8,39E-07	6,07E-03	1,83E-05	1,54E-06	2,01E-08	2,39E-07	2,41E-09
IG_BH06_NG005	HI_378527	2,24E-05	9,58E-07	7,88E-03	2,39E-05	1,86E-06	2,46E-08	2,74E-07	2,79E-09
IG_BH06_NG007	HI_378528	1,81E-05	8,58E-07	9,61E-03	2,97E-05	1,66E-06	2,16E-08	2,51E-07	2,51E-09
IG_BH06_NG009	HI_378529	8,27E-06	6,80E-07	5,09E-03	1,56E-05	7,56E-07	1,03E-08	1,22E-07	1,20E-09

		Isotope ratios			
Sample	**Sample ID**	22/20Ne	err abs.	36/40Ar	err abs.
IG_BH06_NG001	HI_378525	1,03E-01	1,65E-04	2,82E-03	1,16E-04
IG_BH06_NG003	HI_378526	1,02E-01	3,03E-04	2,80E-03	1,09E-04
IG_BH06_NG005	HI_378527	1,03E-01	1,20E-04	2,81E-03	1,08E-04
IG_BH06_NG007	HI_378528	1,03E-01	1,40E-04	1,88E-03	7,40E-05
IG_BH06_NG009	HI_378529	1,03E-01	1,36E-04	1,71E-03	6,88E-05

Table B-6.6: Experimental data of out-gassing experiments (noble gases (NG))

Sample		IG_BH06_NG001	IG_BH06_NG003	IG_BH06_NG005	IG_BH06_NG007	IG_BH06_NG009
Depth a.b.	**m**	**512,5**	**623,6**	**735,6**	**846,9**	**939,6**
Lab Nr.		**378525**	**378526**	**378527**	**378528**	**378529**
Temperature measurement	°C	23,01	22,72	22,86	23,32	22,8
	K	296,01	295,72	295,86	296,32	295,8
Pressure (start)	mbar	0	0	0	0	0
Temperature set-up	°C	16	16	16	16	16
	K	289	289	289	289	289
Pressure (start) corrected STP	mbar	0	0	0	0	0
N2 Volume (start)	ml	0	0	0	0	0
Pressure (end)	mbar	33,55	34,96	34,26	33,78	36,8
Water vapour pressure (P(WV))	mbar	28	28	28	29	28
Pressure end (without P(WV))	mbar	5,5	7,4	6,5	5,2	9,1
Volume corrected for WV	ml	1,22	1,98	1,30	1,34	2,35
Void Volume	ml	221	266	199	256	257
Water content	wt.%	0,22	0,20	0,09	0,20	0,17
PW volume	ml	3,76	3,19	1,58	3,32	2,69
Ratio V(PW):V(void)		0,02	0,01	0,01	0,01	0,01
% of PW of tot Vol	%	1,67	1,18	0,79	1,28	1,04

APPENDIX C

Error Calculations

APPENDIX C-1

Gravimetric Water Content

The water content is calculated according to $WC_{grav} = \frac{m_{pw}}{m_{core,wet}}$

Where WC_{grav} = gravimetric water content, m_{pw} = mass of pore water, $m_{core,wet}$ = mass of the wet core sample

Error calculation after Gaussian error propagation

$$\sigma(WC_{grav}) = \sqrt{\left(dWC_{grav}dm_{PW} \times \sigma(m_{PW})\right)^2 + \left(dWC_{grav}dm_{core,wet} \times \sigma(m_{core,wet})\right)^2}$$

Analytical errors (error of measurement)

$s(m_{pw})$ = difference between $m_{core,dry\ surface}$ before and after drying + 0.05 g (=variations at end of drying); The constant of 0.05 g is the empirically derived uncertainty associated to the drying process of the surface, i.e. loss of water from the core surface.

$s(m_{core,wet})$ = difference between $m_{core,dry\ surface}$ before and after experiment

Both uncertainties include the mass difference of the individual cores before and after the experiments (cf. Appendix II).

Derivations

$$dWC_{grav}dm_{pw} = \frac{100}{m_{core,wet}}$$

$$dWC_{grav}dm_{core,wet} = \frac{-100 \times m_{pw}}{(m_{core,wet})^2}$$

APPENDIX C-2

Water Loss Porosity

The water-loss (connected porosity), ϕ_{WL}, is calculated according to

$$\phi_{WL} = WC_{wet} \times \frac{\rho_{bulk,wet}}{\rho_{water}}$$

where WC_{wet} is the water content based on the wet weight of the rock sample and $\rho_{bulk,wet}$ the bulk wet density of the rock. The density of water, ρ_{water}, is assumed to be 1 g/cm^3.

The conversion of the formula leads to

$$\phi_{WL} = \frac{m_{pw} \times 100}{r^2 \times h \times \pi \times \rho_{water}}$$

where r = radius of the core pieces, h = height of the core.

Error calculation after Gaussian error propagation

$$\sigma(\phi_{WL}) = \sqrt{\left(d\phi_{WL}dm_{PW} \times \sigma(m_{PW})\right)^2 + \left(d\phi_{WL}dr \times \sigma(r)\right)^2 + \left(d\phi_{WL}dh \times \sigma(h)\right)^2 + \left(d\phi_{WL}d\rho_{water} \times \sigma(\rho_{water})\right)^2}$$

Analytical errors (error of measurement)

s(m_{pw}) = difference between $m_{core,dry\ surface}$ before and after drying + 0.05 g (=variations at end of drying)

s(r) = 0.02 cm

s(h) = 0.2 cm

s(r_{water}) = 0.03 g/cm^3

Derivations

$$d\phi dm_{pw} = \frac{100}{r^2 \times h \times \pi \times \rho_{water}}$$

$$d\phi dr = \frac{-m_{pw} \times 100 \times 2r \times h \times \pi \times \rho_{water}}{(r^2 \times h \times \pi \times \rho_{water})^2}$$

$$d\phi dh = \frac{-m_{pw} \times 100 \times r^2 \times \pi \times \rho_{water}}{(r^2 \times h \times \pi \times \rho_{water})^2}$$

$$d\phi dh = \frac{-m_{pw} \times 100 \times r^2 \times \pi \times h}{(r^2 \times h \times \pi \times \rho_{water})^2}$$

APPENDIX C-3

Porewater Cl- and Br Concentration

Calculations

$$C_{PW} = \frac{(m_{PW} + m_{TWi} - \sum^{n} m_s) \times C_{TW\infty} - (m_{TWi} \times C_{TWi}) + \sum^{n} m_s \times C_s}{m_{PW}}$$

where C_{pw} = porewater concentration; m_{pw} = mass of porewater; m_{TWi} = initial mass of test water; C_{TWi} = initial Cl-concentration of test water; m_s = mass of sub sample used for time series; C_s = Cl concentration of sub sample used for time series.

Error calculation after Gaussian error propagation

$$\sigma(C_{PW}) = \sqrt{\begin{aligned}&\left(dC_{PW}dm_{PW} \times \sigma(m_{PW})\right)^2 + \left(dC_{PW}dm_{TWi} \times \sigma(m_{TWi})\right)^2 + \\ &+\left(dC_{PW}dC_{TW\infty} \times \sigma(C_{TW\infty})\right)^2 + \left(dC_{PW}dC_{TWi} \times \sigma(C_{TWi})\right)^2 + \\ &(\sigma(\sum m_S))^2 + (\sigma(\sum m_S \times c_S))^2\end{aligned}}$$

Analytical errors (error of measurement)

$\sigma(m_{PW})$ = difference between $m_{core,dry\ surface}$ before and after drying + 0.05 g (=variations at end of drying

$\sigma(m_{TWi})$ = difference between $m_{TWi} - m_S - m_{TW\infty}$-2ml (2 ml = remaining water in the cylinder

$\sigma(C_{TWi})$ = 5% (Cl) and 10 % (Br) of the analysed concentration

$\sigma(C_{TW\infty})$ = 5% (Cl) and 10 % (Br) of the analysed concentration

$\sigma(m_S)$ = 0.05 ml

$\sigma(C_S)$ = 5% (Cl) and 10 % (Br) of the analysed concentration

Derivations

$$dC_{PW}dm_{PW} = \frac{C_{TW\infty} * m_{PW} - \left[C_{TW\infty} * (m_{PW} + m_{TWi}) - C_{TW} * m_{TWi}\right]}{m_{PW}^2}$$

$$dC_{PW}dm_{TWi} = \frac{(C_{TW\infty} - C_{TWi}) * m_{PW}}{m_{PW}^2}$$

$$dC_{PW}dC_{TW\infty} = \frac{(m_{PW} - m_{TWi}) * m_{PW}}{m_{PW}^2}$$

$$dC_{PW}dC_{TWi} = \frac{-m_{TWi} * m_{PW}}{m_{PW}^2}$$

$$\sigma\left(\sum(m_s)\right) = \left(Nr_S \times \sigma(m_S)\right)$$

$$\sigma\left(\sum(m_S \times C_S)\right) = \left(Nr_S \times C_{S,ave} \times \sigma(m_S)\right) + \left(Nr_S \times m_S \times \sigma(C_S)\right)$$

APPENDIX C-4

Br*1000/Cl Mass Ratio of Porewater

Br*1000/Cl porewater mass ratio = R

Error calculation after Gaussian error propagation

$$\sigma(R) = \sqrt{\left(dRdC_{Br} \times \sigma(C_{Br})\right)^2 + \left(dRdC_{Cl} \times \sigma(C_{Cl})\right)^2}$$

Analytical errors (error of measurement)

$\sigma(C_{Cl})$ = Error of porewater Cl concentration calculated according to AIII-3

$\sigma(C_{Br})$ = Error of porewater Br concentration calculated according to AIII-3

Derivations

$$dRdC_{Br} = \frac{1000}{C_{Cl}}$$

$$dRdC_{Cl} = \frac{-1000 \times C_{Br}}{C_{Cl}^2}$$

APPENDIX C-5

Calculation of Isotopic Signatures of Matrix Porewater

Calculation

$$C_{PW} = \frac{C_{TW\infty(Std1)} \times m_{TW(Std2)} \times m_{Rock(Std1)} \times (C_{TW\infty(Std2)} - C_{TW^0(Std2)}) - C_{TW\infty(Std2)} \times m_{TW(Std1)} \times m_{Rock(Std2)} \times (C_{TW\infty(Std1)} - C_{TW^0(Std1)})}{m_{TW(Std2)} \times m_{Rock(Std1)} \times (C_{TW\infty(Std2)} - C_{TW^0(Std2)}) - m_{TW(Std1)} \times m_{Rock(Std2)} \times (C_{TW\infty(Std1)} - C_{TW^0(Std1)})}$$

m_{PW} = mass of porewater (g)

m_{TW} = mass of test water (g)

C_{TW} = isotopic signature of test water at the beginning of the experiment (‰)

$C_{TW\infty}$ = isotopic signature of test water after equilibration (‰)

Std 1 = Experiment 1 applying standard 1

Std 2 = Experiment 2 applying standard 2

Error calculation after Gaussian error propagation

$$\sigma(C_{PW}) = \sqrt{\begin{array}{l}\left(dC_{PW}dm_{TW(Std1)} \times \sigma(m_{TW(Std1)})\right)^2 + \left(dC_{PW}dm_{TW(Std2)} \times \sigma(m_{TW(Std2)})\right)^2 + \\ +\left(dC_{PW}dC_{TW(Std1)} \times \sigma(C_{TW(Std1)})\right)^2 + \left(dC_{PW}dC_{TW(Std2)} \times \sigma(C_{TW(Std2)})\right)^2 + \\ +\left(dC_{PW}dC_{TW\infty(Std1)} \times \sigma(C_{TW\infty(Std1)})\right)^2 + \left(dC_{PW}dC_{TW\infty(Std2)} \times \sigma(C_{TW\infty(Std2)})\right)^2\end{array}}$$

Analytical errors (error of measurement)

$\sigma(m_{TW(Std1)})$ = 0.002 g

$\sigma(m_{TW(Std2)})$ = 0.002 g

$\sigma(C_{TW(Std1)})$ = 0.1 ‰ for ^{18}O and 1.0‰ for ^{2}H

$\sigma(C_{TW(Std2)})$ = 0.1 ‰ for ^{18}O and 1.0‰ for ^{2}H

$\sigma(C_{TW\infty(Std1)})$ = 0.1 ‰ for ^{18}O and 1.0‰ for ^{2}H

$\sigma(C_{TW\infty(Std2)})$ = 0.1 ‰ for ^{18}O and 1.0‰ for ^{2}H

Derivations

$$dC_{PW}dm_{TW(Std1)} = \frac{(C_{TW(Std1)} - C_{TW\infty(Std1)}) \times C_{TW\infty(Std2)}}{\left(m_{TW(Std1)} \times (C_{TW(Std1)} - C_{TW\infty(Std1)}) - (C_{TW(Std2)} - C_{TW\infty(Std2)}) \times m_{TW(Std2)}\right)} -$$
$$- \frac{\left((C_{TW(Std1)} - C_{TW\infty(Std1)}) \times C_{TW\infty(Std2)} \times m_{TW(Std1)} - (C_{TW(Std2)} - C_{TW\infty(Std2)}) \times C_{TW\infty(Std1)} \times m_{TW(Std2)}\right) \times (C_{TW(Std1)} - C_{TW\infty(Std1)})}{\left(m_{TW(Std1)} \times (C_{TW(Std1)} - C_{TW\infty(Std1)}) - (C_{TW(Std2)} - C_{TW\infty(Std2)}) \times m_{TW(Std2)}\right)^2}$$

$$dC_{PW}dm_{TW(Std2)} = \frac{-(C_{TW(Std2)} - C_{TW\infty(Std2)}) \times C_{TW\infty(Std1)}}{\left(m_{TW(Std1)} \times (C_{TW(Std1)} - C_{TW\infty(Std1)}) - (C_{TW(Std2)} - C_{TW\infty(Std2)}) \times m_{TW(Std2)}\right)} +$$
$$+ \frac{\left((C_{TW(Std1)} - C_{TW\infty(Std1)}) \times C_{TW\infty(Std2)} \times m_{TW(Std1)} - (C_{TW(Std2)} - C_{TW\infty(Std2)}) \times C_{TW\infty(Std1)} \times m_{TW(Std2)}\right) \times (C_{TW(Std2)} - C_{TW\infty(Std2)})}{\left(m_{TW(Std1)} \times (C_{TW(Std1)} - C_{TW\infty(Std1)}) - (C_{TW(Std2)} - C_{TW\infty(Std2)}) \times m_{TW(Std2)}\right)^2}$$

$$dC_{PW}\,dC_{TW(Std1)} = \frac{C_{TW\infty(Std2)} \times m_{TW(Std1)}}{\left(m_{TW(Std1)} \times \left(C_{TW(Std1)} - C_{TW\infty(Std1)}\right) - \left(C_{TW(Std2)} - C_{TW\infty(Std2)}\right) \times m_{TW(Std2)}\right)} -$$
$$- \frac{\left(\left(C_{TW(Std1)} - C_{TW\infty(Std1)}\right) \times C_{TW\infty(Std2)} \times m_{TW(Std1)} - \left(C_{TW(Std2)} - C_{TW\infty(Std2)}\right) \times C_{TW\infty(Std1)} \times m_{TW(Std2)}\right) \times m_{TW(Std1)}}{\left(m_{TW(Std1)} \times \left(C_{TW(Std1)} - C_{TW\infty(Std1)}\right) - \left(C_{TW(Std2)} - C_{TW\infty(Std2)}\right) \times m_{TW(Std2)}\right)^2}$$

$$dC_{PW}\,dC_{TW(Std2)} = \frac{-C_{TW\infty(Std1)} \times m_{TW(Std2)}}{\left(m_{TW(Std1)} \times \left(C_{TW(Std1)} - C_{TW\infty(Std1)}\right) - \left(C_{TW(Std2)} - C_{TW\infty(Std2)}\right) \times m_{TW(Std2)}\right)} +$$
$$+ \frac{\left(\left(C_{TW(Std1)} - C_{TW\infty(Std1)}\right) \times C_{TW\infty(Std2)} \times m_{TW(Std1)} - \left(C_{TW(Std2)} - C_{TW\infty(Std2)}\right) \times C_{TW\infty(Std1)} \times m_{TW(Std2)}\right) \times m_{TW(Std2)}}{\left(m_{TW(Std1)} \times \left(C_{TW(Std1)} - C_{TW\infty(Std1)}\right) - \left(C_{TW(Std2)} - C_{TW\infty(Std2)}\right) \times m_{TW(Std2)}\right)^2}$$

$$dC_{PW}\,dC_{TW\infty(Std1)} = \frac{-\left(C_{TW\infty(Std2)} \times m_{TW(Std1)} + \left(C_{TW(Std2)} - C_{TW\infty(Std2)}\right) \times m_{TW(Std2)}\right)}{\left(m_{TW(Std1)} \times \left(C_{TW(Std1)} - C_{TW\infty(Std1)}\right) - \left(C_{TW(Std2)} - C_{TW\infty(Std2)}\right) \times m_{TW(Std2)}\right)} +$$
$$+ \frac{\left(\left(C_{TW(Std1)} - C_{TW\infty(Std1)}\right) \times C_{TW\infty(Std2)} \times m_{TW(Std1)} - \left(C_{TW(Std2)} - C_{TW\infty(Std2)}\right) \times C_{TW\infty(Std1)} \times m_{TW(Std2)}\right) \times m_{TW(Std1)}}{\left(m_{TW(Std1)} \times \left(C_{TW(Std1)} - C_{TW\infty(Std1)}\right) - \left(C_{TW(Std2)} - C_{TW\infty(Std2)}\right) \times m_{TW(Std2)}\right)^2}$$

$$dC_{PW}\,dC_{TW\infty(Std1)} = \frac{-\left(C_{TW\infty(Std2)} \times m_{TW(Std1)} + \left(C_{TW(Std2)} - C_{TW\infty(Std2)}\right) \times m_{TW(Std2)}\right)}{\left(m_{TW(Std1)} \times \left(C_{TW(Std1)} - C_{TW\infty(Std1)}\right) - \left(C_{TW(Std2)} - C_{TW\infty(Std2)}\right) \times m_{TW(Std2)}\right)} +$$
$$+ \frac{\left(\left(C_{TW(Std1)} - C_{TW\infty(Std1)}\right) \times C_{TW\infty(Std2)} \times m_{TW(Std1)} - \left(C_{TW(Std2)} - C_{TW\infty(Std2)}\right) \times C_{TW\infty(Std1)} \times m_{TW(Std2)}\right) \times m_{TW(Std1)}}{\left(m_{TW(Std1)} \times \left(C_{TW(Std1)} - C_{TW\infty(Std1)}\right) - \left(C_{TW(Std2)} - C_{TW\infty(Std2)}\right) \times m_{TW(Std2)}\right)^2}$$

$$dC_{PW}\,dC_{TW\infty(Std2)} = \frac{\left(m_{TW(Std1)} \times \left(C_{TW(Std1)} - C_{TW\infty(Std1)}\right) + C_{TW\infty(Std1)} \times m_{TW(Std2)}\right)}{\left(m_{TW(Std1)} \times \left(C_{TW(Std1)} - C_{TW\infty(Std1)}\right) - \left(C_{TW(Std2)} - C_{TW\infty(Std2)}\right) \times m_{TW(Std2)}\right)} -$$
$$- \frac{\left(\left(C_{TW(Std1)} - C_{TW\infty(Std1)}\right) \times C_{TW\infty(Std2)} \times m_{TW(Std1)} - \left(C_{TW(Std2)} - C_{TW\infty(Std2)}\right) \times C_{TW\infty(Std1)} \times m_{TW(Std2)}\right) \times m_{TW(Std2)}}{\left(m_{TW(Std1)} \times \left(C_{TW(Std1)} - C_{TW\infty(Std1)}\right) - \left(C_{TW(Std2)} - C_{TW\infty(Std2)}\right) \times m_{TW(Std2)}\right)^2}$$

APPENDIX C-6

Calculation of Mass of Porewater by Isotope Diffusive Exchange Technique

Calculation

$$WC_{IsoEx} = \left[\frac{m_{TW(Std2)} \times m_{Rock(Std1)} \times (C_{TW^0(Std2)} - C_{TW\infty(Std2)}) + m_{TW(Std1)} \times m_{Rock(Std2)} \times (C_{TW\infty(Std1)} - C_{TW^0(Std1)})}{m_{Rock(Std1)} \times m_{Rock(Std2)} \times (C_{TW\infty(Std2)} - C_{TW\infty(Std1)})} \right] \times 100$$

m_{PW} = mass of porewater (g)

m_{TW} = mass of test water (g)

C_{TW} = isotopic signature of test water at the beginning of the experiment (‰)

$C_{TW\infty}$ = isotopic signature of test water after equilibration (‰)

Std 1 = Experiment 1 applying standard 1

Std 2 = Experiment 2 applying standard 2

Error calculation after Gaussian error propagation

$$\sigma(m_{PW}) = \sqrt{\begin{aligned} &\left(dm_{PW}dm_{TW(Std1)} \times \sigma(m_{TW(Std1)})\right)^2 + \left(dm_{PW}dm_{TW(Std2)} \times \sigma(m_{TW(Std2)})\right)^2 + \\ &+\left(dm_{PW}dC_{TW(Std1)} \times \sigma(C_{TW(Std1)})\right)^2 + \left(dm_{PW}dC_{TW(Std2)} \times \sigma(C_{TW(Std2)})\right)^2 + \\ &+\left(dm_{PW}dC_{TW\infty(Std1)} \times \sigma(C_{TW\infty(Std1)})\right)^2 + \left(dm_{PW}dC_{TW\infty(Std2)} \times \sigma(C_{TW\infty(Std2)})\right)^2 \end{aligned}}$$

Analytical errors (error of measurement)

$\sigma(m_{TW(Std1)})$ = 0.002 g

$\sigma(m_{TW(Std2)})$ = 0.002 g

$\sigma(C_{TW(Std1)})$ = 0.1 ‰ for ^{18}O and 1.0‰ for ^{2}H

$\sigma(C_{TW(Std2)})$ = 0.1 ‰ for ^{18}O and 1.0‰ for ^{2}H

$\sigma(C_{TW\infty(Std1)})$ = 0.1 ‰ for ^{18}O and 1.0‰ for ^{2}H

$\sigma(C_{TW\infty(Std2)})$ = 0.1 ‰ for ^{18}O and 1.0‰ for ^{2}H

Derivations

$$dm_{PW}dm_{TW(Std1)} = \frac{\left(C_{TW(Std1)} - C_{TW\infty(Std1)}\right)}{\left(C_{TW\infty(Std1)} - C_{TW\infty(Std2)}\right)}$$

$$dm_{PW}dm_{TW(Std2)} = \frac{-\left(C_{TW(Std2)} - C_{TW\infty(Std2)}\right)}{\left(C_{TW\infty(Std1)} - C_{TW\infty(Std2)}\right)}$$

$$dm_{PW}dC_{TW(Std1)} = \frac{m_{TW(Std1)}}{\left(C_{TW\infty(Std1)} - C_{TW\infty(Std2)}\right)}$$

$$dm_{PW}dC_{TW(Std\,2)} = \frac{-m_{TW(Std\,2)}}{\left(C_{TW\infty(Std\,1)} - C_{TW\infty(Std\,2)}\right)}$$

$$dm_{PW}dC_{TW\infty(Std\,1)} = \left(\frac{-1}{\left(C_{TW\infty(Std\,1)} - C_{TW\infty(Std\,2)}\right)} - \frac{\left(C_{TW(Std\,1)} - C_{TW\infty(Std\,1)}\right)}{\left(C_{TW\infty(Std\,1)} - C_{TW\infty(Std\,2)}\right)^2}\right) \times m_{TW(Std\,1)} + \left(C_{TW(Std\,2)} - C_{TW\infty(Std\,2)}\right) \times m_{TW(Std\,2)}$$

$$dm_{PW}dC_{TW\infty(Std\,2)} = \left(\frac{\left(C_{TW(Std\,1)} - C_{TW\infty(Std\,1)}\right) \times m_{TW(Std\,1)}}{\left(C_{TW\infty(Std\,1)} - C_{TW\infty(Std\,2)}\right)^2} + \frac{1}{\left(C_{TW\infty(Std\,1)} - C_{TW\infty(Std\,2)}\right)^2} - \frac{\left(C_{TW(Std\,2)} - C_{TW\infty(Std\,2)}\right)}{\left(C_{TW\infty(Std\,1)} - C_{TW\infty(Std\,2)}\right)^2}\right) \times m_{TW(Std\,2)}$$



wsp.com

